TWO-DIMENSIONAL MIXING OF CONSERVATIVE POLLUTANTS IN OPEN CHANNELS

A THESIS

submitted in fulfilment of the
requirements for the award of the degree
of

DOCTOR OF PHILOSOPHY

in

CIVIL ENGINEERING

By

SARBJIT SINGH

DEPARTMENT OF CIVIL ENGINEERING
THAPAR INSTITUTE OF ENGINEERING AND TECHNOLOGY
(Deemed University)
PATIALA-147 004 (INDIA)

NOVEMBER, 2004

CERTIFICATE

Certified that the work presented in the thesis entitled "**TWO-DIMENSIONAL MIXING OF CONSERVATIVE POLLUTANTS IN OPEN CHANNELS**" which is being submitted by Mr. Sarbjit Singh in fulfilment of the requirement for the award of the Degree of **Doctor of Philosophy** in the Department of Civil Engineering, Thapar Institute of Engineering and Technology (Deemed University), Patiala is an authentic record of candidate's own work carried out during a period from September 1999 to November 2004 at Thapar Institute of Engineering and Technology (Deemed University), Patiala under the supervision of **Dr. Z.Ahmad** and **Dr. U.C. Kothyari.** The matter presented in the thesis has not been submitted for the award of any other degree in any University.

19/11/04

(Dr. Z. Ahmad)

Assistant Professor
Department of Civil Engineering
Indian Institute of Technology
ROORKEE-247 667.

Kothyari
19/11/04

(Dr. U.C. Kothyari)

Professor
Department of Civil Engineering
Indian Institute of Technology
ROORKEE-247 667.

ABSTRACT

Streams act as sinks for accidental or intentional spillage of pollutants from various industrial and municipal sources. Therefore, it becomes necessary to know the concentration distribution of these pollutants in the downstream, to check whether the required environmental standards are being satisfied or not. Some of the pollutants however, can have devastating impacts on the environment. Therefore, prediction of spreading of pollutants in streams is very important. Accurate prediction of the transport of pollutants is thus crucial for effective water quality management.

As the pollutants travel downstream along the stream, they undergo various stages of mixing and their concentration decreases. The pollutants are mixed longitudinally, transversely and vertically by the action of advection and diffusion (molecular and turbulent) processes and velocity shear. Near the injection site, the mixing is three-dimensional in nature. After some distance from the injection site, the pollutants get mixed uniformly along the depth and the concentration varies only in longitudinal and transverse directions. The assumption of complete vertical mixing within a short reach is accepted because the aspect ratio (flow width/ flow depth) of streams is very large. After a time lapse the pollutants are completely mixed across the cross-section of the stream and the primary variation of concentration is only in the longitudinal direction and mixing beyond this section is called longitudinal dispersion.

If a transverse line source injects tracer uniformly into the stream at any elevation along the depth, instantaneously or continuously, the mixing in the downstream occurs only in longitudinal and vertical directions and a two-dimensional mixing model is required to describe such a mixing process.

Vertical mixing is not as important in water quality management as the transverse mixing. However, vertical mixing has great importance close to the source. Even though it is limited to near the source, the understanding of vertical mixing is required for knowing the concentration of pollutant in the near-field region. The profiles of concentration distribution of the near-field region serve as boundary conditions to the models for simulating mixing in the mid-field and/or far-field region. Compared to transverse and longitudinal mixing, the

vertical mixing is not studied extensively and only a few studies are available in literature on this topic.

The governing equation for two-dimensional mixing of conservative pollutants from a transverse line slug source in steady and uniform flow is of the following form (Nokes et al. 1984):

$$\frac{\partial C}{\partial t}+\frac{\partial}{\partial x}(U_x C)=\frac{\partial}{\partial x}\left[E_x \frac{\partial C}{\partial x}\right]+\frac{\partial}{\partial y}\left[E_y \frac{\partial C}{\partial y}\right] \qquad (A)$$

where C = width-averaged concentration; t = simulation time; U_x = width-averaged longitudinal velocity; E_x = longitudinal mixing coefficient; and E_y = vertical mixing coefficient. For given flow characteristics, analytical or numerical solution of Eq. (A) with suitable boundary conditions yields concentration of pollutants at different longitudinal distances and at different elevations along the depth of flow. Solution of Eq. (A) requires information on channel and flow properties and mixing coefficients E_x and E_y. Analytical solutions of Eq. (A) are available in literature for its simplified form and mainly for a steady source of pollutant (Rutherford 1994).

For a steady source Holley et al. (1972) and Fisher et al. (1979) made the assumption that longitudinal concentration gradients are small compared with vertical concentration gradients and for this case the prediction of pollutant concentration downstream can be modelled by simplifying Eq. (A), to yield:

$$U_x \frac{\partial C}{\partial x}=E_y \frac{\partial^2 C}{\partial y^2} \qquad (B)$$

For the vertically unbounded flow, an analytical solution of Eq. (B) is available in literature (Rutherford 1994). Method of images is used to obtain the tracer concentration for bounded flow. Nokes et al. (1984) solved Eq. (B) for the case of a steady transverse line source by reducing it to a Sturm-Liouville eigen value problem and obtained the solution for different velocity and diffusivity distributions. McNulty and Wood (1984) developed an algorithm to obtain complete downstream concentration for different velocity and diffusivity distributions due to a steady transverse line source. Nokes and Wood (1988) conducted experiments for vertical and lateral mixing from a neutrally buoyant continuous contaminant source in a rectangular tilting flume. Schiller and Sayre (1975) presented a mathematical model based on laboratory flume experiments for predicting vertical distribution of temperatures in open

channels. French (1979) presented an accurate and practical method of computing the solute transfer coefficients in stratified channel flow in terms of easily measurable parameters in either the laboratory or field.

The numerical schemes available for solution of equations similar to Eq. (A) can be generally classified into two types: Split operator and the Combined operator approaches. In the Split-operator approach, the advection and diffusion rates are computed separately by using different numerical schemes, whereas in the Combined operator approach the complete mixing process is simulated without separating the two processes. Furthermore, the computation of diffusion can be executed accurately using a variety of finite difference and finite element methods (Morton 1981). However, it is more difficult to devise numerical schemes of sufficient accuracy for solution of advection process (Li 1990; Schohl and Holly 1991). Among the procedures for solving the pure advection equation, several schemes have been proposed, such as Holly and Preissmann two-point fourth order scheme (Holly and Preissmann 1977); Six-point scheme (Komatsu et al. 1985); Improved six-point scheme (Komatsu et al. 1989); Yang-Hsu time-line interpolation scheme (Yang and Hsu 1990); Spatial cubic spline scheme (Schohl and Holly 1991); SOWMAC scheme (Komatsu et al. 1992; Komatsu et al. 1997); Time line cubic spline scheme (Ahmad and Kothyari 2001). The diffusion process can be accurately computed by several numerical schemes such as Crank-Nicholson central difference scheme; Crank-Nicholson Galerkin finite-element method; alternate-direction implicit (ADI) scheme.

Numerical solution of Eq. (A) with derivative boundary conditions is not available in literature. However, numerical solutions of the varied form of Eq. (A) are available in literature such as, Stefanovic and Stefan (2001); Tsai et al. (2002); Guan et al. (2002).

In the present study a numerical scheme based on Split operator approach has been developed, for the solution of two-dimensional mixing equation. Exact solution of the advection equation has been achieved by adopting the Courant number equal to one for the computational nodes lying on the surface of flow. For the other computational nodes, cubic spline interpolation scheme of Schohl and Holly (1991) has been used to obtain the solution of the advection process because of the velocity defect along the vertical. The computation of diffusion rate has been made by using the alternate-direction implicit method (ADIM) suggested by Smith (1978). This is a two-step approach method in which it is assumed that if the solution is known at any time level, the solution for the next time level is obtained by solving the equations implicitly. To this solution, the advected concentration is added for

obtaining the final concentration. The solution is advanced to the next time level by simply changing the direction of operations. The solution procedure at each individual level is conditionally stable but the combined two levels solution procedure is completely stable. The compensation of errors produced by the alternation of direction gives a scheme, which is stable and convergent.

The proposed numerical scheme has been illustrated by hypothesizing the transverse line injection of tracer at the surface of flow, at mid-depth and at the channel bed. The temporal variation of concentration of transverse line source is assumed to follow a sine curve having equation $C = 100 \sin \omega t$, with $\omega = \frac{\pi}{20}$. The numerical model is mass conservative. The mass conservation of the numerical scheme is confirmed by calculating the mass of the dye injected upstream at a station and mass of the dye recovered at different stations over a long duration of time.

The proposed numerical model describes the mixing of the pollutant due to transverse line slug injection source. The model predicts mixing of the pollutant immediately downstream of an input site in vertical and longitudinal directions (two-dimensional model) as well as in the far-field, *i.e.*, in the longitudinal direction (one-dimensional model). Validation of the proposed numerical scheme was made by using the analytical solution of Fischer (1968) for one-dimensional mixing as well as analytical solution for continuous injection of pollutant as a steady transverse line source.

Vertical mixing is one of the few river-mixing problems for which the vertical mixing coefficient E_y can be predicted satisfactorily on theoretical grounds. Prandtl's mixing length hypothesis provides theoretical formulae for vertical mixing coefficient, which, is found to vary with depth.

Jobson and Sayre (1970a) however noticed that predicted pollutant concentration profiles were not very sensitive to the vertical distribution of vertical mixing coefficient and for many practical problems it is sufficiently accurate to use a depth-averaged value. Jobson and Sayre (1970b); Schiller and Sayre (1975); French (1979); and Nokes (1986) based on laboratory studies found that experimental results match with the vertical mixing coefficient computed based on Prandtl's mixing length hypothesis. Detailed information however, is not available easily for the estimation of longitudinal mixing coefficient E_x.

The numerical scheme proposed herein has been extended by incorporating in it one-dimensional grid search method for determination of E_x values for known values of E_y and concentration versus time (C-t) profiles.

The experiments relating to two-dimensional mixing (longitudinal and vertical) were conducted in the Hydraulics Laboratory of Department of Civil Engineering, Indian Institute of Technology (Formerly: University of Roorkee), Roorkee in a recirculating tilting flume 15.75 m long, 0.39 m wide and 0.50 m deep. Firstly, the experiments were carried out in clear-water flows and were followed by experiments in sediment-laden flows. Rhodamine WT was used as the tracer whose concentration was monitored in the flume using a Turner designed Fluorometer 10-AU-005 of continuous flow type.

The tracer was injected uniformly across the channel width as a transverse slug line source and C-t curves were measured at three elevations along the flow depth, *i.e.*, near the bed, in the middle of the flow depth and near the flow surface at an interval of 1 m at number of stations downstream from the injection site of tracer. The experiments were conducted at four different slopes of the channel. In total 48 runs were conducted for different discharges in clear water and sediment-laden flows. Two uniform sands of average diameter 0.064 mm and 0.024 mm were used as sediment. The concentration of sediment in suspension was varied from 104 ppm to 6178 ppm by weight. In addition, velocity distributions in a cross-section along five verticals were also measured using Prandtl pitot tube for each run.

One requires predictors for E_x and E_y in terms of flow and channel variables, for being able to make calculations of C-t curves at different downstream stations given the C-t curves at an upstream station. E_y can be calculated by using depth-averaged relationship based on Prandtl's logarithmic velocity distribution or by using observed longitudinal velocity at mid-width of the channel. However no predictor is available to estimate longitudinal mixing coefficient E_x.

Values of the mixing coefficients E_x and E_y have been determined by using two-dimensional grid search method, by finding the optimum value of longitudinal mixing coefficient E_x and vertical mixing coefficient E_y. Such values of E_x and E_y are considered to be the optimum ones that produce best matching of the observed and computed C-t curves at all the downstream stations.

The data collected during present experimental study and data available from literature have been used to verify the existing predictors for vertical mixing coefficient E_y. The depth-averaged value of E_y was compared with the optimum (observed) value of E_y. E_y was also computed from measured velocity distribution and compared with observed E_y. In both the cases most of the computed values lie within a scatter band of 2 to 1/2 times the observed values of E_y. The optimum value of E_x was re-determined by using the value of E_y computed from measured longitudinal velocity at mid-width of the channel and by employing one-dimensional grid search method such that error is minimum between the observed and computed C-t curves at all the downstream stations.

A predictor has also been proposed for E_x, based on channel and flow characteristics. It has been found that the predictor produce satisfactory results. The predicted values of E_x are 2 to 1/2 times the observed values.

Sensitivity analysis of the C-t curves to errors in E_x and E_y has also been carried out. It was observed that likely error in E_x due to the use of predictor proposed in the present study would not result in appreciable errors in computation of C-t curves, when the value of E_x is altered with a multiplying factor from 0.2 to 2. A large change in E_x value significantly affects the accuracy of C-t curves. A similar analysis for E_y reveals that accuracy for the computation of C-t curve does not change considerably when optimum value of E_y is altered by factors from 0.5 to 2. Likewise less accurate results are obtained while E_y values are altered beyond these limits.

In addition, alluvial streams carry sediments as suspended load and bed load. To make the tracer transport prediction problems more oriented to field applications, it is necessary to know the effects of sediment on the mixing process. Therefore, the effect of suspended sediment load on the vertical mixing of pollutants has also been studied experimentally. C-t curves were observed for clear water flow and for sediment-laden flow under nearly identical flow conditions. Sand of average diameter 0.064 mm and 0.024 mm with concentration ranging from 104 ppm to 6178 ppm by weight was used as suspended sediment. The cross-sectional velocity distributions in clear-water flows (CWF) and sediment-laden flows (SLF) were also observed.

The C-t curves observed for clear water flow and corresponding sediment-laden flows were superimposed on each other for studying the effect of sediment concentration on C-t curves, at different elevations along the vertical and various downstream locations. The measured vertical velocity distribution for CWF and SLF were also superimposed. From these, it is observed that the presence of sediment does not have appreciable effect on the mixing characteristics for the range of experimental data used in the present study.

ACKNOWLEDGEMENTS

The present work will remain incomplete unless I express my feelings of gratitude to a number of persons who delightfully co-operated with me during the process of this research work. I express my profound sense of heart-felt gratitude to my guides Dr. U.C. Kothyari, Professor, Dr. Z. Ahmad, Assistant Professor, Department of Civil Engineering, Indian Institute of Technology, Roorkee for their valuable guidance and inspiring encouragement in pursuance of this work. They treated me more like a friend than a student. Despite of their busy schedule, they always spared time for me and their guidance precious and genial always kept me on the right track

I would also like to pay my sincere thanks to Dr. M. P. Kapoor, former Director, Dr. S. C. Saxena, Director, Dr. K. K. Raina, Dean, research and sponsored projects, Thapar Institute of Engineering and Technology, Patiala for their enduring inspiration and regular support in various forms, during the course of the work for its successful completion. This work has seen the change of four Heads of Department of Civil Engineering, I thank all of them for their support and help during the various stages of work.

The present research work has been carried out mainly in Hydraulic Engineering Section of Department of Civil Engineering, Indian Institute of Technology, Roorkee. Here I appreciate the facilities extended to me by Hydraulic Engineering Section. I greatly acknowledge the help rendered by the staff of Hydraulic Laboratory of Indian Institute of Technology, Roorkee.

The co-operation received through my friends and colleagues Dr. N. K. Kullar, Dr. Dilbag Singh, Mr. Umesh Sharma, Mr. Sukwinder Singh, Mr. Pardeep Kumar, Dr. Naveen Kwatra, Dr. A. K. Lal, Dr. Maneek Kumar at various stages of the present study is thankfully acknowledged. Dr. Naveen Kwatra deserves a special mention for his invaluable help during the preparation of this manuscript. I am also thankful to my other colleagues of Department of Civil Engineering, Thapar Institute of Engineering and Technology, Patiala for their help and moral support during the period of my work at Roorkee.

The help and support provided by Sh. Satya Narayan, Sh. Ram Lal and other staff of Department of Civil Engineering, Thapar Institute of Engineering and Technology, Patiala is thankfully acknowledged

In the presentation of this work I owe a great deal to publishers and authors of various books and journals. Although appropriate references have been quoted in the bibliography, yet any omissions are totally inadvertent.

I am indeed indebted to my family members who always prayed to God for successful completion of my work.

I owe thanks to my son specially Inderpreet and daughter Supreet for patiently bearing inattentiveness toward them during the work.

I acknowledge my heartiest gratitude to Harpreet, my wife, without whose untiring efforts and enduring patience, I would never have been able to complete this work successfully.

Last but not the least, I wish to express my sincere thanks to all persons who have helped me in the successful completion of this work.

Place: Patiala

Date: November 18, 2004

(Sarbjit Singh)

CONTENTS

LIST OF SYMBOLS

Symbol		Description
A	=	Cross-sectional area of flow
a_k	=	Expansion constants
A_b	=	Area corresponding to bed of the channel
A_{w1}, A_{w2}	=	Areas corresponding to sides walls of the channel
b	=	Bed width of the channel
b^*	=	Dimensionless width of the channel.
b_k	=	Width of the sub-area
B	=	Water surface width of stream
c	=	Tracer concentration at a point
$\bar{c}$	=	Time-averaged tracer concentration
c'	=	Deviation in concentration about $\bar{c}$
C	=	Width-averaged concentration
C'	=	Deviation in concentration about C
C^*	=	Dimensionless concentration
C_p	=	Peak concentration of C-t profile of tracer
C_s	=	Pollutant concentration of source
C_i	=	Concentration of the injected tracer
C_r	=	Courant number
$C^n_{i,j}$	=	Concentration at computational node (i, j) at the n^{th} time level
$\left(C_{i,j+1}\right)^{n+1}_A$	=	Advected concentration at $(i, j+1)$ computational node at the $(n+1)^{th}$ time level
C-t	=	Concentration versus time
$c_1, c_2, \ldots\ldots, c_6$	=	Concentration interpolating coefficients (Six-point scheme)
$c'_1, c'_2, \ldots\ldots, c'_6$	=	Concentration interpolating coefficients (Improved six-point scheme)
d	=	Local depth of flow

d_*	=	Dimensionless local depth of flow
d'_k	=	Depth of the sub-area
D	=	Cross-sectional average flow depth
D_{50}	=	Average size of sediment
$d_1, d_2, ..., d_6$	=	Concentration interpolating coefficients (SOWMAC scheme)
d'_1, d'_2, d'_3, d'_4	=	Concentration interpolating coefficients (Schohl and Holly scheme)
b_{j-1}, d_{j-1}, a_{j-1}	=	Author's known coefficients for $(n_{even}+1)\Delta t$ time levels
b_i, d_i, a_i	=	Author's known coefficients for $(n_{even}+2)\Delta t$ time levels
e_m	=	Molecular diffusion coefficient
e_x	=	Turbulent diffusion coefficient or eddy diffusivity in the x-direction
e_y	=	Turbulent diffusion coefficient or eddy diffusivity in the y-direction
e_z	=	Turbulent diffusion coefficient or eddy diffusivity in the z-direction
E'_x	=	Mixing coefficient in depth-averaged mixing equation
E_x	=	Longitudinal mixing coefficient
E_y	=	Vertical mixing coefficient
E_z	=	Transverse mixing coefficient
E_x^*	=	Dimensionless longitudinal mixing coefficient
E_y^*	=	Dimensionless vertical mixing coefficient
E_z^*	=	Dimensionless transverse mixing coefficient
E_L	=	Longitudinal dispersion coefficient
E_o	=	Vertical mixing coefficient in non-stratified condition
E_s	=	Vertical mixing coefficient in stratified condition
ΔE_x	=	Incremental value of longitudinal mixing coefficient
ΔE_y	=	Incremental value of vertical mixing coefficient
f	=	Foot of trajectory of concentration characteristic on the temporal axes
f_l	=	Friction factor
g	=	Acceleration due to gravity
i	=	Index number along the Y-direction
j	=	Index number along the X-direction

J_x	=	Molecular diffusive flux in the x-direction
J_y	=	Molecular diffusive flux in the y-direction
J_z	=	Molecular diffusive flux in the z-direction
k_1	=	Constant
k_2	=	Constant
k_s	=	Average height of roughness
K	=	Constant
L_y	=	Vertical mixing distance
m	=	Mass of tracer recovered at a section
M	=	Total tracer mass injected
$\dot{M}$	=	Tracer mass inflow rate
n	=	Index number along the time direction
N	=	Total number of computational planes in the time direction (z-direction)
N_1	=	Total number of terms, C-t curves, sub-areas
nX	=	Total number of computational nodes in X-direction
nY	=	Total number of computational nodes in Y-direction
n_{w1}, n_{w2}	=	Manning's coefficient for the side walls of the channel
O	=	Order of local truncation errors
OE_x	=	Optimum value of longitudinal mixing coefficient
OE_y	=	Optimum value of vertical mixing coefficient
P	=	Wetted perimeter
P_b	=	Wetted perimeter corresponding to bed
P_{w1}, P_{w2}	=	Wetted perimeters corresponding to sides walls
ppm	=	Parts per million
q	=	Discharge per unit width
Q	=	Discharge
R_b	=	Hydraulic radius corresponding to bed
R_{w1}, R_{w2}	=	Hydraulic radii corresponding to sides walls
R_c	=	Richardson number
s	=	Depth-averaged concentration
s′	=	Deviation in concentration about s

S	=	Cross-sectional averaged concentration
S'	=	Deviation in concentration about S
S_b	=	Bed slope of the channel
S_f	=	Slope of energy line
t	=	Simulation time
t^*	=	Dimensionless time
t_o	=	Initial time (Time just before the injection of the pollutant)
t_1, t_2, t_3	=	Travelled time of tracer cloud
$\bar{t}$	=	Time of arrival of centroid of the tracer cloud at the observation station
$\bar{t}_1$	=	Time of arrival of centroid of the tracer cloud at first station
$\bar{t}_2$	=	Time of arrival of centroid of the tracer cloud at second station
T_{1R}	=	Elapsed time to the arrival of 25% of peak concentration of the tracer cloud the rising limb
T_{1F}	=	Elapsed time to the arrival of 25% of peak concentration of the tracer cloud the falling limb
T_{2R}	=	Elapsed time to the arrival of 50% of peak concentration of the tracer cloud the rising limb
T_{2F}	=	Elapsed time to the arrival of 50% of peak concentration of the tracer cloud the falling limb
T_{3R}	=	Elapsed time to the arrival of 75% of peak concentration of the tracer cloud the rising limb
T_{3F}	=	Elapsed time to the arrival of 75% of peak concentration of the tracer cloud the falling limb
T_L	=	Elapsed time to the arrival of the leading edge of the tracer cloud
T_T	=	Elapsed time to the arrival of the trailing edge of the tracer cloud
T_P	=	Elapsed time to the arrival of the peak concentration of the tracer cloud
Δt	=	Spacing of the grid in the time direction
u_x	=	Velocity at a point in the x-direction
u_y	=	Velocity at a point in the y-direction
u_z	=	Velocity at a point in the z-direction
$\bar{u}_x$	=	Time-averaged velocity in the x-direction
$\bar{u}_y$	=	Time-averaged velocity in the y-direction
$\bar{u}_z$	=	Time-averaged velocity in the z-direction

u'_x = Deviation in velocity about $\bar{u}_x$ in the x-direction

u'_y = Deviation in velocity about $\bar{u}_y$ in the y-direction

u'_z = Deviation in velocity about $\bar{u}_z$ in the z-direction

U = Average velocity of flow

U_i = Velocity at computational node i

U^* = Dimensionless velocity

U_* = Shear velocity

U_k = Width-averaged velocity over the sub-area (x-direction)

U_x = Width-averaged forward velocity (x-direction)

U_y = Width-averaged velocity in the y-direction

U'_x = Deviation in velocity about U_x

U'_y = Deviation in velocity about U_y

$(U_x)_1$ = Width-averaged velocity up to bottom 1/3 rd depth of flow

$(U_x)_2$ = Width-averaged velocity up to middle 1/3 rd depth of flow

$(U_x)_3$ = Width-averaged velocity up to top 1/3 rd depth of flow

v_x = Depth-averaged velocity in the x-direction

v_z = Depth-averaged velocity in the z-direction

v'_x = Deviation in velocity about v_x in the x-direction

v'_z = Deviation in velocity about v_z in the z-direction

V_x = Cross-sectional averaged velocity

V'_x = Deviation in velocity about V_x

x = Distance in the longitudinal direction

x^* = Dimensionless longitudinal distance

X = Transformed longitudinal distance

X_j = Distance of the j^{th} node from the first node

ΔX = Transformed grid spacing in X-direction

Δx = Grid spacing in x-direction

y = Distance in the vertical direction

y_1 = Arbitrary vertical distance from bottom at which time-averaged velocity is zero

y^* = Dimensionless vertical distance

Y	=	Transformed vertical distance
ΔY	=	Transformed grid spacing in Y-direction
z	=	Distance in the transverse direction
z_1	=	Location of the left bank of the channel
z_2	=	Location of the right bank of the channel
x_o, y_o, z_o	=	Source location
$G(x)$	=	General function of x used in Nokes et al. (1984) model
$H(y)$	=	General function of y used in Nokes et al. (1984) model
$\chi(y)$	=	Non-dimensional velocity
$\psi(y)$	=	Non-dimensional vertical diffusivity
φ	=	Functional term
Δh	=	Pressure head difference
τ	=	Time parameter
τ_o	=	Bed shear stress
τ_t	=	Turbulent shear stress
ν_t	=	Apparent kinematic viscosity or eddy viscosity
κ	=	von Karman's constant
Δ	=	Prefix for incremental quantity
ϕ_x	=	Total flux in the x-direction
ϕ_y	=	Total flux in the y-direction
ϕ_z	=	Total flux in the z-direction
ρ	=	Mass density of water
ξ	=	Foot of trajectory of concentration characteristic line on spatial axes
$\sigma^2(t)$	=	Variance of spatial variation of tracer concentration
γ	=	Constant of separation
σ	=	Sinuosity of the stream
ADIM	=	Alternate-direction implicit method
CWF	=	Clear- water flows
CDCW	=	Tracer concentration data for clear- water flows
CDSL	=	Tracer concentration data for sediment-laden flows
erf	=	Error function
ERS	=	Error between an observed and a predicted C-t curve

ERR	=	Average error between observed and predicted C-t curves at all the stations
int	=	Function used in C language for ignoring fractions
SLF	=	Sediment-laden flows
VDCW	=	Velocity distribution data for clear-water flows
VDSL	=	Velocity distribution data for sediment-laden flows

LIST OF FIGURES

LIST OF TABLES

Chapter 1

INTRODUCTION

1.1 GENERAL

Streams have been used as convenient disposal sites for various industrial and municipal wastes for a long time. These wastes are responsible for wide spread pollution in streams. It is no longer sufficient to deal only with quantities of water. In recent years, more concern has been raised towards the quality management of the riverine system. Many pollutants enter the water environment intentionally or accidentally and are transported and dispersed downstream. Downstream water quality depends upon both the hydrodynamics of transport and mixing, in addition to the chemistry and the biology of natural water systems. The possibility of a contaminant accidentally or intentionally spilled in a river is an ever-present danger to those using water from it downstream. Accidental releases such as rupture of an oil pipe or spill of some toxic material in the stream may have a devastating impact on the environment (Jobson 1997). In order to assess the potential impact of the release of a pollutant in a river, it is necessary to determine the pollutant concentration downstream of the release point. Accurate prediction of the transport of these pollutants is crucial to the effective water quality management.

The scope of study on mixing of pollutants in streams may be summarized as (Young and Wallis 1993):

i) Prediction of the passage of pollutant cloud through river system for water quality management programmes/strategies.

ii) Estimation of the assimilating capacity of rivers to receive urban and industrial effluents for determination of the acceptable limits of effluent input.

iii) Assessment of the ecological impacts of the discharge of cooling water from thermal power stations.

iv) Simulation of the effects of proposed engineering works on mixing patterns.

Fischer et al. (1979) have identified variety of pollutants such as natural inorganic salts, sediments, waste heat, domestic sewage wastes, industrial wastes containing heavy metals, synthetic organic chemicals, radioactive materials, chemical and biological warfare agents etc. Inorganic salts and sediments are not toxic and become pollutants only if used in excessive doses. Waste heat is carried by the effluent from the cooling system of the thermal power plants and discharged into natural water bodies. This may cause rise of temperature in water bodies beyond a certain limit and could be harmful to aquatic life. Domestic sewage wastes can cause stenches and nuisances, but if adequately treated and dispersed, these ecosystem materials can be safely assimilated into large water bodies. Industrial wastes containing heavy residual metals from the industry such as lead, mercury, cadmium etc. if discharged into a water body may increase the concentration of these toxic metals. Synthetic organic materials slowly degrade in environment and are often bioaccumulated in the food chain. Because of high toxicity of radioactive materials e.g. plutonium, even leakage from the storage and discharging into the natural water bodies cause grave concern. A very small dose of chemical and biological warfare agents e.g. anthrax, can cause great danger to human beings.

1.2 PROCESS OF MIXING IN OPEN CHANNEL FLOWS

A common approach for evaluating the mixing characteristics of the flow in an open channel is to inject a tracer into the stream either at a constant rate so that a steady state distribution of concentration is established some time after commencement of injection or as a slug and then to observe its concentration versus time (C-t) profiles at various downstream sections.

Slug injection is more advantageous in the respect of economy in material, feasibility, scientific information, and environmental aspects etc. as compared to continuous injection (Beltaos 1975). The amount of tracer needed to perform a slug test is much less than that is required for a continuous test. This factor is particularly important when an expensive tracer is to be used. Injection of slug is simple as compared to constant injection which requires special equipment. A slug test provides information with respect to mixing and time spread characteristics of the tracer. The same cannot be obtained from a continuous test (since time variations vanish). Using high or moderate concentrations of tracer concentrations for long times may affect the aquatic life adversely.

A decrease in concentration of pollutants occurs with distance as the pollutant is mixed in the ever-increasing volume of water. This process is highly complex and main mechanisms involved are advection, diffusion and velocity shear. The mixing of pollutants associated with molecular action and turbulent action is called diffusion while bodily movement of pollutants with the flow velocity is called advection. Two types of diffusion may be identified: molecular diffusion and turbulent diffusion. Molecular diffusion is due to the random motion of the fluid particles and turbulent diffusion is due to the turbulent nature of flow as most stream flows are turbulent in nature. Turbulent diffusion is generally many orders of magnitude larger than molecular diffusion, so that molecular diffusion is generally neglected in the analysis of turbulent flows (Holley 1969, Fisher et al. 1979). Due to non-uniform distribution of velocity, *i.e.*, velocity shear in open channel flows, the pollutant is differentially advected at the local flow velocity downstream, with pollutant in the faster moving water carried downstream earlier than pollutant in the slower moving water.

Figure 1.1 shows general distribution of a tracer concentration resulting from a slug injection. In the tracer transport problems, it is convenient to define three mixing zones; the near-field, mid-field and far-field. In the **near-field** (immediate downstream of the injection site), tracer disperses vertically, transversally and longitudinally as it is advected downstream and it requires the use of full three-dimensional mixing equation for its study. However, if a transverse line source at any depth of flow injects tracer instantaneously or continuously, the mixing is only in longitudinal and vertical directions and a two-dimensional mixing equation is required to describe such a mixing process. The **mid-field** is the region in which vertical concentration gradients are considered to be small. In other words, the complete vertical mixing is assumed to have taken place in the vertical direction within a short distance from the point of tracer injection. This assumption of complete vertical mixing prior to mid-field region is valid because in most of the streams, the aspect ratio (flow width/flow depth) is large, as a result vertical gradients of stream velocity and hence vertical mixing rates are usually higher than the transverse mixing rates. In the mid-field attention can be focussed on transverse and longitudinal changes in the depth-averaged concentration and therefore in this zone, the mixing process is well described by the two-dimensional mixing equation. A photograph showing transverse mixing of pollutants from East Bein in river Sutluj near Nakodar (Punjab) is shown in Fig. 1.2. In the **far-field**, transverse concentration gradients also become insignificant and attention is focussed on the variation in cross-sectionally

averaged concentrations. The primary variation of concentration in the far-field is in longitudinal direction, known as longitudinal dispersion.

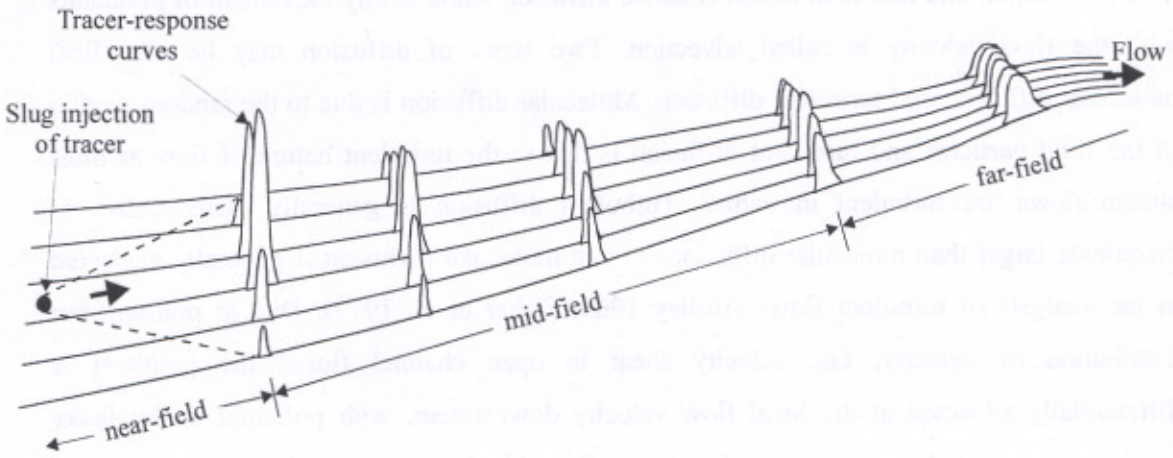

Fig. 1.1 Process of tracer mixing in open channels

In present study, the variation in C-t profiles along the streams due to slug injection of tracer only at an upstream location is studied.

1.3 THE MODELLING APPROACH

The concentration measurement of various pollutants in water bodies such as rivers, lakes, coastal areas etc. is very costly. For this reason, methods are required to be developed to predict the temporal and spatial distribution of pollutants in water bodies. Since, the fate of pollutants is governed by a combination of physical, chemical and biological processes, there is a lot of interest and research in developing improved predictive models for combining all these effects.

The hydrodynamics of pollutant transport in streams is explained by flow continuity equation, flow momentum equation and pollutant continuity equation. The solution of first two equations provides the values in flow domain of the hydraulic parameters like velocity, depth of flow, area of flow etc. These parameters are used for solving the third equation (mass transport equation) for prediction of pollutant concentration. All the above three equations are partial differential equations. Analytical solutions of these equations are

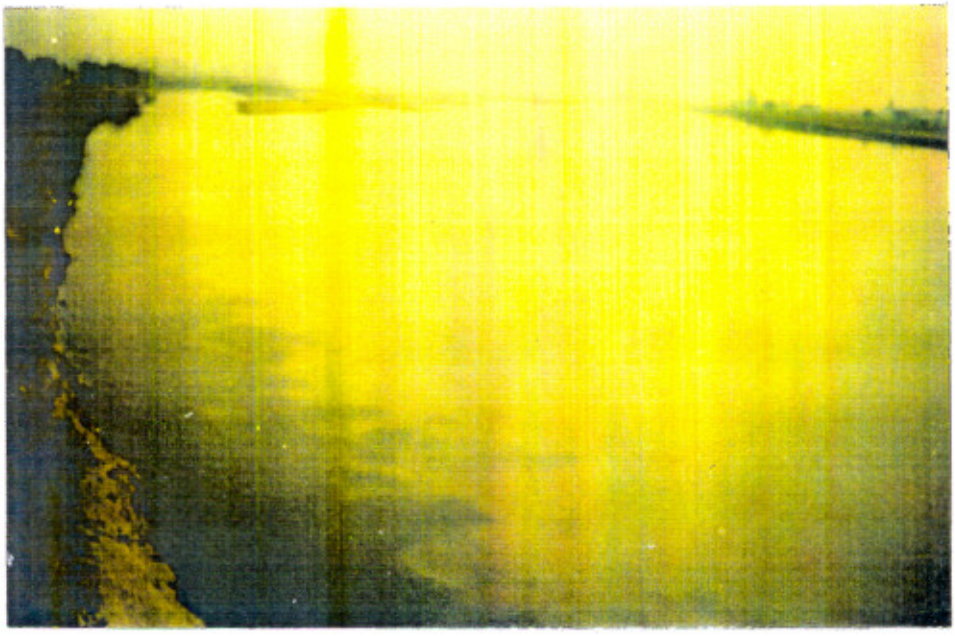

Fig. 1.2 Transverse mixing of pollutants in river Satluj

available only for simplified cases which do not usually occur in practice. The numerical models are mostly versatile and take care of variable coefficients of the governing equation and different boundary conditions. However, accuracy of the numerical model should be critically examined prior to using it for the prediction of pollutant concentration as some numerical models are plagued by numerical diffusion and/or numerical oscillations in the solution, which is sometimes stronger than the physical diffusion rendering the solution useless. The level of numerical diffusion however, depends on the type of numerical scheme used.

1.3.1 Two-Dimensional Mixing Model

A two-dimensional mixing model can be used to analyze vertical mixing of pollutants downstream from a transverse line slug source and to determine both the pollutant concentration profiles and the distance below the source where pollutant is well mixed over the flow depth.

Vertical mixing is not as important in water quality management as is transverse mixing. However, vertical mixing has great importance close to the source. Even though it is limited to near the source, the understanding of vertical mixing is required for knowing the concentration of pollutant in the near-field region. The profiles of pollutant concentration near the end of the near-field region serve the purpose of boundary conditions to the models for simulation of mixing in mid-field and/or far-field. Compared to transverse and longitudinal mixing, the vertical mixing is not studied extensively and only a few studies are available in literature on this topic.

In open channel flows, the principal mechanism causing vertical mixing of a neutrally buoyant tracer is the turbulence generated by velocity shear at the bed. Vertical mixing can be increased locally by secondary currents (notably at sharp bends) and by obstacles in the flow. Experimental studies indicate that in plane shear flows, Prandtl's mixing length hypothesis provides an economical and tolerably accurate model for estimation of the vertical mixing coefficient.

From the principle of mass conservation of pollutants, a three-dimensional mixing equation for concentration of a conservative pollutant at a point in the flow field may be written as (Fischer et al. 1979, James and Helinsky 1984):

$$\frac{\partial \bar{c}}{\partial t} + \bar{u}_x \frac{\partial \bar{c}}{\partial x} + \bar{u}_y \frac{\partial \bar{c}}{\partial y} + \bar{u}_z \frac{\partial \bar{c}}{\partial z} = \frac{\partial}{\partial x}\left(e_x \frac{\partial \bar{c}}{\partial x}\right) + \frac{\partial}{\partial y}\left(e_y \frac{\partial \bar{c}}{\partial y}\right) + \frac{\partial}{\partial z}\left(e_z \frac{\partial \bar{c}}{\partial z}\right) \quad (1.1)$$

where x-, y- and z- are longitudinal, vertical and transverse distances respectively; $\bar{c}$ is the time-averaged concentraion; t is simulation time; $\bar{u}_x, \bar{u}_y$ and $\bar{u}_z$ are time-averaged velocities in the x-, y- and z- directions, respectively; e_x, e_y and e_z are the turbulent diffusion coefficients or eddy diffusivities in the respective directions.

A two-dimensional mixing equation for mixing of pollutant from a transverse line source may be deduced by integrating Eq. (1.1) across the flow width, to yield (Nokes et al. 1984):

$$\frac{\partial C}{\partial t} + \frac{\partial}{\partial x}(U_x C) = \frac{\partial}{\partial x}\left[E_x \frac{\partial C}{\partial x}\right] + \frac{\partial}{\partial y}\left[E_y \frac{\partial C}{\partial y}\right] \quad (1.2)$$

where C = width-averaged concentration; U_x = width-averaged forward velocity; E_x = longitudinal mixing coefficient and E_y = vertical mixing coefficient. For given flow characteristics, the analytical or numerical solution of Eq. (1.2) with the suitable boundary conditions yield concentration of pollutants at different elevations along the depth and in the longitudinal direction, injected through transverse line source. A brief review of literature on studies for two-dimensional mixing in streams due to transverse line source is given below.

1.4 BRIEF REVIEW

Equation (1.2) is the governing equation for two-dimensional mixing of pollutants in streams due to transverse line source. Its solution requires information on channel and flow properties and mixing coefficients E_x and E_y. For given flow characteristics, the analytical solutions of Eq. (1.2) are available in the literature for its simplified form. Holley et al. (1972) and Fischer et al. (1979) made the assumption that longitudinal concentration gradients are small compared with vertical concentration gradients and for this case the prediction of pollutant concentration downstream can be modeled by simplifying Eq. (1.2), to yield:

$$U_x \frac{\partial C}{\partial x} = E_y \frac{\partial^2 C}{\partial y^2} \quad (1.3)$$

For the vertically unbounded flow, an analytical solution of Eq. (1.3) is given by (Rutherford 1994). Method of images was used to obtain the tracer concentration for bounded flow. Nokes et al. (1984) solved Eq. (1.3) for the case of a steady transverse line source by reducing it to a Sturm-Liouville eigen value problem and obtained the solution for different velocity and diffusivity distributions. McNulty and Wood (1984) also developed an algorithm to obtain complete downstream concentration for different velocity and diffusivity distributions for a steady transverse line source. Nokes and Wood (1988) conducted experiments for vertical and lateral mixing from a neutrally buoyant continuous contaminant source in 12 m long, 560 mm wide and 430 mm deep tilting flume of rectangular cross section. Schiller and Sayre (1975) presented a mathematical model based on laboratory flume experiments for predicting vertical distribution of temperatures in open channels. French (1979) presented an accurate and practical method of computing the solute transfer coefficients in stratified channel flows in terms of easily measurable parameters in either the laboratory or the field.

The numerical schemes available for solution of equations similar to Eq. (1.2) can be generally classified into two types: Split operator and the Combined operator approaches. In the Split-operator approach, the advection and diffusion processes are separately computed by using different numerical schemes, whereas in the Combined operator approach the complete mixing process is simulated without separating the two processes. Furthermore, the computation of diffusion can be executed accurately using a variety of finite difference and finite element methods (Morton 1981). However, it is more difficult to devise numerical schemes of sufficient accuracy for solution of advection process (Li 1990; Schohl and Holly 1991). Among the procedures for solving the pure advection equation, several schemes have been proposed, such as Holly and Preissmann two-point fourth order scheme (Holly and Preissmann 1977); Six-point scheme (Komatsu et al. 1985); Improved six-point scheme (Komatsu et al. 1989); Yang-Hsu time-line interpolation scheme (Yang and Hsu 1990); Spatial cubic spline scheme (Schohl and Holly 1991); SOWMAC scheme (Komatsu et al. 1992, Komatsu et al. 1997) and Time line cubic spline scheme (Ahmad and Kothyari 2001). The diffusion process can be accurately computed by several numerical schemes such as Crank-Nicholson central difference scheme; Crank-Nicholson Galerkin finite-element method; alternate-direction implicit (ADI) scheme.

Numerical solution of Eq. (1.2) with derivative boundary conditions is not available in the literature. However, numerical solutions of the varied form of Eq. (1.2) are available in literature such as, Stefanovic and Stefan (2001); Tsai et al. (2002); Guan et al. (2002).

Vertical mixing is one of the few mixing problems where theoretical estimates of the mixing coefficient are available. Prandtl's mixing length hypothesis provides theoretical formulae for vertical mixing coefficient, which is found to vary parabolically with depth. Jobson and Sayre (1970a) however found that predicted pollutant concentration profiles were not very sensitive to the vertical distribution of mixing coefficient and for many practical problems it is sufficiently accurate to use a depth-averaged value. Jobson and Sayre (1970b); Schiller and Sayre (1975); French (1979) and Nokes (1986) based on laboratory studies found that experimental results match with the vertical mixing coefficient computed based on Prandtl's mixing length hypothesis. Little or no information is however, available for the estimation of longitudinal mixing coefficient E_x.

Arora (1983); Samaga et al. (1986); Umeyama and Gerritsen (1992); Ahmad et al. (1999) have studied the velocity distribution in open channels carrying suspended sediment load. They found that these velocity distributions deviate from the velocity distributions in flows without sediment. Dispersion is considered to be significantly affected by the advection process (Holley 1969). Therefore, the dispersion characteristics of flows transporting suspended sediments are expected to be different from those of clear-water flows.

Studies on vertical mixing of pollutants in sediment-laden flows are not available so far. However a few of studies are available for the process of longitudinal dispersion. Singh (1987) performed experiments on 400 mm wide channel for longitudinal dispersion. It was observed that the presence of sediments did not have any noticeable effect on the mixing of pollutant in the range of suspended sediment concentration studied (< 5000 ppm) (Singh et al. 1992). Ahmad et al. (2004) observed that more dispersion occurs in sediment-laden flows than in the corresponding clear-water flows and dispersion increases with an increase in concentration of suspended sediment in the flow. This was attributed to the fact that velocity defect in the vertical increases with an increase in sediment concentration (Lau 1983; Samaga et al. 1986; Umeyama and Gerritsen 1992). Ahmad et al. (2004) proposed a predictor for longitudinal dispersion coefficient for sediment-laden flow.

1.5 OBJECTIVES

The present investigations were taken up keeping in view the gaps in knowledge mentioned above. The broad objectives of the present investigations were to conduct a carefully controlled set of experiments to study in detail the mixing process in clear-water and sediment-laden flows in a laboratory channel due to transverse line source and also propose a numerical model for solution of Eq. (1.2). The specific objectives were:

(i) To conduct a carefully controlled set of experiments on a laboratory flume for collecting data regarding process of vertical mixing in clear-water and sediment-laden flows.

(ii) To propose a mathematical model for the numerical solution of the two-dimensional mixing equation for the prediction of pollutants concentration in streams due to transverse line slug (source).

(iii) Determination of the mixing coefficients using data available in the literature and those data collected through present experimental study for both clear-water and in the presence of suspended sediments.

(iv) To study the sensitivity of the computed C-t profiles at different locations to the variations in the mixing coefficients.

(v) To study the effect of suspended sediment load on the mixing process.

1.6 LIMITATIONS

The laboratory experiments for the present investigation are limited to steady, sub-critical and uniform flows in a rigid rectangular channel. Two sizes of sediments of average diameter 0.064 mm and 0.024 mm with concentrations ranging from 104 ppm to 6178 ppm by weight were used in suspension. The tracer used was conservative, neutrally buoyant for which the solution of Rhodamine WT dye prepared in distilled water was used.

The numerical scheme is developed for computation of pollutants concentrations at downstream sections of the streams due to transverse line slug source only. Due to non-availability of other data, the proposed numerical scheme could only be tested mainly using the data collected during the present experimental study.

Chapter

2

BASIC THEORY AND REVIEW OF LITERATURE

2.1 PRELIMINARY REMARKS

The process of mixing of pollutants in natural streams is highly complex and the mechanisms involved therein have not been understood completely. In general the main mechanisms involved in mixing of pollutants are molecular and turbulent diffusions and velocity shear. The relative contribution of molecular diffusion to the mixing process is considered as negligible. When a slug of the pollutant is injected in the form of line source along width of the stream, the mixing in the near-field zone is two-dimensional with pollutant concentration varying in longitudinal and vertical directions. The present chapter deals with the basic theory and a review of the previous studies on vertical mixing in open channel. Furthermore previous studies on transverse and longitudinal dispersion have been reviewed briefly.

2.2 BASIC THEORY

The basic aim of present study on solute transport is to develop a model for prediction of the concentration of a dispersing material at downstream stations from the place of injection of the pollutants in an open channel. This is best comprehended by way of analysis of the mass-balance equation of the tracer being transported. The mass-balance is expressed by differential equation, which incorporates all the aspects affecting the transport of the pollutant. The transport of pollutant consists of the processes of diffusion and advection. Two types of diffusion are identified: molecular diffusion and turbulent diffusion. Molecular

diffusion is due to the random motion of the fluid particles and the turbulent diffusion is due to turbulent nature of flow. Advection is bodily movement of tracer due to velocity of flow.

2.2.1 Molecular Diffusion

Analysis of molecular diffusion uses the continuum hypothesis and Fick's Law. Molecular diffusion itself is not of great direct consequences in environmental problems except on the microscopic scale of chemical and biological reactions. However, its study is fundamental for understanding the process of dispersion.

If a neutrally buoyant tracer is slowly introduced into a stagnant fluid, it will spread out slowly at the same rate, in all the directions. This spreading is due to the random molecular motion within the fluid, called Brownian motion and the process is termed molecular diffusion. Molecular diffusion is the fundamental process, which causes tracer to diffuse from a region of high concentration to a region of low concentration. According to Fick, the mass of tracer crossing a unit area per unit time (called tracer flux) in a given direction is proportional to the concentration gradient of tracer in that direction (Holley 1969). This is known as Fick's Law. In the x-direction, Fick's Law can be mathematically expressed as (Fischer et al. 1979):

$$J_x = -e_m \frac{\partial c}{\partial x} \tag{2.1}$$

Where x = distance in longitudinal direction; J_x = molecular diffusive flux in the x-direction; c = tracer concentration at a point and e_m = molecular diffusion coefficient. The negative sign in Eq. (2.1) arises because tracer diffuses from a region of higher concentration to a region of lower concentration.

By using the principle of conservation of mass within the control volume, the mass balance equation for the tracer can be written as (Fischer et al. 1979):

$$\frac{\partial c}{\partial t} = -\left[\frac{\partial J_x}{\partial x} + \frac{\partial J_y}{\partial y} + \frac{\partial J_z}{\partial z}\right] \tag{2.2}$$

Where y = distance in vertical direction; z = distance in transverse direction; J_y and J_z are the molecular diffusive fluxes in the y- and z- directions, respectively.

Using Eq. (2.1), one can write (Fischer et al. 1979):

$$\frac{\partial c}{\partial t} = e_m\left(\frac{\partial^2 c}{\partial x^2} + \frac{\partial^2 c}{\partial y^2} + \frac{\partial^2 c}{\partial z^2}\right) \tag{2.3}$$

Equation (2.3) describes the spreading of mass of tracer in a stagnant fluid. The molecular diffusion coefficient e_m is a property of the fluid and for a given temperature, its value is considered to be the same in all directions of flow. The values of e_m for inert tracers in water are in the range of 0.5×10^{-9} m²/s to 2.0×10^{-9} m²/s (Rutherford 1994).

Thus for one-dimension (x-direction) case, Eq. (2.3) can be written as:

$$\frac{\partial c}{\partial t} = e_m \frac{\partial^2 c}{\partial x^2} \tag{2.4}$$

Equation (2.4) is parabolic linear partial different equation and is called one-dimensional Fickian diffusion model. This equation can be used for the computation of molecular diffusion coefficient e_m in terms of variance $\sigma^2(t)$ of spatial variation of tracer concentration as (Fischer 1967; Graf and Altinakar 1998):

$$e_m = \frac{1}{2}\frac{\partial \sigma^2(t)}{\partial t} \tag{2.5}$$

From Eq. (2.5), it is clear that the variance of the spatial distribution of tracer concentration increases linearly with time. It is also a property of diffusion equation that any finite initial distribution eventually decays into a Gaussian distribution (Fischer et al. 1979). In field studies, it is often observed that the variance of observed tracer distribution increases with time at a linear rate (Rutherford 1994).

2.2.2 Advection Process

Advection is a bodily movement of tracer or pollutant cloud resulting from current or velocity of the flow. It is most important in flowing water which carries the tracer downstream away from the source. Pure advection does not cause any change of concentration within a tracer cloud. The amount of tracer transported per unit time per unit area perpendicular to the current is termed as advective flux and is the product of the velocity and the tracer concentration. If u_x is the velocity at a point in the x-direction and c is the concentration at that point, then advective flux in x-direction is $u_x c$.

2.2.3 Advection-Diffusion Equation In Laminar Flow

The spreading of tracer concentration in laminar flow is due to both advection and molecular diffusion processes. It is assumed that transport by these two processes is independent and additive (Rutherford 1994).

The total flux in the x-direction (ϕ_x) is then the sum of advective flux and diffusive flux, *i.e.*,

$$\phi_x = u_x c - e_m \frac{\partial c}{\partial x} \tag{2.6 a}$$

Similarly, the total fluxes in the y- and z- directions can be written as:

$$\phi_y = u_y c - e_m \frac{\partial c}{\partial y} \tag{2.6 b}$$

and

$$\phi_z = u_z c - e_m \frac{\partial c}{\partial z} \tag{2.6 c}$$

Here u_y and u_z are the point velocities in y- and z- directions, respectively.

Substituting Eq. (2.6) in Eq. (2.2) after replacing J_x, J_y and J_z with ϕ_x, ϕ_y and ϕ_z, to yield three-dimensional Fickian advection-diffusion equation in Cartesian co-ordinates as (Graf and Altinakar 1998; Deng et al. 2002):

$$\frac{\partial c}{\partial t} + u_x \frac{\partial c}{\partial x} + u_y \frac{\partial c}{\partial y} + u_z \frac{\partial c}{\partial z} = e_m \left[\frac{\partial^2 c}{\partial x^2} + \frac{\partial^2 c}{\partial y^2} + \frac{\partial^2 c}{\partial z^2} \right] \tag{2.7}$$

Equation (2.7) can be solved to predict the pollutant concentration with time and location if the three-dimensional velocity field, the molecular diffusion coefficient as well as suitable initial and boundary conditions for concentrations are specified (Cunge et al.1980; Rutherford 1994).

2.2.4 Advection-Diffusion Equation In Turbulent Flow

Most rivers and open channels are characterized by high Reynolds number and flow in them is turbulent (Henderson 1967).

Equation (2.7) can be modified to predict the tracer transport in turbulent flow. In turbulent flow, the instantaneous velocities and concentration can be expressed as:

$$u_x = \bar{u}_x + u'_x \tag{2.8a}$$

$$u_y = \bar{u}_y + u'_y \tag{2.8b}$$

$$u_z = \bar{u}_z + u'_z \tag{2.8c}$$

$$c = \bar{c} + c' \tag{2.8d}$$

Here the over bar denotes the time-averaged values of the quantities and prime denotes fluctuations about the time-averaged values.

u'_x, u'_y and u'_z are the velocity fluctuations in the x-, y- and z-directions about the time averaged velocities, respectively; c' is the fluctuation in concentration about $\bar{c}$; $\bar{u}_x$, $\bar{u}_y$ and $\bar{u}_z$ are the time-averaged velocities in the x-, y- and z-directions, respectively and $\bar{c}$ is the time-averaged concentration.

Substituting Eq. (2.8) into Eq. (2.7), to yield (Rutherford 1994; Deng et al. 2002):

$$\frac{\partial \bar{c}}{\partial t} + \bar{u}_x \frac{\partial \bar{c}}{\partial x} + \bar{u}_y \frac{\partial \bar{c}}{\partial y} + \bar{u}_z \frac{\partial \bar{c}}{\partial z} = e_m \left[\frac{\partial^2 \bar{c}}{\partial x^2} + \frac{\partial^2 \bar{c}}{\partial y^2} + \frac{\partial^2 \bar{c}}{\partial z^2} \right] - \left[\frac{\partial (\overline{u'_x c'})}{\partial x} + \frac{\partial (\overline{u'_y c'})}{\partial y} + \frac{\partial (\overline{u'_z c'})}{\partial z} \right] \tag{2.9}$$

The first term of left hand side of Eq. (2.9) represents the rate of change of mean concentration and the next three terms quantify advection of the time-averaged concentration. The first three terms of right hand side quantify molecular diffusion and the remaining terms quantify the additional transport due to turbulent fluctuations, *i.e.*, u'_x, u'_y and u'_z. This additional transport is termed turbulent diffusion or eddy diffusion (Rutherford 1994; Deng et al. 2002).

In natural channels, turbulent diffusion causes tracer to spread far more rapidly than due to only molecular diffusion (Fischer et al. 1979). This does not mean that molecular diffusion plays no part in turbulent mixing. As per Fischer et al. (1979) molecular diffusion is still the fundamental process, which causes tracer to diffuse from a region of high concentration to a region of low concentration. Turbulence has the effect of tearing apart tracer cloud thereby increasing local concentration gradients and accelerating molecular diffusion. It is the combination of turbulent and molecular diffusion which causes rapid tracer mixing in turbulent flow.

Taylor (1921) made a theoretical analysis of the spreading of a tracer cloud in stationary and homogeneous turbulence. He showed that after some time since the injection of the tracer, the variance of the tracer cloud increases linearly with time. In Fickian diffusion model, the

variance of a tracer cloud was also considered to increase linearly with time as discussed in Section 2.2.1. This suggests that turbulent diffusion can also be modeled using Fick's law provided sufficient time has elapsed since tracer injection. By analogy with molecular diffusion, one can write (Holley 1969; Deng et al. 2002):

$$\overline{u'_x c'} = -e_x \frac{\partial \bar{c}}{\partial x} \tag{2.10a}$$

$$\overline{u'_y c'} = -e_y \frac{\partial \bar{c}}{\partial y} \tag{2.10b}$$

$$\overline{u'_z c'} = -e_z \frac{\partial \bar{c}}{\partial z} \tag{2.10c}$$

Here e_x, e_y and e_z are turbulent diffusion coefficients or eddy diffusivities in the respective directions. The turbulent diffusion coefficients are the property of the flow and vary with the velocity, turbulence and geometry of the flow. The eddy diffusivities are of the order of 10^{-3} m^2/s which are many order of magnitude larger than molecular diffusivity (10^{-9} m^2/s), so that molecular diffusion is generally neglected in the analysis of turbulent flows (Holley 1969; Fischer et al. 1979). Assuming e_x, e_y and e_z are not functions of spatial coordinates (homogeneous turbulence), substitution of Eq. (2.10) into Eq. (2.9) yields (Deng et al. 2002):

$$\begin{aligned} &\frac{\partial \bar{c}}{\partial t} + \bar{u}_x \frac{\partial \bar{c}}{\partial x} + \bar{u}_y \frac{\partial \bar{c}}{\partial y} + \bar{u}_z \frac{\partial \bar{c}}{\partial z} \\ &= (e_m + e_x)\frac{\partial^2 \bar{c}}{\partial x^2} + (e_m + e_y)\frac{\partial^2 \bar{c}}{\partial y^2} + (e_m + e_z)\frac{\partial^2 \bar{c}}{\partial z^2} \end{aligned} \tag{2.11}$$

Rewriting Eq. (2.11) with assumption that the molecular diffusion is very small as compared to turbulent diffusion coefficients and turbulence is non-homogenous, one gets (Fischer et al. 1979; James 1984):

$$\begin{aligned} &\frac{\partial c}{\partial t} + u_x \frac{\partial c}{\partial x} + u_y \frac{\partial c}{\partial y} + u_z \frac{\partial c}{\partial z} \\ &= \frac{\partial}{\partial x}\left(e_x \frac{\partial c}{\partial x}\right) + \frac{\partial}{\partial y}\left(e_y \frac{\partial c}{\partial y}\right) + \frac{\partial}{\partial z}\left(e_z \frac{\partial c}{\partial z}\right) \end{aligned} \tag{2.12}$$

The over bars are removed for clarity from Eq. (2.12). Equation (2.12) is the three-dimensional mass balance equation of tracer transport in turbulent flow and is known as advection-diffusion equation. Equation (2.12) is widely used for solving practical mixing problems. However, this equation cannot be solved either analytically or numerically unless

the three-dimensional velocity field and the mixing coefficients are known a priori. In practical mixing problems, some of the terms in Eq. (2.12) can be negligibly small and hence can be dropped. For example for instantaneous transverse line source, in the near-field zone, the mixing is in x- and y- directions. After complete mixing in the vertical direction, the mixing is in x-direction only. However for instantaneous vertical line source, the mixing is in x- and z- directions. Equation (2.12) can be integrated over depth/width and area to yield simplified mixing equations.

2.3 WIDTH AVERAGING OF ADVECTION-DIFFUSION EQUATION

A derivation for depth-averaged advection-diffusion is available in literature (Rutherford 1994; Deng et al. 2002). Following similar approach, the width-averaged advection-diffusion equation is derived herein.

If the pollutant is instantaneously injected as a transverse line source, then the concentration gradients in the transverse directions are relatively small and the mixing takes place dominantly in the vertical and longitudinal directions only. For solving these types of tracer transport problems, width averaging of advection-diffusion equation is required. Therefore, Eq. (2.12) can be integrated from the left bank of the channel, *i.e.*, $z = z_1(x, y)$ to the right bank of the channel, $z = z_2(x, y)$. Extensive use is made of Leibnitz's rule in this exercise (Rutherford 1994).

$$\int_{z_1}^{z_2} \frac{\partial}{\partial x}\varphi(x,z)dy = \frac{\partial}{\partial x}\int_{z_1}^{z_2}\varphi(x,z)dz - \varphi(x,z_2)\frac{\partial z_2}{\partial x} + \varphi(x,z_1)\frac{\partial z_1}{\partial x} \tag{2.13}$$

Integrating Eq. (2.12) term by term leads to:

$$\int_{z_1}^{z_2}\frac{\partial c}{\partial t}dz + \frac{\partial}{\partial x}\int_{z_1}^{z_2}u_x c dz - (u_x c)_{z_2}\frac{\partial z_2}{\partial x} + (u_x c)_{z_1}\frac{\partial z_1}{\partial x} + \frac{\partial}{\partial y}\int_{z_1}^{z_2}u_y c dz - (u_y c)_{z_2}\frac{\partial z_2}{\partial y} + (u_y c)_{z_1}\frac{\partial z_1}{\partial y}$$

$$+ (u_z c)_{z_2} - (u_z c)_{z_1}$$

$$= \frac{\partial}{\partial x}\int_{z_1}^{z_2} e_x\frac{\partial c}{\partial x}dz - \left(e_x\frac{\partial c}{\partial x}\right)_{z_2}\frac{\partial z_2}{\partial x} + \left(e_x\frac{\partial c}{\partial x}\right)_{z_1}\frac{\partial z_1}{\partial x} + \frac{\partial}{\partial y}\int_{z_1}^{z_2} e_y\frac{\partial c}{\partial y}dz - \left(e_y\frac{\partial c}{\partial y}\right)_{z_2}\frac{\partial z_2}{\partial y} + \left(e_y\frac{\partial c}{\partial y}\right)_{z_1}\frac{\partial z_1}{\partial y}$$

$$+ \left(e_z\frac{\partial c}{\partial z}\right)_{z_2} - \left(e_z\frac{\partial c}{\partial z}\right)_{z_1} \tag{2.14}$$

Rearranging Eq. (2.14) gives

$$\int_{z_1}^{z_2} \frac{\partial c}{\partial t} dz + \frac{\partial}{\partial x} \int_{z_1}^{z_2} u_x c \, dz + \frac{\partial}{\partial y} \int_{z_1}^{z_2} u_y c \, dz$$

$$= \frac{\partial}{\partial x} \int_{z_1}^{z_2} e_x \frac{\partial c}{\partial x} dz + \frac{\partial}{\partial y} \int_{z_1}^{z_2} e_y \frac{\partial c}{\partial y} dz + \left[c \left(u_x \frac{\partial z_2}{\partial x} + u_y \frac{\partial z_2}{\partial y} - u_z \right) \right]_{z_2} - \left[c \left(u_x \frac{\partial z_1}{\partial x} + u_y \frac{\partial z_1}{\partial y} - u_z \right) \right]_{z_1}$$

$$- \left(e_x \frac{\partial c}{\partial x} \frac{\partial z_2}{\partial x} + e_y \frac{\partial c}{\partial y} \frac{\partial z_2}{\partial y} - e_z \frac{\partial c}{\partial z} \right)_{z_2} + \left(e_x \frac{\partial c}{\partial x} \frac{\partial z_1}{\partial x} + e_y \frac{\partial c}{\partial y} \frac{\partial z_1}{\partial y} - e_z \frac{\partial c}{\partial z} \right)_{z_1} \quad (2.15)$$

The boundary conditions are that at both the banks of the channel, the fluxes of water and tracer normal to the boundaries are zero. With the use of these boundary conditions, all the right hand terms of Eq. (2.15) except first two terms are reduced to zero (Rutherford 1994).

Equation (2.15) reduces to:

$$\frac{\partial}{\partial t}\left(b\bar{c}\right) + \frac{\partial}{\partial x}\left(b\overline{u_x c}\right) + \frac{\partial}{\partial y}\left(b\overline{u_y c}\right) = \frac{\partial}{\partial x}\left(b\overline{e_x \frac{\partial c}{\partial x}}\right) + \frac{\partial}{\partial y}\left(b\overline{e_y \frac{\partial c}{\partial y}}\right) \quad (2.16)$$

Where the over bar denotes width-averaged values and b = width of the channel.

The velocities and concentrations can be expressed as the sum of a width-averaged and a width deviation, *i.e.*,

$$u_x = U_x + U'_x \quad (2.17a)$$

$$u_y = U_y + U'_y \quad (2.17b)$$

$$c = C + C' \quad (2.17c)$$

Where U_x, U_y and C are the width-averaged velocities and concentration, respectively. U'_x, U'_y and C′ are the deviations of u_x, u_y and c about U_x, U_y and C, respectively.

$$\text{Also } U_x = \frac{1}{b} \int_{z_1}^{z_2} u_x dz \quad (2.18a)$$

$$U_y = \frac{1}{b} \int_{z_1}^{z_2} u_y dz \quad (2.18b)$$

$$C = \frac{1}{b}\int_{z_1}^{z_2} c\,dz \tag{2.18c}$$

$$\overline{u_x c} = \overline{(U_x + U'_x)(C + C')} = U_x C + \overline{U'_x C'} \tag{2.19a}$$

The width-averaged of the deviations U'_x, U'_y and C' are zero.

If e_x and e_y do not vary with width, then

$$\overline{e_x \frac{\partial c}{\partial x}} = e_x \frac{\partial C}{\partial x} \tag{2.19b}$$

$$\overline{e_y \frac{\partial c}{\partial y}} = e_y \frac{\partial C}{\partial y} \tag{2.19c}$$

Substituting these in Eq. (2.16) yields (Rutherford 1994):

$$\frac{\partial}{\partial t}(bC) + \frac{\partial}{\partial x}(bU_x C) + \frac{\partial}{\partial y}(bU_y C) = \frac{\partial}{\partial x}\left(-b\overline{U'_x C'} + be_x \frac{\partial C}{\partial x}\right) + \frac{\partial}{\partial y}\left(-b\overline{U'_y C'} + be_y \frac{\partial C}{\partial y}\right) \tag{2.20}$$

By applying Taylor's analysis (Taylor 1953, 1954), it is shown that at asymptotically large times, the longitudinal diffusive flux is proportional to the longitudinal gradient of the width-averaged concentration. Thus

$$-\overline{U'_x C'} = E_x \frac{\partial C}{\partial x} \tag{2.21}$$

Where E_x is the longitudinal mixing coefficient, which accounts for variations in the longitudinal velocity across the width.

By analogy with Eq. (2.21), the vertical diffusive flux is written as:

$$-\overline{U'_y C'} = E_y \frac{\partial C}{\partial y} \tag{2.22}$$

Where E_y is the vertical mixing coefficient which accounts for the effects on the width-averaged concentration of width variations in the vertical velocity.

Substituting Eqs. (2.21) and (2.22) into Eq. (2.20) yields:

$$\frac{\partial}{\partial t}(bC) + \frac{\partial}{\partial x}(bU_x C) + \frac{\partial}{\partial y}(bU_y C) = \frac{\partial}{\partial x}\left[b(E_x + e_x)\frac{\partial C}{\partial x}\right] + \frac{\partial}{\partial y}\left[b(E_y + e_y)\frac{\partial C}{\partial y}\right] \tag{2.23}$$

For the flow in the predominant x-direction ($U_y = 0$), Eq. (2.23) reduces to:

$$\frac{\partial}{\partial t}(bC)+\frac{\partial}{\partial x}(bU_x C)=\frac{\partial}{\partial x}\left[b(E_x+e_x)\frac{\partial C}{\partial x}\right]+\frac{\partial}{\partial y}\left[b(E_y+e_y)\frac{\partial C}{\partial y}\right] \qquad (2.24)$$

In Eq. (2.24) even though the average motion is in x-direction, it will transport the tracer in the other direction also (Young and Wallis 1993). Equation (2.24) is the two-dimensional width-averaged advection-diffusion equation and can be used to solve tracer transport problems in streams due to instantaneous transverse line source.

2.4 DEPTH AVERAGING OF ADVECTION-DIFFUSION EQUATION

In most rivers, vertical mixing is completed within a distance 50 times the river depths or 1 to 10 times the river width (Rutherford 1994). For mixing in mid-field zone, Eq. (2.12) can be integrated over the depth of flow to predict the transverse and longitudinal changes of the depth-averaged concentration.

Integrating Eq. (2.12) from the bed to the surface and making use of the boundary condition that at both the water surface and the river bed, the fluxes of water and tracer normal to the boundaries are zero, to yield (Rutherford 1994; Deng et al. 2002):

$$\frac{\partial}{\partial t}\left(d\bar{c}\right)+\frac{\partial}{\partial x}\left(d\overline{\overline{u_x c}}\right)+\frac{\partial}{\partial z}\left(d\overline{\overline{u_z c}}\right)=\frac{\partial}{\partial x}\left(de_x\overline{\overline{\frac{\partial c}{\partial x}}}\right)+\frac{\partial}{\partial z}\left(de_z\overline{\overline{\frac{\partial c}{\partial z}}}\right) \qquad (2.25)$$

Where the double over bar denotes the depth-averaged values and d = local depth of flow.

The velocities and concentrations can be expressed as the sum of a depth-averaged and a vertical deviation, *i.e.*,

$$u_x = v_x + v'_x \qquad (2.26a)$$

$$u_z = v_z + v'_z \qquad (2.26b)$$

$$c = s + s' \qquad (2.26c)$$

Where v_x and v_z are the depth-averaged velocities and s is the depth-averaged concentration; v'_x, v'_z are the deviation of u_x and u_z about v_x and v_z respectively and s' is the deviation of c about s.

Making these substitutions into Eq. (2.25) and assuming that e_x and e_z do not vary with depth, one can get:

$$\frac{\partial}{\partial t}(ds)+\frac{\partial}{\partial x}(dv_x s)+\frac{\partial}{\partial z}(dv_z s)=\frac{\partial}{\partial x}\left(-d\overline{\overline{v'_x s'}}+de_x\frac{\partial s}{\partial x}\right)+\frac{\partial}{\partial z}\left(-d\overline{\overline{v'_z s'}}+de_z\frac{\partial s}{\partial z}\right) \quad (2.27)$$

The terms $-\overline{\overline{v'_x s'}}$ and $-\overline{\overline{v'_z s'}}$ quantify the additional transport due to non-uniformities of velocity and concentration over the depth, and is termed dispersion. It is to be noted that dispersion is not a fundamental physical process but arises due to averaging (Rutherford 1994). It is not possible to solve Eq. (2.27) until the dispersive fluxes are related to some property of the depth-averaged concentration. Using Taylor's (1954) asymptotic analysis of shear dispersion in a pipe flow, one can write:

$$-\overline{\overline{v'_x s'}}=E'_x\frac{\partial s}{\partial x} \quad (2.28)$$

Where E'_x is the mixing coefficient in the x-direction which accounts for the variations in the longitudinal velocity over the depth.

By analogy with Eq. (2.28), the transverse dispersive flux can be written as:

$$-\overline{\overline{v'_z s'}}=E_z\frac{\partial s}{\partial z} \quad (2.29)$$

Where E_z is the transverse mixing coefficient which accounts for the vertical variations of transverse velocity.

Substituting Eqs. (2.28) and (2.29) into Eq. (2.27) yields (Rutherford 1994):

$$\frac{\partial}{\partial t}(ds)+\frac{\partial}{\partial x}(dv_x s)+\frac{\partial}{\partial z}(dv_z s)=\frac{\partial}{\partial x}\left[d(E'_x+e_x)\frac{\partial s}{\partial x}\right]+\frac{\partial}{\partial z}\left[d(E_z+e_z)\frac{\partial s}{\partial z}\right] \quad (2.30)$$

Equation (2.30) is the two-dimensional depth-averaged advection-diffusion equation and is extensively used to solve pollutants transport problems in the mid-field zone (transverse mixing).

2.5 CROSS-SECTION AVERAGING OF ADVECTION-DIFFUSION EQUATION

At considerable distance downstream from the site of injection of tracer, the tracer mixes uniformly across the channel cross-section and the primary variation of the concentration is

only in the longitudinal direction and mixing beyond this section is called longitudinal dispersion.

The time required from the instant of injection to the complete cross-sectional mixing is called 'mixing time or initial time' and the distance travelled during this time is called 'mixing length'. The value of mixing length depends on the nature of the tracer injection e.g. impulsive/continuous injection as well as the geometry of the source e.g. point/line/plane injection in addition to flow and channel characteristics. Longitudinal dispersion arises because vertical and transverse velocity shear carry the pollutants downstream more slowly near the bed and the banks than in mid-channel. Fischer (1967) showed that in river channels transverse velocity shear makes a greater contribution to longitudinal dispersion than vertical velocity shear. Turbulent diffusion causes localized spreading both along and across the channel. Turbulent diffusion counteracts the effects of velocity shear. The rate of longitudinal dispersion reflects the balance between velocity shear, which acts to spread tracer along the channel and transverse mixing, which promotes uniform concentrations and hence counteracts the effects of velocity shear.

Longitudinal dispersion is of interest only when the input tracer is unsteady (e.g. slug injection) as for a steady source; the fully mixed concentration of a conservative tracer is constant. Beltaos (1980) and El-Hadi et al. (1984) categorically stated that the longitudinal dispersion is not likely to be encountered in large streams within length of practical interest.

The governing equation of longitudinal dispersion can be obtained by integrating Eq. (2.30) across the channel and making use of the boundary conditions that at both the banks of the channel, the fluxes of water and tracer normal to the boundaries are zero (neglecting the contribution of turbulent diffusion coefficient and considering unidirectional flow), to yield (Rutherford 1994):

$$\frac{\partial}{\partial t}\left(A\bar{s}\right)+\frac{\partial}{\partial x}\left(A\overline{v_x s}\right)=\frac{\partial}{\partial x}\left(A(\overline{E'_x})\frac{\partial s}{\partial x}\right) \tag{2.31}$$

Where the over bar denotes a cross-sectional averaged and A = cross-sectional area of flow.

The depth-averaged velocity and concentration can be expressed as the sum of cross-sectional averaged and a cross-sectional deviation.

$$v_x = V_x + V'_x \tag{2.32a}$$

$$s = S + S' \tag{2.32b}$$

Where V_x and S are the cross-sectional averaged velocities and concentration, respectively; V_x' and S′ are the deviations of v_x and s about V_x and S, respectively.

Substituting Eq. (2.32) into Eq. (2.31) yields:

$$\frac{\partial}{\partial t}(AS)+\frac{\partial}{\partial x}(AV_xS)=\frac{\partial}{\partial x}\left[-A\overline{V_x'S'}+AE_x'\frac{\partial S}{\partial x}\right] \tag{2.33}$$

By analogy to Eq. (2.10), one can write

$$-\overline{V_x'S'}=E_L\frac{\partial S}{\partial x} \tag{2.34}$$

Where E_L is known as longitudinal dispersion coefficient which accounts for variation of longitudinal velocity over the channel cross-section.

Substituting Eq. (2.34) into Eq. (2.33) and replacing (E_L+E_x') by E_L, which incorporates E_x', to yield (Fischer et al. 1979; Deng et al. 2002):

$$\frac{\partial}{\partial t}(AS)+\frac{\partial}{\partial x}(AV_xS)=\frac{\partial}{\partial x}\left(AE_L\frac{\partial S}{\partial x}\right) \tag{2.35}$$

Here V_x is the cross-sectional averaged velocity and S is the cross-sectional averaged concentration. Equation (2.35) is called one-dimensional advection-dispersion equation and is used for study mixing process in the far-field zone.

2.6 TWO-DIMENSIONAL MIXING DUE TO TRANSVERSE LINE SOURCE (VERTICAL MIXING)

The three-dimensional advection-diffusion equation, *i.e.*, Eq. (2.12) is the basis of analysing mixing problems in rivers. But the solution of such equation requires detailed information on channel and flow properties and mixing coefficients, which cannot be gathered conveniently during field experiments in natural channels. For instantaneous horizontal line source, the mixing of pollutants is in longitudinal and vertical directions only, and Eq. (2.24) can be solved for predicting the pollutants concentrations changes.

In open channels, the principle mechanism causing the vertical mixing of a neutrally buoyant tracer is the turbulence generated by vertical velocity shear which arises as a result of bed friction. As a result the tracer becomes vertically well mixed within a short distance from the site of injection. Vertical mixing is completed with in a distance 50 times the river depths or

1-10 times the river width (Rutherford 1994). Vertical mixing is increased locally due to secondary currents and obstacles in the flow.

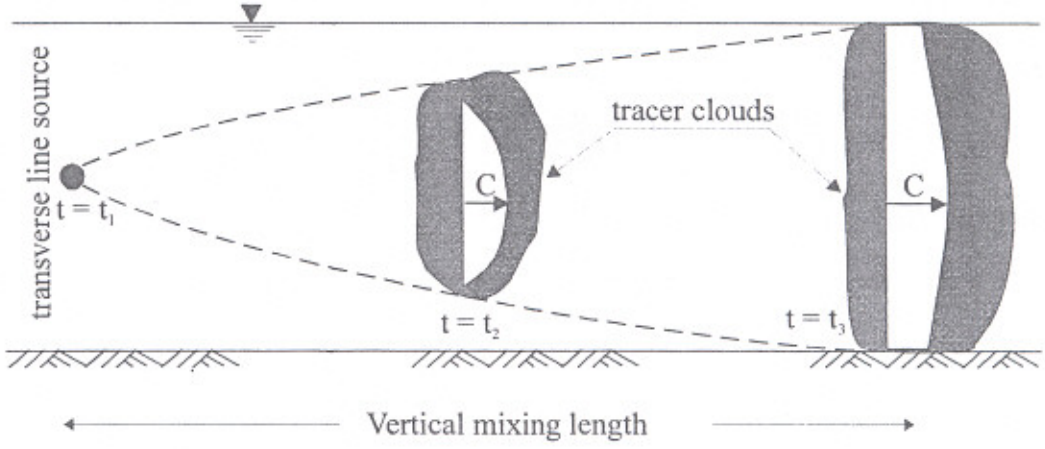

Fig. 2.1 Vertical mixing in plane shear flow

Figure 2.1 shows vertical mixing of a transverse unsteady line source (perpendicular to the plane of figure) located at mid-depth in a plane shear flow. At $t = t_1$ the tracer is concentrated to a line, however, it disperses in vertical direction as it moves in the downstream from the injection site, (it also disperses in longitudinal direction as well). The position of clouds are shown at $t = t_2$ and t_3. At $t = t_2$, the tracer has not mixed uniformly over the depth, however, at $t = t_3$, tracer has mixed completely in the vertical direction. The distance requires for complete vertical mixing is known as vertical mixing distance. In addition to flow characteristics, the vertical mixing distance also depends upon geometry and location of the source.

By combining turbulent diffusion and dispersion coefficients, the width-averaged Eq. (2.24) can be written as (Nokes et al. 1984):

$$\frac{\partial}{\partial t}(bC)+\frac{\partial}{\partial x}(bU_x C)=\frac{\partial}{\partial x}\left[bE_x\frac{\partial C}{\partial x}\right]+\frac{\partial}{\partial y}\left[bE_y\frac{\partial C}{\partial y}\right] \tag{2.36}$$

Longitudinal mixing coefficient plays important role for unsteady source only. Predictor for computation of longitudinal mixing coefficient is not available in the literature. For steady source, the time derivative of concentration is negligible and hence can be dropped from Eq. (2.36) and may be written as (Holley et al.1972; Fischer et al. 1979):

$$\frac{\partial}{\partial x}(bU_x C) = \frac{\partial}{\partial y}\left[bE_y \frac{\partial C}{\partial y}\right] \tag{2.37}$$

In Eq. (2.37), the rate of vertical mixing is determined by vertical mixing coefficient.

2.6.1 Vertical Mixing Coefficient

Vertical mixing in plane shear flow is one of the few river-mixing problems for which the vertical mixing coefficient E_y can be predicted satisfactorily on theoretical grounds. Prandtl's mixing length hypothesis provides an economical and tolerably accurate model for estimating the vertical variation of velocity and vertical mixing coefficient in plane shear flow.

By analogy with the coefficient of viscosity in laminar flow, Reynolds stress in turbulent flow as given by Boussinesq can be written as:

$$\tau_t = \rho \nu_t \frac{\partial u_x}{\partial y} \tag{2.38}$$

Where τ_t = turbulent shear stress, ν_t = apparent kinematic viscosity or eddy viscosity which is much greater than the corresponding kinematic viscosity for laminar flow and ρ is the mass density of water.

The logarithmic velocity distribution in turbulent flow in open channels can be expressed as (Ranga Raju 1993):

$$\frac{u_x}{U_*} = \frac{1}{\kappa} \log\left(\frac{y}{y_1}\right) \tag{2.39}$$

Where U_* = shear velocity, κ = von-Karman's constant and y_1 = arbitrary vertical distance from bottom at which time-averaged velocity is zero.

Reynolds analogy states that

$$E_y = \nu_t \tag{2.40}$$

Experimental studies show that Eq. (2.40) holds within 5-10 % for dilute solution of neutrally buoyant tracers in shear flows (Rutherford 1994).

In plane turbulent shear flow, the shear stress varies linearly with depth and vanishes at the surface (French 1986; Rutherford 1994), so

$$\tau_t = \tau_o\left(1 - \frac{y}{d}\right) \tag{2.41}$$

Where τ_o = bed shear stress

From Eqs. (2.38), (2.40) and (2.41), one can get:

$$E_y = \left[\tau_o\left(1 - \frac{y}{d}\right) \Big/ \left(\rho \frac{\partial u_x}{\partial y}\right)\right] \tag{2.42}$$

Substituting Eq (2.39) into Eq. (2.42) yields (Elder 1959; Rutherford 1994;Garde and Ranga Raju 2000):

$$E_y = \kappa U_* y\left(1 - \frac{y}{d}\right) \tag{2.43}$$

Thus the vertical mixing coefficient varies parabolically with depth, vanishing at both the bed and water surfaces. Jobson and Sayre (1970a) found that predicted concentration profiles were not very sensitive to the vertical distribution of E_y and for many practical problems it is sufficiently accurate to use the depth-averaged value of E_y, *i.e.*,

$$\bar{E}_y = \frac{1}{d}\int_0^d E_y \, dy \tag{2.44}$$

$$\bar{E}_y = \frac{\kappa}{6} d U_* = 0.067 \, d U_* \, ; \kappa = 0.4. \tag{2.45}$$

Over bar is dropped here onward from vertical mixing coefficient for simplicity. Experimental results from several laboratory studies match closely to Eq. (2.45) (Jobson and Sayre 1970b; Schiller and Sayre 1975; French 1979 and Nokes 1986) and are shown in Table 2.1.

Generally, velocity profiles in open channels are approximately logarithmic and in such cases Eq. (2.44) can be expected to provide reasonable estimates of the vertical mixing coefficient. In some parts of the channel due to existence of secondary currents, velocity profiles depart from logarithmic variation. Thus the estimates would be not so good.

2.6.2 Solutions Of Vertical Mixing Equation

Computation of concentration at the downstream stations due to transverse line source requires either analytical or numerical solution of Eq. (2.36). Analytical solutions are not

Table 2.1: Vertical Mixing Coefficient

Width b (m)	Depth d (m)	Velocity u_x (m/s)	Shear velocity U_* (m/s)	$\frac{E_y}{dU_*}$	Reference
Laboratory Channels Unstratified flow					
2.44	0.4	---	0.049-0.136	0.063	Jobson and Sayre (1970b)
0.76	0.071	0.046	0.04	0.042	Schiller and Sayre (1975)
0.56	0.039-0.076	---	0.041-0.058	0.067	McNulty (1983)
0.56	0.05-0.065	0.034-0.028	0.024-0.016	0.067	Nokes (1986)
Stratified flow					
0.76	0.071	0.031	0.0037	0.004	Schiller and Sayre (1975)
0.040	0.037	0.04	0.0690	0.004	French (1979)

flexible enough to handle the complex mixing of transport problems. Numerical models are flexible but they suffer from numerical dispersion errors. In addition, analytical solutions to the equation exist only for some particular simplified flows and tracer injection configuration but for most practical situations only numerical methods are used.

Analytical or numerical solutions of Eq. (2.36) are available in the literature for its simplified forms. Some of these are described herein.

2.6.2.1 Analytical solutions

The analytical solutions are simple to evaluate and can also be used to validate numerical models. Some of these are discussed as:

(a) ***Steady transverse line source*****:** Holley et al. (1972) and Fischer et al. (1979) assumed that longitudinal concentration gradients are small compared with vertical concentration gradients. Under this assumption, the prediction of pollutant concentration downstream can be modeled by Eq. (2.37). For the source location at $x = 0$ and $y = y_o$ from the bed of the channel, analytical solution of Eq. (2.37) for constant velocity and vertical mixing coefficient in a vertically unbounded flow is given as:

$$C(x,y)=\frac{\dot{M}}{d\sqrt{4\pi E_y x U_x}}\exp\left[\frac{-U_x(y-y_0)^2}{4E_y x}\right] \tag{2.46}$$

Where $\dot{M}$ = tracer mass inflow rate

For the bounded flow, the method of images can be used to obtain the tracer concentration. The method of images is based on the principle of superposition which states that if an equation and its boundary conditions are linear, then it is possible to superimpose any number of individual solutions of the equation to obtain the desired solution.

The boundary conditions for Eq. (2.37) are that the tracer flux is zero at the bed and the water surface, *i.e.*,

$$\frac{\partial C}{\partial y}=0;\ \text{at } y=0 \text{ and } y=d \tag{2.47}$$

With these boundary conditions, the bounded solution of Eq. (2.45) is:

$$C(x,y)=C(x,y+y_o)+C(x,y-y_o)+\sum_{k=1}^{N_1}\begin{bmatrix}C(x,2kd-y-y_o)+C(x,2kd+y+y_o)\\+C(x,2kd-y+y_o)+C(x,2kd+y-y_o)\end{bmatrix} \tag{2.48}$$

In practice it is only necessary to evaluate the summation as far as $N_1 = 6$ throughout most of the near-field zone, but larger value of N_1 are required once the tracer becomes well mixed vertically.

Concentration profile for a real source at height $y = y_o$ is shown in Fig. 2.2. It is clear from the figure that vertical concentration gradient is not zero at y = 0. To make it zero, an imaginary source is required at $y=-y_o$. The resulting tracer concentration is the sum of concentrations due to real and imaginary sources as shown in Fig. 2.2.

However if the transverse source is spread over a depth from y_1 to y_2, the solution of Eq. (2.37) can be obtained following the analogy with the solution of transverse mixing equation by Yotsukura and Cobb (1972). For constant U_x and E_y, Eq. (2.37) may be written as:

$$\frac{\partial C}{\partial x}=\frac{E_y}{U_x}\frac{\partial^2 C}{\partial y^2} \tag{2.49}$$

Solution of Eq. (2.49) for boundary conditions of Eq. (2.47) for transverse source spread over the depth from y_1 to y_2 is (Lipsett and Beltaos 1978):

$$\frac{C}{S}=\frac{1}{2(\eta_2-\eta_1)}\left[\begin{array}{l}\frac{1}{2}\left\{\operatorname{erf}\left(\frac{\eta_2+\eta}{\sqrt{2\varsigma}}\right)+\operatorname{erf}\left(\frac{\eta_2-\eta}{\sqrt{2\varsigma}}\right)-\operatorname{erf}\left(\frac{\eta_1+\eta}{\sqrt{2\varsigma}}\right)-\operatorname{erf}\left(\frac{\eta_1-\eta}{\sqrt{2\varsigma}}\right)\right\}+\\ \sum_{k=1}^{\infty}\left\{\begin{array}{l}\operatorname{erf}\left(\frac{\eta_2+2k-\eta}{\sqrt{2\varsigma}}\right)+\operatorname{erf}\left(\frac{\eta_2-2k-\eta}{\sqrt{2\varsigma}}\right)-\operatorname{erf}\left(\frac{\eta_1+2k-\eta}{\sqrt{2\varsigma}}\right)\\ -\operatorname{erf}\left(\frac{\eta_1-2k-\eta}{\sqrt{2\varsigma}}\right)+\operatorname{erf}\left(\frac{\eta_2+2k+\eta}{\sqrt{2\varsigma}}\right)+\operatorname{erf}\left(\frac{\eta_2-2k+\eta}{\sqrt{2\varsigma}}\right)\\ -\operatorname{erf}\left(\frac{\eta_1+2k+\eta}{\sqrt{2\varsigma}}\right)-\operatorname{erf}\left(\frac{\eta_1-2k+\eta}{\sqrt{2\varsigma}}\right)\end{array}\right\}\end{array}\right] \quad (2.50)$$

Where S = cross-sectional averaged concentration of pollutants; $\eta=\frac{y}{d}$; $\eta_1=\frac{y_1}{d}$; $\eta_2=\frac{y_2}{d}$;

$\varsigma=\frac{2E_y x}{U_x d^2}$ and erf denotes error function.

Nokes et al. (1984) variable-coefficient model

Nokes et al. (1984) solved Eq. (2.37) by reducing it to a Sturm-Liouville eigen value problem and obtained the solution for any velocity and diffusivity distributions. They derived eigen functions and eigen values for a logarithmic velocity and parabolic diffusivity distributions by using power series solution technique and compared the solution with Holley et al. (1972), obtained for a uniform velocity and diffusivity distribution. Equation (2.37) may be written as:

$$U_x\frac{\partial C}{\partial x}=\frac{\partial}{\partial y}\left[E_y\frac{\partial C}{\partial y}\right] \quad (2.51)$$

With boundary conditions, *i.e.*, Eq. (2.47), Eqs. (2.45) and (2.51) can be non-dimensionalized by the following transformations:

$$x^*=\frac{x}{d}\;;\;\; y^*=\frac{y}{d}\;;U_x=v_x\chi(y)\;\;;E_y=U_*d\psi(y) \quad (2.52)$$

Here x^* is non-dimensional longitudinal distance; y^* is non-dimensional vertical distance; $\chi(y)$ is non-dimensional velocity and $\psi(y)$ is non-dimensional vertical diffusivity.

Rewriting Eqs. (2.47) and (2.51), the resulting advection-diffusion equation becomes (dropping the primes for clarity):

$$\left(\frac{8}{f_1}\right)^{\frac{1}{2}}\chi(y)\frac{\partial C}{\partial x}=\frac{\partial}{\partial y}\left\{\psi(y)\frac{\partial C}{\partial y}\right\} \tag{2.53}$$

With $$\psi(y)\frac{\partial C}{\partial y}=0 \quad \text{at} \quad y=0,1 \tag{2.54}$$

Here $f_1=8\left(\frac{U_*}{U_x}\right)^2$, is the friction factor.

Equation (2.51) may be transformed into two ordinary differential equations by assuming a separated solution of the form:

$$C(x,y)=G(x)H(y) \tag{2.55}$$

The functions G(x) and H(y) satisfy the equations:

$$\frac{dG}{dx}+\frac{1}{8}f_1\gamma G=0 \tag{2.56}$$

and $$\frac{d}{dy}\left[\psi(y)\frac{dH}{dy}\right]+\gamma\chi(y)H=0 \tag{2.57}$$

Where γ is constant of separation.

Equation (2.56) has the solution

$$G(x)=K\exp\left[-\frac{1}{8}f_1\gamma x\right] \tag{2.58}$$

Where K is a constant.

Equation (2.57) together with separated form of Eq. (2.54), *i.e.*, $\psi(y)\frac{dH}{dy}=0 \quad \text{at} \quad y=0,1$ constitutes an eigen value problem governed by Sturm-Liouville theory. Nokes et al. (1984) stated that the eigen values of this problem are real, discrete and non-degenerate and that the eigen functions are mutually orthogonal with respect to the weighing function $\chi(y)$ over the interval $0\le y\le 1$. The eigen functions are also assumed to form a complete set, thus allowing any well-behaved function in the interval $0\le y\le 1$ to be expressed as an infinite series of the eigen functions.

The general solution of Eq. (2.53) can be written as:

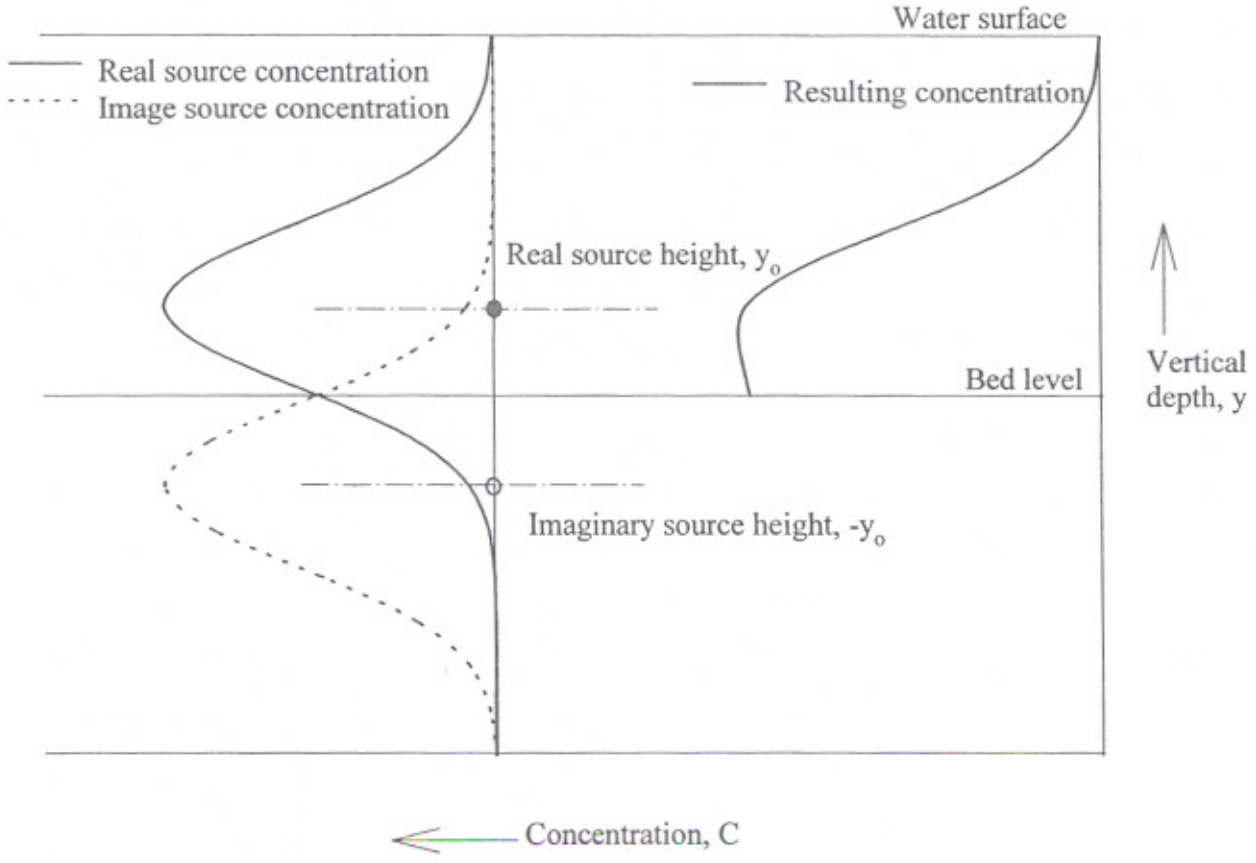

Fig. 2.2 Demonstration of method of images for computation of concentration in bounded flow

$$C(x,y) = \sum_{\gamma} a_{\gamma} \exp\left[-\frac{1}{8}\gamma f_1 x\right] H_{\gamma}(y) \qquad (2.59)$$

In Eq. (2.59) only positive values of γ are accepted with $\gamma = 0$ is the smallest eigen value, which correspond to the equilibrium condition, when the pollutant is uniformly mixed over the cross-section. The eigen values may thus be placed in order of increasing magnitude and Eq. (2.59) can be written as:

$$C(x,y) = \sum_{k=0}^{\infty} a_k \exp\left[-\frac{1}{8}\gamma_k f_1 x\right] H_k(y) \qquad (2.60)$$

The expansion constants a_k are determined by the concentration of source at x = 0, *i.e.*, $C(0,y) = C_s(y)$ and the orthogonality of the eigen functions as:

$$a_k = \frac{\int_0^1 C_s(y)\chi(y)H_k(y)dy}{\int_0^1 \chi(y)H_k^2(y)dy}; \quad (k = 0,1,\ldots\ldots\ldots,\infty) \qquad (2.61)$$

Equations (2.60) and (2.61) represent a complete solution of a steady two-dimensional mixing of a continuous release.

To verify their theoretical work, Nokes et al. (1984) conducted experiments on a laboratory flume: 15 m long, 560 mm wide and 150 mm deep. To obtain approximately two-dimensional flow, they placed roughness strips covering 50% of the width, 20 mm x 7 mm, spaced at 20 mm in the direction perpendicular to the flow. A tracer of salt (NaCl) solution was injected into the flume as a continuous horizontal line source at the surface and bottom of flow. Observations were taken at various depths and distances from the source. Samples were passed from conductivity probes via. a salinity meter. Average velocity profiles were measured across and along the flume with an 8 mm pitot tube and a Kent mini-flow impeller-type current meter. From their theoretical and experimental results, they concluded that the use of logarithmic-velocity and parabolic diffusivity yields better prediction of concentration than the constant-coefficient model.

McNulty and Wood (1984) developed an algorithm for Eq. (2.37) to obtain the complete downstream concentration for any velocity and diffusivity distribution. They used Aris method of moments to generate the required solution and compared the results with those obtained using assumptions of negligible longitudinal concentration gradients and constant velocity and diffusivity distribution. They concluded that assumptions of uniform flow conditions are conservative in terms of predicting vertical mixing.

Nokes and Wood (1988) conducted experiments for vertical and lateral mixing from a neutrally buoyant continuous contaminant source in 12 m long, 560 mm wide and 430 mm deep tilting flume of rectangular cross section. They stated that the experimental results of vertical mixing supported the use of eigen function solution with a parabolic diffusivity and logarithmic velocity distribution.

Nokes and Huges (1994) presented a semi-analytical model for solving three-dimensional turbulent diffusion equation for a steady neutrally buoyant conservative pollutant in open channels with an arbitrary but uniform cross-section of any shape and any distribution of longitudinal velocity and turbulent diffusivities. They extended the two-dimensional eigen function solution technique of Nokes and Wood (1988) to a three-dimensional eigen function technique for predicting the concentration downstream in the near-field mixing zone where three-dimensional mixing effects are present.

Lung and Connor (1984) developed an analytical method for computing two-dimensional tidally averaged estuarine transport where the two-dimensional circulation is characterized by a horizontal seaward velocity in the upper layer and a landward velocity in the lower layer, with a compensating vertical velocity to maintain hydraulic continuity. The analysis provides solution for the horizontal and vertical velocities as well as the values of vertical eddy viscosity which characterizes the vertical exchange of momentum.

Analytical solution of some other equation that govern the vertical mixing are discussed below:

(b) Steady point source: For a pipe flow discharging into a stream, the tracer concentration can be modeled by:

$$U_x \frac{\partial C}{\partial x} = \frac{\partial}{\partial y}\left[E_y \frac{\partial C}{\partial y}\right] + \frac{\partial}{\partial z}\left[E_z \frac{\partial C}{\partial z}\right] \tag{2.62}$$

For constant velocity and mixing coefficients an analytical solution of Eq. (2.62) in an unbounded channel for a point source at $x = 0$, $y = y_o$ and $z = z_o$ is obtained as (Clearly and Adrain 1973; Rutherford 1994):

$$C(x,y,z) = \dot{M} \frac{\exp\left[\frac{-U_x (y-y_0)^2}{4E_y x}\right]}{\sqrt{4\pi E_y x}} \frac{\exp\left[\frac{-U_x (z-z_0)^2}{4E_z x}\right]}{\sqrt{4\pi E_z x}} \tag{2.63}$$

The boundary conditions in this case require zero flux at the water surface, channel bed and walls as:

$$\frac{\partial C}{\partial z} = 0; \quad \text{at} \quad z = 0, b \tag{2.64a}$$

$$\frac{\partial C}{\partial y} = 0; \quad \text{at} \quad y = 0, d \tag{2.64b}$$

Equations (2.62) and (2.64) are linear, the bounded solution can be obtained by using the method of images which would satisfy Eq. (2.64).

(c) Unsteady point source: The governing equation for unsteady point source for constant velocity and diffusivities coefficients is:

$$\frac{\partial C}{\partial t} + U_x \frac{\partial C}{\partial x} = E_x \frac{\partial C}{\partial x} + E_y \frac{\partial C}{\partial y} + E_z \frac{\partial C}{\partial z} \tag{2.65}$$

The analytical solution of Eq. (2.65) for instantaneous input of mass M occurring at time t = 0 located at x = 0, y = y_0 and z = z_0 in an unbounded channel is obtained by (Rutherford 1994; Graf 1998) as:

$$C(x,y,z,t) = M \frac{\exp\left[\frac{-(x-U_x t)^2}{4E_x t}\right]}{\sqrt{4\pi E_x t}} \frac{\exp\left[\frac{-(y-y_0)^2}{4E_y t}\right]}{\sqrt{4\pi E_y t}} \frac{\exp\left[\frac{-(z-z_0)^2}{4E_z t}\right]}{\sqrt{4\pi E_z t}} \qquad (2.66)$$

Where M = Total tracer mass injected

The no flux boundary conditions at y = 0, d and z = 0, b can again be accommodated using the method of images. Equation (2.66) gives a tolerably accurate prediction of concentrations provided the tracer cloud lies mid depth at the center of the channel. Once the tracer cloud approaches the bed, assumption of uniform velocity becomes invalid and thus does not give realistic results.

Zoppou and Knight (1997, 1999) provided analytical solution for the two- and three-dimensional advection-diffusion equation with spatially variable velocity and diffusion coefficients. They assumed that each velocity components has a linear dependence on the distance and each diffusion coefficient is proportional to the square of the corresponding velocity component and then by using a simple transformation, they reduced the spatially variable equation into a linear equation with constant coefficients.

2.6.2.2 Numerical solutions

Equation (2.36) may be divided into two processes: advection and diffusion, *i.e.*,

Advection process:
$$\frac{\partial C}{\partial t} + \frac{\partial}{\partial x}(U_x C) = 0 \qquad (2.67)$$

Diffusion process:
$$\frac{\partial C}{\partial t} = \frac{\partial}{\partial x}\left[E_x \frac{\partial C}{\partial x}\right] + \frac{\partial}{\partial y}\left[E_y \frac{\partial C}{\partial y}\right] \qquad (2.68)$$

The numerical schemes available for solving equations similar to Eq. (2.36) could be classified into two types: split operator and the combined operator approach. By the split-operator approach, the advection and diffusion processes are separately computed using different numerical schemes, whereas the combined operator approach simulates the mixing equation without separating the two processes. Furthermore, the computation of diffusion can be executed accurately using a variety of finite difference and finite element methods (Morton 1981). On the other hand, it has been more difficult to attain sufficient accuracy in

the numerical computation of advection (Li 1990; Schohl and Holly 1991). Most finite difference methods for the calculation of advection are plagued by artificial or numerical diffusion, which is sometimes stronger than the physical diffusion. This artificial diffusion has no physical meaning and can cause erroneous results or sometimes even negative concentration. The level of numerical diffusion however depends on the numerical scheme used.

Among the procedures for solving the pure advection equation, several accurate schemes have been proposed, such as Holly and Preissmann two-point fourth order scheme (Holly and Preissmann 1977); Six-point scheme (Komatsu et al. 1985); Improved six-point scheme (Komatsu et al. 1989); Yang-Hsu time-line interpolation scheme (Yang and Hsu 1990); Spatial cubic spline scheme (Schohl and Holly 1991); SOWMAC scheme (Komatsu et al. 1992, Komatsu et al. 1997); Time line cubic spline scheme (Ahmad and Kothyari 2001).

Although the split-operator approach clearly has considerable advantages, it is comparatively more intensive and complicated when applied to multidimensional flow problems because the advection and diffusion processes must be handled separately. Combined operator approach offers an alternative to the split-operator approach due to its simplicity and efficiency.

(a) Computation of advection equation

The backward characteristics method with interpolating approximation of the exact solution is widely used in the solution of the pure advection equation. The choice of the interpolating function affects the accuracy of the solution significantly. From Eq. (2.67), pure advection equation for uniform velocity can be written as:

$$\frac{\partial C}{\partial t} + U_x \frac{\partial C}{\partial x} = 0 \tag{2.69}$$

The above equation may be written in terms of total derivatives as:

$$\frac{dC}{dt} = 0 \quad \text{along} \quad \frac{dx}{dt} = U_x \tag{2.70}$$

These ordinary differential equations simply state that the concentration must be constant along the space-time trajectory defined by $U_x(x,t)$. Implementation of Eq. (2.70) in a mathematical model on the fixed Eulerian space-time grid of Fig. 2.3 implies:

$$C_j^{n+1} = C_\xi^n = C_f \tag{2.71}$$

Here superscript n denotes time level, subscript j denotes a spatial step, ξ and f denote the coordinate of the foot of the trajectory of concentration characteristic along spatial axes and temporal axes leading to the point (x_j, t_{n+1}). The problem of finding the concentration at point x_j at time t_{n+1} reduces to the problem of knowing the concentration at ξ at time t_n. For that reason the accuracy of the scheme is dependent on how accurately one estimates C_ξ^n. A number of interpolating schemes are available for the determination of C_ξ^n. Some of the schemes are described as here:

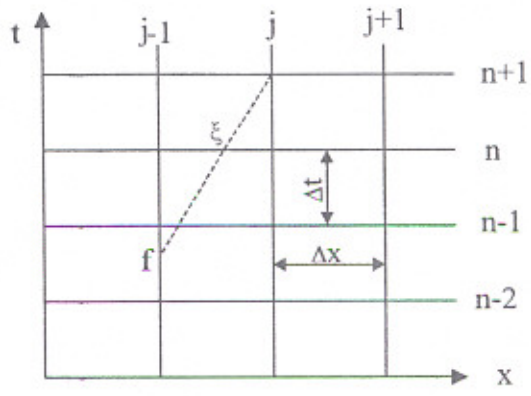

Fig. 2.3 Finite difference grid for the computation of advection in one-direction

(i) Improved six-point scheme

When applied to two- or three- dimensional advection-diffusion equation, the six-point scheme (Komatsu et al. 1985) has proved to be less accurate than for the one-dimensional case. This is due to increased opportunity of accumulation of truncation error because of repeated use of the interpolating polynomial. To improve the results, an improved six-point scheme (Komatsu et al. 1989) was developed in which an artificial correction term was added to the results.

The improved six-point scheme is as follows:

$$C_\xi^n = c_1' C_{j-3}^n + c_2' C_{j-2}^n + c_3' C_{j-1}^n + c_4' C_j^n + c_5' C_{j+1}^n + c_6' C_{j+2}^n \qquad (2.72)$$

Where

$$c_l' = c_l + \frac{0.275 C_r}{12} D_l$$

$$c_2' = c_2 - \frac{C_r \lambda S_1}{2} D_2 - \frac{(-1 + 3C_r) \times 0.275}{12} D_1$$

$$c_3' = c_3 - \frac{(1 - 3C_r) \lambda S_1}{2} D_2 - \frac{(1 - C_r) \times 0.275}{6} D_1$$

$$c_4' = c_4 - \frac{(-2 + 3C_r) \lambda S_1}{2} D_2 + \frac{C_r \times 0.275}{6} D_1$$

$$c_5' = c_5 - \frac{(1 - C_r) \lambda S_1}{2} D_2 - \frac{(-2 + 3C_r) \times 0.275}{12} D_1$$

$$c_6' = c_6 - \frac{(1 - C_r) \times 0.275}{12} D_1$$

Here

$$C_r = \frac{(x_j - x_\xi)}{(x_j - x_{j-1})} \text{ is Courant number.}$$

$$\lambda = \begin{cases} \frac{\omega}{|\omega|}; & (\omega \neq 0) \\ 0; & (\omega = 0) \end{cases}$$

$$\omega = -\frac{\partial C}{\partial x} \frac{\partial^2 C}{\partial x^2} \frac{\partial^4 C}{\partial x^4} \frac{\partial^5 C}{\partial x^5}, \quad \frac{\partial C}{\partial x} = \frac{C_j - C_{j-1}}{\Delta x}, \quad \frac{\partial^2 C}{\partial x^2} = \frac{C_{j+1} - C_j - C_{j-1} + C_{j-2}}{2(\Delta x)^2}$$

$$\frac{\partial^4 C}{\partial x^4} = \frac{C_{j+2} - 3C_{j+1} + 2C_j + 2C_{j-1} - 3C_{j-2} + C_{j-3}}{2(\Delta x)^4}$$

$$\frac{\partial^5 C}{\partial x^5} = \frac{C_{j+2} - 5C_{j+1} + 10C_j - 10C_{j-1} + 5C_{j-2} - C_{j-3}}{(\Delta x)^5}$$

$$D_1 = 4.74 \times 10^{-2} \left(C_r^2 - C_r \right)$$

$$D_2 = -3.16 \times 10^{-2} \left(C_r^2 - C_r \right)$$

$$S_1 = \frac{23.6}{(n + 18.7)^{0.758}}$$

$c_1, c_2, \ldots\ldots\ldots, c_6$ are the coefficients of the six-point scheme and are given as:

$$c_1 = -0.01806 C_r^3 - 0.03828 C_r^2 + 0.05633 C_r$$

$$c_2 = 0.2570C_r^3 + 0.05276C_r^2 - 0.3097C_r$$

$$c_3 = -0.6806C_r^3 + 0.6480C_r^2 + 1.033C_r$$

$$c_4 = 0.6806C_r^3 - 1.394C_r^2 + 0.2869C_r + 1$$

$$c_5 = -0.2570C_r^3 + 0.8236C_r^2 - 0.5667C_r$$

$$c_6 = 0.01806C_r^3 - 0.09245C_r^2 + 0.07439C_r$$

(ii) SOWMAC scheme

Komatsu et al. (1992), developed a refined implicit scheme namely SOWMAC (Second order wave equation method for advection calculation) based on the concept of solving second order wave equation instead of first order advection equation. SOWMAC scheme is given as follows:

$$d_1C_{j-1}^{n+1} + d_2C_j^{n+1} + d_3C_{j+1}^{n+1} = d_4C_{j-1}^n + d_5C_j^n + d_6C_{j+1}^n \qquad (2.73)$$

Where $d_1, d_2, \ldots\ldots\ldots, d_6$ are coefficients and are functions of Courant number.

$$d_1 = 0.3776C_{r0+} + 0.3152C_{r0-} - 0.5467C_{r1+} + 0.4843C_{r1-} + C_r^2$$

$$d_2 = 1.3072 + 0.0624|C_r| - 0.3382C_r^2$$

$$d_3 = 0.3152C_{r0+} + 0.3776C_{r0-} + 0.4843C_{r1+} - 0.5467C_{r1-} + 0.1691C_r^2$$

$$d_4 = 0.3776C_{r0+} + 0.3152C_{r0-} + 0.5157C_{r1+} - 0.4533C_{r1-} + 0.1381C_r^2$$

$$d_5 = 1.3072 + 0.0624|C_r| - 0.2762C_r^2$$

$$d_6 = 0.3152C_{r0+} + 0.3776C_{r0-} - 0.4533C_{r1+} + 0.5157C_{r1-} + 0.1381C_r^2$$

$$C_{r0+} = (\text{int})\left\{\frac{C_r + 1}{1 + |C_r|}\right\}$$

$$C_{r0-} = (\text{int})\left\{\frac{1 - C_r}{1 + |C_r|}\right\}$$

$$C_{r1+} = \frac{|C_r| + C_r}{2}$$

$$C_{r1-} = \left| \frac{C_r - |C_r|}{2} \right|$$

In the above, (int) is an incorporated function used in C language for ignoring fractions.

The above scheme uses only three computational grid points, so there is no need for special treatment of the boundary condition.

(iii) Cubic spline scheme

Schohl and Holly (1991) interpolated the value of C_ξ^n using two point bracketing ξ by cubic spline interpolation viz.

$$C_\xi^n = d_1' \left.\frac{\partial^2 C}{\partial x^2}\right|_{j-1}^n + d_2' \left.\frac{\partial^2 C}{\partial x^2}\right|_j^n + d_3' C_{j-1}^n + d_4' C_j^n \qquad (2.74)$$

Where $d_1' = \frac{C_r(C_r^{\,2} - 1)\Delta x^2}{6}$, $d_2' = -\frac{C_r(C_r - 1)(C_r - 2)\Delta x^2}{6}$, $d_3' = C_r$ and $d_4' = 1 - C_r$

Solution of Eq. (2.74) requires the value of second spatial derivatives of concentration at all the nodal points at time level, n (See; Fig.2.3). The same is calculated by the following equation:

$$\left.\frac{\partial^2 C}{\partial x^2}\right|_{j-1}^n + \left.\frac{\partial^2 C}{\partial x^2}\right|_j^n + \left.\frac{\partial^2 C}{\partial x^2}\right|_{j+1}^n = \frac{6}{\Delta x^2}\left(C_{j-1}^n - 2C_j^n + C_{j+1}^n\right) \qquad (2.75)$$

Equation (2.75) is a special form of linear system of equations which are solved through inversion of a tri-diagonal matrix. The natural spline condition in which the upstream and downstream second spatial derivatives are taken equal to zero are taken by Schohl and Holly (1991).

Egan and Mahoney (1972) introduced Lagarangian second moment method (SMM) scheme for the computation of advection for two-dimensional air-pollution transport. It has been successfully used by Pepper and Baker (1980) for three-dimensional atmosphere pollution transport as well as by Nassiri and Babarusti (1997) to compute the dye concentration distribution in shallow recirculating flow dominated by advection. The method considers the zero, the first and the second moment of the spatial distribution of concentration. The time evaluation of moments is calculated using a Lagrangian approach. At each time step, the advected distribution is projected to a fixed Eulerian grid.

(b) Computation of diffusion equation

The one-dimensional diffusion process can be accurately computed by numerical schemes such as Crank-Nicholson central difference scheme and Crank-Nicholson Galerkin finite-element method. However, computation of diffusion in two-dimensions is obtained using alternate-direction implicit (ADI) scheme (Smith 1978; Luk et al.1990).

Numerical solution of Eq. (2.36) with derivative boundary conditions is not available in the literature. However, numerical solutions of the similar type of equations by using combined operator approach are available in literature such as, Stefanovic and Stefan (2001); Tsai et al. (2002); Guan et al. (2002).

2.6.3 Distance for Complete Vertical Mixing

The distance required for 98% complete mixing of tracer along the vertical from a steady transverse line source located at mid-depth is obtained from the Eq. (2.46) (Rutherford 1994):

$$L_y = 0.134 \frac{U_x d^2}{E_y} \tag{2.76}$$

The 98% complete mixing means that the ratio of minimum and maximum concentration over the depth is 0.98. The constant-coefficient model predicts that the vertical mixing distance is shorter for a source located at mid-depth than for a source at any other depth. However, by assuming logarithmic velocity and parabolic diffusivity distributions, it has been obtained that the optimum source location is not at mid-depth but is slightly closer to the surface. For a point source at the bed or at the surface, the vertical mixing distance is four times larger, *i.e.*,

$$L_y = 0.536 \frac{U_x d^2}{E_y} \tag{2.77}$$

For a source at mid-depth, substitution of Eq. (2.45) into Eq. (2.76) yields

$$\frac{L_y}{d} = 2 \frac{U_x}{U_*} \tag{2.78}$$

In river $\frac{U_x}{U_*}$ rarely exceeds 25 (Rutherford 1994) and so Eq. (2.78) indicates that

$$\frac{L_y}{d} \leq 50 \qquad (2.79)$$

Thus a neutrally buoyant tracer becomes fully mixed vertically within 50 depth of the flow, downstream of the source.

2.6.4 Buoyancy Effects on Vertical Mixing

Buoyancy effects on vertical mixing are to be considered when warm water e.g. waste heat from the power stations is discharged into a stream. Also, buoyancy effects are important in tidal rivers where density stratification occurs with saline water having more density underlying fresh water having less density. In both situations vertical mixing is subdued because turbulence has to perform additional work to lift dense fluid and depress light fluid. Officer (1976) and Bowden (1983) have shown that stratification reduces the vertical mixing coefficient. Based on experimental studies, the vertical mixing coefficient in non-stratified and stratified conditions can be expressed in the following form:

$$E_s = E_o(1 + k_1 R_c)^{k_2} \qquad (2.80)$$

Where E_o and E_s = vertical mixing coefficient in non-stratified and stratified condition respectively; k_1 and k_2 = constants; R_c is Richardson number and is defined as the ratio of the buoyancy forces to the inertial forces acting in the flow.

Schiller and Sayre (1975) presented a mathematical model based on laboratory flume experiments for predicting vertical distribution of temperatures in the far-field region in a uniform two-dimensional flow. They concluded that in the far-field region, the turbulence of the ambient flow dominates the mixing process and cooling losses to the atmosphere cannot be neglected unlike in the near-field mixing zone where jet momentum and entrainment are dominant and cooling losses to the atmosphere are negligible.

French (1979) presented an accurate and practical method of computing the solute transfer coefficients in stratified channel flow in terms of easily measured parameters in either the laboratory or field. He concluded that vertical mixing in stratified steady two-dimensional channel flow can be described in terms of homogeneous vertical momentum transfer coefficient and flow Richardson number (Flow Richardson number is the ratio of the energy added to the flow by buoyancy to the turbulent energy added by shear at the boundary) when density stratification is continuous and the primary source of turbulence is the bottom boundary.

For the continuity in the subject of mixing of pollutants in streams, the transverse and longitudinal mixing are also discussed here briefly.

2.7 TRANSVERSE MIXING

Transverse mixing arises from turbulence and vertical variations in transverse velocity. Transverse mixing is important in water quality management especially when dealing with the discharge of wastes/pollutants from point sources or the mixing of tributary inflows. In such problems, vertical mixing occurs rapidly and is only important very close to the source, whereas, longitudinal dispersion is only important in far-field if the source is unsteady.

The depth-averaged mixing equation, presented in Section 2.4 in rectangular Cartesian coordinates is

$$\frac{\partial}{\partial t}(ds)+\frac{\partial}{\partial x}(dv_x s)+\frac{\partial}{\partial z}(dv_z s)=\frac{\partial}{\partial x}\left[dE'_x\frac{\partial s}{\partial x}\right]+\frac{\partial}{\partial z}\left[dE_z\frac{\partial s}{\partial z}\right] \qquad (2.30)$$

Here E'_x and E_z take care of e_x and e_z respectively.

Yotsukura and Cobb (1972); Yotsukura and Sayre (1976) developed the cumulative discharge concept, which permits an analytical solution of simplified form of Eq. (2.30) for steady injection. Lau and Krishnappan (1981) adopted an implicit finite difference scheme proposed by Stone and Brain (1963) to solve simplified form of Eq. (2.30). Based on Split operator approach, Luk et al. (1990) employed explicit finite difference scheme to solve the transverse mixing equation for non-conservative substances and unsteady pollutant source in streams. They divided the stream tubes into variable elements so that Courant number for the grid space is always equal to unity. But such approach complicates the transverse calculations considerably. A great deal of computation effort is spent for bookkeeping tasks Guan et al. (2002); Ahmad and Kothyari (2001); Stefanovic and Stefan (2001); Tsai et al. (2002). Guan et al. (2002) also proposed numerical schemes for the solution of Eq. (2.30) or its simplified form for constant mixing coefficients.

Several attempts have been made to establish the relationship between transverse mixing coefficient and bulk parameters representing channel and flow characteristics such as width, depth, shear velocity, friction factor, curvature and sinuosity (Lau and Krishnappan 1977, 1981; Fischer 1969; Webel and Schatzmann 1984; Deng et al. 2001; Boxall and Guymer 2003 a and b). Based on published data from a number of sources on transverse mixing

Boxall and Guymer (2003 a and b) has proposed empirical formulae for transverse mixing coefficient which are given in Table 2.2.

Table 2.2: Empirical Formulae For Transverse Mixing Coefficient

Straight Channels	$0.15 < E_z / dU_* < 0.30$
Gentle meandering channels	$0.30 < E_z / dU_* < 0.90$
Curved channels	$1.0 < E_z / dU_* < 3.0$

Here E_z = Transverse mixing coefficient, d = Local depth of flow and U_* = Shear velocity

It is to be noted that the value of transverse mixing coefficient is relatively higher in meandering and curved channels due to the presence of secondary currents.

2.8 LONGITUDINAL MIXING

After a time lapse and considerable distance from the injection site, the tracer is completely mixed over the cross-section of the stream and the primary variation of the concentration is only in the longitudinal direction and dispersion beyond this section is called longitudinal dispersion. Longitudinal dispersion arises because vertical and transverse velocity shear carry the tracer downstream more slowly near the bed and the banks than in mid-channel. Fischer (1967) showed that in river channels transverse velocity shear makes a greater contribution to longitudinal dispersion than vertical velocity shear. Equation (2.35) is the governing equation of longitudinal dispersion in open channels.

To understand the process of longitudinal dispersion, it is necessary to solve Eq. (2.35) either analytically or numerically. The most commonly used analytical solution by Fischer (1968) is described in the following section.

2.8.1 Fischer's Analytical Solution

Fischer (1968) obtained a solution of Eq. (2.35) for constant values of A, V_x and E_L. The observed C-t curve on an upstream section of the channel is used as initial tracer distribution. The solution given is:

$$S(x_2,t) = \int_{-\infty}^{\infty} S(x_1,\tau) \frac{\exp\left[\frac{-\{V_x(\bar{t}_2 - \bar{t}_1 - t + \tau)\}^2}{4E_L(\bar{t}_2 - \bar{t}_1)}\right]}{\sqrt{4\pi E_L(\bar{t}_2 - \bar{t}_1)}} U d\tau \qquad (2.81)$$

Here $S(x_2,t)$ is the predicted value of concentration at station x_2 at time t, $S(x_1,\tau)$ is the value of concentration at station x_1 at time τ, and $\bar{t}_1$ and $\bar{t}_2$ are the respective times of passage of the tracer cloud past the two stations calculated assuming that the cross-sectional mean velocity is equal to the velocity of the tracer cloud. Thus if the C-t curve, flow parameters and E_L value are known at one station, one can find the C-t curve at the second station.

Bansal (1971); Prakash (1977); Nokes et al. (1984) and Alavian (1986) have also proposed analytical solutions of the dispersion equation under simplified assumptions.

The numerical schemes available for solution of Eq. (2.35) are either based on Split-operator approach or Combined operator approach. Some such schemes proposed more recently are those by Ahmad et al. (1999); Li and Yu (1994); Yang and Hsu (1990); Wu and Tsanis (1994); Jaque and Ball (1994) and Tsai et al. (2002).

2.8.2 Estimation of Longitudinal Dispersion Coefficient

Longitudinal dispersion coefficient is a fundamental parameter in hydraulic modelling of river pollution, as it is a measure of the intensity of the mixing of the pollutants in river channels. Longitudinal dispersion coefficient can be estimated from the pollutant concentration profiles, stream velocity profiles and channel and flow parameters (empirical equations). Methods which use concentration profiles for the estimation of E_L are change of moment method, routing procedure method and diffusive transport method proposed by Fischer (1968); Frozen Cloud method and Hayami solution by Barnett (1983).

Longitudinal dispersion rises mainly as a result of transverse and vertical velocity shear. Some of the longitudinal dispersion does also occur due to a transverse shear resulting from secondary currents. Fischer et al. (1979) found that in natural streams, the transverse profile of longitudinal velocity is 100 or more times effective in producing longitudinal dispersion than the vertical velocity profile and therefore the longitudinal dispersion coefficient can be estimated knowing the velocity distribution over the cross-section of the channel. Fischer

(1967) developed an integral equation based on the balance between longitudinal advection and transverse diffusion and derived equation for E_L as:

$$E_L = -\frac{1}{A}\int_0^{z=B} dV_x' \int_0^z \frac{1}{E_z d}\int_0^z dV_x' dz dz dz \qquad (2.82)$$

Where B = water surface width of stream; Fischer et al. (1979) considered transverse mixing coefficient $E_z = 0.15 dU_*$ for the idealized rivers with a uniform, straight and infinitely wide channels of constant depth.

Seo and Baek (2004) also developed a theoretical method for predicting the longitudinal dispersion coefficient based on the beta function for transverse velocity distribution in natural streams.

Various empirical equations for estimation of E_L are recommended by investigators (Asai et al. 1991; Seo and Cheong 1998; Ahmad et al. 1999; Deng et al. 2001; Deng et al. 2002).

For straight alluvial rivers and using the hydraulic geometry relationship for stable rivers, Deng et al. (2001) derived equations for transverse profile for channel shape, local flow depth and lateral distribution of the deviation of the local velocity from the cross-sectional velocity. Using these equations in the Fischer's triple integration equation, they proposed the following equation for predicting the longitudinal dispersion coefficient for natural streams.

$$\frac{E_L}{DU_*} = \frac{0.15}{8E_{z^*}}\left(\frac{B}{D}\right)^{\frac{5}{3}}\left(\frac{V_x}{U_*}\right)^2 \qquad (2.83)$$

Where D = Cross-sectional average flow depth

E_z^* = Dimensionless transverse mixing coefficient

$$= 0.145 + \left(\frac{1}{3520}\right)\left(\frac{U}{U_*}\right)\left(\frac{B}{D}\right)^{1.38}$$

By comparing with field data and the equations proposed by other investigators, they found that Eq. (2.83) has least error in predicting the longitudinal dispersion coefficient for natural streams.

Later Deng et al. (2002) proposed a new equation for longitudinal dispersion coefficient in straight and natural meandering streams by using new channel shape and local flow depth equations. The proposed equation is:

$$\frac{E_L}{U_* D} = -\left(\frac{I}{E_z^*}\right)\left(\frac{V_x}{U_*}\right)^2\left(\frac{B}{D}\right)^2 \tag{2.84}$$

Where E_z^* = Dimensionless transverse mixing coefficient given by Deng et al. (2001)

For straight channels,

$$I = 0.0013\left(\frac{B}{D}\right)^{-0.3523}$$

and for meandering channels,

$$I = 0.0061\sigma^3 - 0.0259\sigma^2 + 0.0422\sigma - 0.0224, \text{ for } B/D = 10$$

$$I = 0.0077\sigma^3 - 0.0379\sigma^2 + 0.0686\sigma - 0.0387, \text{for } B/D = 20$$

$$I = 0.0094\sigma^3 - 0.0502\sigma^2 + 0.0954\sigma - 0.0553, \text{for } B/D = 54.6$$

$$I = 0.0105\sigma^3 - 0.058\sigma^2 + 0.112\sigma - 0.0651, \text{for } B/D = 148.4$$

Here σ = Sinuosity of the stream

For other cases of width to depth ratio, I value can be linearly interpolated from the neighboring values computed from the corresponding above regression equations.

They verified the proposed relationship using 70 sets of field data from 30 streams in United States ranging from straight channels to sinuous natural channels and was found to predict 90% longitudinal dispersion coefficient values within the range of 0.5 to 2 times the observed ones.

2.9 MIXING OF POLLUTANTS IN SEDIMENT-LADEN FLOWS

Alluvial streams carry sediments as suspended load and bed load. To make the tracer transport prediction problems more oriented to field applications, it is necessary to know the effects of sediment on the mixing process.

Einstein and Chien (1955); Arora (1983); Samaga et al. (1986); Umeyama and Gerritsen (1992); Ahmad et al. (2004) have studied the velocity distribution in open channels carrying suspended sediment load. They found that these velocity distributions deviate from the velocity distributions in flows without sediment. Dispersion is considered to be significantly affected by the advection process (Holley 1969). Therefore, the dispersion characteristics of

flows transporting suspended sediments may be expected to be different from those of clear-water flows.

No systematic study is available so far on vertical mixing of pollutants in sediment-laden flows. However a limited number of studies are available on longitudinal dispersion. Singh (1987) and Singh et al. (1992) performed experiments on 400 mm wide channel for longitudinal dispersion and observed that the presence of sediments does not have any noticeable effect on the mixing of pollutant beyond the initial period in the range of concentration studied (<5000 ppm). However, it is well known that the presence of sediment affects the friction factor, which can have a significant effect on dispersion. Ahmad (1999) and Ahmad et al. (2004) have observed that more dispersion occurs in sediment-laden flows than in the corresponding clear-water flows and dispersion increases with an increase in sediment concentration in the flow, as the deviation of velocity distribution from the mean velocity also increases with an increase in sediment concentration (Lau 1983; Samaga et al. 1986; Umeyama and Gerritsen 1992). Ahmad et al. (2004) also proposed a predictor for longitudinal dispersion coefficient for sediment-laden flows.

2.10 CONCLUDING REMARKS

A review of pertinent literature concerning the two-dimensional mixing (vertical mixing) of neutrally buoyant dispersants from an instantaneous transverse line source in laboratory flumes and natural streams presented in this chapter indicates that the following points regarding the mixing which need careful consideration.

1. Analytical and/or numerical schemes are yet to be identified for complete solution of the governing equation for the process of two-dimensional mixing, *i.e.*, Eq. (2.36) for transverse line slug source.
2. Analytical solutions are available for simplified form of Eq. (2.36) and for steady injection of pollutants.
3. Based on sound theoretical ground and verified with experimental results, vertical mixing coefficient can be predicted satisfactorily by using Prandtl's mixing length hypothesis.
4. No predictor for longitudinal mixing coefficient is available in the literature.
5. Due to increased velocity defects, more dispersion occurs in sediment-laden flows than in the corresponding clear-water flows and dispersion increases with an increase

in sediment concentration in the flow. However, no information is available as yet on the effect of suspended sediment concentration on the process of two-dimensional mixing or vertical mixing.

Chapter

3

NUMERICAL MODELLING

3.1 INTRODUCTION

It is practically difficult to measure the concentration distribution of disposed off pollutants in water bodies such as rivers, lakes and coastal areas on routine basis and at the same time, it is very costly. Analytical modelling of dispersion process is limited to the simplified form of governing equation which does not hold good for real situations. Numerical modelling therefore is adopted for solution of the mass balance equation of tracer transport for prediction of pollutant distribution in water bodies. The numerical models allow for the analysis of the variabilities in channel characteristics, water quality and other transport parameters. Such models have a wide range of applications such as calculation of dilution rates of pollutants, delineation of mixing zones, evaluation of risk from accidental or intentional spillage of pollutants and assessment of pollution control strategies.

The solution of the mass transport equation using a numerical model requires a priori information on velocity field, mixing coefficients and channel properties. A successful numerical model must be able to solve accurately the advection and diffusion processes of the transport equation. The computation of diffusion can be executed accurately using a variety of finite difference and finite element methods (Morton 1981). On the other hand, it has been more difficult to attain sufficient accuracy in the numerical computation of advection (Li 1990; Schohl and Holly 1991). Most finite difference methods for the calculation of advection are plagued by artificial or numerical diffusion, which is sometimes stronger than the physical diffusion. This artificial diffusion has no physical meaning and can cause erroneous results or sometimes even negative concentration. The level of numerical diffusion however depends on the numerical method used.

The literature pertaining to the numerical solution of the two-dimensional mixing of a conservative pollutant showed that none of the numerical schemes available in literature is

directly applicable for impulsive injection of pollutant involving the two-dimensional mixing, as in this case concentration gradient in longitudinal as well as lateral directions is significant. In the present chapter therefore, a numerical scheme has been proposed for modelling of two-dimensional advection and diffusion. The proposed numerical scheme is stable and convergent.

3.2 PROPOSED NUMERICAL SCHEME FOR THE SOLUTION OF TWO-DIMENSIONAL MIXING EQUATION

A numerical scheme based on Split operator approach is presented herein, for the solution of equation of two-dimensional mixing. In this approach, the advection and diffusion rates are computed separately using different numerical schemes. The exact solution of the advection equation has been achieved by adopting the Courant number equal to one for the computational nodes on the flow surface (*i.e.*, where y/d = 1.0). For the other computational nodes (*i.e.*, while y/d < 1.0), cubic spline interpolation scheme of Schohl and Holly (1991) has been used to obtain the solution of the advection process because of the velocity defect along the vertical. The computation of diffusion rate has been made by using the alternate-direction implicit method (ADIM) suggested by Smith (1978). This is a two-step approach method in which it is assumed that if the solution is known at any time level, the solution for the next time level is obtained by solving the equations implicitly. To this solution, the advected concentration is added for obtaining the final concentration. The solution is advanced to the next level by simply changing the direction of operations. The solution procedure at each individual level is conditionally stable but the combined two levels solution procedure is completely stable (Peaceman and Rachford 1955; Smith 1978). The compensation of errors produced by the changing the direction of operations gives a scheme, which is stable and convergent.

3.2.1 Non-dimensional Form of the Equation

The two-dimensional mixing equation, *i.e.*, Eq. (2.36) is a linear parabolic partial differential equation which describes the spatial and temporal variations of the solute concentration, requiring for its solution: upstream and downstream boundary conditions, derivative boundary condition as well as initial state of flow domain (initial condition). The assumptions involved in the development of the equation are as follows:

i) Pollutant is conservative

ii) Buoyancy effects are neglected

iii) Flow is predominately in x-direction

iv) Horizontal line source is uniformly spread across the width of the channel

v) The flow is steady and uniform

The order of magnitude of various terms appearing in Eq. (2.36) could be very different in problems involving real data. However it is considered that the order of magnitude of various terms in non-dimensional form of the equation will not vary much from each other. Hence it is appropriate to solve Eq. (2.36) in non-dimensional form (Ahmad et al. 1999).

Defining the following non-dimensional variables as:

$$b^* = \frac{b}{d}; \qquad C^* = \frac{C}{C_i}; \qquad U^* = \frac{U_x}{\sqrt{gd}}; \qquad x^* = \frac{x}{d}; \qquad y^* = \frac{y}{d};$$
$$E_x^* = \frac{E_x}{d\sqrt{gd}}; \qquad E_y^* = \frac{E_y}{d\sqrt{gd}} \quad \text{and} \quad t^* = t\sqrt{\frac{g}{d}} \tag{3.1}$$

Where superscript '$*$' indicates the dimensionless value of that variable, b^* dimensionless width; C^* dimensionless concentration; E_x^* dimensionless longitudinal mixing coefficient; E_y^* dimensionless vertical mixing coefficient; t^* dimensionless time; U^* dimensionless velocity; x^* dimensionless longitudinal distance and y^* dimensionless vertical distance.

C_i is the concentration of the injected tracer and d is the local depth of flow. Substituting the values of the variables from Eq. (3.1) into Eq. (2.36), to yield:

$$\frac{\partial}{\partial t^*}\left(b^* C^*\right) + \frac{\partial}{\partial x^*}\left(b^* U^* C^*\right) = \frac{\partial}{\partial x^*}\left(b^* E_x^* \frac{\partial C^*}{\partial x^*}\right) + \frac{\partial}{\partial y^*}\left(b^* E_y^* \frac{\partial C^*}{\partial y^*}\right) \tag{3.2}$$

Equation (3.2) is the non-dimensional form of Eq. (2.36). The results from Eq. (3.2) are to be multiplied by the corresponding scaling parameters, for obtaining the values of desired variables. For steady and uniform flow and for constant E_x and E_y, Eq. (3.2) gets simplified to:

$$\frac{\partial C}{\partial t} + U\frac{\partial C}{\partial x} = E_x \frac{\partial^2 C}{\partial x^2} + E_y \frac{\partial^2 C}{\partial y^2} \tag{3.3}$$

Asterisks ($*$) are dropped from Eq. (3.3) for convenience.

Transforming Eq. (3.3) by using, the following functions:

$$X = \frac{x}{\sqrt{E_x}} \quad \text{and} \quad Y = \frac{y}{\sqrt{E_y}} \tag{3.4}$$

The transformation yields:

$$\frac{\partial C}{\partial t} + \frac{U}{\sqrt{E_x}} \frac{\partial C}{\partial X} = \frac{\partial^2 C}{\partial X^2} + \frac{\partial^2 C}{\partial Y^2} \tag{3.5}$$

A finite difference method is proposed for solution of Eq. (3.5) as described below.

3.2.2 Finite Difference Method

Based on the Split operator approach, Eq. (3.5) is solved using cubic spline scheme for the solution of advection process and alternate-direction implicit scheme for diffusion process.

Let us consider a space XY as shown in Fig. 3.1. Divide XY space into a rectangular computational mesh having spacing ΔX in the X-direction and ΔY in the Y-direction. The corresponding spacing in the time direction is Δt.

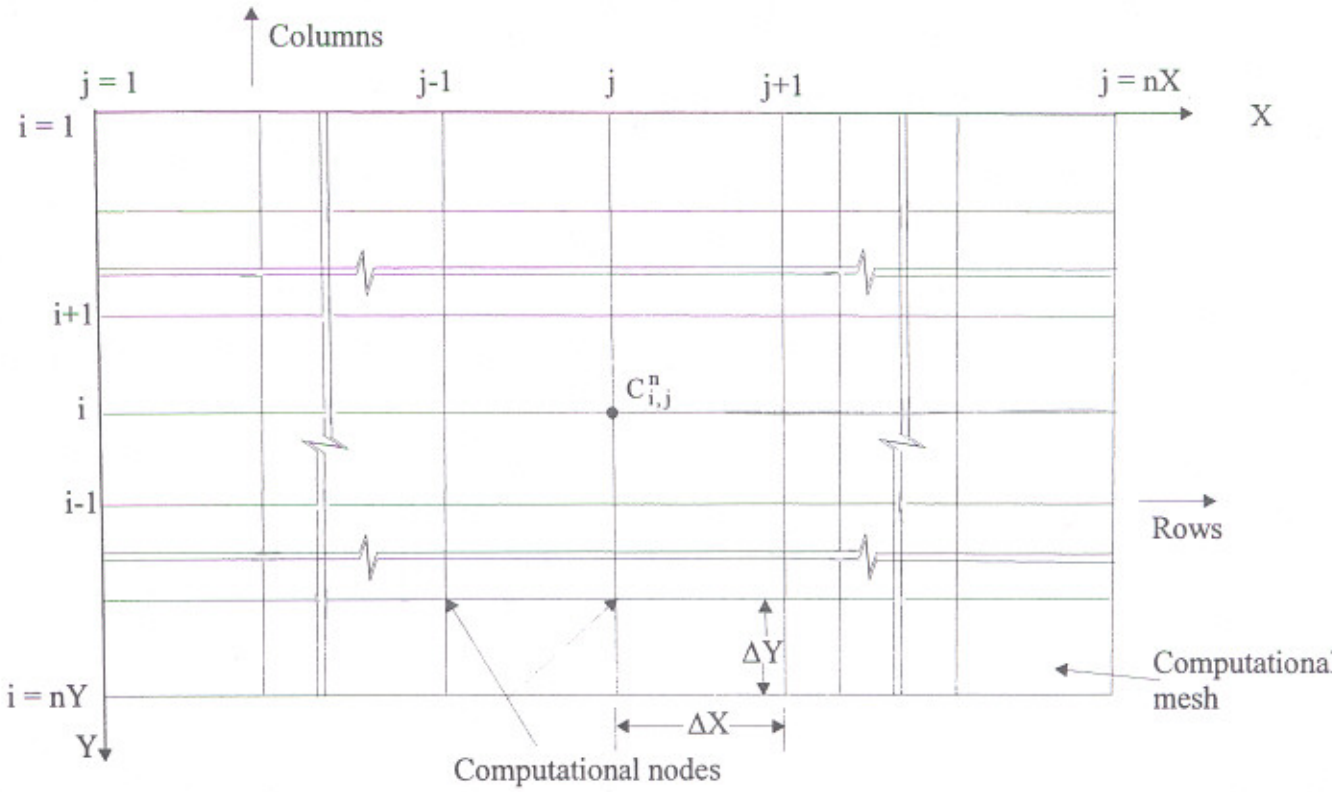

Fig. 3.1 Description of a computational plane at time level $n\Delta t$

The co-ordinates (X, Y, t) of the computational nodes of the solution domain are defined as:

$$X = j\Delta X;\quad j = 1, 2, 3, \ldots\ldots\ldots\ldots, nX$$

$$Y = i\Delta Y;\quad i = 1, 2, 3, \ldots\ldots\ldots\ldots, nY$$

$$t = n\Delta t;\quad n = 0, 1, 2, \ldots\ldots\ldots\ldots, N$$

Here nX = Total number of computational nodes in the X-direction; nY = Total number of computational nodes in the Y-direction; N = Total number of computational planes in the time direction (Z-direction) and i, j and n are indices. Any computational node of the mesh can be represented as ($i\Delta Y$, $j\Delta X$, $n\Delta t$) or simply (i, j, n). Hence concentration at the n^{th} time level can be written as $C^n_{i,j}$.

Solutions of advection and diffusion processes are discussed in the following section.

(a) Advection process

Pure advection equation can be written as:

$$\frac{\partial C}{\partial t} + \frac{U}{\sqrt{E_x}}\frac{\partial C}{\partial X} = 0 \tag{3.6}$$

Use of forward difference approximation for the partial derivative $\frac{\partial C}{\partial t}$ and backward difference approximation for $\frac{\partial C}{\partial X}$ yields (Smith 1978; Jain 1991):

$$\frac{\partial C}{\partial t} = \frac{C^{n+1}_{i,j} - C^n_{i,j}}{\Delta t} + O(\Delta t) \tag{3.7}$$

$$\frac{\partial C}{\partial X} = \frac{C^n_{i,j} - C^n_{i,j-1}}{\Delta X} + O(\Delta X) \tag{3.8}$$

The terms $O(\Delta t)$ and $O(\Delta X)$ are the order of local truncation errors.

Substituting Eqs. (3.7) and (3.8) into Eq. (3.6), one obtains (Abbot 1980):

$$\frac{C^{n+1}_{i,j} - C^n_{i,j}}{\Delta t} + \frac{U_i}{\sqrt{E_x}}\frac{C^n_{i,j} - C^n_{i,j-1}}{\Delta X} = 0 \tag{3.9}$$

Where $\Delta X = X_j - X_{j-1}$; U_i = velocity at node i; X_j and X_{j-1} = distance of j^{th} and $(j-1)^{th}$ nodes from the first node, respectively.

When Courant number (C_r) defined as $\frac{U_i}{\sqrt{E_x}}\frac{\Delta t}{\Delta X}$ is set to be unity, we have

$$U_i \Delta t = \sqrt{E_x}\,\Delta X \tag{3.10}$$

By substituting Eq. (3.10) into Eq. (3.9), we get

$$C_{i,j}^{n+1} = C_{i,j-1}^{n} \tag{3.11}$$

This is the exact solution of advection process. Here the values of $\Delta X = \frac{U_i}{\sqrt{E_x}}\Delta t$ are so chosen that for computational nodes at the flow surface, *i.e.*, while y/d = 1.0, the root of concentration characteristic line falls at the node for previous time step. For computational nodes in the spatial levels with y/d < 1.0, the flow velocity shall be different due to velocity defect, therefore the root of the characteristic line will not fall on the computational node but it will intersect the spatial axes at point ξ (See; Fig. 3.2). Therefore, interpolation will be required to be made at these computational nodes. The problem of finding the concentration at $C_{i-1,j}^{n+1}$ reduces to the problem of knowing the concentration at $C_{i-1,\xi}^{n}$ (See; Fig. 3.2). For that reason the accuracy of the scheme is dependent on how accurately one estimates the concentration at $C_{i-1,\xi}^{n}$. Schohl and Holly's (1991) cubic spline interpolation scheme is used to determine the concentration at $C_{i-1,\xi}^{n}$. They used two points bracketing ξ by cubic spline interpolation viz.

$$C_{i-1,\xi}^{n} = d_1' \left.\frac{\partial^2 C}{\partial X^2}\right|_{i-1,j-1}^{n} + d_2' \left.\frac{\partial^2 C}{\partial X^2}\right|_{i-1,j}^{n} + d_3' C_{i-1,j-1}^{n} + d_4' C_{i-1,j}^{n} \tag{3.12}$$

Where $d_1' = \frac{C_r(C_r^{\,2} - 1)\Delta X^2}{6}$, $d_2' = -\frac{C_r(C_r - 1)(C_r - 2)\Delta X^2}{6}$, $d_3' = C_r$ and $d_4' = 1 - C_r$

Solution of Eq. (3.12) requires the value of second spatial derivatives of concentration at all the nodal points at (i-1) spatial level. The same is calculated by the following equation:

$$\left.\frac{\partial^2 C}{\partial X^2}\right|^{n}_{i-1,j-1} + \left.\frac{\partial^2 C}{\partial X^2}\right|^{n}_{i-1,j} + \left.\frac{\partial^2 C}{\partial X^2}\right|^{n}_{i-1,j+1} = \frac{6}{\Delta X^2}\left(C^{n}_{i-1,j-1} - 2C^{n}_{i-1,j} + C^{n}_{i-1,j+1}\right) \qquad (3.13)$$

Equation (3.13) is a special form of system of linear equations which is solved through inversion of a tri-diagonal matrix. The natural spline condition in which the upstream and downstream second spatial derivatives are taken equal to zero, are used in Eq. (3.13). In the same manner concentration at the lower spatial levels (i-2, i-3,.....,nY) are determined.

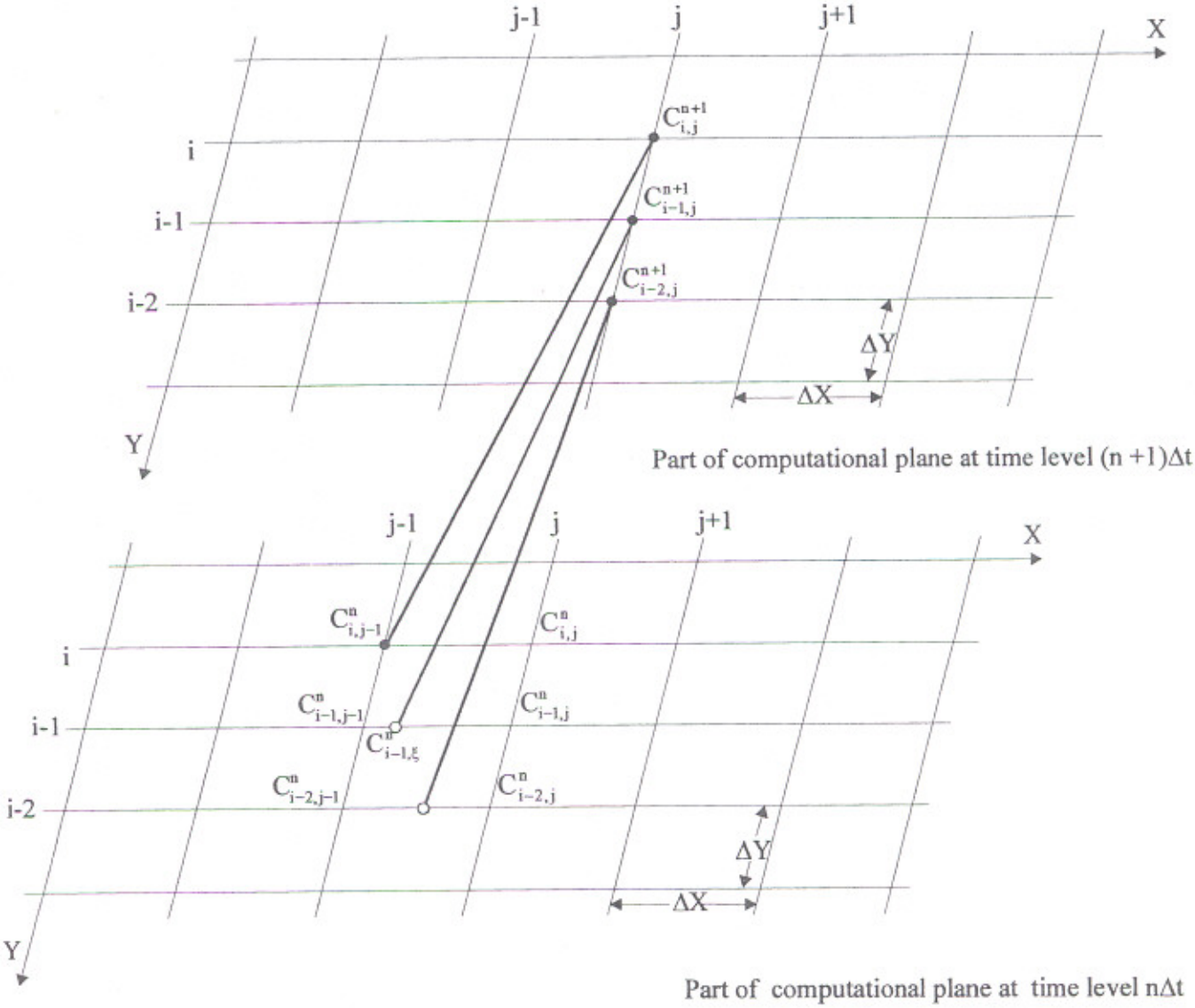

Fig. 3.2 Two-dimesional computational mesh for computation of advection component.

(b) Diffusion process

Diffusion equation in two dimensions may be written as:

$$\frac{\partial C}{\partial t} = \frac{\partial^2 C}{\partial X^2} + \frac{\partial^2 C}{\partial Y^2} \tag{3.14}$$

Equation (3.14) is a two-dimensional parabolic partial differential equation and can be solved by alternate-direction implicit method (ADIM) suggested by Smith (1978). This is a two-step approach method, which requires minimum computer storage and is therefore widely used for computations.

Computation of concentration at time level $(n_{even}+1)\Delta t$

In ADIM, it is assumed that the solution is known at the n^{th} level, *i.e.*, for time $t = n\Delta t$, the solution for the $(n+1)^{th}$ level, *i.e.*, for the time $t = (n+1)\Delta t$, (while index n is even) is obtained by replacing one of the second order derivatives say $\frac{\partial^2 C}{\partial X^2}$ by the implicit finite difference approximation in terms of unknown pivotal values of C from the $(n+1)^{th}$ time level. The other second order derivative $\frac{\partial^2 C}{\partial Y^2}$ is replaced by explicit finite difference approximation at the n^{th} level and $\frac{\partial C}{\partial t}$ is replaced by forward difference approximation. With these discretization, one can write (Smith 1978):

$$\frac{\partial C}{\partial t} = \frac{C_{i,j}^{n+1} - C_{i,j}^{n}}{\Delta t} + O(\Delta t) \tag{3.15a}$$

$$\frac{\partial^2 C}{\partial X^2} = \frac{C_{i,j-1}^{n+1} - 2C_{i,j}^{n+1} + C_{i,j+1}^{n+1}}{\Delta X^2} + O(\Delta X^2) \tag{3.15b}$$

$$\frac{\partial^2 C}{\partial Y^2} = \frac{C_{i-1,j}^{n} - 2C_{i,j}^{n} + C_{i+1,j}^{n}}{\Delta Y^2} + O(\Delta Y^2) \tag{3.15c}$$

The terms $O(\Delta t)$, $O(\Delta X^2)$ and $O(\Delta Y^2)$ are the order of local truncation errors.

In Eq. 3.15(a), the term $C_{i,j}^{n}$ can be replaced by $\left(C_{i,j+1}^{n+1}\right)_A$, which is the advected concentration obtained from the advection process. Substituting Eq. (3.15) into Eq. (3.14), one gets:

$$-r_1 C_{i,j-1}^{n+1} + (1+2r_1) C_{i,j}^{n+1} - r_1 C_{i,j+1}^{n+1} = r_2 C_{i-1,j}^{n} - 2r_2 C_{i,j}^{n} + r_2 C_{i+1,j}^{n} + \left(C_{i,j+1}^{n+1}\right)_A \quad (3.16)$$

where $r_1 = \dfrac{\Delta t}{\Delta X^2}$ and $r_2 = \dfrac{\Delta t}{\Delta Y^2}$

Equation (3.16) can also be written as:

$$b_{j-1} C_{i,j-1}^{n+1} + d_{j-1} C_{i,j}^{n+1} + a_{j-1} C_{i,j+1}^{n+1} = C_{i,j}^{n} \quad (3.17)$$

Here $b_{j-1} = -r_1$; $d_{j-1} = (1+2r_1)$; $a_{j-1} = -r_1$;

$$C_{i,j}^{n} = r_2 C_{i-1,j}^{n} - 2r_2 C_{i,j}^{n} + r_2 C_{i+1,j}^{n} + \left(C_{i,j+1}^{n+1}\right)_A \quad (3.18)$$

$$j = 2, 3, \ldots\ldots\ldots\ldots, nX-1 \;;\; i = 1, 2, 3, \ldots\ldots\ldots\ldots, nY$$

For a square computational mesh, $\Delta X = \Delta Y$ and $r_1 = r_2 = r$, one can get

$$-rC_{i,j-1}^{n+1} + (1+2r) C_{i,j}^{n+1} - rC_{i,j+1}^{n+1} = rC_{i-1,j}^{n} - 2rC_{i,j}^{n} + rC_{i+1,j}^{n} + \left(C_{i,j+1}^{n+1}\right)_A \quad (3.19)$$

Equation (3.17) or Eq. (3.19) cannot be solved by itself because it contains three unknown values at time level t = (n+1)Δt. However the application of the corresponding finite difference equation to each of the computational nodes along a row parallel to X-axis gives (nX-2) implicit equations involving nX unknowns. Here nX is the total number of computational nodes in the spatial grid along X-axis. To solve this system of equations two boundary conditions are to be used: one at the upstream and second at downstream end of the flow domain. Each row then results in a tridiagonal linear system of equations and can be solved by using Thomas or double sweep algorithm.

Computations are carried out at time level (n+1) for computational nodes with i = 2 to i = (nY-1). Computation of concentrations for remaining computational nodes having i = 1 and i = nY require introduction of the computational nodes having i = 0 and i = (nY+1) at n^{th} level as shown in Fig. 3.3 and by incorporating derivative boundary conditions meaning that at both the water surface and the channel bed, the fluxes of water and tracer normal to the boundaries are zero, *i.e.*, concentration gradient at the water surface and the channel bed are zero, *i.e.*, $\dfrac{\partial C}{\partial Y} = 0$ at y = 0, d.

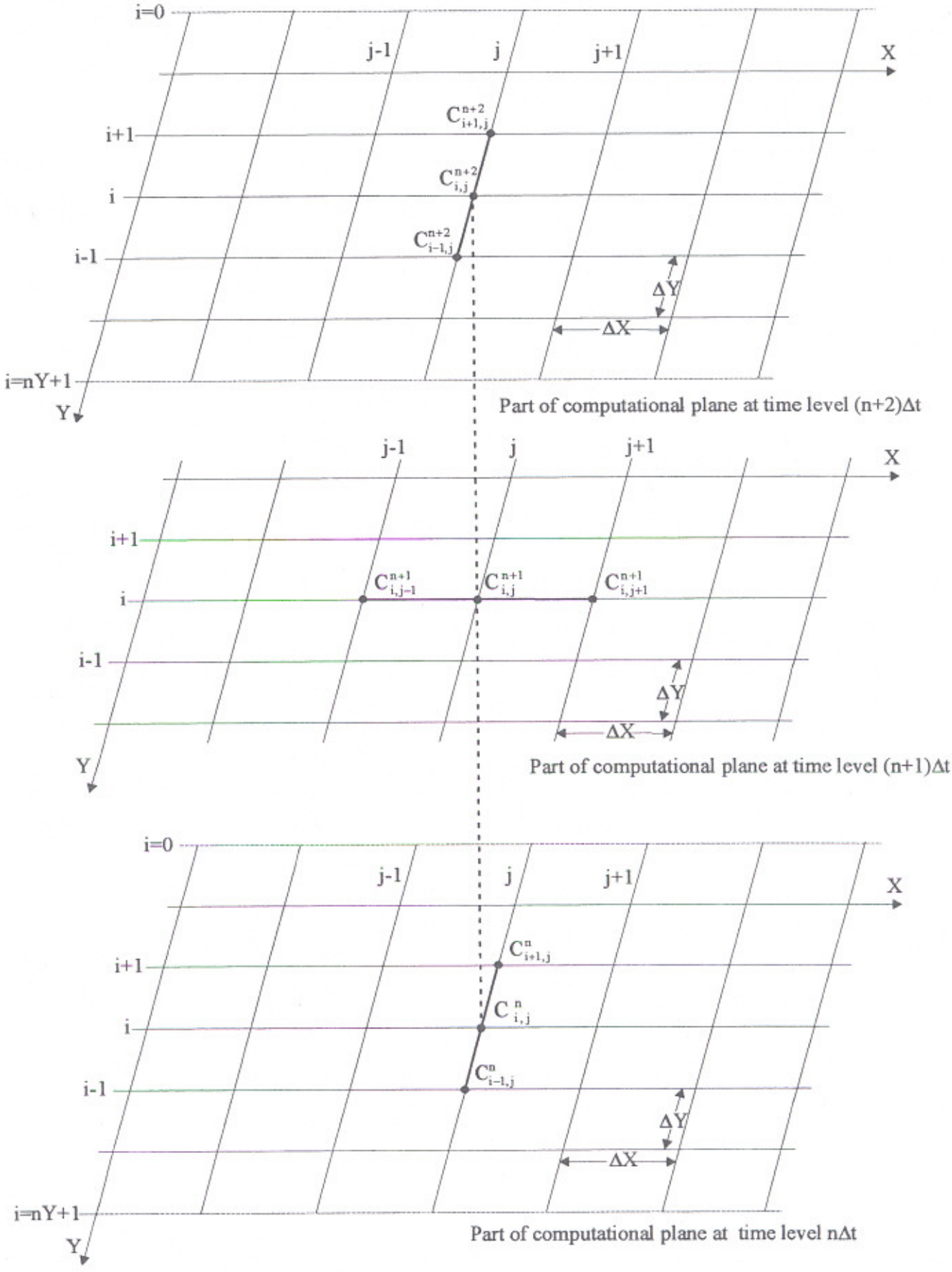

Fig. 3.3 Two-dimesional computational mesh for computations of diffusion compmnent.

Using the central difference approximation for $\frac{\partial C}{\partial Y}$, one can write

$$\frac{C^{n}_{i+1,j} - C^{n}_{i-1,j}}{2\Delta Y} = 0$$

$$C^{n}_{i+1,j} = C^{n}_{i-1,j} \quad \text{at} \quad i = 1 \text{ and } i = nY \tag{3.20}$$

Equation (3.20) reflects that concentration at i = 0 row is equal to concentration at row i = 2 for the same value of j at n^{th} level. Likewise concentration at i = (nY+1) row is equal to concentration at row i = (nY-1). In this way concentration is obtained in entire domain at time level (n+1). The solution of the system of equations for one computational row is discussed in the Section 3.2.3.

Computation of concentration at time level $(n_{even}+2)\Delta t$

To achieve stable solution, the direction of operations for the evaluation of concentration at the next time level, *i.e.*, t = (n+2)Δt, (while index n is even) is now reversed and the solution is advanced from $(n+1)^{th}$ plane to $(n+2)^{th}$ plane by replacing the second order derivative $\frac{\partial^2 C}{\partial Y^2}$ by an implicit finite difference approximation at the $(n+2)^{th}$ level and $\frac{\partial^2 C}{\partial X^2}$ by an explicit one at the $(n+1)^{th}$ level (See; Fig. 3.3). Thus one can write:

$$\frac{\partial C}{\partial t} = \frac{C^{n+2}_{i,j} - C^{n+1}_{i,j}}{\Delta t} + O(\Delta t) \tag{3.21a}$$

$$\frac{\partial^2 C}{\partial X^2} = \frac{C^{n+1}_{i,j-1} - 2C^{n+1}_{i,j} + C^{n+1}_{i,j+1}}{\Delta X^2} + O(\Delta X^2) \tag{3.21b}$$

$$\frac{\partial^2 C}{\partial Y^2} = \frac{C^{n+2}_{i-1,j} - 2C^{n+2}_{i,j} + C^{n+2}_{i+1,j}}{\Delta Y^2} + O(\Delta Y^2) \tag{3.21c}$$

Replacing $\left(C^{n+1}_{i,j}\right)$ in Eq. (3.21a) by $\left(C^{n+2}_{i,j+1}\right)_A$, which is the advected concentration obtained from advection process and substituting Eq. (3.21) into Eq. (3.14), yields:

$$-r_2 C^{n+2}_{i-1,j} + (1 + 2r_2) C^{n+2}_{i,j} - r_2 C^{n+2}_{i+1,j} = r_1 C^{n+1}_{i,j-1} - 2r_1 C^{n+1}_{i,j} + r_1 C^{n+1}_{i,j+1} + \left(C^{n+2}_{i,j+1}\right)_A \tag{3.22}$$

Equation (3.22) can be written as:

$$b_i C_{i-1,j}^{n+2} + d_i C_{i,j}^{n+2} + a_i C_{i+1,j}^{n+2} = C_{i,j}^{n+1} \tag{3.23}$$

Here $b_i = -r_2 ; d_i = (1 + 2r_2); \ a_i = -r_2;$

$$C_{i,j}^{n+1} = r_1 C_{i,j-1}^{n+1} - 2r_1 C_{i,j}^{n+1} + r_1 C_{i,j+1}^{n+1} + \left(C_{i,j+1}^{n+2}\right)_A \quad \text{and} \tag{3.24}$$

$i = 1, 2, 3, \ldots\ldots\ldots\ldots, nY; \qquad j = 2, 3, \ldots\ldots\ldots\ldots, nX - 1$

Application of Eq. (3.23) to each of the computational nodes along a column parallel to Y-axis gives nY implicit linear equations involving (nY+2) unknown values of concentration with two fictitious values at rows i = 0 and i =(nY+1). Application of derivative boundary condition at i =1 and i = nY, *i.e.*, $C_{i-1,j}^{n+2} = C_{i+1,j}^{n+2}$ reduces number of unknowns from (nY+2) to nY for a particular column parallel to Y-axis. Unique solution is obtained, as the numbers of equations are equal to the numbers of unknowns. Similarly computations are made at all other points of the computational mesh of other columns. The solution of the system of equations for any one of the columns is discussed in the Section 3.2.3.

The solution is advanced from $(n+2)^{th}$ level to $(n+3)^{rd}$ level by again reversing the direction of operations and the process is continued until the solution procedure is obtained at all the remaining time levels, every time reversing the direction of operations. The time interval Δt must be the same during the time marching.

ADIM is stable for any value of r_1 and r_2 or r as long as the same time increment is used for all levels. Each individual level is conditionally stable but the combined two levels are completely stable (Smith 1978). The compensation of errors produced by the alternation of direction of operations gives a scheme, which is convergent and stable for all values of r_1 and r_2.

3.2.3 Solution of the System of Equations

(a) Solution of the system of equations at time level $(n_{even}+1)\Delta t$

As discussed in the previous section that finite difference solution of Eq. (3.17) at time t = (n+1)Δt, (while index n is even) along a row parallel to X-axis results in (nX-2) linear equations involving nX unknown at these points. Two boundary conditions: one at the upstream and second at downstream end should be known to reduce number of unknown to (nX-2), *i.e.*, equal to number of linear equations to have unique solution of system of equations. The system of linear equations is tridiagonal in form and can be solved by using Thomas or double sweep algorithm as discussed herein.

Making use of the boundary conditions, the system of linear equations, *i.e.*, Eq. (3.17) for the first row (*i.e.*, for i =1) of computational mesh at time level t = (n+1)Δt can be written as:

$$\begin{bmatrix} d_1 & a_1 & 0 & 0 & 0 & 0 & 0 & 0 \\ b_2 & d_2 & a_2 & 0 & 0 & 0 & 0 & 0 \\ 0 & b_3 & d_3 & a_3 & 0 & 0 & 0 & 0 \\ - & - & - & - & - & - & - & - \\ - & - & - & - & - & - & - & - \\ - & - & - & - & - & - & - & - \\ 0 & 0 & 0 & 0 & b_{nX-3} & d_{nX-3} & a_{nX-3} & 0 \\ 0 & 0 & 0 & 0 & 0 & 0 & b_{nX-2} & d_{nY-2} \end{bmatrix} \times \begin{bmatrix} C_{1,2}^{n+1} \\ C_{1,3}^{n+1} \\ C_{1,4}^{n+1} \\ - \\ - \\ - \\ C_{1,nX-2}^{n+1} \\ C_{1,nX-1}^{n+1} \end{bmatrix} = \begin{bmatrix} C_{1,2}^{n} \\ C_{1,3}^{n} \\ C_{1,4}^{n} \\ - \\ - \\ - \\ C_{1,nX-2}^{n} \\ C_{1,nX-1}^{n} \end{bmatrix} \qquad (3.25)$$

The value of $C_{1,1}^{n+1}$ and $C_{1,nX}^{n+1}$ are known as upstream and downstream boundary conditions. Hence the value of $C_{1,2}^{n}$ and $C_{1,nX-1}^{n}$ calculated by Eq. (3.18) are modified as:

$$C_{1,2}^{n}(\text{new}) = C_{1,2}^{n}(\text{old}) - b_1 C_{1,1}^{n+1}$$

$$C_{1,nX-1}^{n}(\text{new}) = C_{1,nX-1}^{n}(\text{old}) - a_{nX-2} C_{1,nX}^{n+1}$$

The new values of $C_{1,2}^{n}$ and $C_{1,nX-1}^{n}$ are used in Eq. (3.25). The solution of such equations can be obtained using Thomas or Double Sweep algorithm. A computational procedure due to Thomas is described below (Conte and deBoor 1980; Sastry 1995):

(i) Compute b_{j-1}, d_{j-1} and a_{j-1} for j = 2, 3, ..., nX-1.

(ii) Set $\alpha = a_1$; $\beta = d_1$; $rr = \dfrac{b_2}{d_1}$ and compute

$$d_2 = d_2 - rr \times a_1$$

$$C_{1,3}^{n} = C_{1,3}^{n} - rr \times C_{1,2}^{n}$$

(iii) Set $rr = \dfrac{b_{j+1}}{d_j}$; j = 2,3, ..., nX-3 and compute

$$d_{j+1} = d_{j+1} - rr \times a_j$$

$$C_{1,j+2}^{n} = C_{1,j+2}^{n} - rr \times C_{1,j+1}^{n}$$

(iv) Finally compute $C_{1,nX-1}^{n+1}, C_{1,nX-2}^{n+1}, \ldots\ldots\ldots\ldots, C_{1,2}^{n+1}$ by back substitution as:

$$C_{1,nX-1}^{n+1} = \frac{C_{1,nX-1}^{n}}{d_{nX-2}}$$

$$C_{1,j}^{n+1} = \left(\frac{C_{1,j}^{n} - a_{j-1} C_{1,j+1}^{n+1}}{d_{j-1}} \right); \; j = nX\text{-}2,\ nX\text{-}3, \ldots\ldots\ldots\ldots, 3.$$

$$C_{1,2}^{n+1} = \frac{\left(C_{1,2}^{n} - \alpha C_{1,3}^{n+1} \right)}{\beta}$$

Similarly the solution at all other computational nodes of the grid *i.e.* for rows with i = 2 to i = nY at time t = (n+1)Δt is obtained.

(b) Solution of the system of equations at time level $(n_{even}+2)\Delta t$

Application of Eq. (3.23) to each of 'nY' nodal points of the computational mesh along the column parallel to Y-axis gives nY equations for obtaining values of (nY+2) unknowns at time t = (n+2)Δt, (while n is even). Using the derivative boundary conditions, the number of unknowns are reduced to nY. The system of linear equations, *i.e.*, Eq. (3.23) is tridiagonal in form and can be solved again by using Thomas or double sweep algorithm.

Making use of the derivative boundary condition, the linear system of equations for the second column (*i.e.*, for j = 2) parallel to the first column (*i.e.*, when j = 1 and Y-axis at time t = (n+2)Δt can be expressed as:

$$\begin{bmatrix} d_1 & a_1 & 0 & 0 & 0 & 0 & 0 & 0 \\ b_2 & d_2 & a_2 & 0 & 0 & 0 & 0 & 0 \\ 0 & b_3 & d_3 & a_3 & 0 & 0 & 0 & 0 \\ - & - & - & - & - & - & - & - \\ - & - & - & - & - & - & - & - \\ - & - & - & - & - & - & - & - \\ 0 & 0 & 0 & 0 & b_{nY-1} & d_{nY-1} & a_{nY-1} & 0 \\ 0 & 0 & 0 & 0 & 0 & 0 & b_{nY} & d_{nY} \end{bmatrix} \times \begin{bmatrix} C_{1,2}^{n+2} \\ C_{2,2}^{n+2} \\ C_{3,2}^{n+2} \\ - \\ - \\ - \\ C_{nY-1,2}^{n+2} \\ C_{nY,2}^{n+2} \end{bmatrix} = \begin{bmatrix} C_{1,2}^{n+1} \\ C_{2,2}^{n+1} \\ C_{3,2}^{n+1} \\ - \\ - \\ - \\ C_{nY-1,2}^{n+1} \\ C_{nY,2}^{n+1} \end{bmatrix} \quad (3.26)$$

Solution of these equations can be obtained using Thomas or Double Sweep algorithm as:

(i) Compute b_i, d_i and a_i, for i = 1,2,3, ..., nY.

(ii) Set $\alpha = a_1$; $\beta = d_1$; $rr = \frac{b_2}{d_1}$ and compute

$$d_2 = d_2 - rr \times a_1$$

$$C_{2,2}^{n+1} = C_{2,2}^{n+1} - rr \times C_{1,2}^{n+1}$$

(iii) Set $\frac{b_{i+2}}{d_{i+1}} = rr$ for i = 2,3, ..., nY-1 and compute

$$d_{i+1} = d_{i+1} - rr \times a_i$$

$$C_{i+1,2}^{n+1} = C_{i+1,2}^{n+1} - rr \times C_{i,2}^{n+1}$$

(iv) Finally compute $C_{nY,2}^{n+2}, C_{nY-1,2}^{n+2}, \ldots\ldots\ldots\ldots, C_{1,2}^{n+2}$ by using back substitution as:

$$C_{nY,2}^{n+2} = \frac{C_{nY,2}^{n+1}}{d_{nY}}$$

$$C_{i,2}^{n+2} = \left(\frac{C_{i,2}^{n+1} - a_i C_{i+1,2}^{n+2}}{d_i} \right) ; \text{ for } i = nY-1, nY-2, \ldots\ldots\ldots\ldots, 2.$$

$$C_{1,2}^{n+2} = \left(\frac{C_{1,2}^{n+1} - \alpha C_{2,2}^{n+2}}{\beta} \right)$$

Similarly the solution is obtained at all nodes of the computational mesh, *i.e.*, for the other columns with j = 3 to j = nX-1 and time t = (n+2)Δt.

The solution is advanced from (n+2)Δt time level to (n+3)Δt by reversing the direction of operations and obtaining solution as described before. The process is continued till the solution at all time levels is known. This procedure has been found to be robust and very efficient (Sastry 1995). A flow chart depicting the computational procedure described above is shown in Fig. 3.4.

3.2.4 Initial, Boundary and Derivative Boundary Conditions

The initial, boundary and derivative boundary conditions are required to obtain unique solution of two-dimensional advection-diffusion model as discussed above. The initial condition is to be specified over the considered reach length of the stream for the initial time

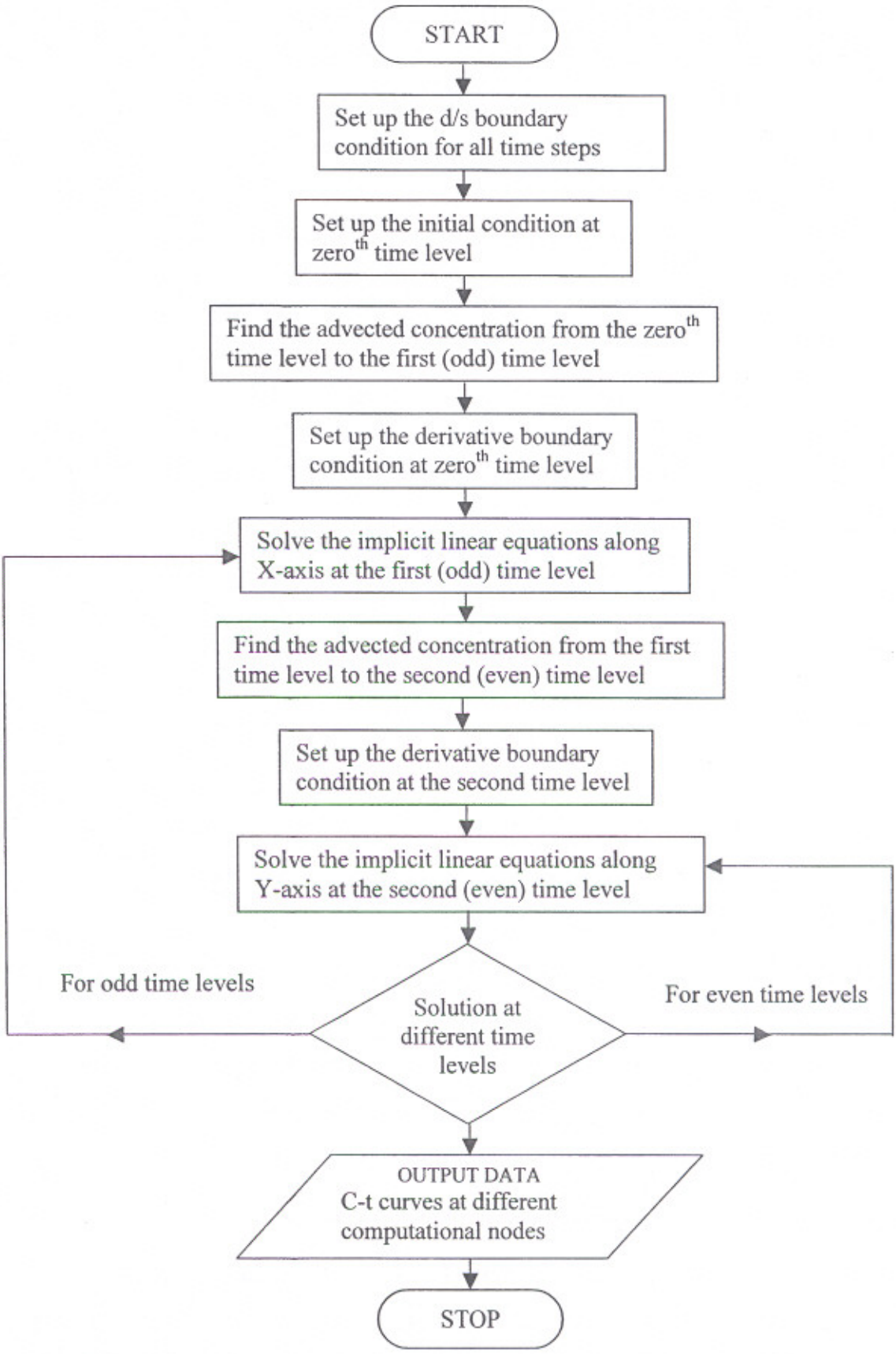

Fig. 3.4 Flow chart depicting the computational procedure

t_o (it is the time before the injection of the pollutant) in the form of spatial concentration profile $C(X,Y)_{t_o}$. Generally before the injection of the pollutant, $C(X,Y)_{t_o} = 0$. However, if in some cases $C(X,Y)_{t_o} \neq 0$, its value should be known at all sections of the stream.

The upstream boundary condition is that the value of concentration is known at all the computational nodes at upstream in the form of concentration profiles. The downstream boundary condition is that at a very large distance from the injection point of the pollutant, the concentration of the pollutant is known, generally it is equal to zero for slug injection.

The derivative boundary condition is required to eliminate the fictitious computational nodes, outside the boundary of computational mesh. The derivative boundary condition is that the flux of tracer normal to the boundaries are zero, at the water surface and at the channel bed, *i.e.*, there is no concentration gradient at the water surface and the channel bed.

The initial, boundary and derivative conditions may be summarized as follows:

Initial condition:

$$C(X,Y)_{t_o} = 0 \text{ or Known; for } X, Y \geq 0 \tag{3.27}$$

Where t_o is the time before the injection of the pollutant.

Boundary conditions:

$$\text{(a) } C(X_1, Y_i, t) = \text{Known; for } t \geq 0 \tag{3.28}$$

X_1 and Y_i are the upstream nodal points

$$\text{(b) } C(X_\infty, Y_\infty, t) = 0 \text{ (for slug injection); for } t > 0 \tag{3.29}$$

Derivative boundary condition:

$$E_y \frac{\partial C}{\partial Y} = 0 \quad \text{at} \quad y = 0, d \tag{3.30}$$

3.3 DETERMINATION OF E_x USING THE NUMERICAL SCHEME

As discussed in Chapter-II, the values of vertical mixing coefficient E_y can be satisfactorily predicted using relationships available in literature, however the value of longitudinal mixing coefficient E_x cannot be computed reliably. Therefore it is proposed to extend the proposed

numerical scheme for the purpose of determination of E_x by using observations of C-t profiles. The method of one-dimensional grid search method used for the purpose is described below.

3.3.1 One-Dimensional Grid Search Method

This method is based on the bisection procedure, which is used to find roots of one-dimensional functions. Also by this method, one can find the optimum value of E_x, which is such that it produces maximum agreement between the predicted and the observed C-t curves at the stations. The agreement between the predicted and the observed C-t curves can be judged in this case in terms of error (ERS), which is defined as (See; Fig. 3.5)

$$\text{ERS, \%} = \left(1 - \frac{\text{Overlapping (shaded area)}}{\text{Area of observed C - t curve}}\right) \text{x } 100 \tag{3.31}$$

For a number of C-t curves at different elevations at a station, weighted error is computed as:

$$\text{Weighted error} = \frac{\sum_{k=1}^{N_1} \text{ERS}(k) \text{ x } A(k)}{\sum_{k=1}^{N_1} A(k)} \tag{3.32}$$

Here A (k) = area of observed C-t curves 'k'; ERS(k) = error in the C-t curves 'k' and N_1 = total number of C-t curves at a station.

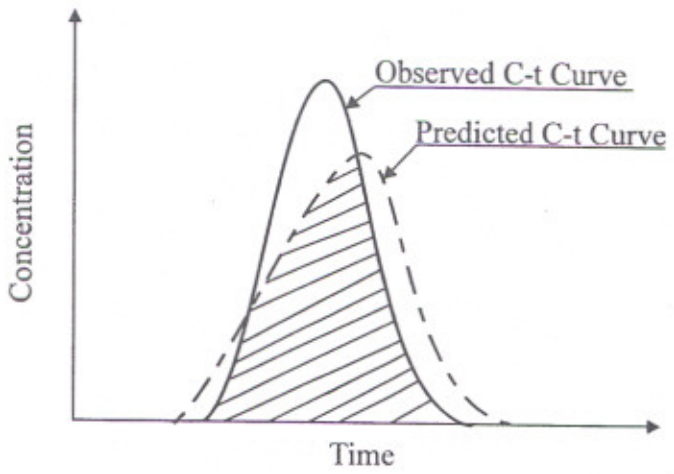

Fig. 3.5 Definition of error

Using observed tracer concentration profiles at the upstream most station as input, C-t curves at the downstream stations and at different elevations along the depth are predicted by the

proposed numerical scheme by first using a trial value of E_x. Thus computed C-t curves are compared with the corresponding observed C-t curves and the weighted error at each station is calculated by using Eq. (3.32). Average error, ERR is calculated next by taking arithmetic mean of all the weighted errors. The values of E_x producing minimum value of ERR, is considered as the optimum one and same is determined using the procedure illustrated below.

A global optimum value of E_x exists due to parabolic nature of Eq. (2.36) (See; Fig. 3.6). The initial approximate value of E_x is calculated by method of Fischer et al. (1979) involving triple integration of longitudinal velocity profile in transverse direction. Let the initial E_x correspond to point ① (See; Fig. 3.6). An incremental value, ΔE_x of longitudinal mixing coefficient equal to one tenth of the initial E_x is taken and error is calculated at the points ② and③. The point corresponding to minimum error is searched. As in this case, such point shall be ②. Now error is calculated at the next point say ④ and again the minimum error is searched; such point again shall be ②. This means that the optimum value of E_x lies somewhere in the bracketing triplet (①, ② and ④). Now the grid is bisected and ERR at ⑤ and ERR at ⑥ are calculated. Now if ERR at ② < ERR at ⑤ and ERR at⑥, then the grid is again bisected and same process is followed, until one attains the desired accuracy as illustrated in Fig. 3.6.

The algorithm for the determination of E_x using the proposed method is described through flow chart shown in Fig. 3.7.

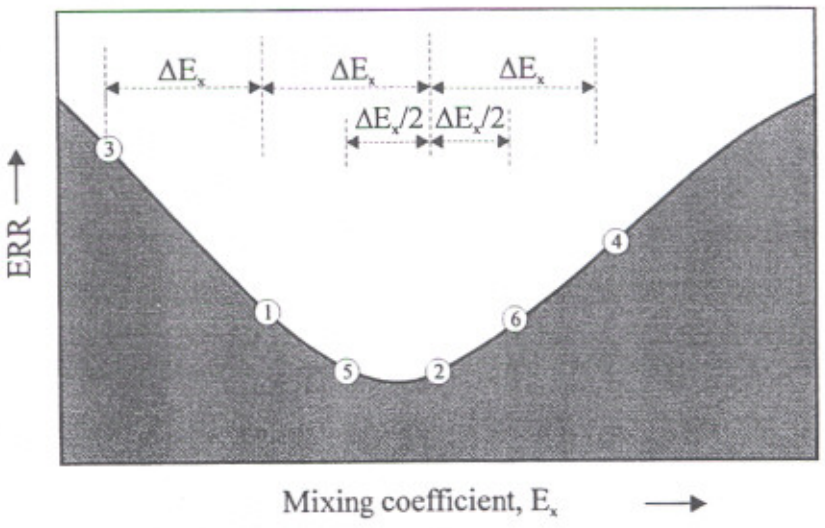

Fig. 3.6 One-dimensional grid search method

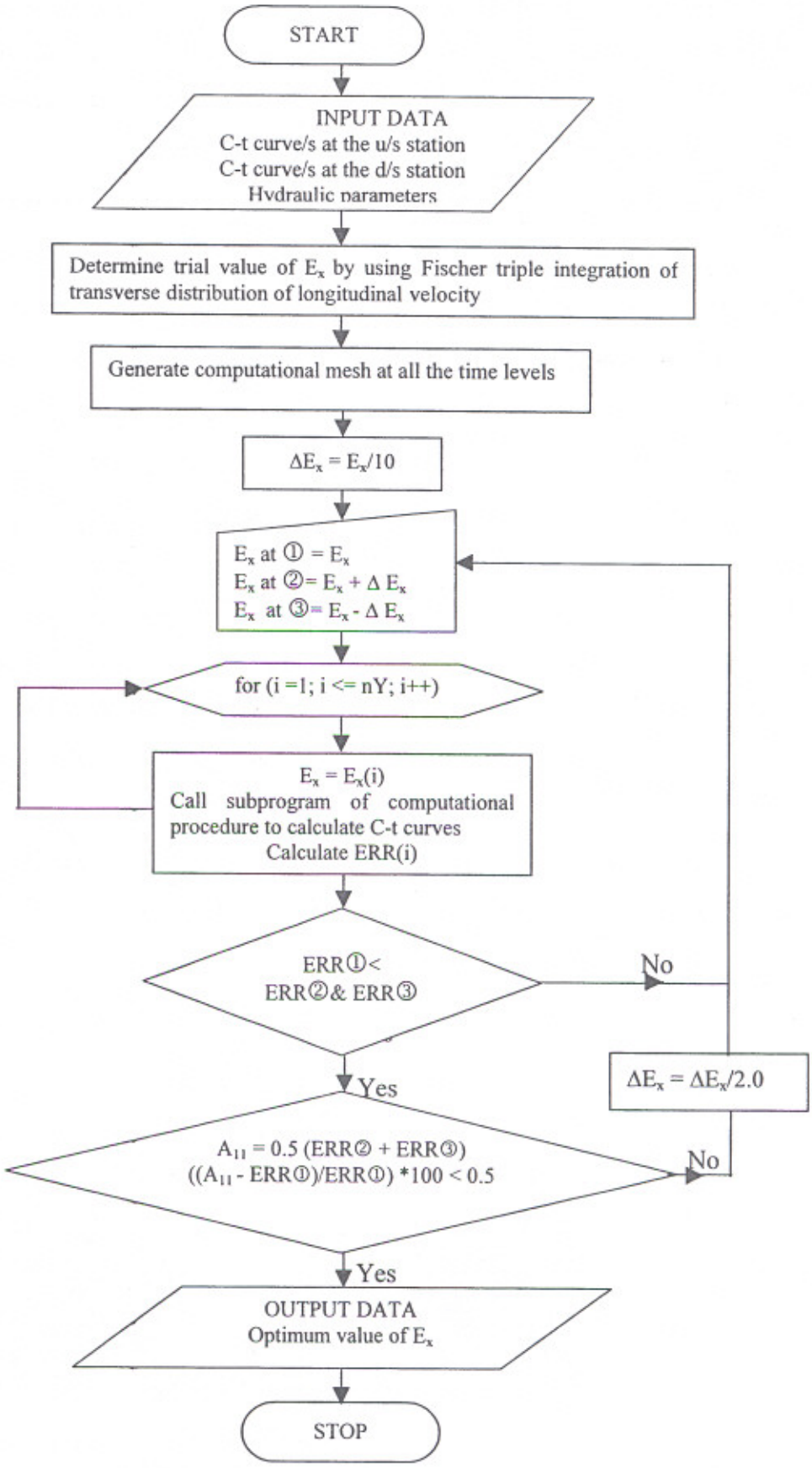

Fig. 3.7 Flow chart for the determination of E_x

3.4 PROCEDURE FOR THE COMPUTATION OF C-t CURVES USING THE PROPOSED NUMERICAL SCHEME

The stepwise procedure for the determination of C-t curves in clear-water and sediment-laden flows using the proposed numerical scheme, for given channel and flow characteristics, E_x and E_y values and the concentration profiles at the boundary section is described below. Observed C-t profiles at different elevations along the flow depth at the upstream most station are to be used as input.

1. Generate the computational mesh for different time planes from known values of velocity at the computational nodes along the depth of flow.
2. Set up the initial condition, upstream and downstream boundary condition as well as the derivative boundary condition for all the time planes.
3. Determine the advected concentration at each of the computational nodes at the first time level (odd) from zeroth time level (*i.e.*, initial condition).
4. Compute the concentration due to diffusion process at the first time level by using alternate-direction implicit method by writing the equations implicitly along a row in terms of explicit equations at the zeroth time level. To this solution advected concentration is added for obtaining the final concentration. Solve these implicit equations by using double sweep algorithm. Repeat the computations for all the computational nodes of the other rows.
5. For the second time level (even) change the direction of operations by writing the equations implicitly along a column in terms of explicit equations at the first time level and adding the advected concentration obtained from the first time level. Again solve these implicit equations by using double sweep algorithm. Repeat the computations for all the computational nodes of the other columns.
6. Find the solution at the remaining time levels by reversing the direction of operations every time for each time plane movement.
7. List C-t curves ordinates at the desired downstream stations and at desired elevations along the flow depth.

The computer code for the above procedure is described in a flow chart given in Fig. 3.8.

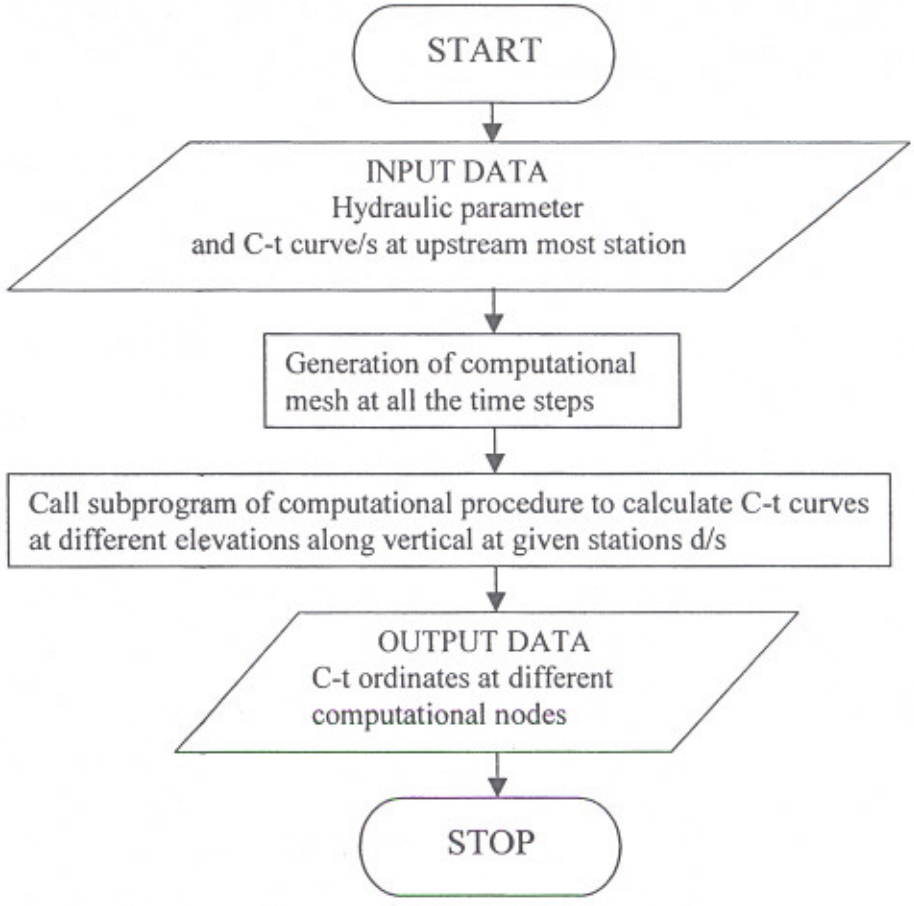

Fig. 3.8 Flow chart for the computation of C-t curves

3.5 THE COMPUTER CODE

The mathematical formulations described in this chapter are developed into a computer program that is used to study the various aspects pertaining to the two-dimensional mixing of conservative pollutants in open channels. The computer code has been developed in object-oriented C^{++} programme which typically consists of a number of objects, which communicate with each other by calling one another's member functions.

The flow charts for the various modules of the programs have been shown in Figs. 3.4, 3.7 and 3.8. The computer programme has been tested on IBM compatible computer Pentium-IV turbo C^{++} complier version 3.0.

3.6 ILLUSTRATION OF THE PROPOSED NUMERICAL SCHEME

Application of the proposed numerical scheme is illustrated by hypothesizing the transverse line injection of tracer at the surface of flow, mid-depth and at the channel bed. The temporal

variation of concentration of transverse line source is assumed to follow a sine curve having equation $C = 100 \sin \omega t$, with $\omega = \frac{\pi}{20}$. The values of other parameters are $d = 0.15\,m$, $E_x = 0.026\ m^2/s$, $E_y = 0.00035\ m^2/s$. Using proposed scheme and above input data, the tracer concentration profiles at three elevations viz. at the water surface, mid-depth and bottom at an interval of 1 m distance along longitudinal direction are computed and shown in Figs. 3.9, 3.10 and 3.11. Figure 3.9 shows computed profiles of tracer concentration at different elevations along the vertical while transverse line tracer was injected at the flow surface. Figure 3.9 shows that at distances near the source, the concentration at the depth with y/d = 0.5 and near channel bottom while y/d = 0.0 is zero but as the tracer travels downstream, the concentration at y/d = 1.0 starts decreasing whereas the concentration at y/d = 0.5 and zero starts increasing while the tracer mixes vertically. After some distance, the tracer mixes completely in the vertical direction and the three concentration profiles overlap indicating beginning the zone of longitudinal mixing. Figure 3.9(b) shows spatial variation of peak concentration. The similar trend is indicated while the tracer is injected at y/d = 0.5 (See; Fig. 3.10) and at y/d = 0.0 (See; Fig. 3.11). It is noticed that for input data considered herein the mixing length is about 12 m for the transverse line source placed at y/d = 0.5 whereas for line source at y/d = 1.0 and zero, the mixing length is more than 14 m.

The proposed numerical model is mass conservative. The mass conservation of the proposed numerical scheme is verified by calculating the mass of the dye injected upstream at a station and mass of the dye recovered at different stations.

3.7 CONCLUDING REMARKS

A numerical scheme based on the Split operator approach is proposed for the solution of two-dimensional advection-diffusion equation. Exact solution of advection process has been obtained by developing a variable spatial grid corresponding to the velocity of flow for computational nodes at y/d = 1.0 so that the root of the trajectory of the concentration at y/d = 1.0 fall at the computational nodes where the concentration is known. For the computational nodes with y/d < 1.0, velocity of flow is smaller due to velocity defect in the vertical therefore, cubic spline interpolation scheme of Schohl and Holly (1991) has been used to obtain the solution of the advection process at such computational nodes. For simulation of diffusion process, alternate-direction implicit method (ADIM) suggested by Smith (1978) has been used. This is two-step approach method which is stable and convergent. The proposed

scheme has been extended for determination of E_x values by incorporating in it the one-dimensional grid search.

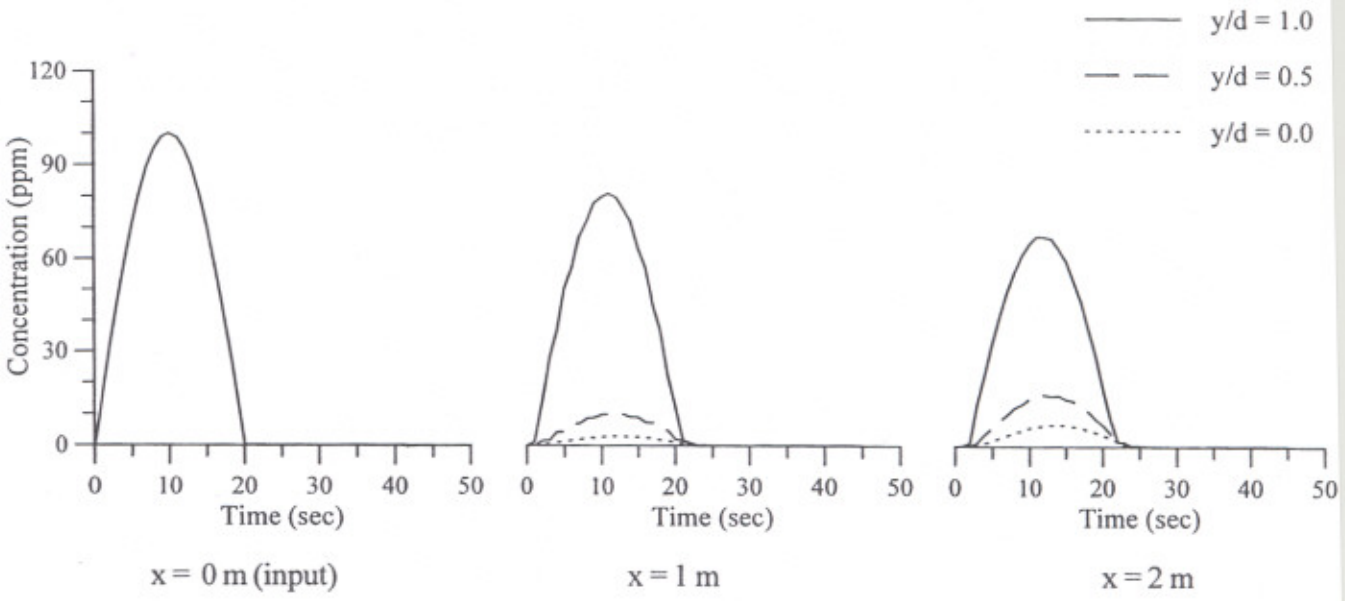

x = 0 m (input) x = 1 m x = 2 m

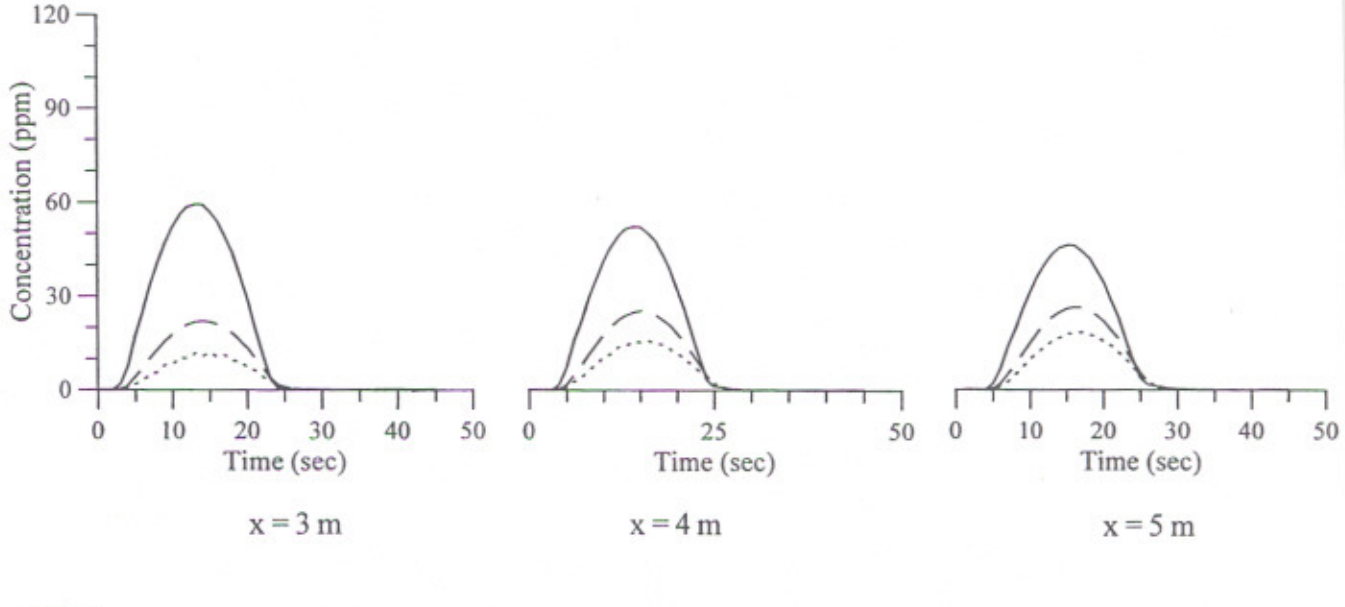

x = 3 m x = 4 m x = 5 m

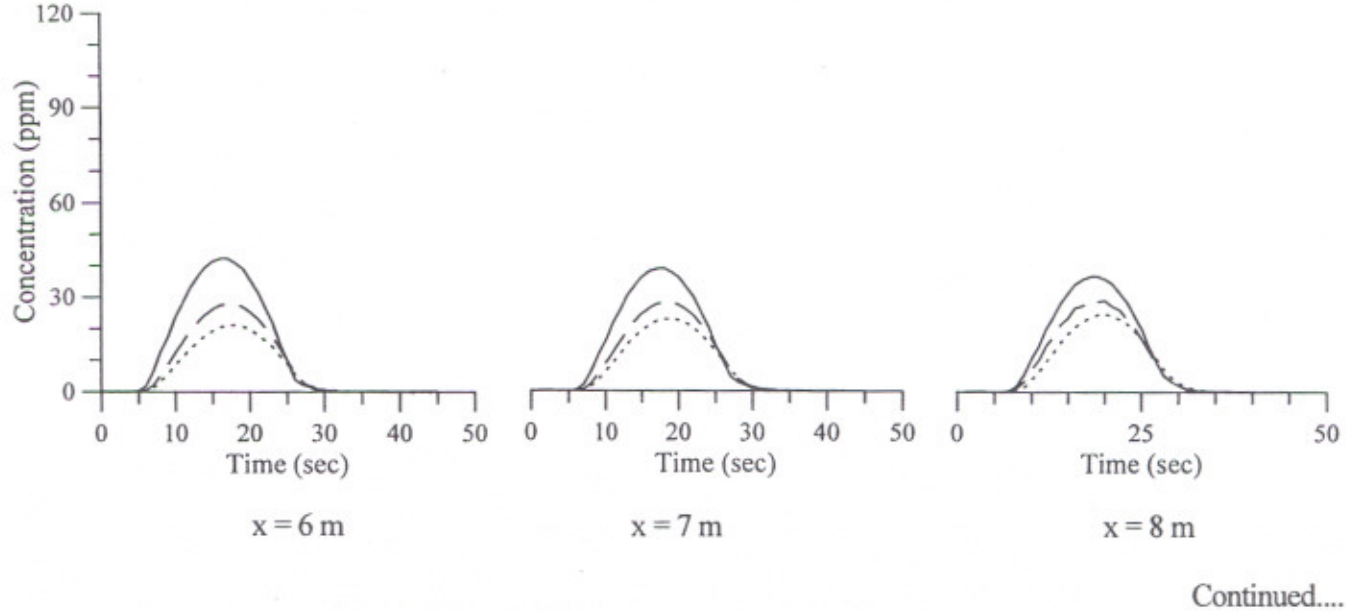

x = 6 m x = 7 m x = 8 m

Continued....

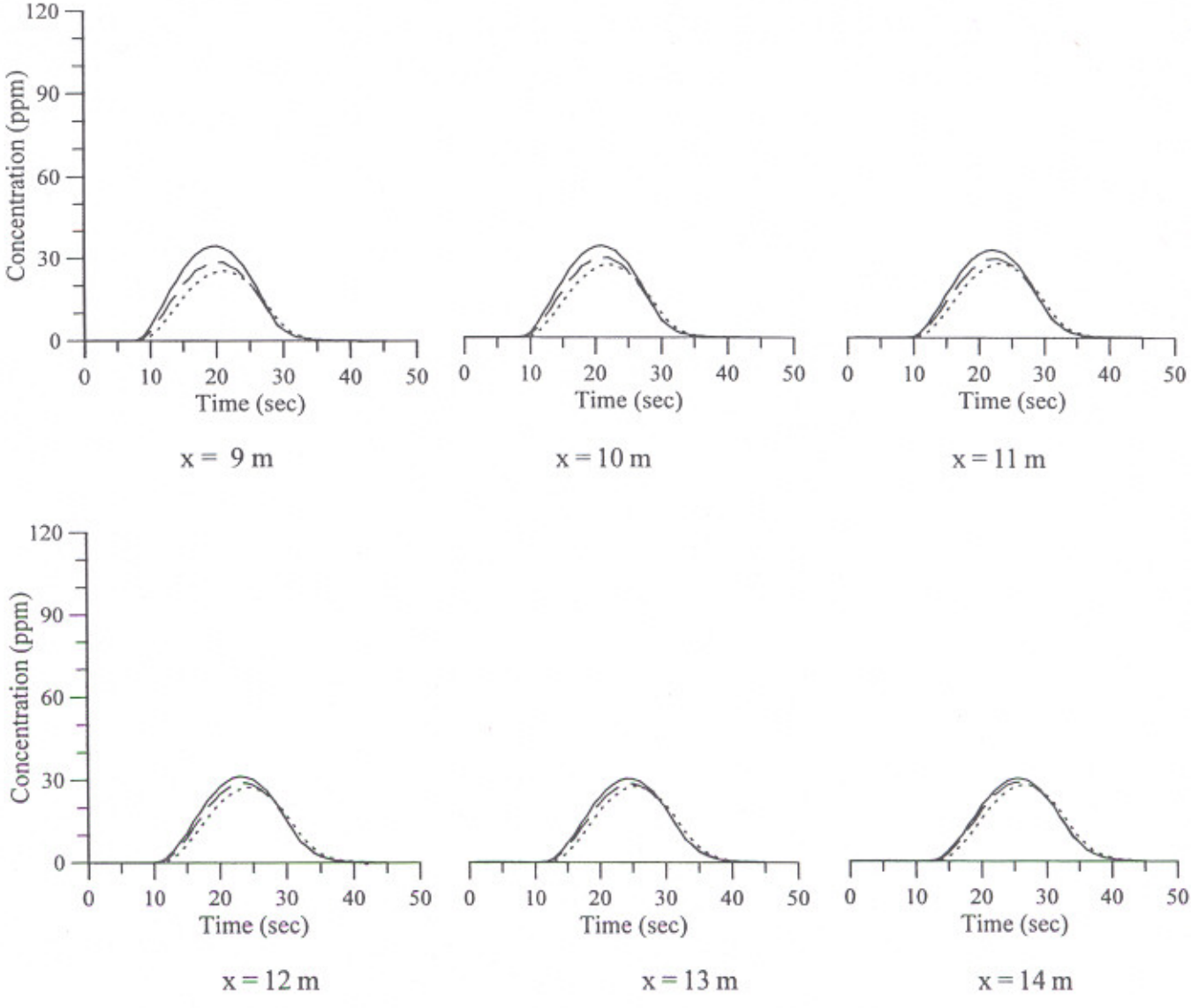

Fig.3.9 (a) Variations in concentration profiles at three sections along vertical in downstream of the injection section (Transverse line source at y/d = 1.0)

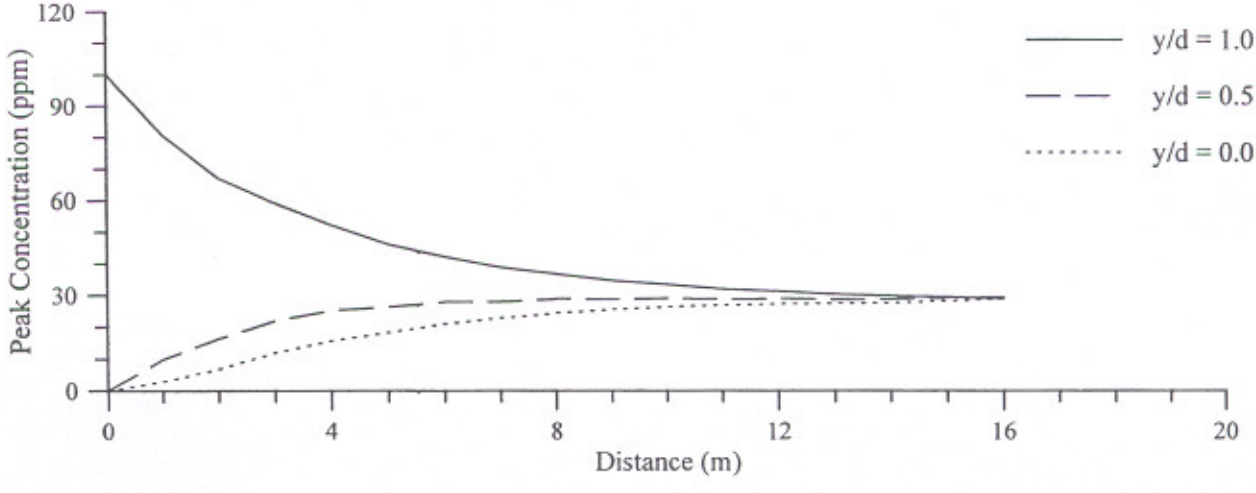

Fig.3.9(b) Spatial variation of peak concentration for transverse line source at y/d =1.0

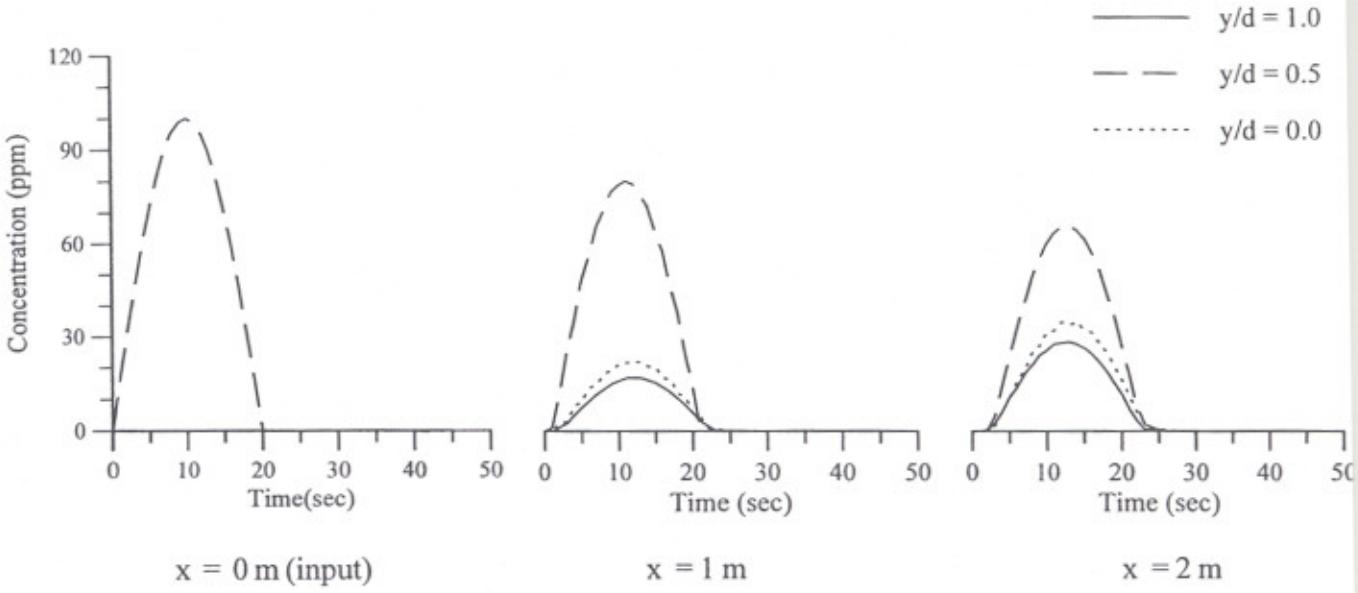

x = 0 m (input) x = 1 m x = 2 m

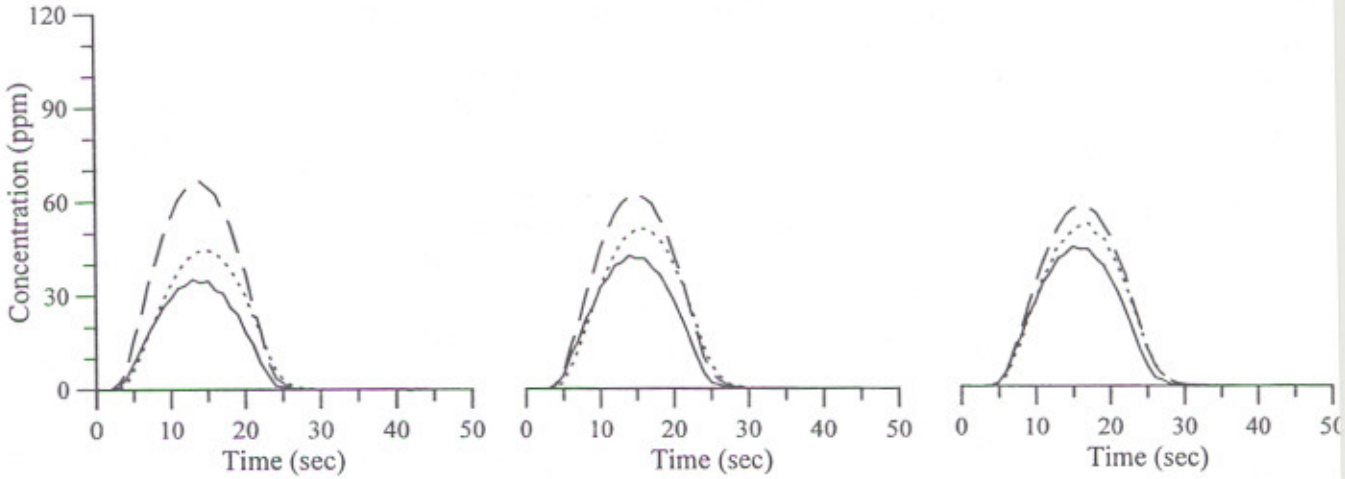

x = 3 m x = 4 m x = 5 m

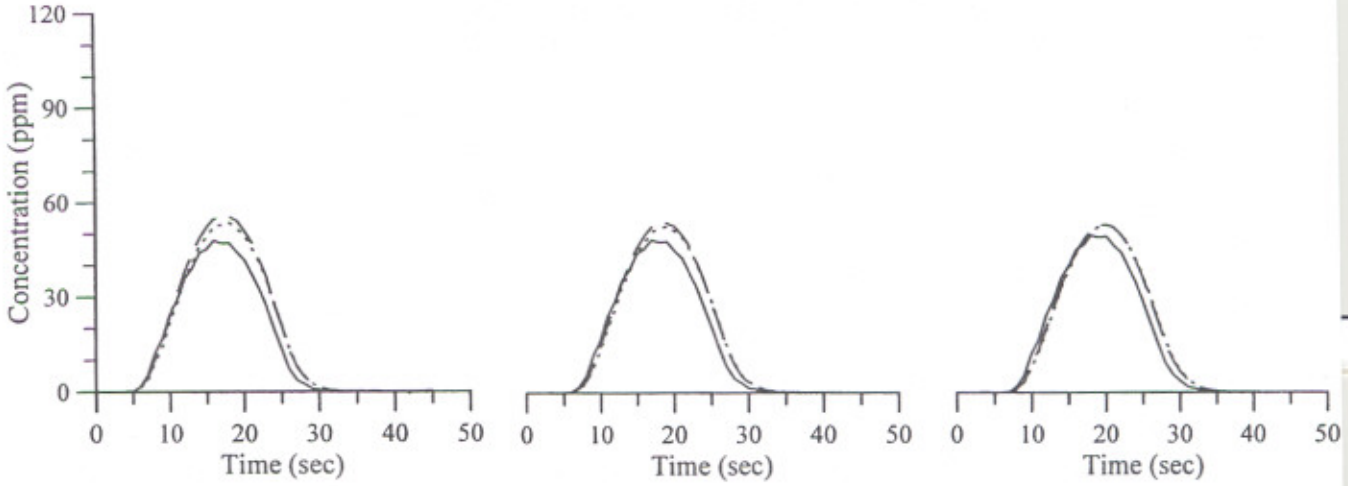

x = 6 m x = 7 m x = 8 m

Continued....

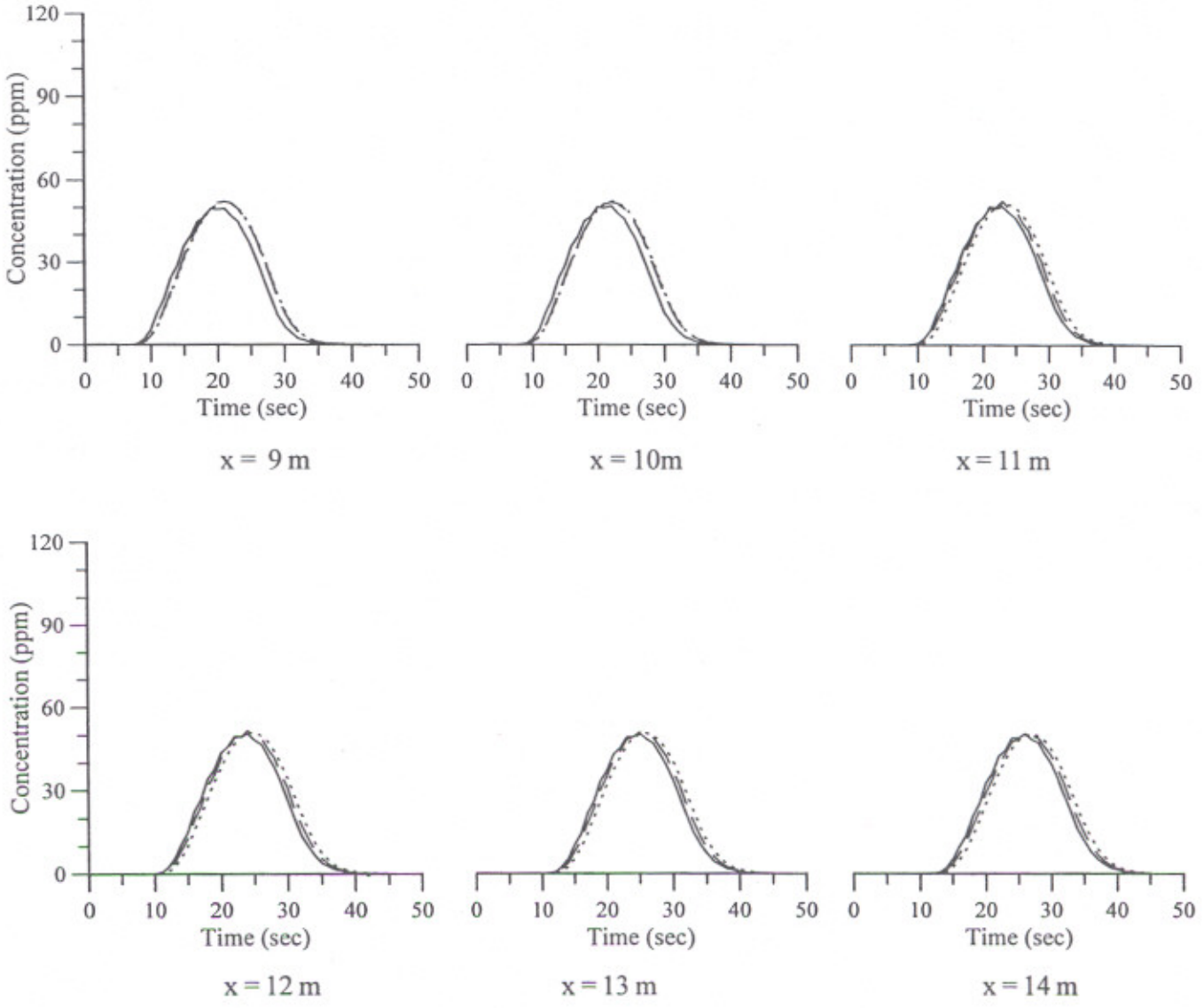

Fig. 3.10 (a) Variations in concentration profiles at three sections along vertical in downstream of the injection section (Transverse line source at y/d = 0.5)

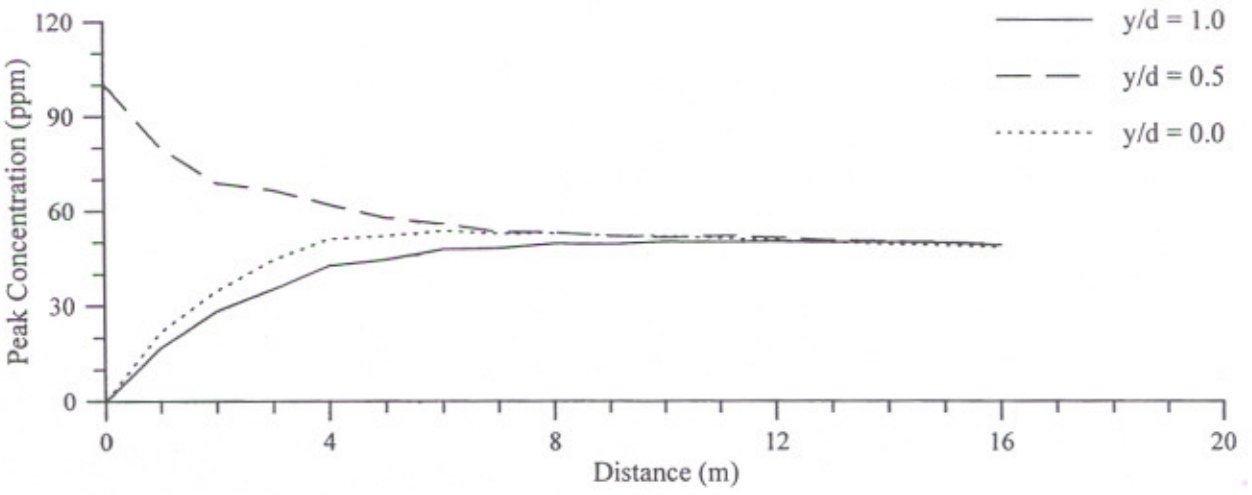

Fig. 3.10 (b) Spatial variation of peak concentration for transverse line source at y/d = 0.5

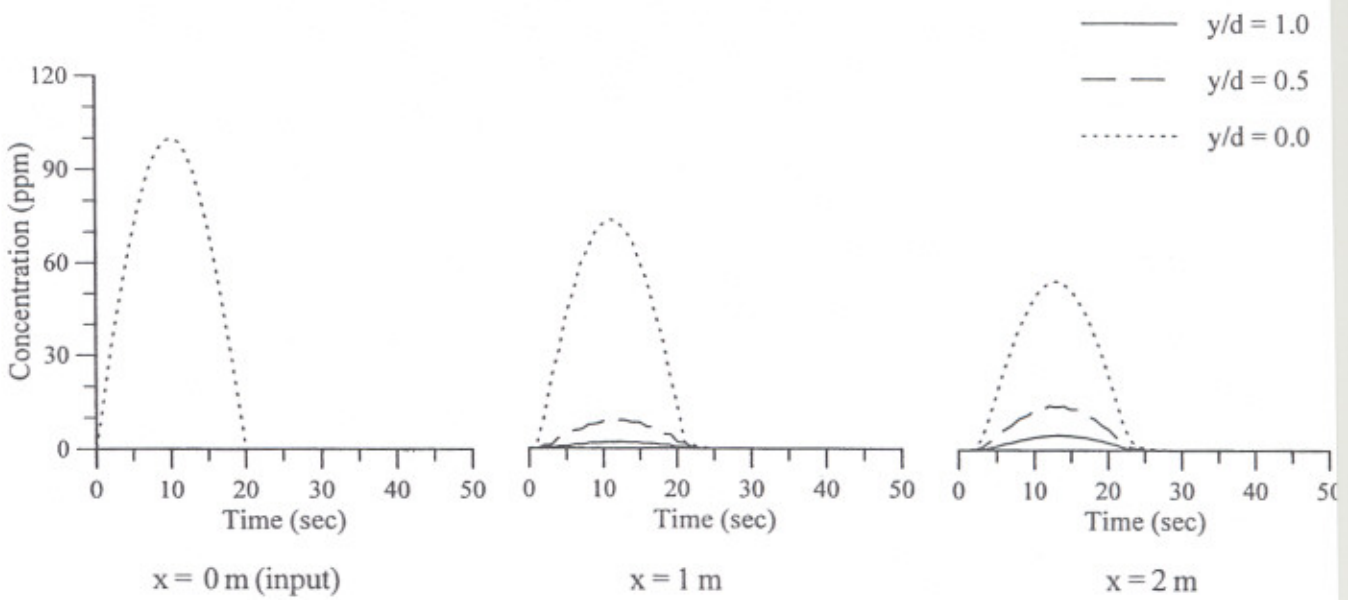

x = 0 m (input) x = 1 m x = 2 m

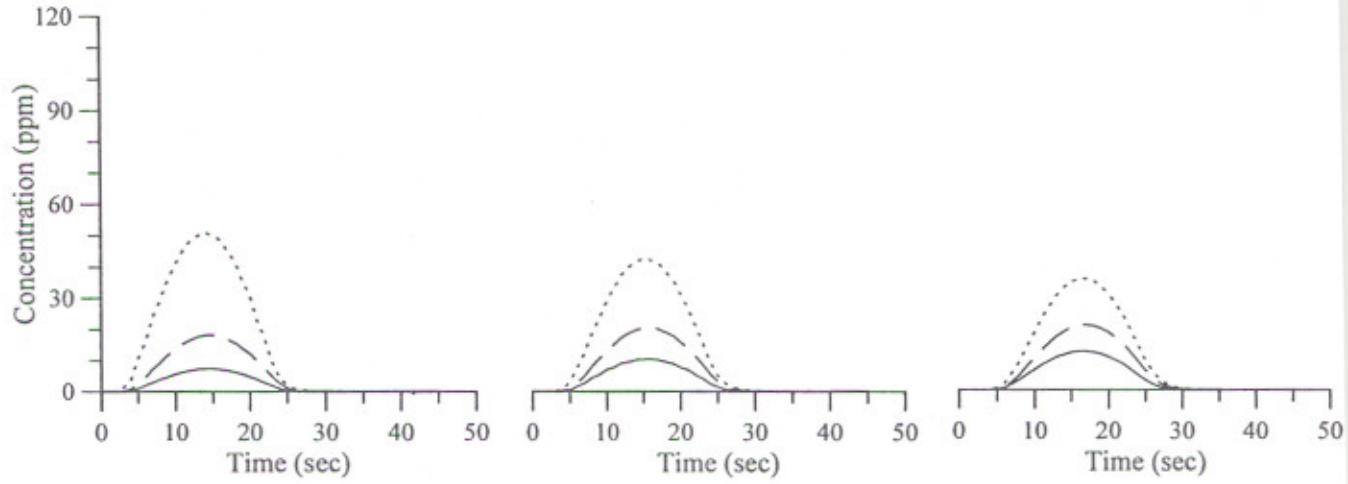

x = 3 m x = 4 m x = 5 m

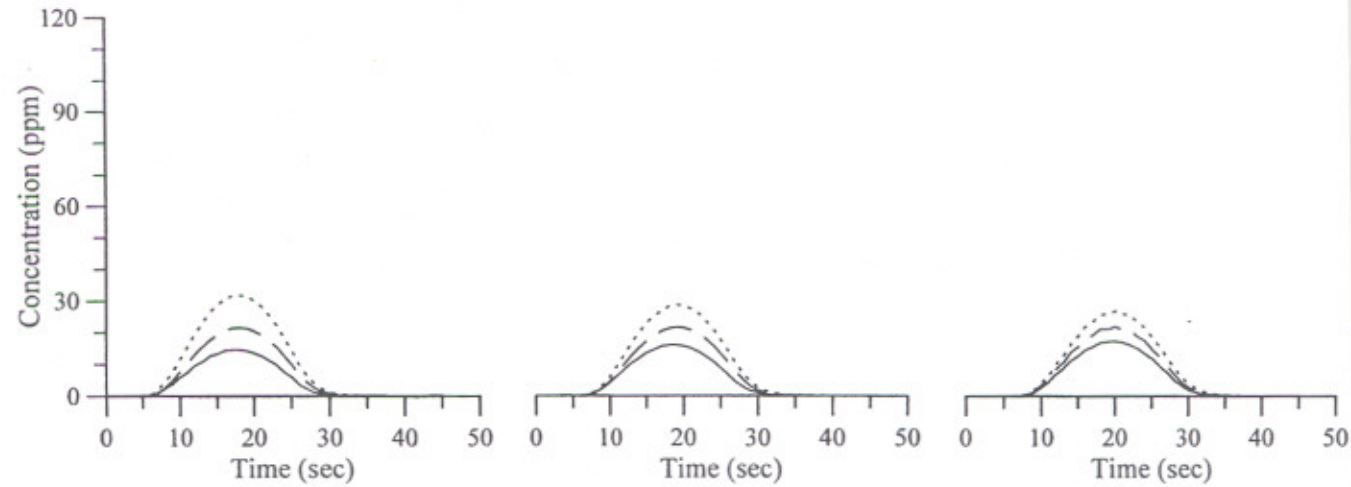

x = 6 m x = 7 m x = 8 m

Continued....

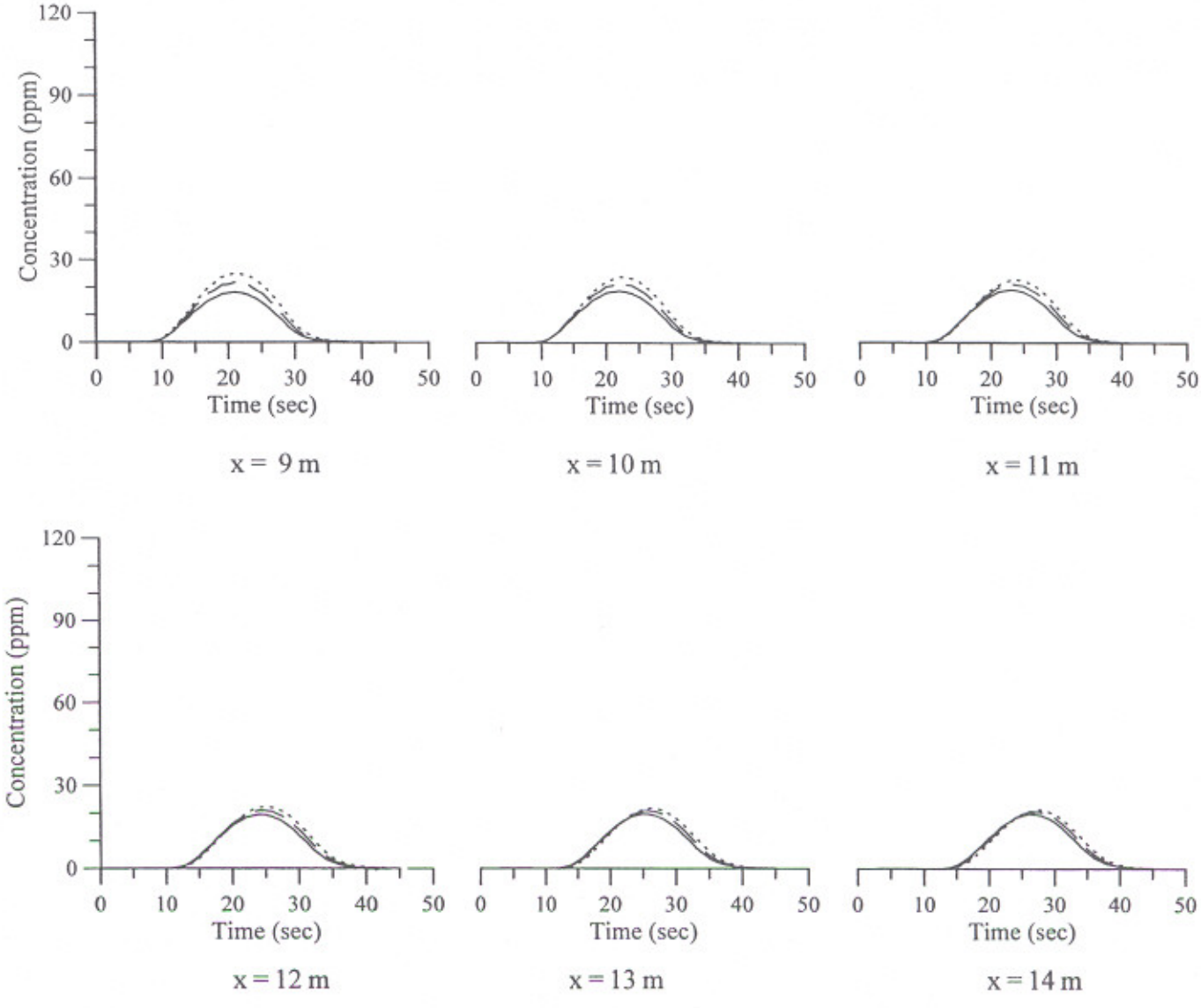

Fig. 3.11 (a) Variations in concentration profiles at three sections along vertical in downstream of the injection section (Transverse line source at y/d = 0.0)

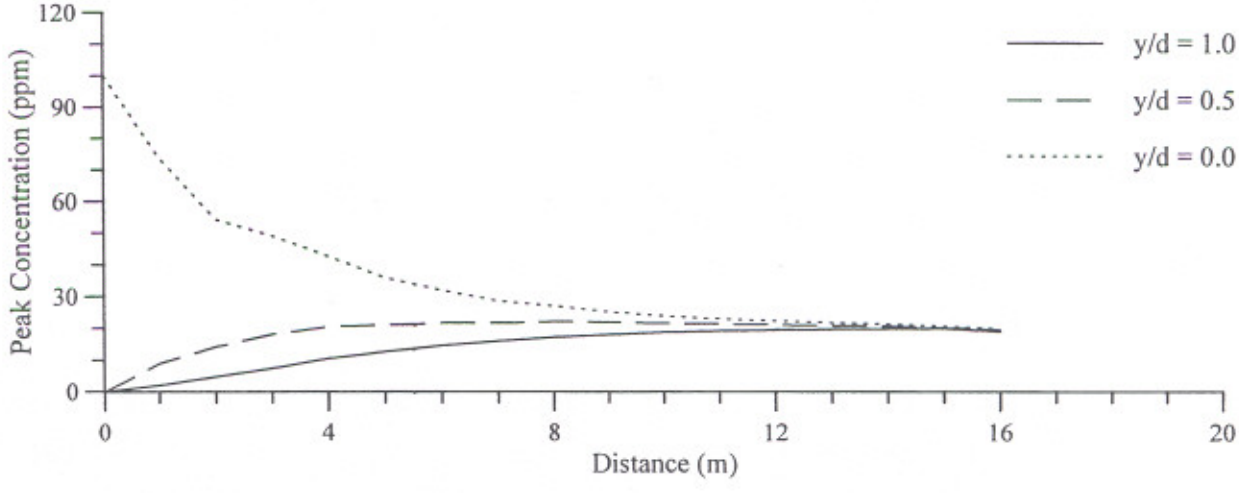

Fig. 3.11 (b) Spatial variation of peak concentration for transverse line source at y/d = 0.0

Chapter

4

EXPERIMENTAL PROGRAMME

4.1 INTRODUCTION

Experiments were conducted in the Hydraulics Laboratory of Department of Civil Engineering, Indian Institute of Technology, Roorkee (Erstwhile University of Roorkee, Roorkee).

The review of literature presented in Chapter-II and the theoretical work presented in Chapter-III revealed that detailed data are required on the following aspects of the two-dimensional mixing of pollutants.

i) Two-dimensional mixing of conservative pollutants in clear-water flows due to a transverse line slug injection source.

ii) Effect of suspended sediment load on the two-dimensional mixing of conservative pollutants due to a transverse line slug injection source.

iii) Effect of velocity distribution on the two-dimensional mixing in clear-water and sediment-laden flows.

iv) Predictors for mixing coefficients for both clear-water and in the presence of suspended sediments.

The present experimental programme was designed to procure data on the above aspects. The experiments were conducted for both clear-water and sediment-laden flows under steady and uniform flow conditions. Rhodamine WT dye was used as a tracer. Tracer concentrations were continuously measured by Fluorometer. Two uniform sands of sizes 0.064 mm and 0.024 mm were used as sediment.

4.2 EXPERIMENTAL SET UP

Carefully controlled experiments were planned to study the process of two-dimensional mixing of conservative pollutants in open channel flows. The experiments were conducted in

a rectangular flume. A sector orifice meter was used to measure the discharge passing through the flume. Point velocities were measured by using Prandtl pitot tube. A Fluorometer was used to measure the tracer concentration downstream of its injection site. Tracer injection sampler and collecting sampler were used to inject and collect the tracer, respectively. Rhodamine WT fluorescent dye was used as the tracer because of its:

i) Conservative nature (low decay rate)
ii) Neutral behavior with water and sediment
iii) High sensitivity
iv) Satisfactory recovery ratio
v) Detectability and simplicity of fluorometric testing procedures

Tai and Rathbun (1988) reported that Rhodamine WT dye decay photochemically at the rate of about 2 - 4% per day. Kilpatrick et al. (1967) noted higher decay rates in rivers (about 5% per day) compared to estuaries (about 3%).

Width-integrated sediment collecting sampler was used to collect representative sediment concentration in the sediment-laden flows.

4.2.1 Flume

The experiments were conducted in 15.75 m long, 0.39 m wide and 0.50 m deep recirculating tilting flume. The details of the flume along with its flow system are shown in Figs. 4.1 and 4.2. The flume was provided with transparent glass walls on both sides held between vertical angle iron posts fitted to a steel bottom. The channel bottom was made smooth using cement plaster. The presence of different surfaces on the sides and at the bottom necessitates a side wall correction for calculating the hydraulic radius corresponding to the bed. Such a modified method was given by Einstein (1942) and the same has been used for computations herein. The flume was also provided with two circular pipe rails with adjustable supports on the sides of the flume for positioning the pointer gauge, tracer injection sampler and continuous tracer sampling system. The rails were made parallel to the flume bed before the start of the experimental programme. A tail gate was provided at the end of the flume to maintain uniform flow in the flume. Flow straightners were provided to straighten the flow and two sheets of stainless steel mesh walls were placed on the upstream of the straightners to break large size eddies in the flow. A perforated wooden wave suppressor was provided after the straightners to damp surface disturbances. Bell-shaped entrance section of the flume was provided to minimize the separation of flow.

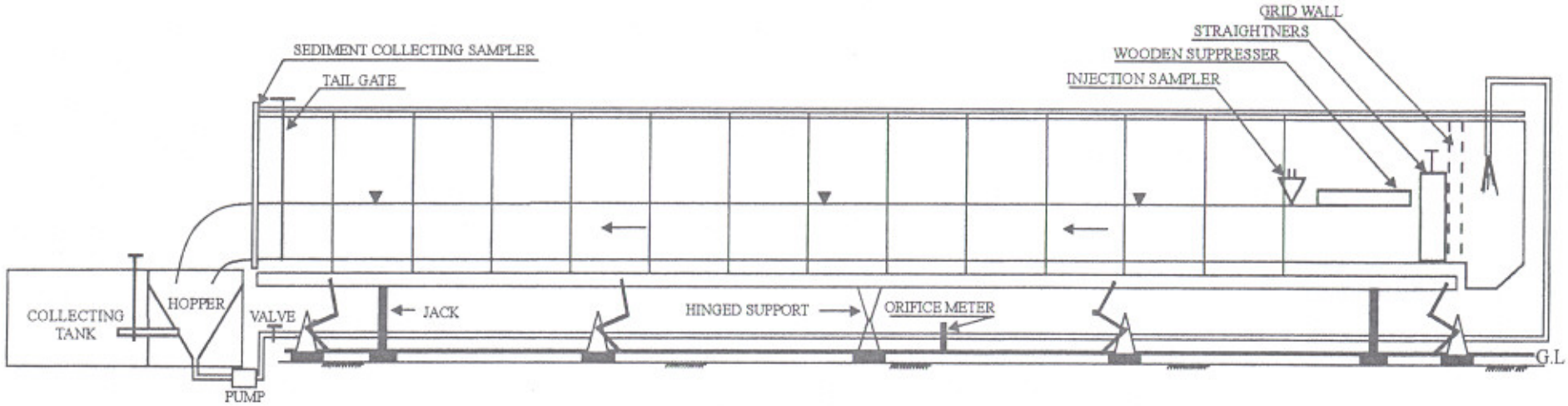

ELEVATION

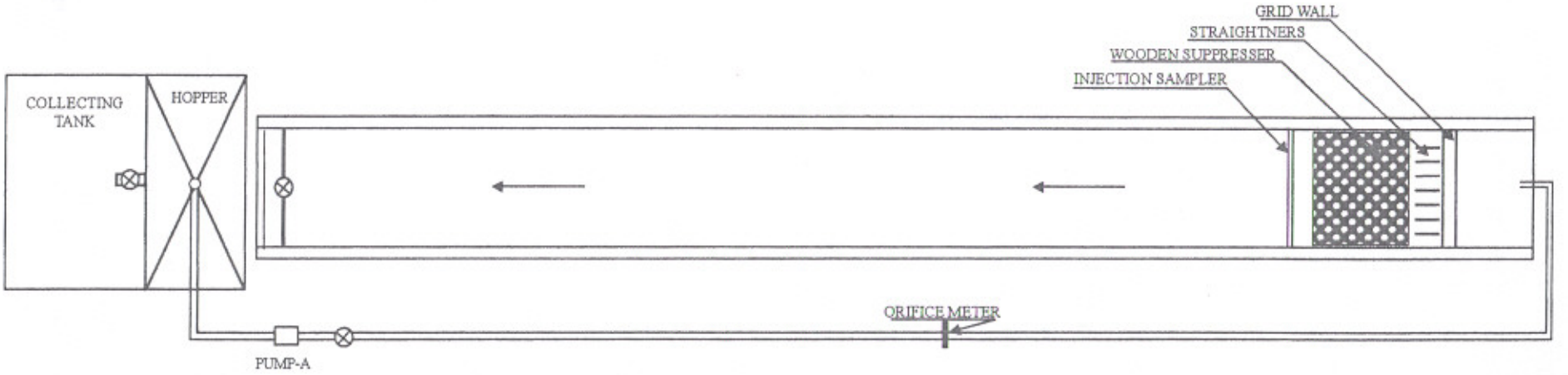

PLAN

Fig. 4.1 Layout of the Experimental Set-up

The recirculating system of the flume consisted of a rectangular tank of dimensions (2.6 m x 1.2 m x 0.9 m) divided into two compartments; a hopper was provided in the first compartment. The two compartments were connected by a valve, which prevented the entry of sediment into the second compartment. Water was supplied to the flume through a supply pipe from the hopper fitted with a centrifugal pump coupled to a 30 kW motor. A valve for regulating discharge, and a sector orifice meter for measuring the discharge were provided in the supply pipe. A line diagram of the flow system is shown in Fig. 4.3.

4.2.2 Orificemeter

A sector orifice meter (designated as A in Fig. 4.3) installed in the 0.10 m diameter supply pipe was used to measure discharge through the pipe. Sector orifice meter was used to avoid the deposition of sediment on its upstream side. The orifice meter was calibrated through velocity measurements using a Prandtl pitot tube. Velocity profiles were measured at five different vertical sections across the width of the flume for a given discharge. The discharge was obtained by integrating these velocity profiles over the area of flow. The results of these experiments are plotted in Fig. 4.4 along with the data of the earlier investigators (Arora 1983; Singh 1987; Patel 1995). The data points of the present study are in close agreement with the data points of the earlier investigators. Thus Fig. 4.4 was used as calibration curve for the orifice meter.

4.2.3 Prandtl Pitot Tube

Prandtl pitot tube of diameter 1.5 mm was used to measure the velocity of flow in clear water as well as sediment-laden flows. In the case of sediment-laden flows, regular cleaning of the tube was done in order to prevent the clogging of the tube. Prandtl pitot tube was connected to an inclined U-tube manometer for measuring the total and static heads difference, *i.e.*, dynamic pressure head.

4.2.4 Tracer Injection Sampler

The tracer was injected into the flow as a slug in the form of transverse line source by an injection sampler shown in Fig. 4.5. A photograph of the tracer injection sampler is shown in Fig. 4.6. This sampler consisted of a metallic tray of triangular cross-section of length 350 mm and depth 100 mm. The inner surface of the injection sampler was coated with impervious packing material so as to prevent the leakage of the tracer. One spring at each end of the sampler was provided so as to keep the two sides of the triangular sampler in the closed

Fig. 4.2 A photograph of the flume

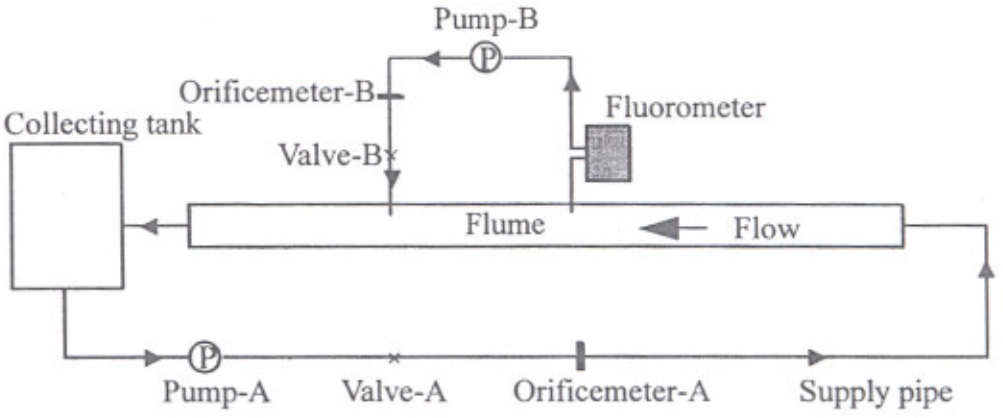

Fig. 4.3 Line diagram of flow system

position. The tray could be hinged to the sides of the flume at any height keeping it in a horizontal position and spanning the full width of the flume. Two handles with a separator in between were also provided at top on each sides of the sampler for equal opening at the bottom for each injection. For all the injections, tracer solution was filled up in the sampler and positioned slightly above the water surface. The handles of triangular sampler were pressed instantaneously to inject the tracer on the water surface as a line source.

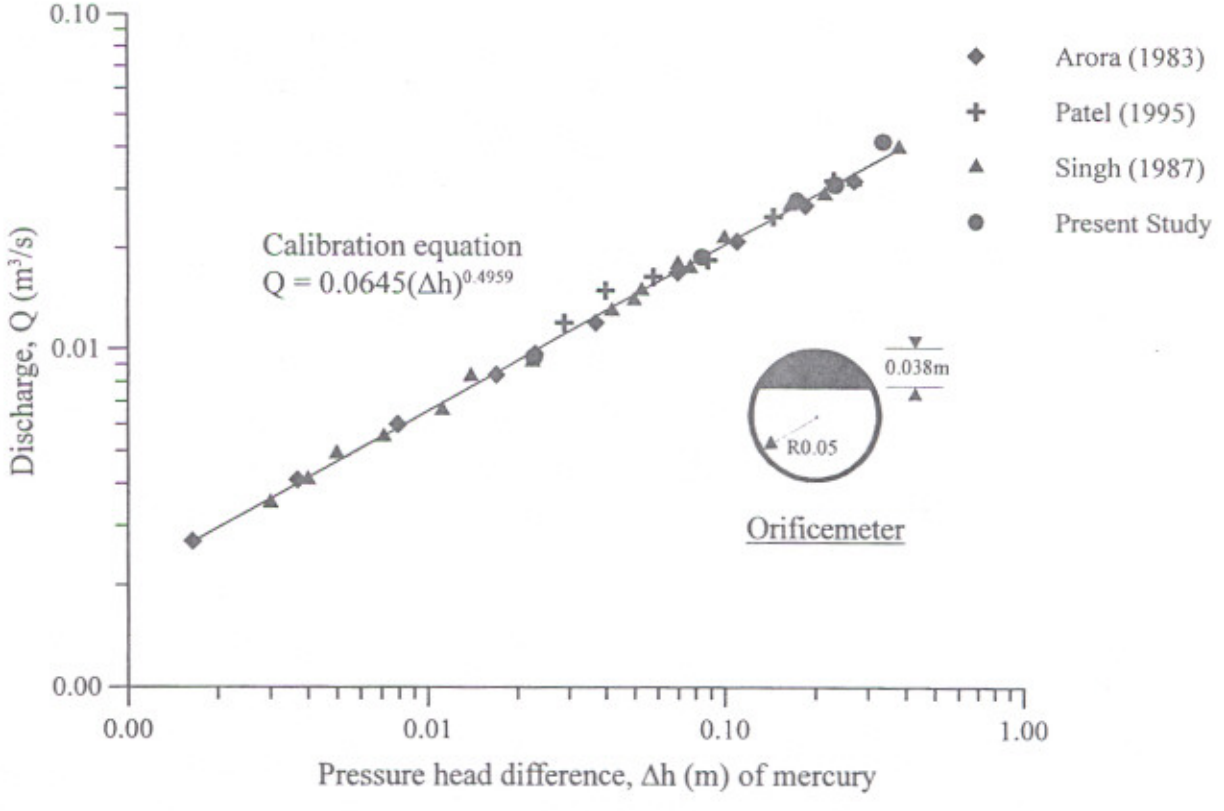

Fig. 4.4 Calibration curve of orificemeter-A

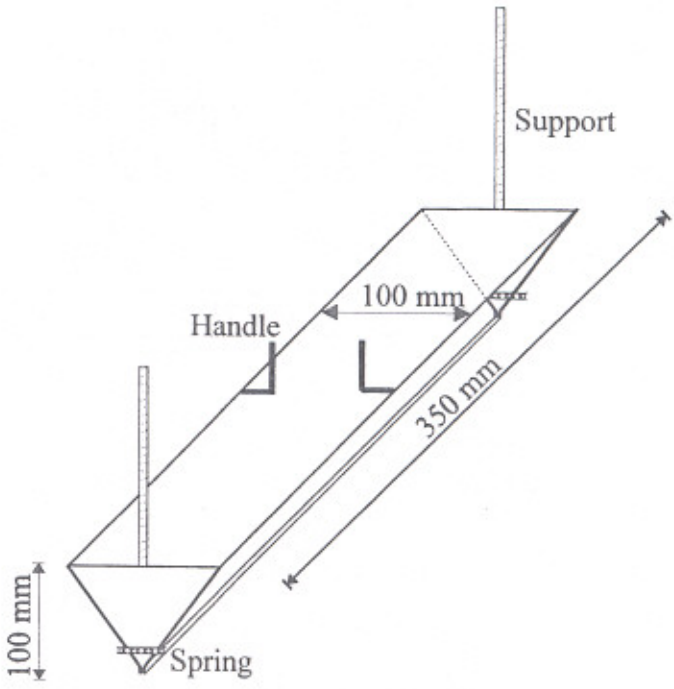

Fig. 4.5 Tracer injection sampler

4.2.5 Tracer Collecting Sampler

The tracer collecting sampler consisted of five vertical copper tubes of 8 mm diameter each fixed to a brass flat at 90 mm center to center spacing (See; Figs. 4.7 and 4.8) and pointing against the direction of flow. The purpose of providing five tubes was to collect continuously the width-integrated tracer sample. The sample from these tubes entered into a manifold of 50 mm diameter and 25 mm height, whose outlet was connected to the inlet of the Fluorometer through a 10 mm diameter polyethylene pipe. The use of manifold ensured width-integrated sample having a concentration equal to the width-averaged concentration of tracer at any elevation along the depth of flow in the flume.

4.2.6 Fluorometer

Fluorometer is an instrument which is used to measure the concentration of various analytes in samples via fluorescence. The Fluorometer used in present study is the model 10-AU-005, designed by the Turner Designs Sunnyvale, USA. The model 10-AU-005 measures samples with high sensitivity and stability.

The operating principle of the Fluorometer is based on the property of the fluorescent material, which has the ability to absorb light at one wavelength and instantaneously emit it at a new and longer wavelength. Light from a light source (the lamp) is passed through a coloured filter (excitation filter) that transmits light of the chosen wavelength range (See;

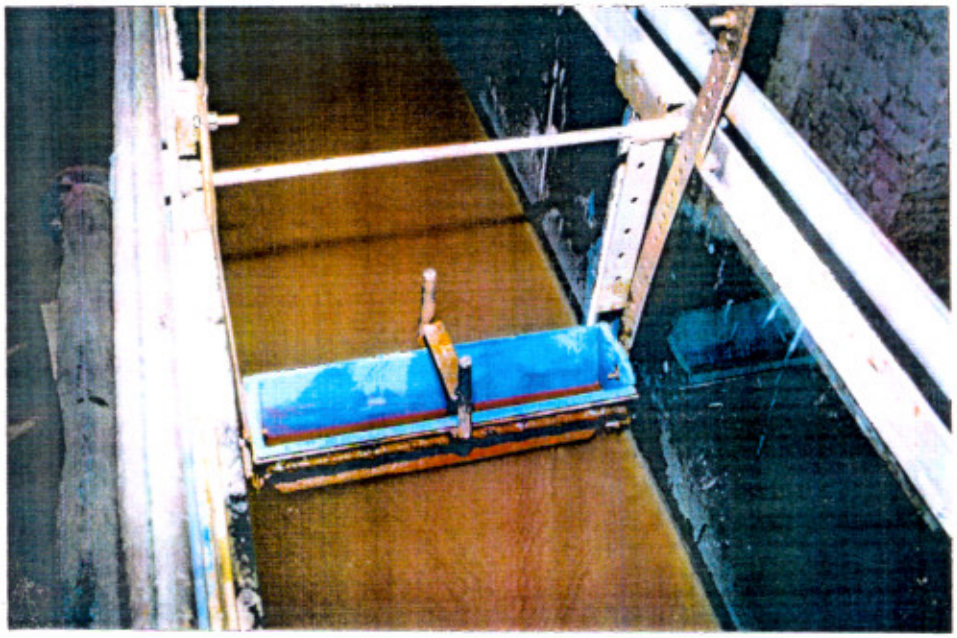

Fig. 4.6 A photograph of tracer injection sampler

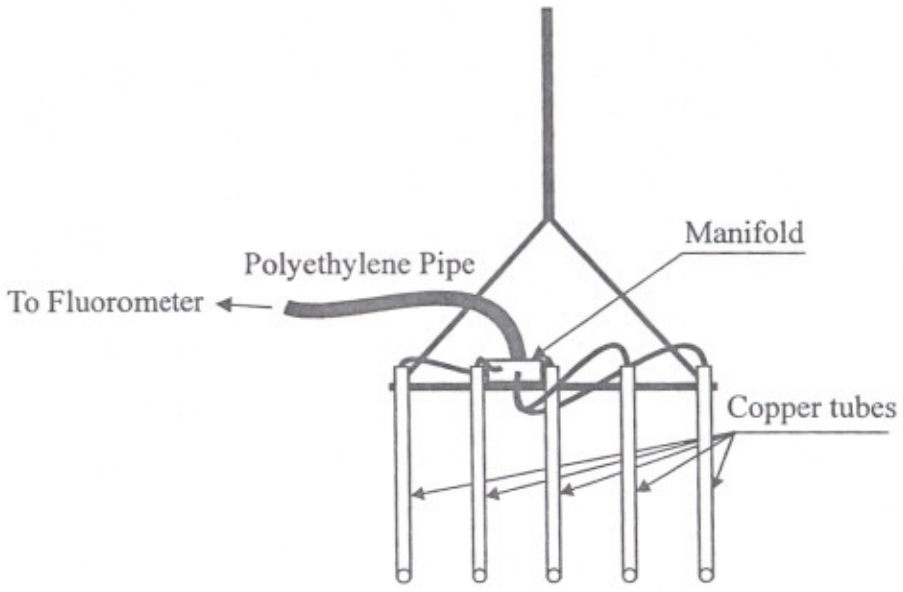

Fig. 4.7 Tracer collecting sampler

Fig.4.9). This light passes through the sample which emits light proportional to the concentration of the fluorescent material present and proportional to the intensity of the exciting filter. The emitted light is passed through another optical filter (emission filter) to prevent any scattered exciting light from reaching the detector (in this case a photo multiplier tube) and to pass the emitted colour which is specific to the analyte of interest. The photo multiplier tube is just like a vacuum tube and it generates electrons (electric current) in response to photons (light). The photo multiplier contains nine stages to multiply the electrons coming from the previous stage. Thus the current is multiplied many times before the amplification in the Fluorometer takes place. Since the same light source and detector are involved in both the measurement and reference path, variations in intensity of the lamp and in sensitivity of the detector are automatically compensated. Moreover, sensitivity of the nine-stage photo multiplier tube varies with the ninth power of the voltage. The model achieves stability by recalibrating itself ten times a second. This makes the instrument more stable and accurate under harsh conditions. The optical system of the Fluorometer is shown in Fig. 4.9.

Operation of Fluorometer consists of three steps: (i) Activation and initial verification of operational parameters; activation involves supplying power and operational parameters involve review of default values which are assigned according to the application. (ii) Calibration, which consists of setting the sensitivity of the instrument to a level appropriate to the samples and blank. A sample of known concentration is taken as standard and a blank is a

sample of the solution to be worked with, before any of the substance to be measured has been added. This fluid is the matrix for the standard and is used to set the instrument to read zero. (iii) Running the samples. Once the instrument is calibrated, a cuvette containing sample is inserted into the sample compartment or by letting the sample flow through the flow cell (for continuous flow cuvette), the concentration is read on the home screen. The data are stored in the Fluorometer (internal data logging). The Fluorometer can log up to 64,800 data points depending upon the format which includes index, time interval, date, sample read out, temperature and units of measurements. The data can be logged at an interval of varying from one to thirty seconds or one to thirty minutes. Depending on the data logging parameters chosen, one can log from 5 hours to 1350 days before the memory is full. The logged data is transferred to a Computer through RS-232 serial port using the Fluorometer internal data logger output software. The limit of detectability (sensitivity) of the instrument is 5 parts per trillion of Rhodamine WT in potable water or 10 parts per billion of crude oil in pure water (Turner Designs 1993).

4.2.7 Tracer Concentration Monitoring System

Rhodamine WT dye was injected using the injection sampler at a section in the upstream part of the flume, the injection section of the flume was beyond the development length of the flow. Water samples were collected continuously by using tracer collector sampler at every meter length of the flume downstream of the injection section. These concentration samples were passed through the Fluorometer for monitoring the concentration distribution by using a monoblock centrifugal pump. After passing through the Fluorometer the samples were returned to the flume. An orificemeter (designated as B in Fig. 4.3) was used to measure discharge. Valve B was provided to regulate the discharge so as to maintain the velocity of flow through the monitoring system equal to the velocity of flow in the channel. The line diagram of water flow for the whole system is depicted in Fig. 4.3.

The calibration curve for the orificemeter B is shown in Fig. 4.10 and a photographic view of the concentration monitoring system is shown in Fig. 4.11.

Samples were collected at three or two elevations along the flow depth viz. first near the bottom at about 5 mm above the bed, the second at the mid-depth and the third at about 10 mm below the top surface of the flow depending on the depth of flow.

Fig. 4.8 A photographic view of tracer collecting sampler

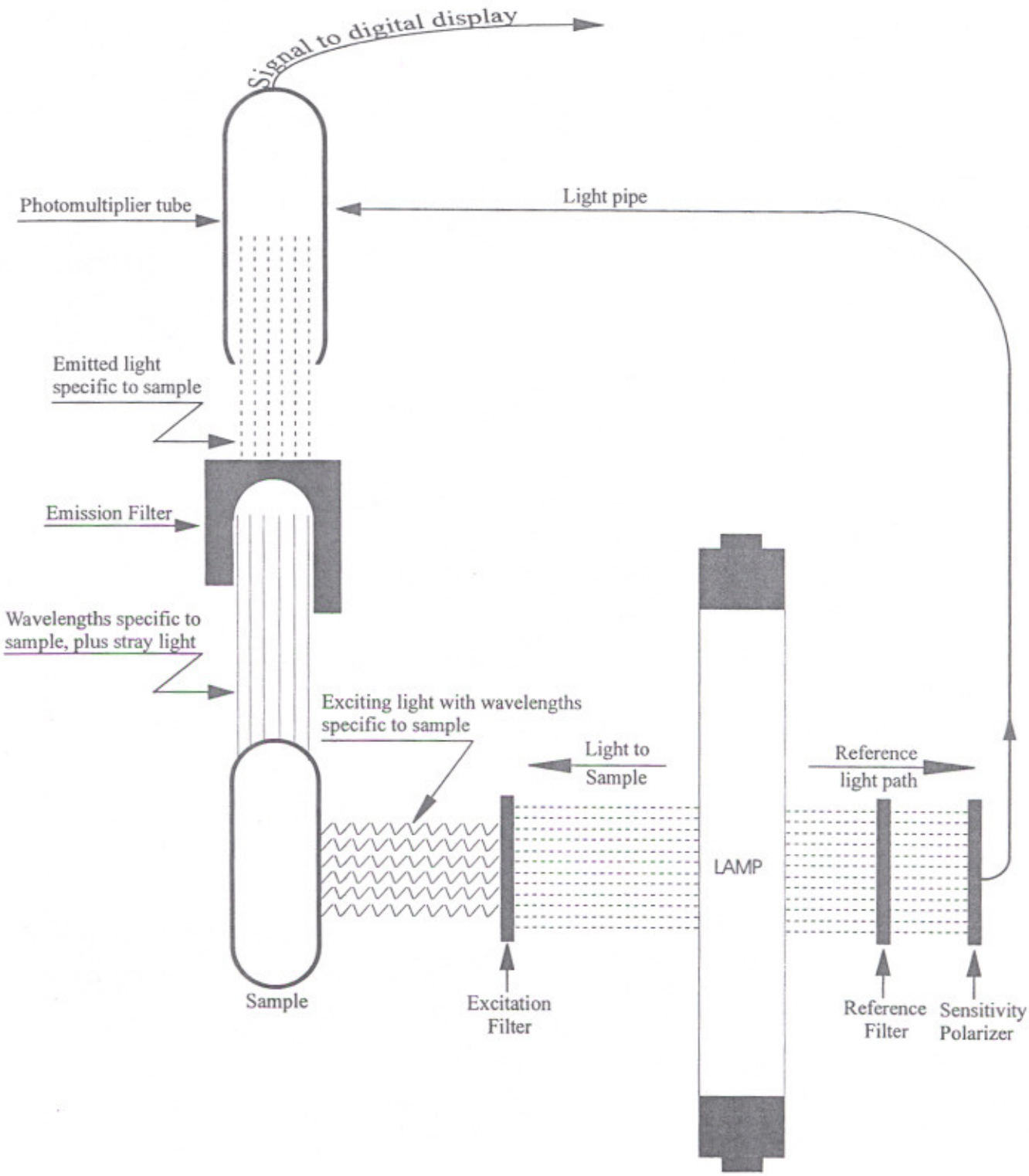

Fig. 4.9 Optical system of the Fluorometer model 10-AU-005

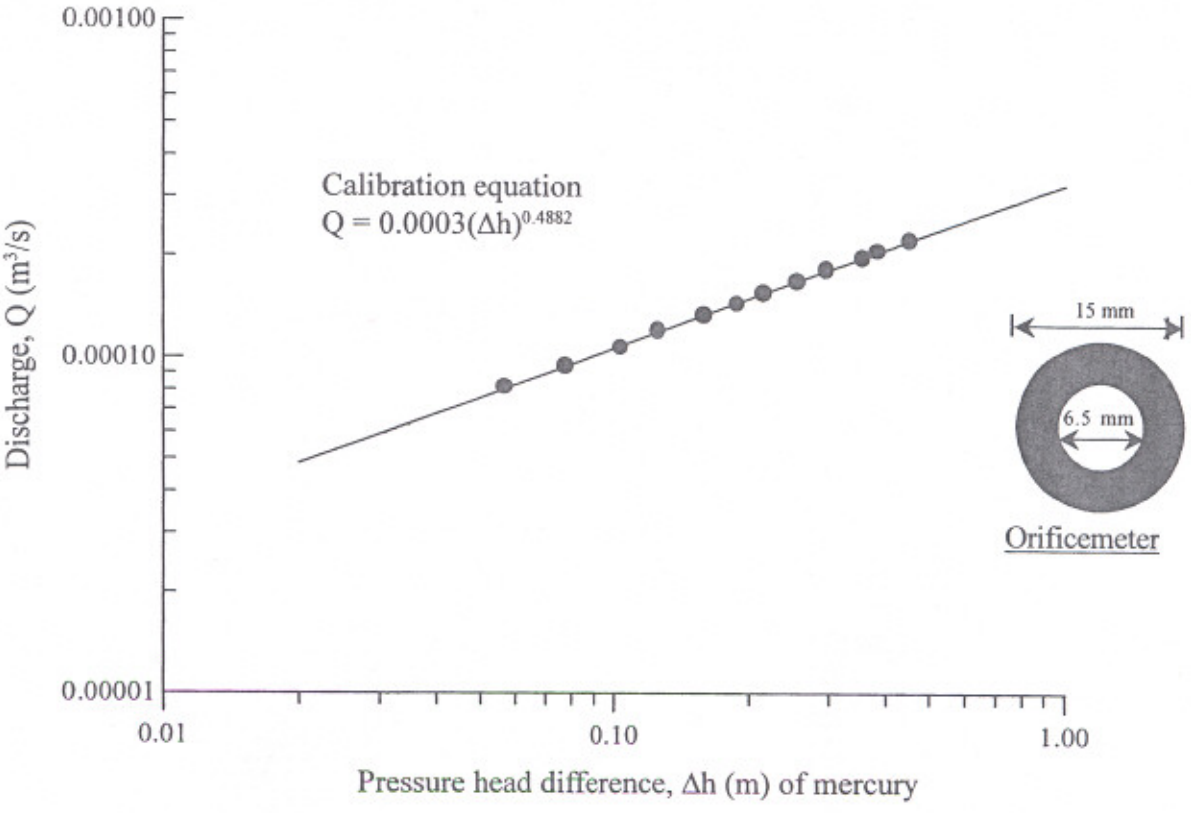

Fig.4.10 Calibration curve of orificemeter-B

4.2.8 Sediment Sampling and the Sediments Used

Experiments were conducted in sediment-laden flows to study the effect of suspended sediment on the dispersion. For each run in sediment-laden flow, flow sample was also taken to calculate the rate of suspended sediment transport.

Fine sand of relative density 2.65 was used as sediment in the experimental work, so that only suspended load occurred even at low velocities. Two sizes of sand were used. The first size of sand was passed through 90μ sieve and was retained on 45μ sieve, giving an average diameter of sand particle equal to 0.064 mm. The second size of sediment was passed through 45μ sieve. Therefore hydrometer analysis of the sample was carried out, the grain size distribution of its sample is shown in Fig. 4.12. The average size of the sediment (D_{50}) was worked out as 0.024 mm.

Cross-sectional averaged concentration of the suspended load in the flow was measured by a width-integrating sampler, which sampled sediment over the depth of flow. This sampler was installed at the downstream end of the flume (See; Fig. 4.13). The sample of sediment-laden

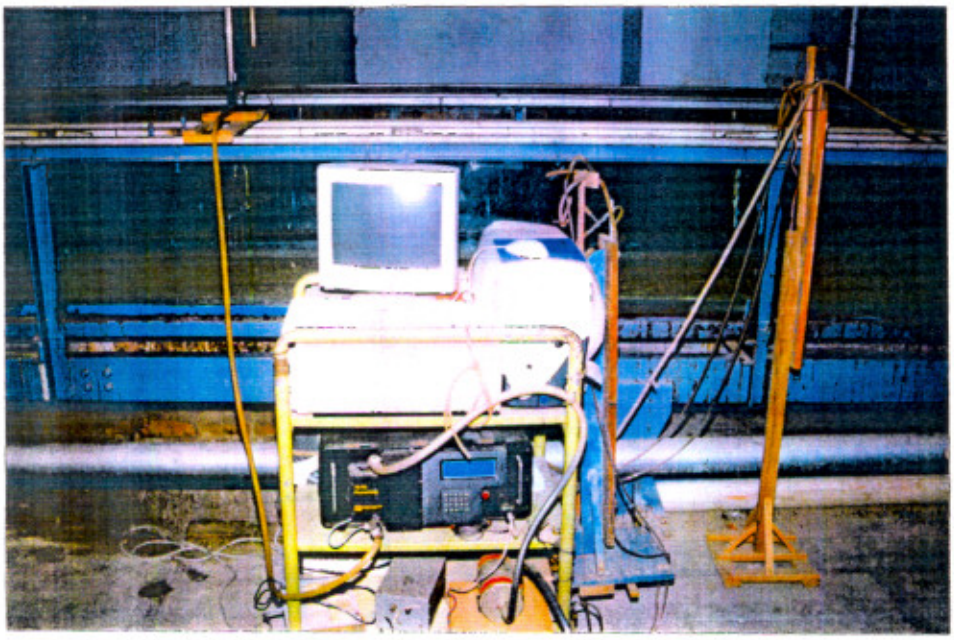

Fig. 4.11 Concentration monitoring system

flow was collected from the sampler through a rubber tube in a bucket. The sediment was allowed to settle at the bottom and the excess water was drained carefully. The sediment was then filtered on a filter paper and the filtered material was dried in an electric oven for 24 hours and weighed on an electronic balance. Knowing the initial weights, the concentration in parts per million (ppm) by weight for each sample was determined.

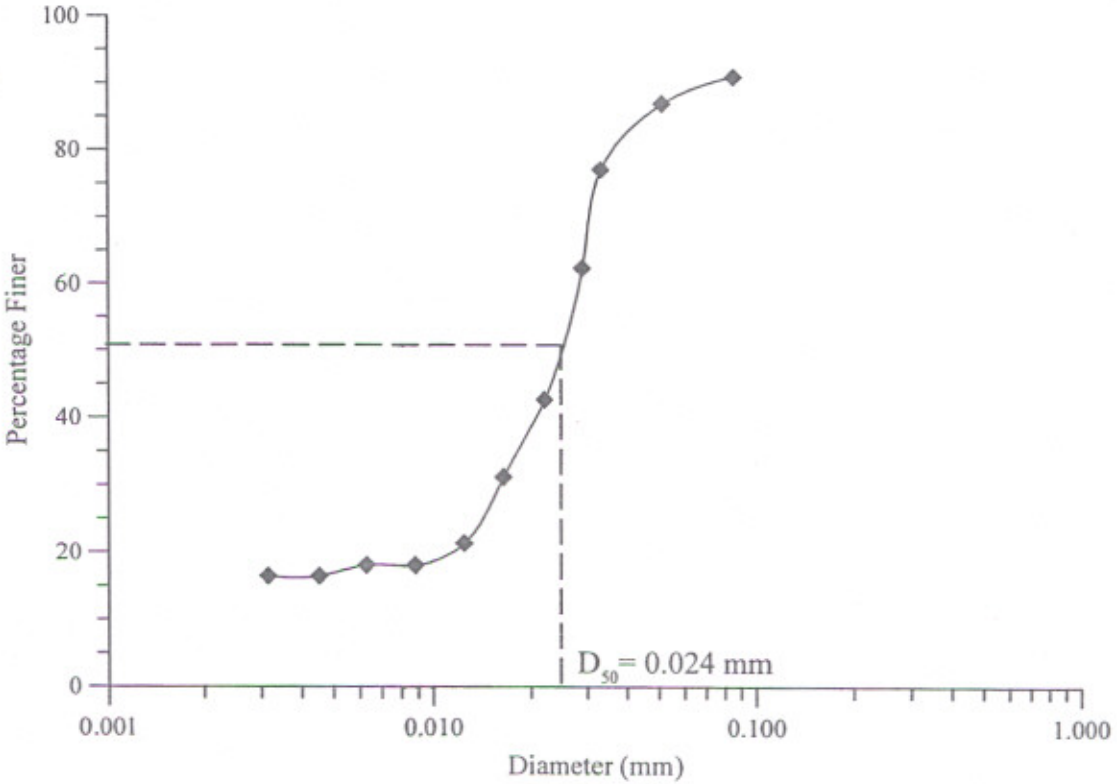

Fig. 4.12 Grain size distribution of the sediment used (Hydrometer analysis)

4.3 EXPERIMENTAL PROCEDURE

The flume was set horizontal by adjusting its titling mechanism. The railings of the flume were then made parallel to the bed by using a dumpy level and by adjusting the railings through use of screws. To cover a wide range of data, the experiments were conduced for four bed slopes 0.000917, 0.001176, 0.002041 and 0.001475 and designated as 1CDCW, 2CDCW, 3CDCW and 4CDCW, respectively for clear-water run. The corresponding sediment laden runs were designated as 1CDSL, 2CDSL, 3CDSL and 4CDSL, respectively.

For example data set 3CDCW2 refers to data on tracer concentration for clear-water run number two on slope number 3, *i.e.*, 0.002041 and the corresponding to this, the equivalent sediment laden run number five was designated as 3CDSL25. Similarly the velocity distributions were designated as 1VDCW, 2VDCW, 3VDCW and 4VDCW, respectively.

The bed slope was measured by using two small boxes connected to each other through a rubber tube and placed at known distance apart. After sufficient long period, the water levels in each of these two boxes were measured by using a pointer gauge. The difference of water levels divided by the distance between the two locations gives the slope of the bed. For each slope, the experiments were first carried out for different discharges in clear-water flows. For each discharge, uniform flow was first established by adjusting the tail gate and measuring the depth of flow along the flume. A known concentration of Rhodamine WT dye solution was poured into the tracer injection sampler fitted near the upstream end of the flume. The location of injection sampler was changed depending upon the discharge and the flow establishment length. The sampler was positioned slightly above the water surface by adjusting the side screws. The collecting sampler was first located at first station at a distance 1 m from the injection sampler and about 5 mm above the bed. The monitoring system was activated and allowed to warm up for 10 minutes. The sample withdrawal pump B was started so that a continuous flow was maintained through the Fluorometer-cuvette. The flow through the Fluorometer was regulated with the help of valve B, so that velocity of flow through the monitoring system is equal to the velocity of flow in the flume at that depth. The dye was injected instantaneously in the flume as a horizontal line source and in synchronization with the switching on of the data logging of the Fluorometer. After the passage of dye cloud, the data logging was stopped. Now the collecting sampler was raised and placed at the mid-depth of flow. An equal volume of dye solution was injected and the data was again logged up in the Fluorometer as in the previous one. Between the two tracer injections a sufficient time was allowed to thoroughly mix up the dye in the recirculating water. The collecting sampler was then brought about 10 mm below the top water surface and data was again logged up in the Fluorometer. The whole exercise resulted in the recording of three tracer concentration versus time profiles in the Fluorometer at a distance of 1 m from the injection sampler.

The movable trolley housing the monitoring system was then moved to the 2 m distance from the injection sampler. In the same manner as at the first station, the three concentration versus

Fig. 4.13 A downstream view of flume
(Sediment collecting sampler)

time curves were obtained by using the same quantity of dye. The same procedure was repeated for a number of downstream stations each separating the previous one by 1 m.

During the experimentation when the blank concentration in the water had increased significantly, the water was removed from the tank and further experiments were conducted after filling it with fresh water.

After the clear-water runs were completed for a given slope, a predetermined amount of sediment was added to the recirculating system and sufficient time was given for mixing the sediment uniformly in the recirculating water. The sediment load was determined by collecting the width-integrated sample using sediment-collecting sampler. The width-integrated sampler was moved slowly across the width so that about 10 litres of sample was collected in the time required for the sampler to traverse the flume width ten times. The collected sediment sample was passed through a filter paper and dried in an oven. The dried weight of sediment was measured on an electronic balance. The average concentration of sediment was then expressed in parts per million (ppm) as dry weight of solids per unit weight of sediment-water mixture.

Tracer concentration versus time profiles were recorded at different longitudinal distances and at three or two elevations along the depth using the Fluorometer in the same manner as for clear-water runs. More sediment was added to the recirculating water and runs for suspended sediment concentration were taken. When the sediment started showing sign of deposition, the water-sediment mixture was removed and the tank again filled with fresh water. The same procedure was adopted for the other sediment having a different size. As stated earlier, the withdrawal velocity (during measurement of tracer concentration) was kept equal to the velocity of flow in the flume to obtain true mixing of the tracer in the water.

Clear-water runs were taken at all the four slopes. However, sediment-laden flow runs were taken at two slopes only, *i.e.*, 0.001475 and 0.002041. For the other two sets of slopes, *i.e.*, 0.000917 and 0.001176 even addition of small amount of sediment showed deposition and therefore no sediment-laden data were taken for these sets.

The logged up data in the Fluorometer was transferred to an interfaced computer by internal data logging (IDL) software and the further analysis of data was done on the computer.

For each type of run either in clear-water or sediment-laden flow, the velocity distribution in a cross-section along five verticals was measured by Prandtl pitot tube.

A typical set of observed C-t curves for clear-water and sediment-laden flow at downstream stations at three elevations are shown in Figs. 4.14 and 4.15, respectively. Also shown in Figs. 4.16 are the observed isovels for some of the data sets.

Figures 4.14 and 4.15 show that peak concentration of the C-t curves measured near the water surface decreases in the downstream as the tracer is being mixed in the ever increasing volume of water whereas peak concentration of C-t curves measured at the mid-depth and near the bed increases in the downstream. After some distance, all the three peak concentrations become nearly equal thereby showing complete cross-sectional mixing of the tracer.

The measured velocities are an important indicator of the presence or absence of secondary currents and lateral velocity gradients in the flow. These two phenomenon cause additional mixing over and above caused by vertical shear. As depicted in Figs. 4.16 velocity distribution exhibit a high degree of two-dimensionality over the central region of the channel. The depressed velocity maxima in the vertical profiles near the channel walls imply the presence of secondary currents in this region. This feature of the profiles are not evident in the central region of the flow and thus, provided the flow has no significant lateral velocity gradients, secondary currents are not an important feature in the central region of the flow. Also the measured velocities were checked by integrating the velocity over the flow cross-section to compute the discharge and comparing this value with the value of discharge measured through calibration of orifice meter. For most of the runs, the computed and the measured discharges showed a satisfactory comparison.

All the experimental data collected during the present study are listed in Appendix-I and Appendix-II.

4.4 COMPUTATION OF HYDRAULIC RADIUS

Knowledge of shear velocity U_* is required to study the effect of velocity distribution on the mixing process. In the field as well as laboratory there are a number of instances where bed and side roughness are different e.g. glass walled flume with roughened bed, side walls of flume made of different materials, alluvial streams with rocky sides and gravel bed etc. In all such cases, the primary interest is to know about the hydraulic radius with respect to the bed. This necessitates a sidewall correction to be applied in order to get the hydraulic radius with respect to the bed.

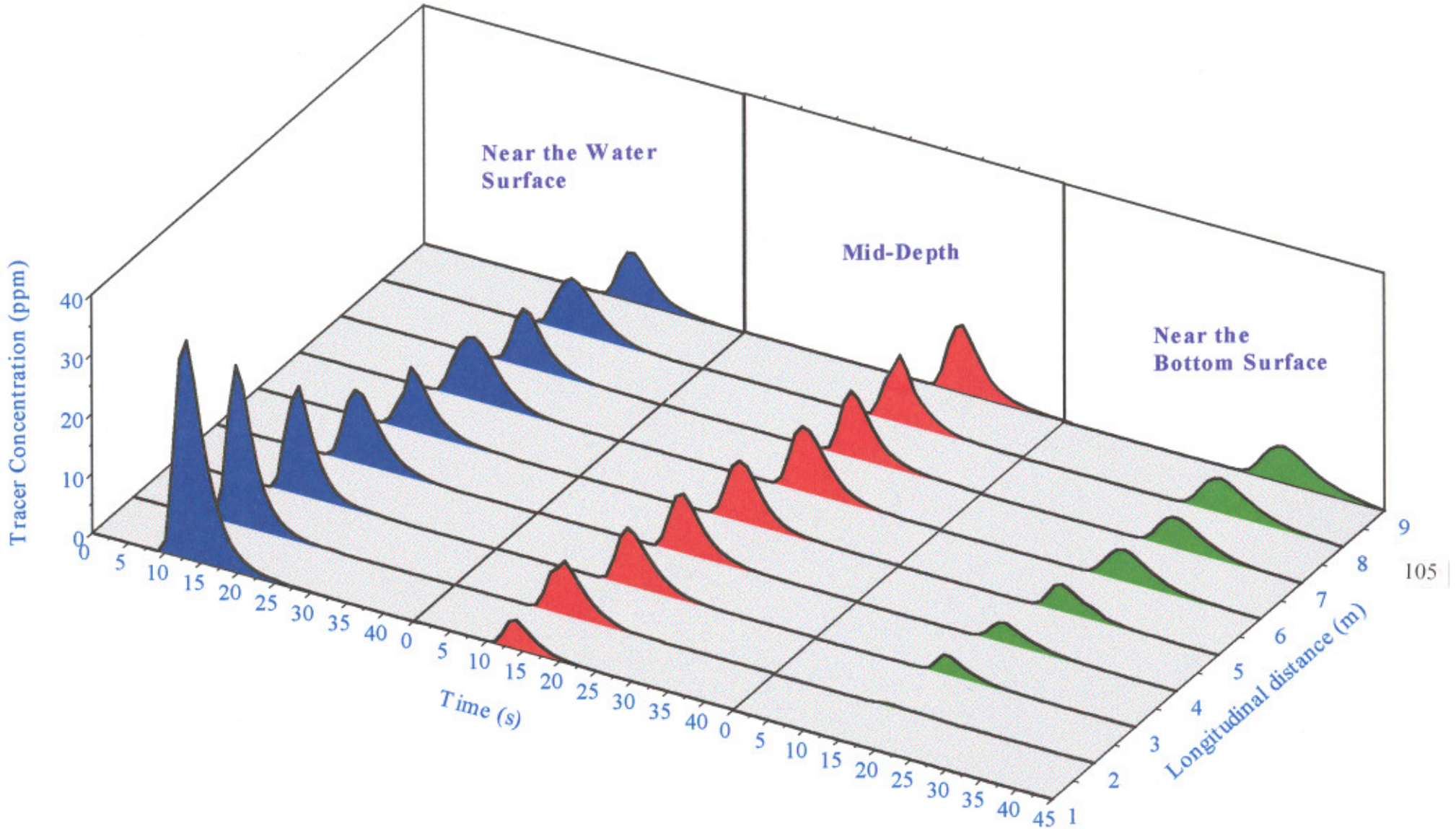

Fig. 4.14 Observed tracer conentration versus time curves (Data set 1CDCW5).

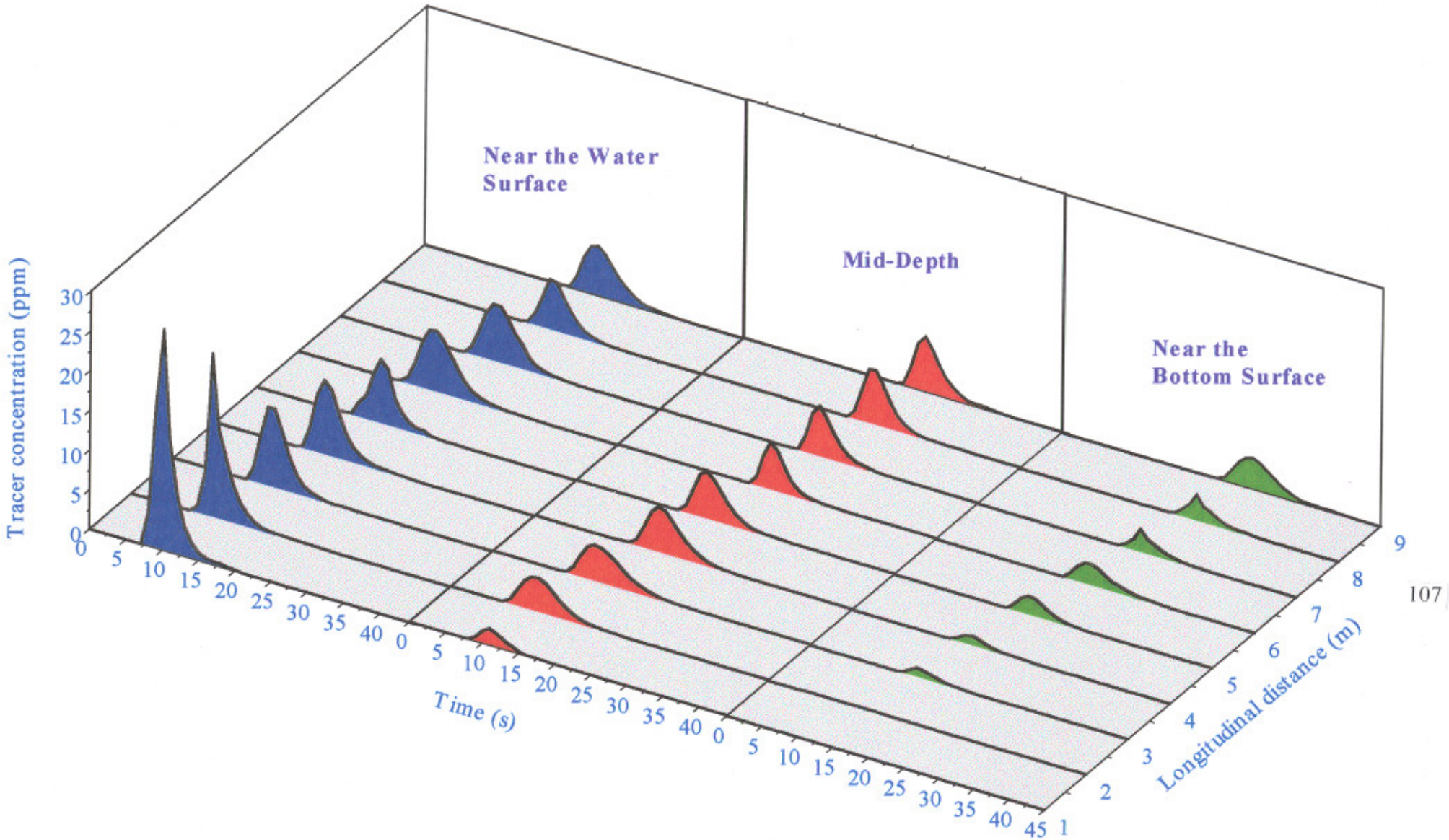

Fig. 4.15 Observed tracer conentration versus time curves (Data set 4CDSL32)

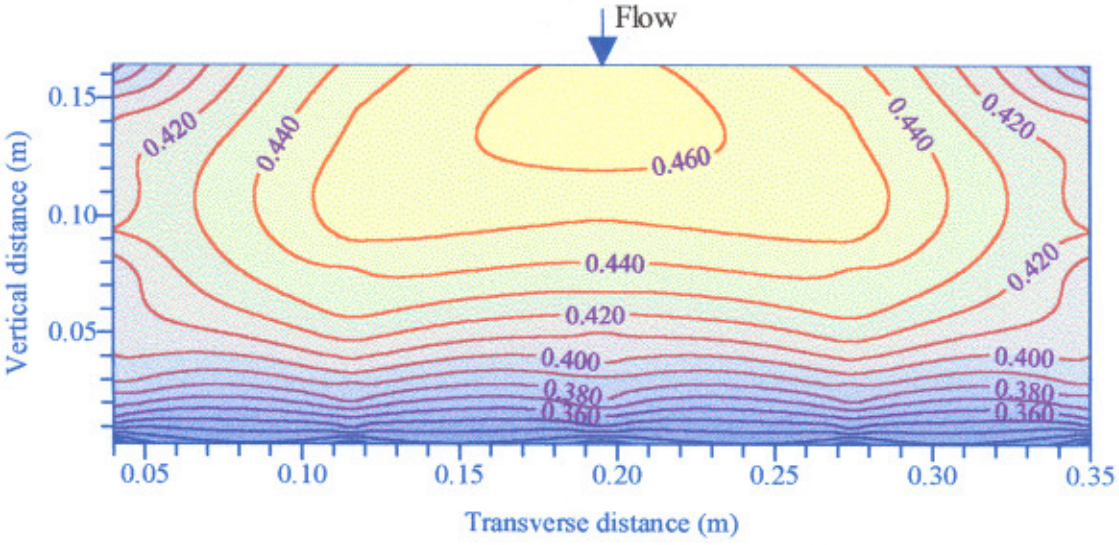

(Data set 1VDCW5)

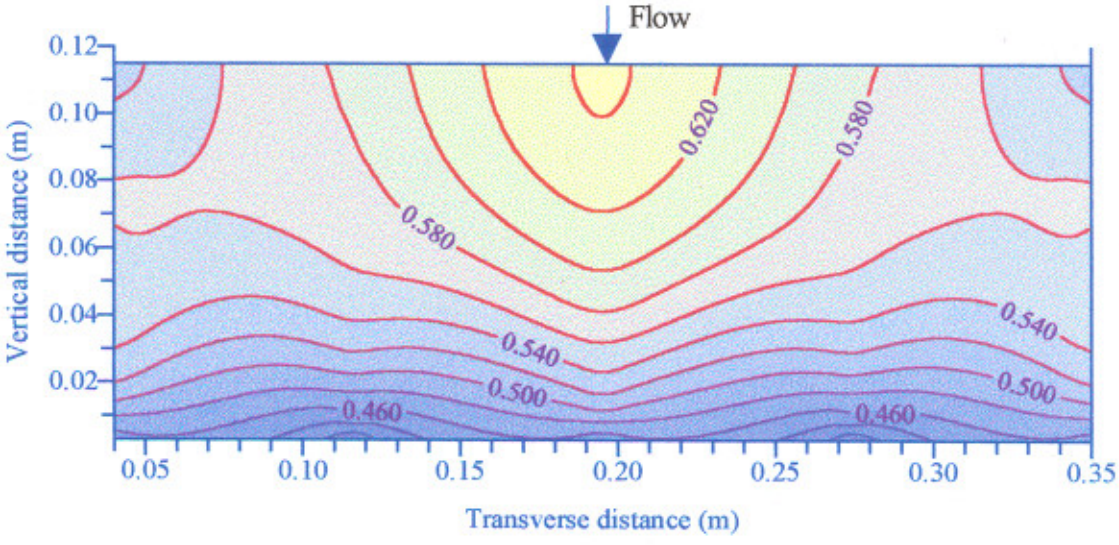

(Data set 3VDSL18)

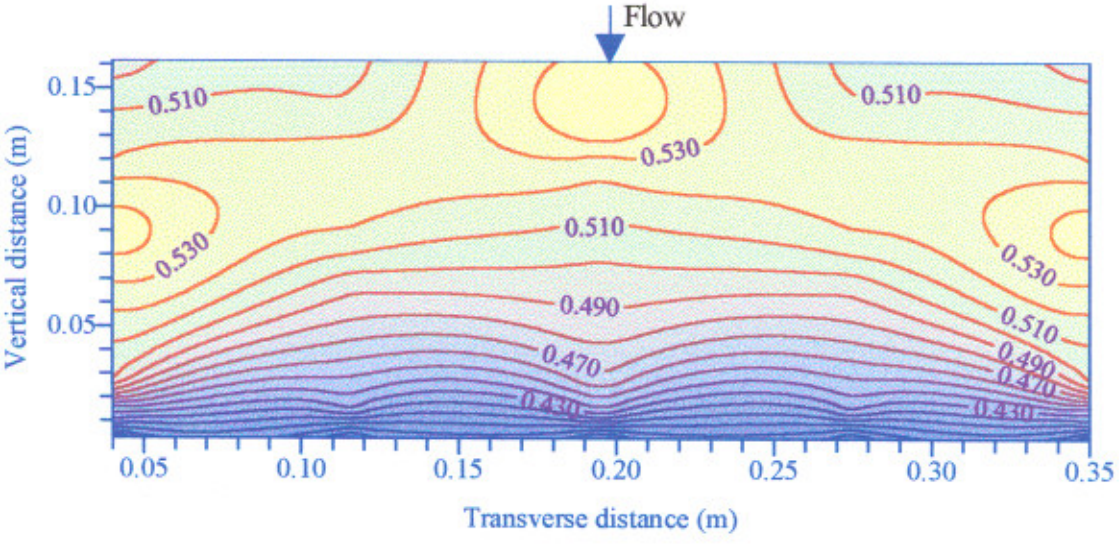

(Data set 4VDSL32)

All velocities are in m/s.

Fig.4.16 Isovels for some of the observed data sets

According to Einstein (1942), the cross-sectional area of flow of a channel, A can be divided into the area corresponding to the bed (A_b) and the areas corresponding to the side walls, *i.e.*, (A_{w1}) and (A_{w2}).

$$A = A_b + (A_{w_1}) + (A_{w_2}) \tag{4.1}$$

$$bd = P_b R_b + (P_{w_1})(R_{w_1}) + (P_{w_2})(R_{w_2}) \tag{4.2}$$

$$bd = bR_b + d(R_{w_1}) + d(R_{w_2}) \tag{4.3}$$

Here b is the bed width of the channel; d is the local depth of flow; P_b, (P_{w_1}) and (P_{w_2}) are wetted perimeters and R_b, (R_{w_1}) and (R_{w_2}) are the hydraulic radii of bed and sides walls respectively. He further assumed that Manning's equation can be applied to the bed and side walls independently using the same mean velocity and slope. Accordingly, one can write:

$$U = \frac{1}{(n_{w_1})}(R_{w_1})^{2/3} S_f^{1/2} \tag{4.4}$$

$$U = \frac{1}{(n_{w_2})}(R_{w_2})^{2/3} S_f^{1/2} \tag{4.5}$$

Here U is the average velocity of flow; S_f is the slope of energy line and (n_{w_1}) and (n_{w_2}) are Manning's coefficients for the side walls and. Knowing the value of Manning's coefficients, depending on the type of material, (R_{w_1}) and (R_{w_2}) can be computed as:

$$(R_{w_1}) = \left(\frac{U(n_{w_1})}{\sqrt{S_f}}\right)^{1.5} \text{ and} \tag{4.6}$$

$$(R_{w_2}) = \left(\frac{U(n_{w_2})}{\sqrt{S_f}}\right)^{1.5} \tag{4.7}$$

Using Eqs. (4.6 and 4.7), the value of R_b can be computed from Eq. (4.3) as:

$$R_b = d\left[1 - \frac{U^{1.5}}{bS_f^{0.75}}\left\{(n_{w_1})^{1.5} + (n_{w_2})^{1.5}\right\}\right] \tag{4.8}$$

If the side walls are of same material, (n_{w_1}) = (n_{w_2}), then Eq. (4.8) reduces to:

$$R_b = d\left[1 - \frac{2}{b}\left(\frac{U n_w}{\sqrt{S_f}}\right)^{1.5}\right] \tag{4.9}$$

The value of R_b has been obtained by using the above stated method. It was found that value of R_b obtained by this method was less than R, obtained by considering the same material for the bed and the sides.

4.5 NORMALIZATION OF C-t CURVES

Rhodamine WT dye is conservative in nature. Thus quantity of dye injected at the upstream should be equal to tracer amount recovered at any station in the downstream of injection site. For all the data sets in the present experimental programme the recovered mass is computed. It is found that mass recovered compare very closely with the mass injected. In addition, the magnitude of the tracer concentration in a stream is in direct proportion to the mass of tracer injected. Doubling the amount of tracer injected for a given flow will double the observed concentrations, but the shape and direction of the tracer response curve will remain the same. Similarly any error in the volume of tracer injected will incorporate equal error for that C-t curve. The data at each station were normalized by utilizing the above principles. The procedure of normalization is mentioned below.

After deduction of the blank from observed concentration of the tracer, area under resulting C-t curves were computed. The cross-sectional area at a section is divided into three or two horizontal strips (sub-areas) depending on the number of C-t curves available at that section. For each sub-area, the average velocity and depth of flow are calculated. The mass of tracer, m recovered at the section is calculated from:

$$m = \sum_{k=1}^{N_1} (\Sigma C \Delta t)_k b_k d'_k U_k \tag{4.10}$$

Where N_1 = total number of sub-areas; $\sum C\Delta t$ = area under C-t curve; b_k = width of the sub-area; d'_k = depth of the sub-area and U_k = width-averaged velocity over the sub-area.

The mass of the recovered tracer at the subsequent stations was calculated from Eq. (4.10). Finally the arithmetic average of the mass recovered was calculated. Thus the observed C-t curves at each station were then normalized with respect to the average mass.

Tracer concentration versus time curves for sediment-laden runs are also normalized due to the fact that sediment particles adsorb the tracer. To ascertain adsorption of Rhodamine WT dye on the sediments, known volume of water and tracer concentration was taken in a bucket. The sample was continuously passed through the Fluorometer, which showed a constant reading. Sediment was then added into the bucket. The mixture was continuously stirred with a mechanical stirrer. A decrease in the reading was shown by Fluorometer. More addition of sediment showed further decrease in the dye concentration. The variation of tracer concentration with the sediment concentration for two sediment sizes 0.064 mm and 0.116 mm is shown in the Fig. 4.17. All the observed C-t curves for sediment-laden flows were normalized therefore, accordingly.

4.6 RANGE OF DATA

The range of data collected in the present study is given in Table 4.1.

Table 4.1 Range of data collected in the present study

S. No.	*Parameters*	*Range*
1.	Slope	0.0009174 to 0.0020408
2.	Discharge	0.0158 m^3/s to 0.0367 m^3/s
3.	Flow velocity	0.370 m/s to 0.587 m/s
4.	Depth of Flow	0.0895 m to 0.196 m
5.	Width of flume	0.39 m
6.	Hydraulic radius with respect to bed	0.063 m to 0.138 m
7.	Size of sediment	0.024 mm and 0.064 mm
8.	Concentration of sediment	104 ppm to 6178 ppm by weight
9.	Total numbers of runs	48
10.	Spacing of stations	1 m

4.7 CONCLUDING REMARKS

Experiments were conducted to measure tracer concentration versus time profiles at the downstream sections at two to three elevations along the flow depth resulting due to horizontal line injection of tracer on the water surface at the upstream section of the flume.

Experiments were conducted both for clear-water and sediment-laden flows at four different values of bed slopes, *i.e.*, 0.000917, 0.001176, 0.002041 and 0.001475 and with various discharges. All the observed C-t curves were appropriately normalized. Velocity distributions along five verticals were also measured across the width of flow, for clear-water as well as sediment-laden flow runs.

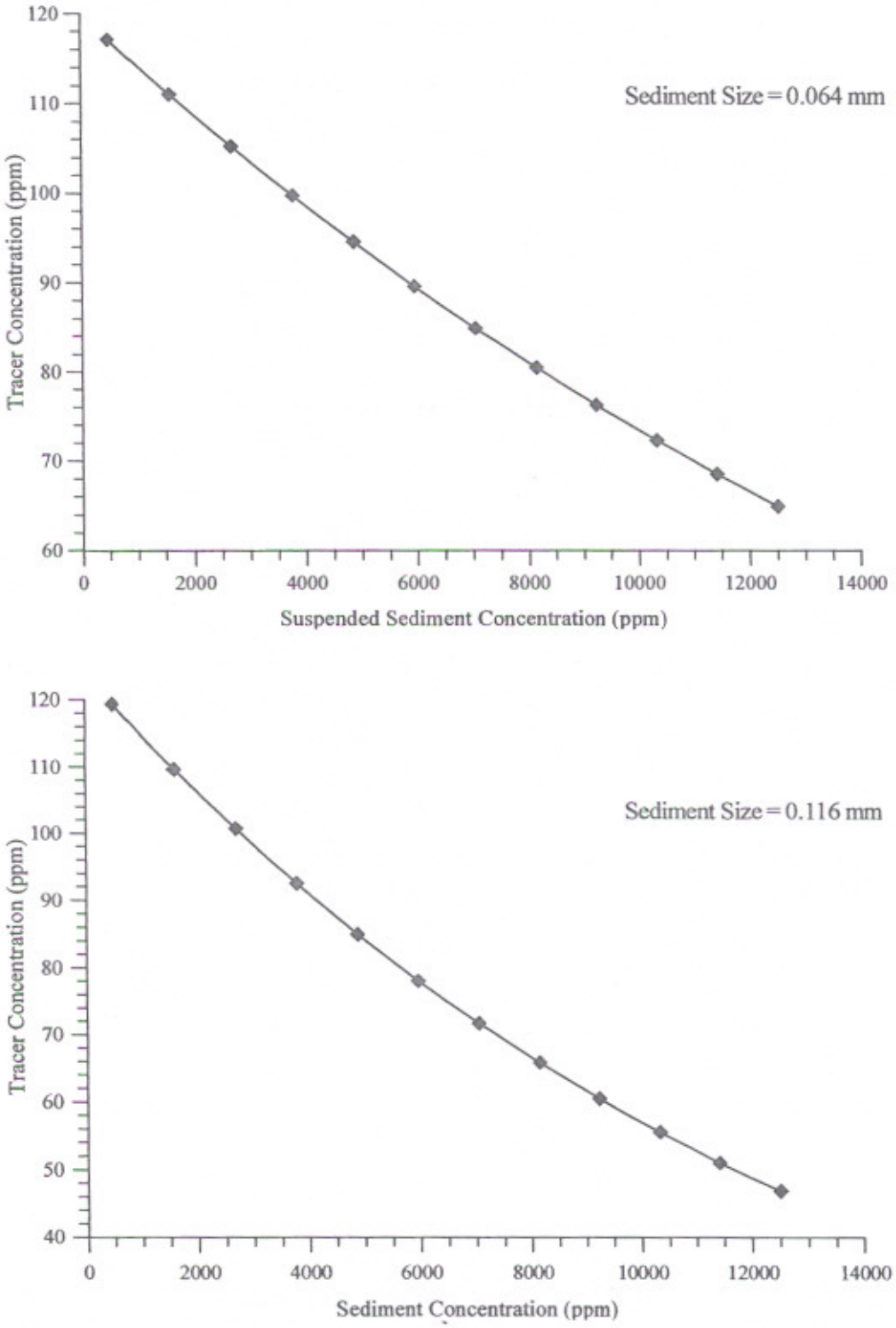

Fig. 4.17 Variation of tracer concentration with sediment concentration

Chapter

5

ANALYSIS OF DATA AND RESULTS

5.1 INTRODUCTION

Data collected through experiments and those available from earlier studies are analyzed in this chapter. The proposed numerical scheme is first validated by comparing its results with analytical solution for continuous tracer injection from transverse line source and Fischer's (1968) analytical solution for one-dimensional mixing of pollutants in open channels. The mixing coefficients E_x and E_y are analysed and a new predictor for E_x is proposed. The effect of suspended load on process of mixing is studied using the experimental data. The sensitivity of the C-t curves to errors in E_x and E_y is also studied.

5.2 VALIDATION OF THE PROPOSED NUMERICAL SCHEME

The proposed numerical model describes mixing of the pollutant in streams due to transverse line slug injection source. It predicts concentration of pollutants downstream of the injection site both in near-field (*i.e.*, in longitudinal and vertical directions) and far-field (*i.e.*, in longitudinal direction). The scheme is validated by comparing its results with analytical solution for continuous injection of transverse line source and Fischer's (1968) analytical solution for one-dimensional mixing of pollutants in channels.

Analytical solution of transverse mixing equation for constant discharge and continuous transverse line injection, *i.e.*, Eq. (2.50) is used for validation of the proposed numerical scheme. The hypothetical continuous injection of pollutant of concentration 20 ppm is assumed to spread

uniformly up to a depth of 0.2 m below the free surface. The total depth of flow equal to 1m is assumed. The channel is considered to be wide having a bed slope (S_b) of 1 in 6000 and hence shear velocity $U_* = \sqrt{gdS_b} =$ 0.04 m/s. Logarithmic velocity distribution $\left(\frac{u}{U_*} = 5.75 \log \frac{y}{k_s} + 8.5; \text{with } k_s = 1.5\,\text{mm}\right)$ is assumed to be followed producing an average velocity, U = 0.9 m/s. From Eq. (2.45), the value of E_y comes out to be 0.00271 m^2/s. The concentration computed through analytical solution at x = 3, 5 and 10 m are shown in Fig. 5.1. For the computation of concentration using proposed numerical scheme, the entire depth of flow is divided into 10 computational grids with spacing $\Delta y = 0.1\,m$. Velocity at each grid point is calculated using the above stated logarithmic velocity distribution and concentration of pollutant at the three computational nodes at the free water surface was taken as 20 ppm. The computed concentration by the proposed numerical scheme at x = 3, 5 and 10 m are also shown in Fig. 5.1. A close agreement between the analytical and numerical results may be noted.

Applicability of the proposed numerical scheme for the computation of tracer concentration in one-dimensional mixing is also proven by comparing its results with Fischer's (1968) analytical solution of one-dimensional mixing equation. For this purpose two input C-t curves of the present study, *i.e.*, 1CDCW7 and 4CDCW5 and one input C-t curve of Ahmad (1997) were used (See; Figs. 5.2, 5.3 and 5.4). For 1CDCW7 and 4CDCW5 sets of data E_L was computed by using Fischer's (1967) triple integral equation, using the velocity distribution in lateral direction (See; Figs. 5.5 and 5.6), however, for third data set $E_L = 0.037\,m^2/s$ was derived by Ahmad (1997). Using Eq. (2.81), the tracer concentration was computed at downstream stations in the flow and the same are also shown in Figs. 5.2, 5.3 and 5.4. For the computation of tracer concentration using the proposed numerical scheme, the values of E_x and E_y were needed. Since no predictor is available in literature for E_x, in the present study a predictor is proposed for E_x (See; Eq. 5.2), which is used for its computation. E_y is computed using Eq. (2.45). In all the three data sets, the depth of flow was divided in vertical direction by six computational nodes and at each computational node at input section the tracer concentrations were taken equal to that given by input C-t curves. C-t curves at downstream stations were calculated next. It is found

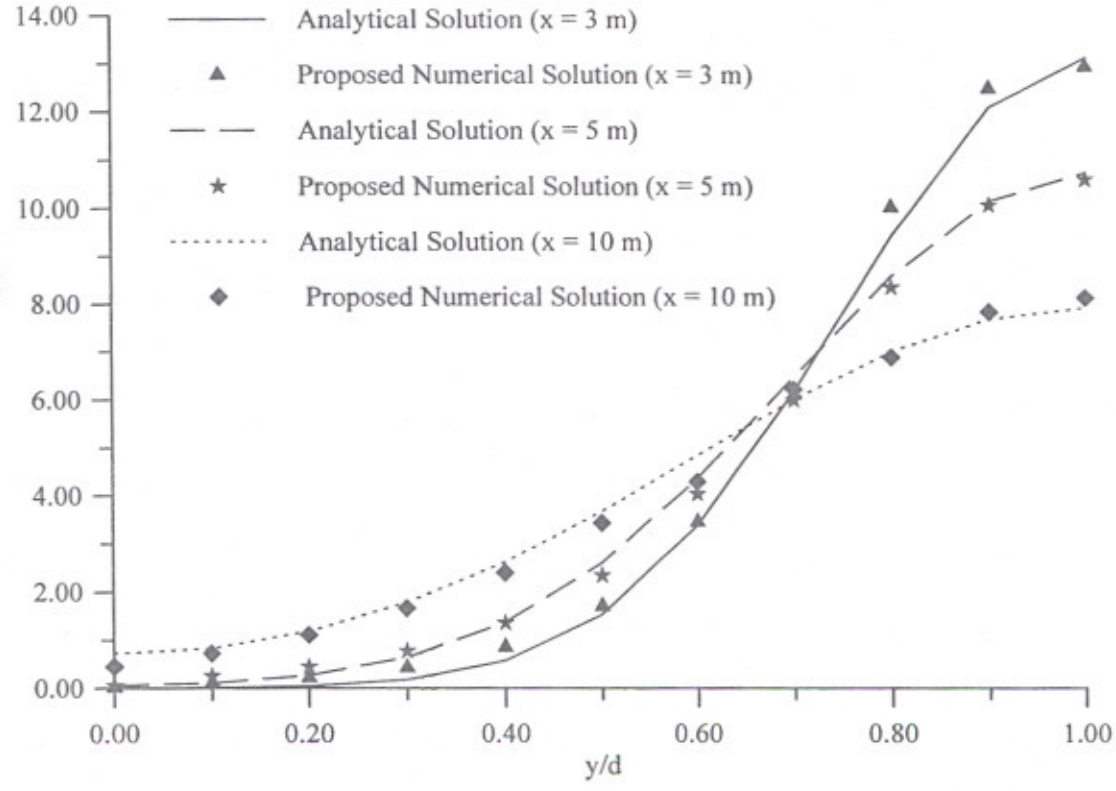

Fig. 5.1 Comparison of results obtained using the proposed numerical scheme and analytical solution for continuos injection of transverse line source

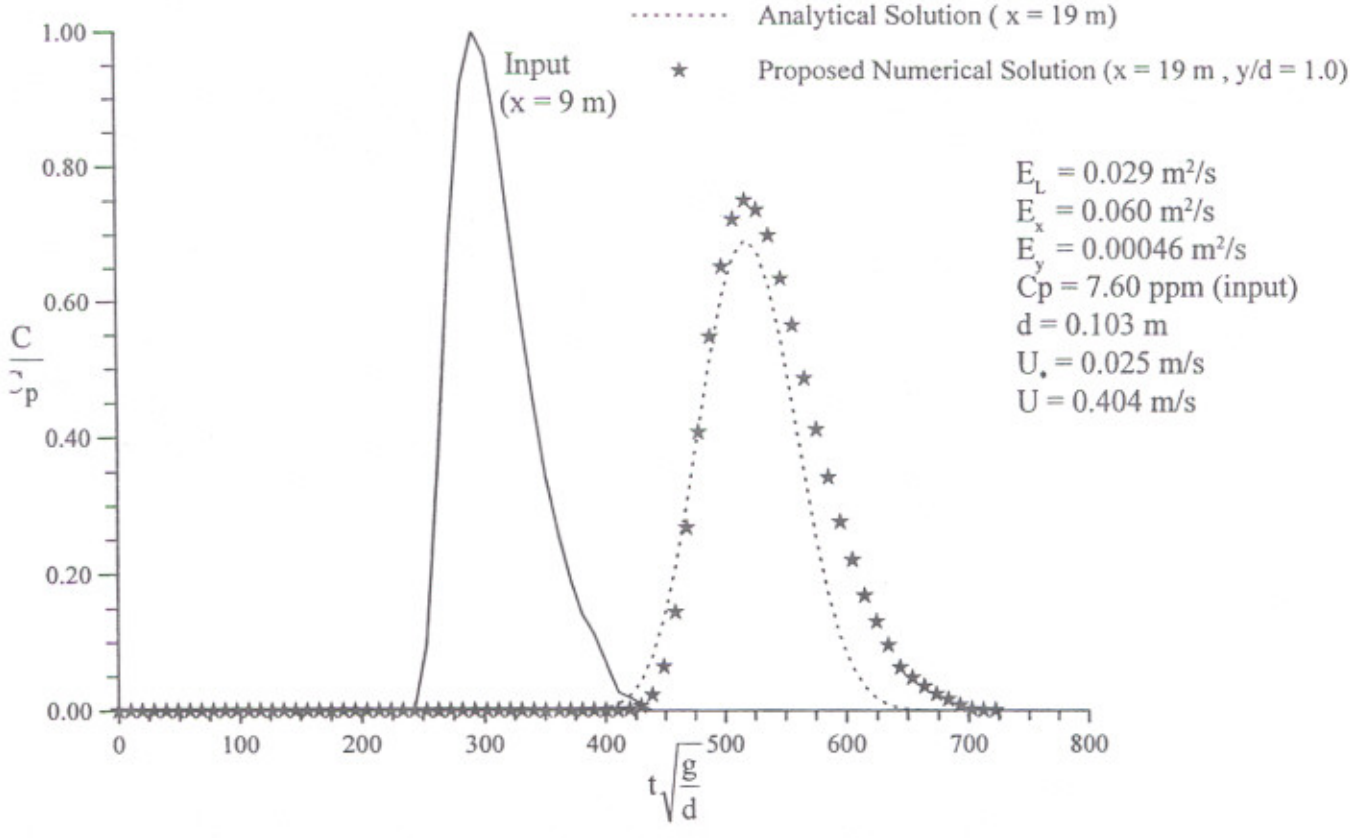

Fig. 5.2 Comparison of results obtained using Fischer's analytical solution and the proposed numerical scheme (Data set 1CDCW7)

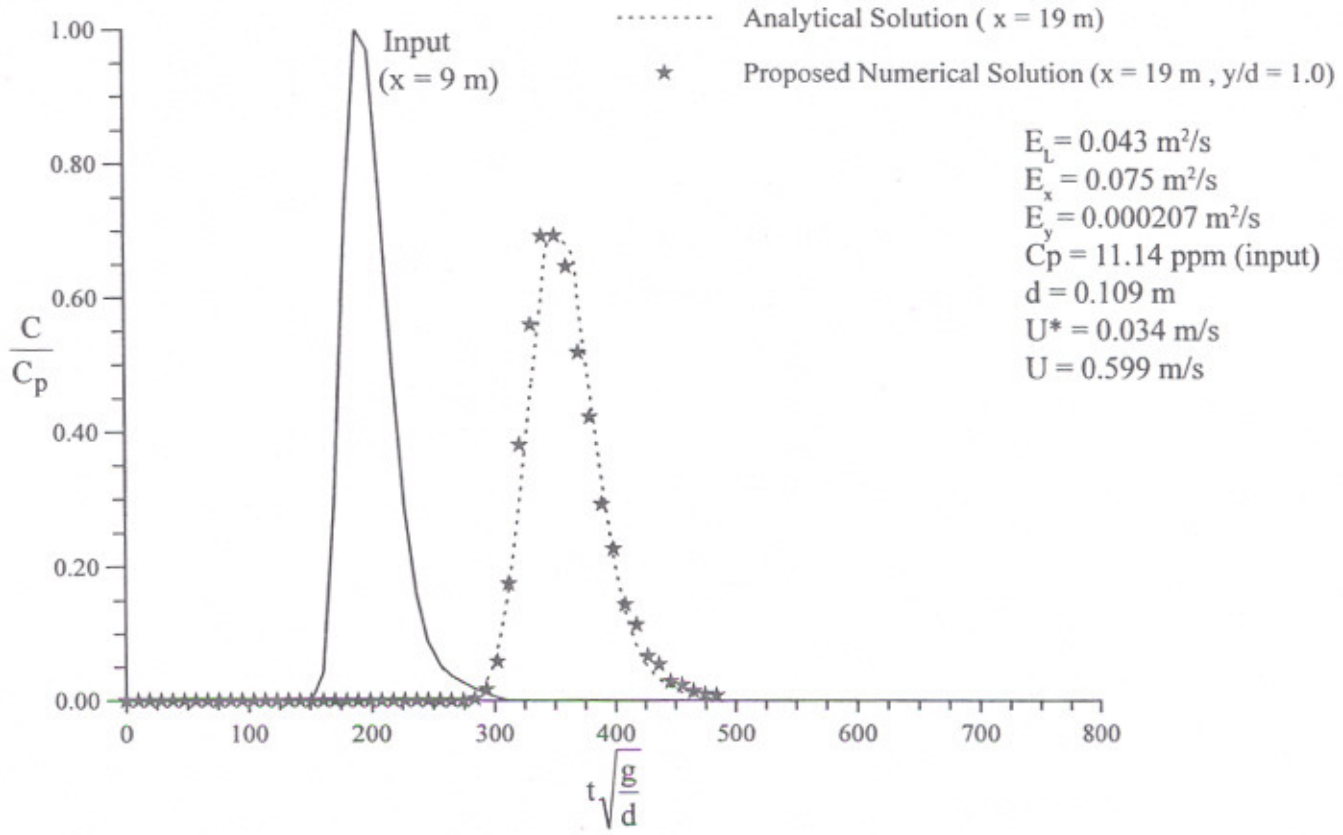

Fig. 5.3 Comparison of results obtained using Fischer's analytical solution and the proposed numerical scheme (Data set 4CDCW5)

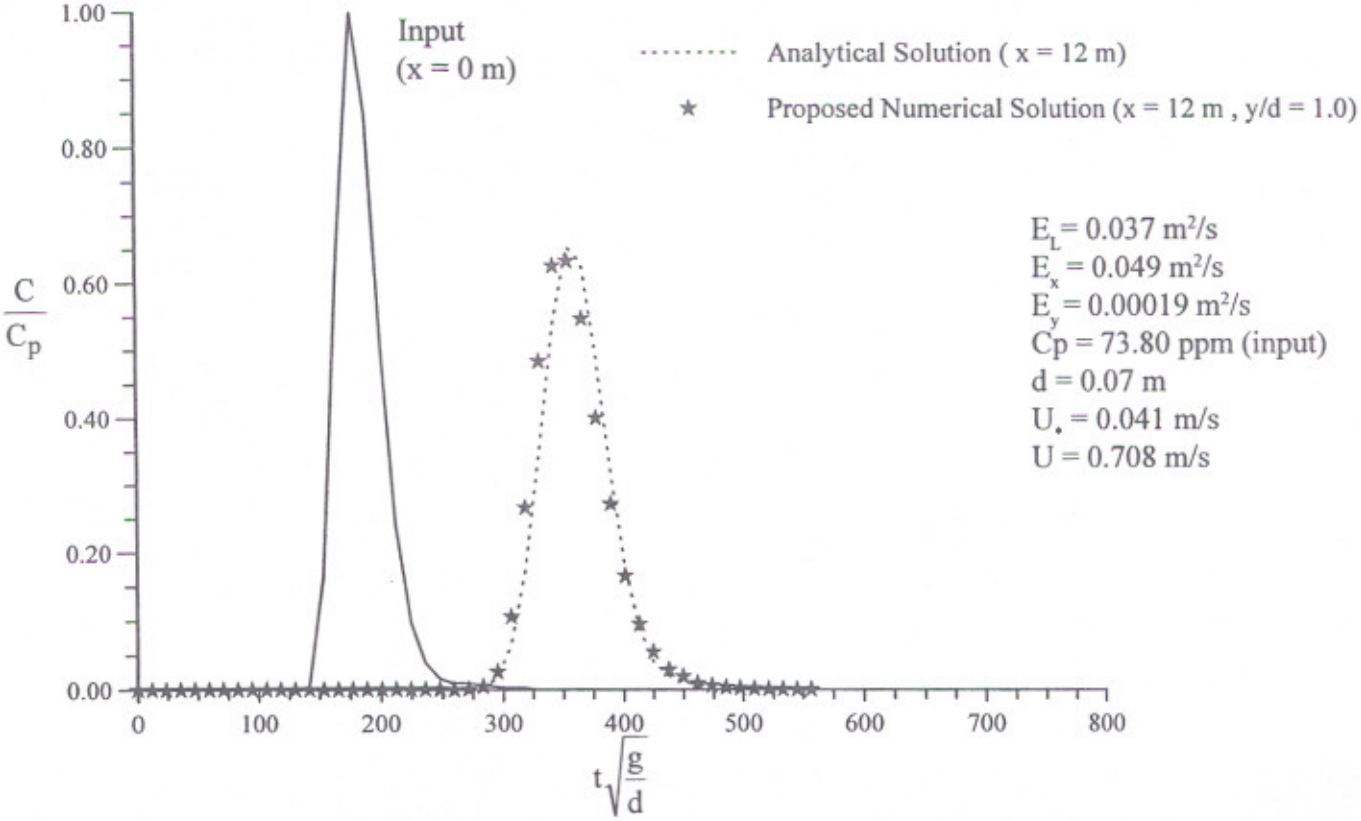

Fig. 5.4 Comparison of results obtained using Fischer's analytical solution and the proposed numerical scheme (Data set of Ahmad 1997)

that C-t curves at various elevations along the depth are practically same, thus computed C-t curves at y/d = 1.0 (*i.e.*, at surface of water) are shown in Figs. 5.2, 5.3 and 5.4. Comparison of analytical and numerical results reveals that agreement between them is satisfactory in some cases (Figs. 5.3 and 5.4 particularly) while it is not satisfactory in some other cases as revealed by Fig. 5.2. The discrepancy is attributed to the error in prediction of E_L and E_x. It is to be noted that longitudinal mixing coefficient, E_x is based on the width-averaged variation of longitudinal velocity whereas longitudinal dispersion coefficient, E_L takes into account the cross-sectional average variation of longitudinal velocity. Thus it is concluded that provided realistic estimates for E_x and E_L are available, the proposed scheme can satisfactorily predict the C-t curves for mid-field and far-field regions due to transverse line slug injection of pollutant.

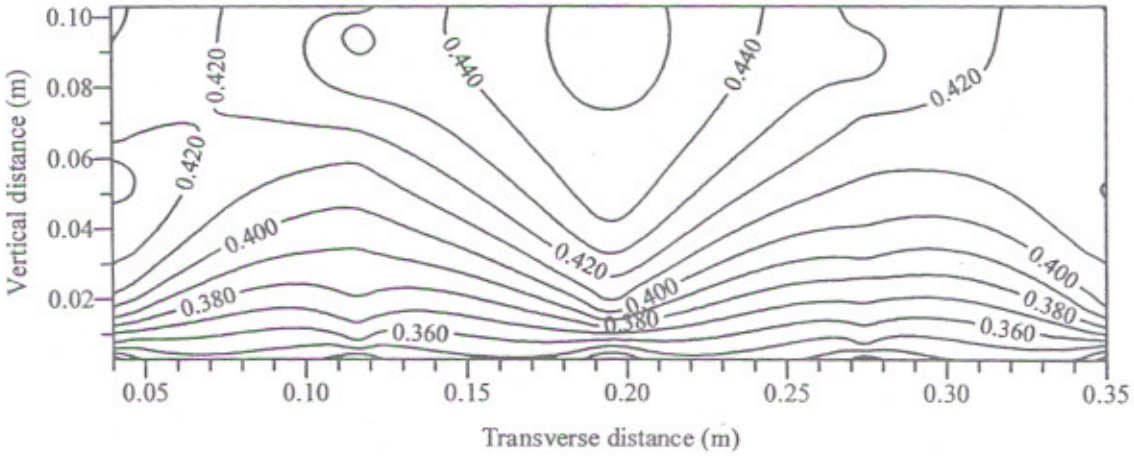

Fig. 5.5 Isovels for data set 1VDCW7

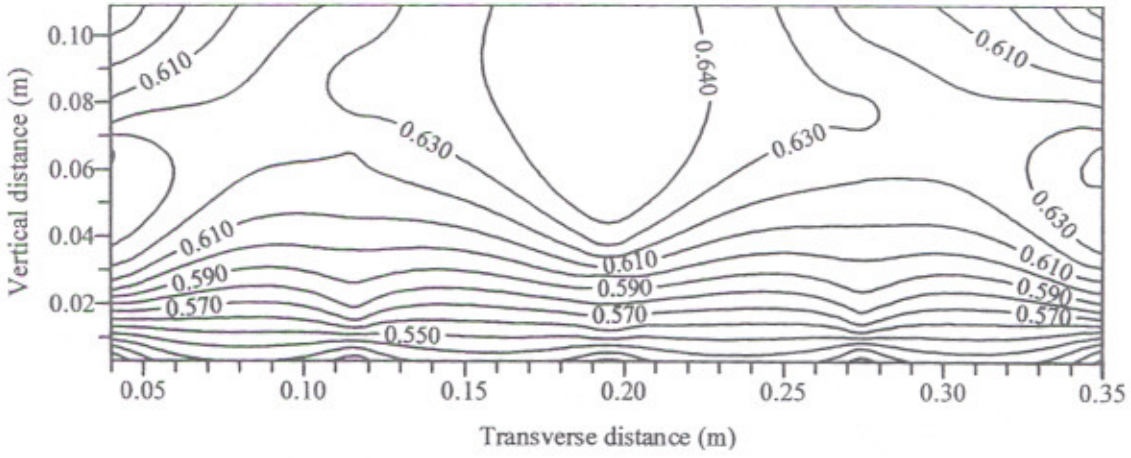

Fig. 5.6 Isovels for data set 4VDCW5

(All values are in m/s)

5.3 STUDY OF THE VARIATION IN MIXING COEFFICIENTS E_x AND E_y

The proposed numerical scheme is extended for determining the values of mixing coefficients E_x and E_y using the observed C-t curves at downstream stations and at different elevations in a vertical. As mentioned in Chapter-II, a sound theoretical study is available in the literature for the determination of E_y. However no method is available for the estimation of E_x (Rutherford 1994).

A two-dimensional grid search method has been employed to determine optimum value of longitudinal mixing coefficient E_x and vertical mixing coefficient E_y, for best matching of the observed and computed C-t curves. E_x results due to deviation of longitudinal velocity from the width-averaged velocity, therefore, the initial estimate for E_x was obtained by using Fischer et al. (1979) triple integration of transverse profile of observed longitudinal velocity. This is to be noted that in natural streams transverse profile of longitudinal velocity is several or more times effective in producing longitudinal mixing than the vertical profile of longitudinal velocity (Fischer et al. 1979). Initial estimate of E_y was obtained by using observed longitudinal velocity at mid-width of the channel and also by assuming Prandtl's logarithmic velocity distribution over the vertical.

Those values of E_x and E_y are considered to be the optimum ones for which the error as defined in Chapter-III (See; Fig. 3.4) is minimum between the observed and computed C-t curves at all the downstream stations. Let initial guess for these values be designated as OE_x and OE_y. To make the search for the optimum values, a two-dimensional computational grid is constructed as shown in Fig. 5.7. The incremental values of OE_x and OE_y are taken as equal to 1/10 and 1/2 of the initial values of E_x and E_y respectively. The feasible region consists of positive values of E_x and E_y.

Let the computation starts from a point P, the error ERR as defined in Section 3.3.1 of Chapter-III (viz. Eq. 3.32) is calculated at the neighborhood of P, at points R and Q lying vertically above and below P, respectively (See; Fig. 5.7). If the error is minimum at the point P, the grid was

refined by taking $\Delta E_y = OE_y / 2.0$ and the computation is repeated along the vertical line of computations till one gets the desired accuracy. But if the error is minimum at either point R or Q, the computation is shifted to the required position; unless one gets some other point where the error is minimum in its neighborhood, say at the point M_C (See; Fig. 5.7). The value of OE_x and OE_y at the point M_C are the local optimum values. To get global optimum values of OE_x and OE_y, the computation is shifted horizontally in both the directions, for E_x equal to $(OE_x + \Delta E_x)$ and $(OE_x - \Delta E_x)$. The local minimum is determined in the same way for both increasing and decreasing values of E_x. Let thus identified local optimum points be M_R and M_L for the values of E_x equal to $(OE_x + \Delta E_x)$ and $(OE_x - \Delta E_x)$, respectively. Out of the three local optimum points, the one finally selected has minimum error. If this point is M_C, the point is considered as global optimum value. But if the point is M_R or M_L, the computation is shifted in the required direction, computational traversing as explained above is continued till the entire feasible region is covered.

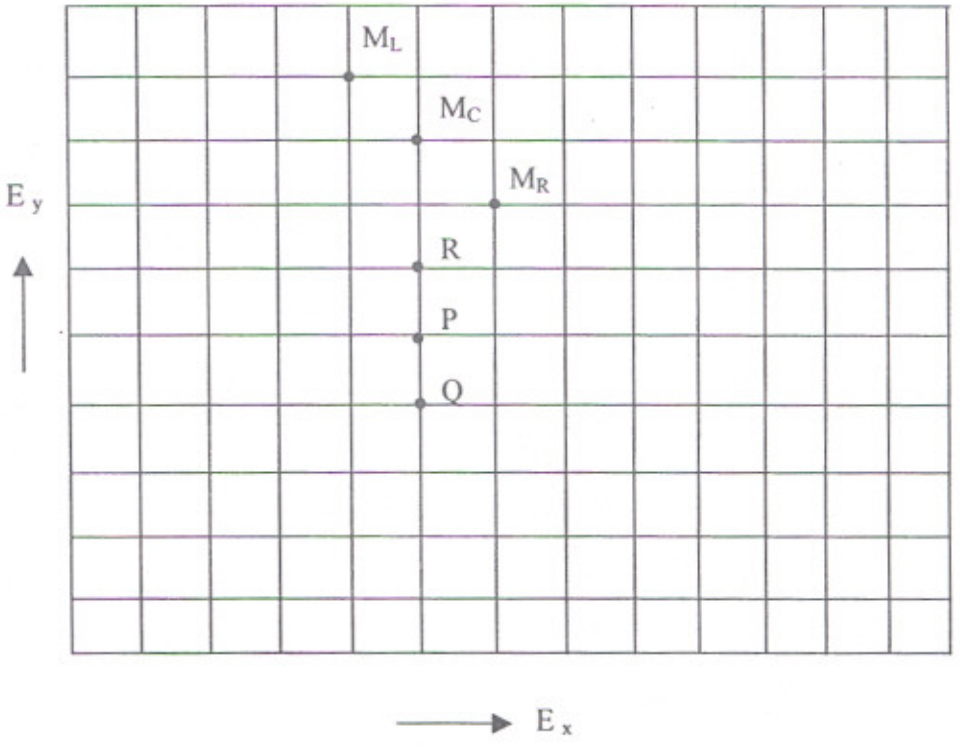

Fig. 5.7 Determination of optimum mixing coefficients OE_x and OE_y

To judge how closely the predicted C-t curves compare with the observed ones for above derived optimum values of E_x and E_y, the C-t curves computed using the proposed numerical scheme at y/d = 1.0 (*i.e.*, at surface of flow) and y/d = 0.0 (*i.e.*, at bed of the channel) are plotted in Fig. 5.8 for the data set 4CDCW5. As expected a close agreement is obtained between these two curves. A similar agreement was also observed for the other data sets (not shown here).

5.4 VERIFICATION OF RELATIONSHIPS FOR E_y

The experimental data collected during present study and data available from literature have been used to verify the existing predictors for vertical mixing coefficient E_y. The depth-averaged value of E_y, computed using Eq. (2.45) is compared with the optimum (observed) value of E_y as shown in Fig. 5.9. Optimum values of E_y were derived as per the procedure illustrated in section 5.3, for the data of present study, however for other data the optimum values of E_y were available in literature. It is clear from Fig. 5.9 that most of the E_y values predicted by Eq. (2.45) lie within a range of 2 to 1/2 times the observed values of E_y. The values of E_y were also estimated from measured velocity distribution at mid width of the channel in vertical direction and using Eq. (2.42). These were compared with observed E_y as shown in Fig. 5.10. As the velocity distribution for data taken from literature were not available, Fig. 5.10 is prepared only for experimental data of present study. The agreement between E_y computed from vertical velocity distribution with observed one is slightly better than E_y computed using Eq. (2.45). Such result is understandable because Eq. (2.45) is based on assumption of logarithmic velocity distribution, whereas the observed velocity distribution differs from the logarithmic velocity distribution. Therefore henceforth E_y values computed using measured velocity distribution are utilized for further computations. Equation (2.45) is used for computation of E_y when observations on velocity distribution are available. The optimum values of E_x were re-determined by using the proposed numerical scheme, by using the E_y values determined through use of observed velocity distribution in vertical direction.

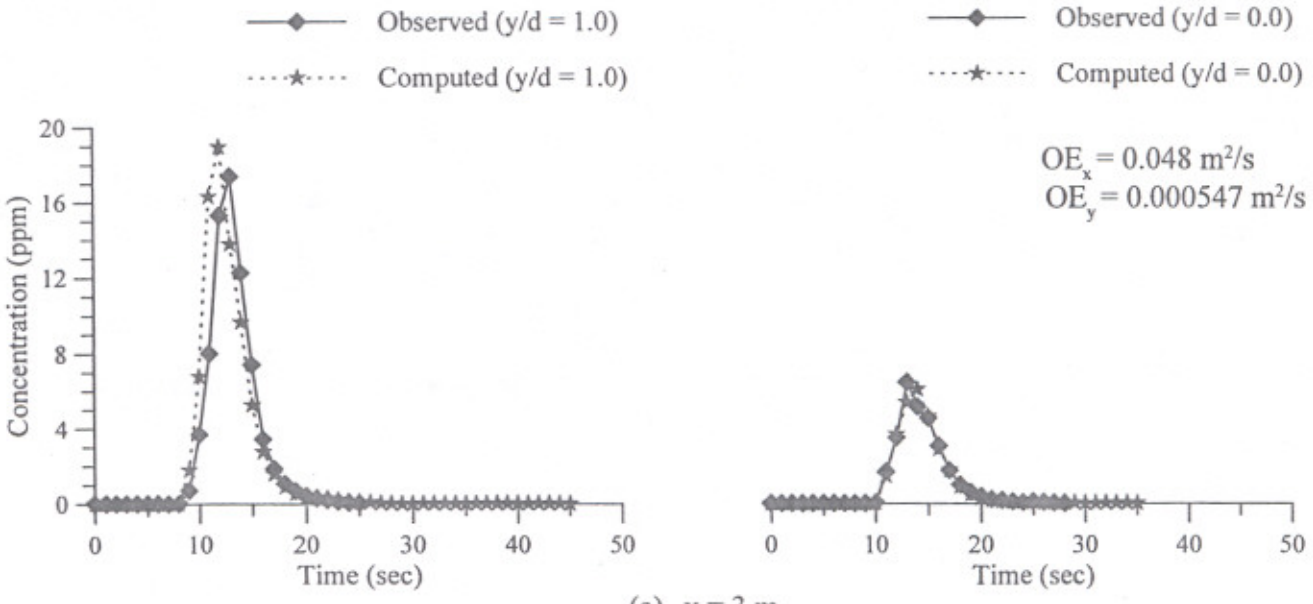

(a) x = 3 m

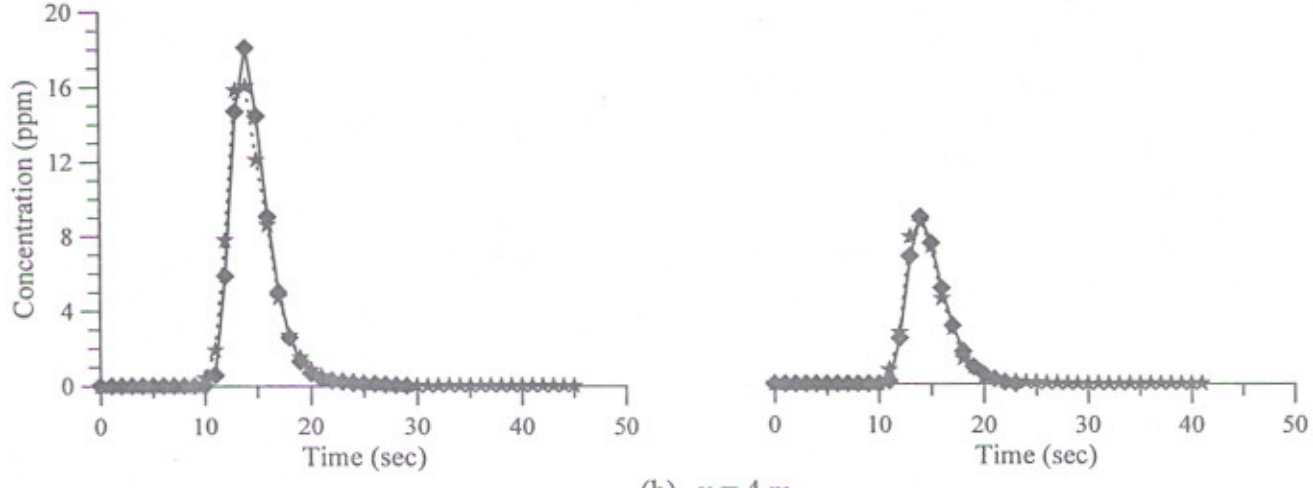

(b) x = 4 m

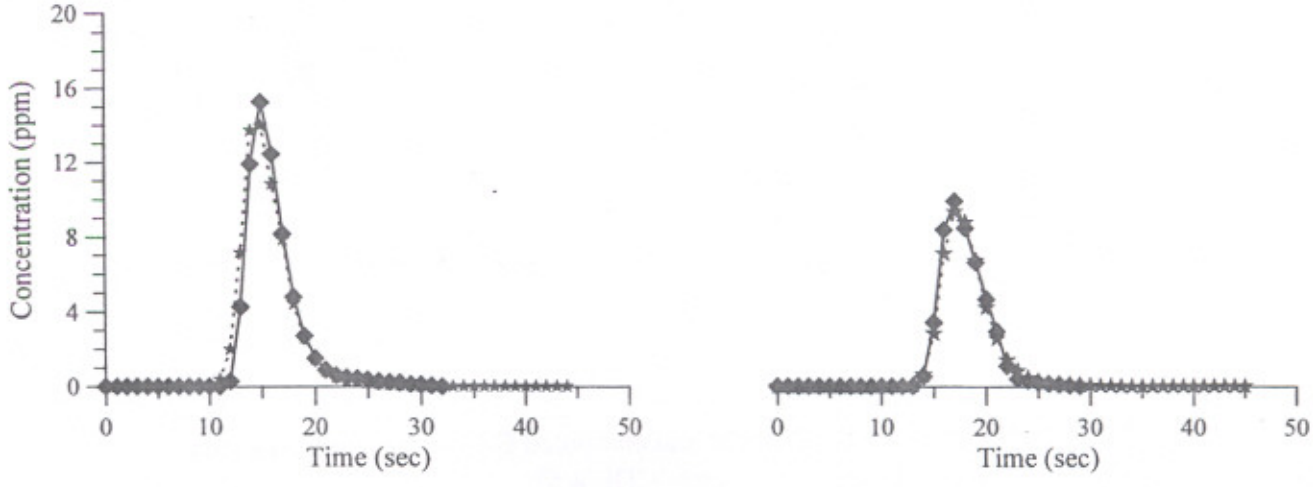

(c) x = 5 m

Continued....

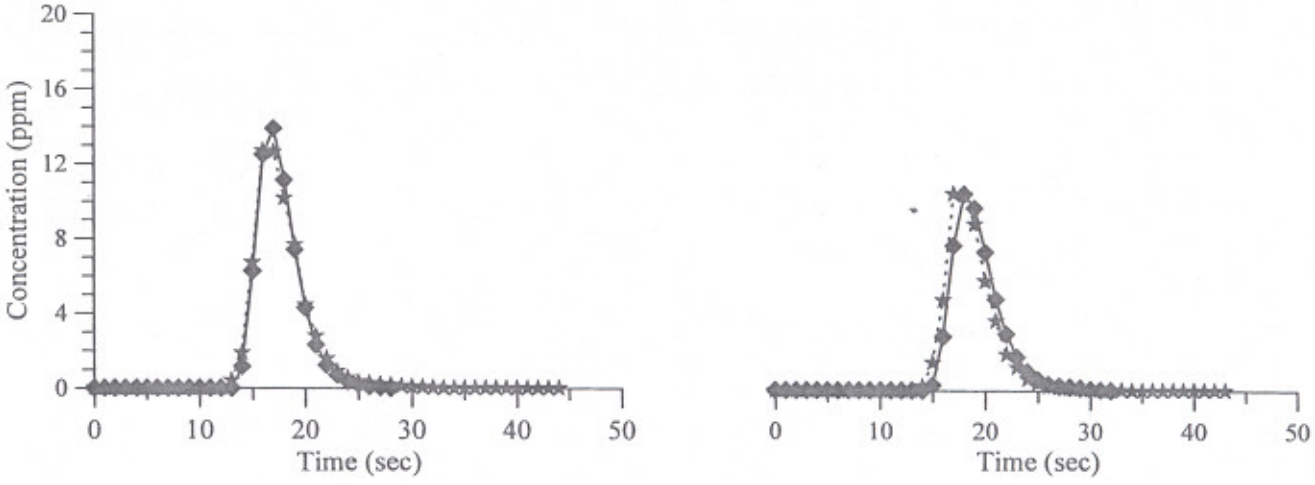

(d) x = 6 m

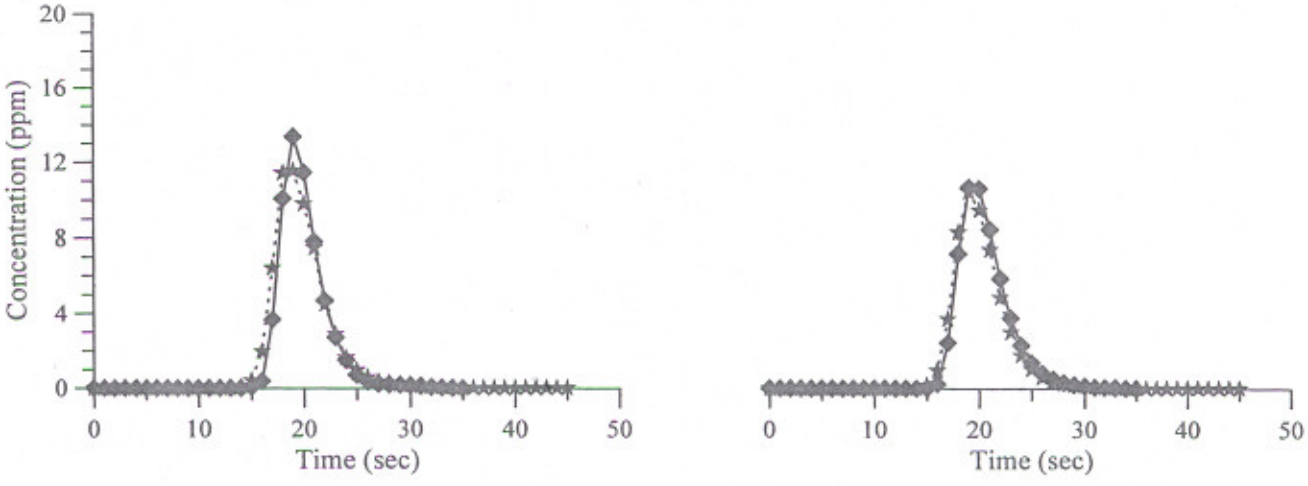

(e) x = 7 m

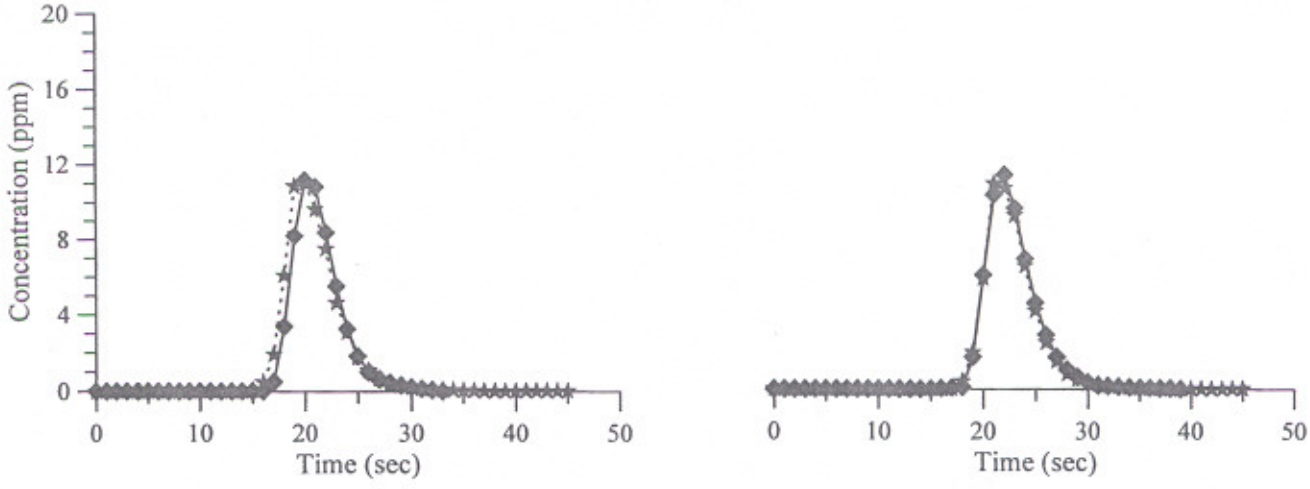

(f) x = 8 m

Fig. 5.8 Comparison of observed and computed C-t curves using optimum value of E_x and E_y (Data set 4CDCW5)

Those values of E_x are considered to be the optimum ones for which error as defined by Eq. (3.32) is minimum between the observed and computed C-t curves at all the downstream stations. The variation of E_x values with the corresponding values of associated errors are shown in Fig. 5.11 and Fig. 5.12 for two data sets 1CDCW7 and 4CDCW1 as illustration.

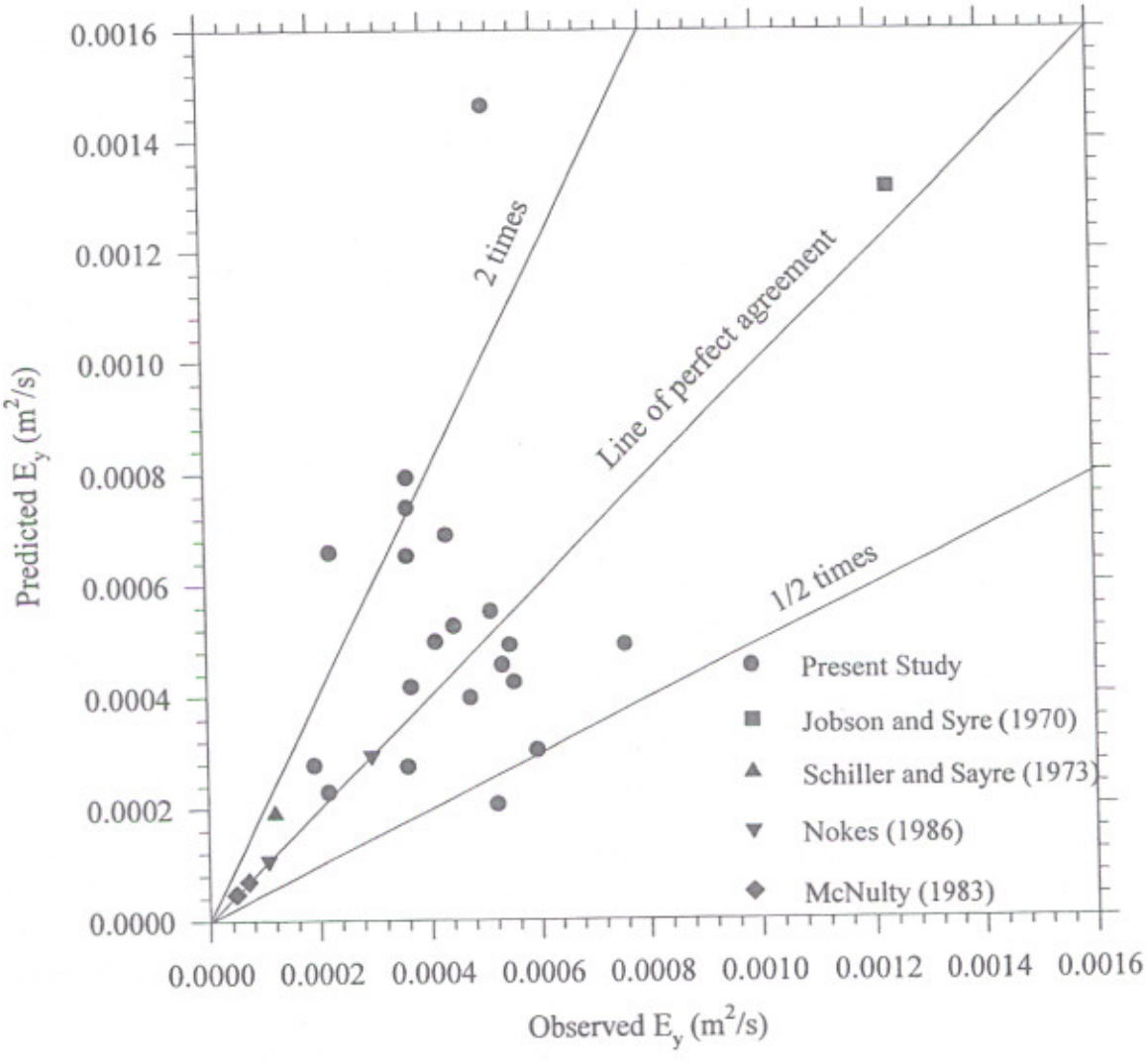

Fig. 5.9 Verfication of depth averaged value of E_y computed by Eq. (2.45)

Using thus determined optimum values of E_x and E_y obtained from observed velocity distribution in vertical direction at mid-width of the channel, the C-t curves are computed using

the proposed numerical scheme and these are plotted in Fig. 5.13 along with the observed C-t curves for the data set 2CDCW3. The values of E_x computed as above for different data sets are listed in Appendix-II.

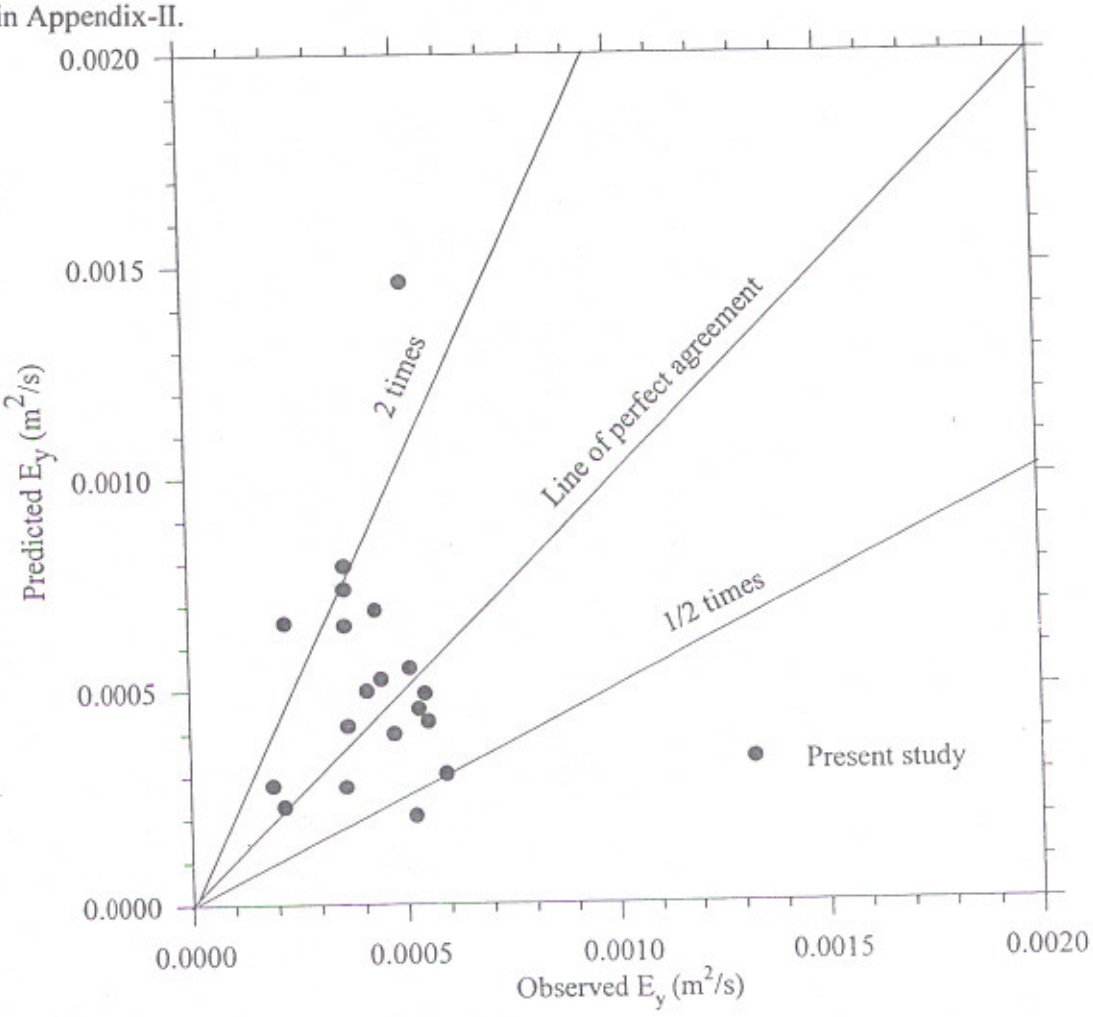

Fig.5.10 Verification of E_y computed from measured velocity distribution in vertical direction

5.5 PROPOSED RELATIONSHIP FOR E_x

As discussed above, E_y may be computed reasonably accurately from the velocity distribution in vertical direction or by using Eq. (2.45), however no predictor is available for longitudinal mixing coefficient, E_x. Ahmad et al. (2004) presented analysis for the identification of flow and

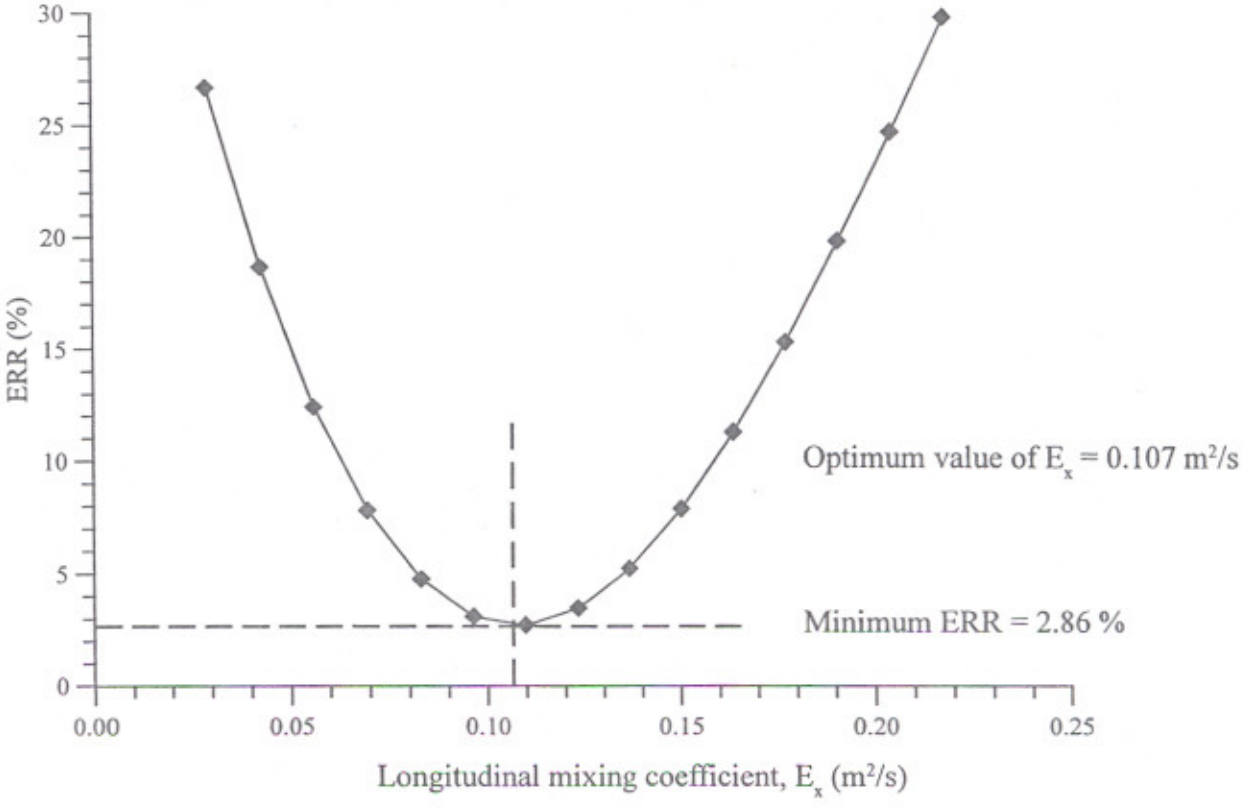

Fig.5.11 Determination of longitudinal mixing coefficient (Data set 1CDCW7)

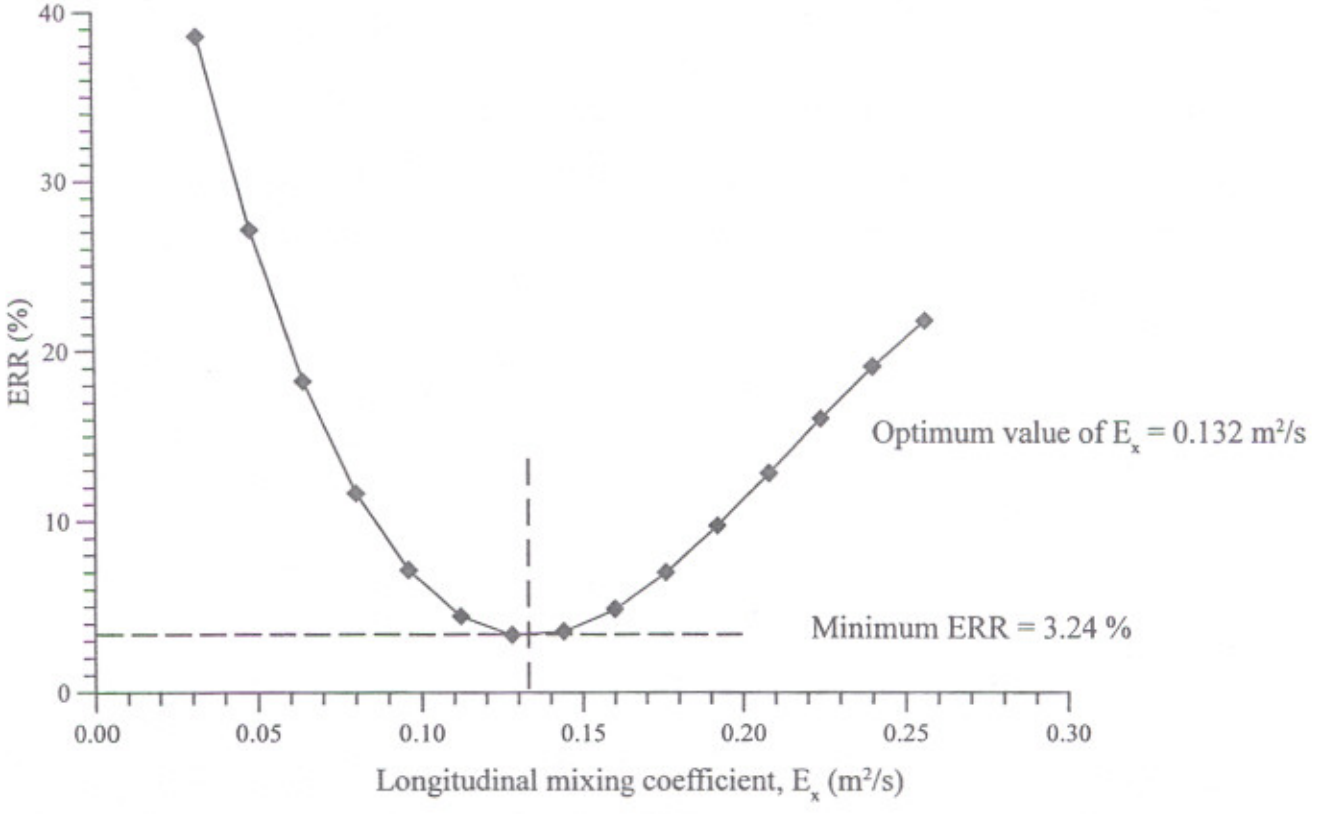

Fig.5.12 Determination of longitudinal mixing coefficient (Data set 4CDCW1)

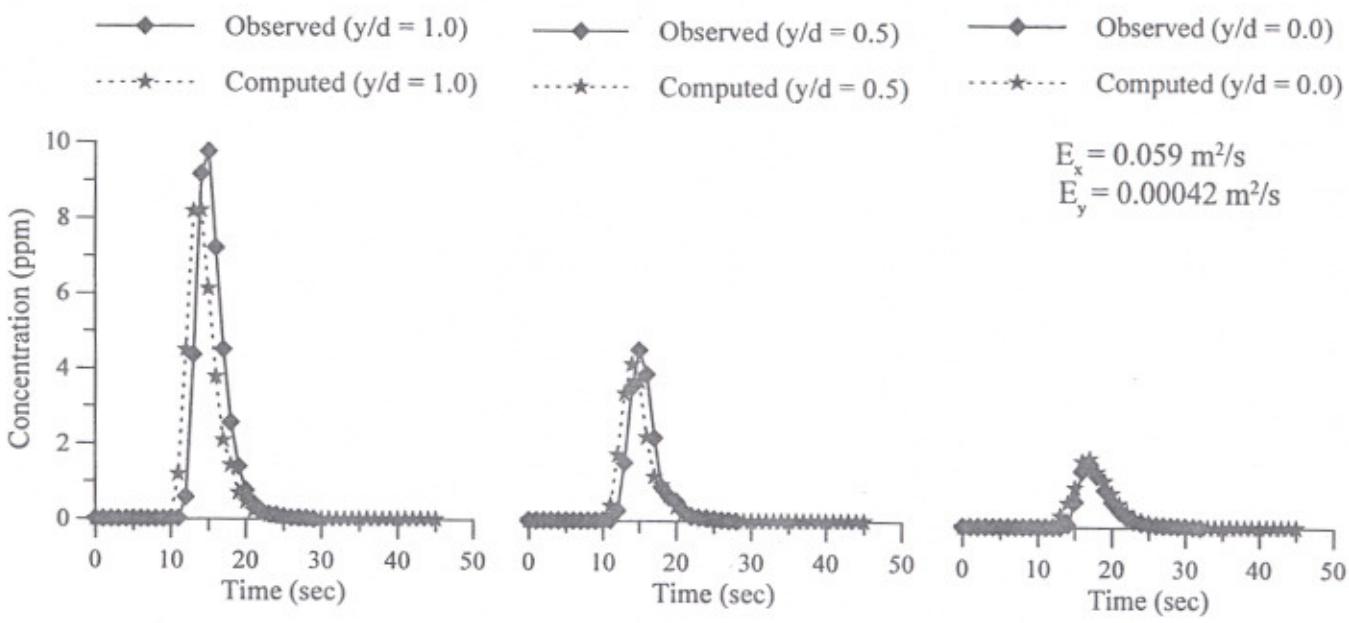

(a) x = 3 m

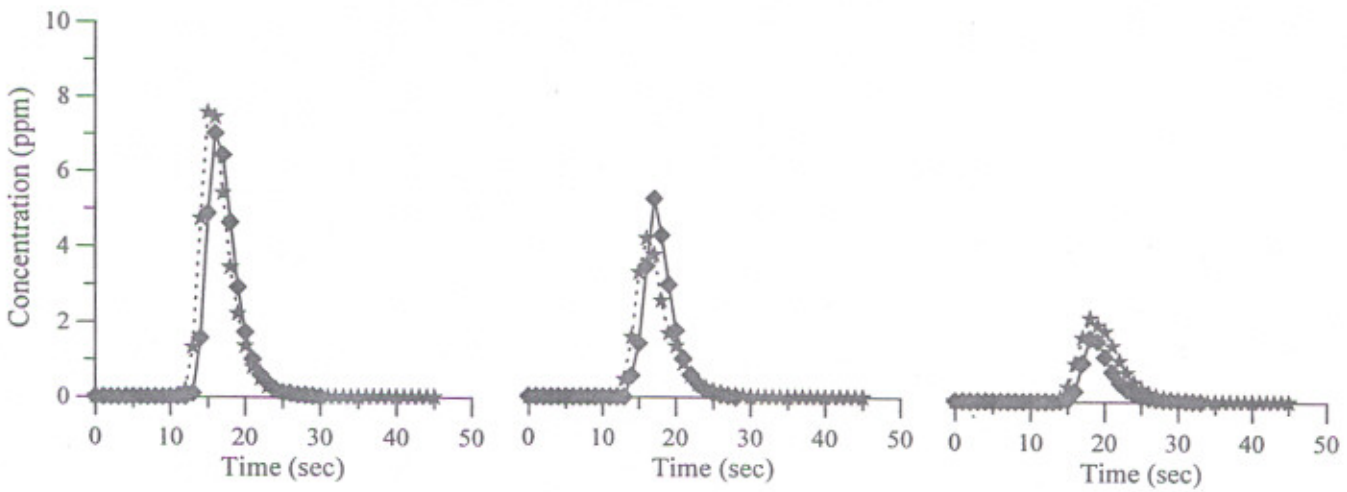

(b) x = 4 m

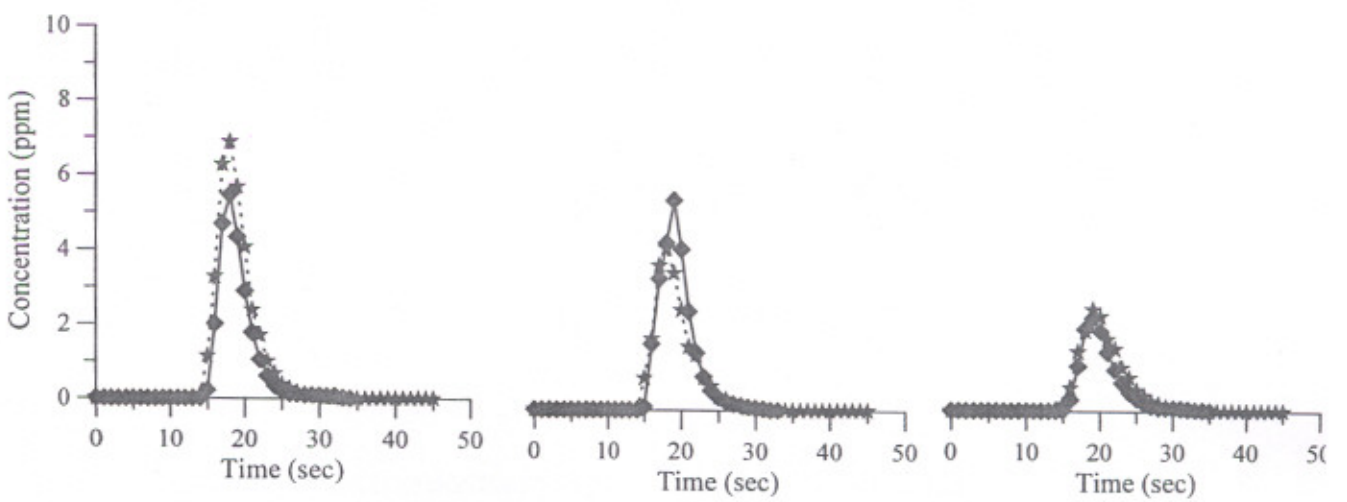

(c) x = 5 m

Continued...

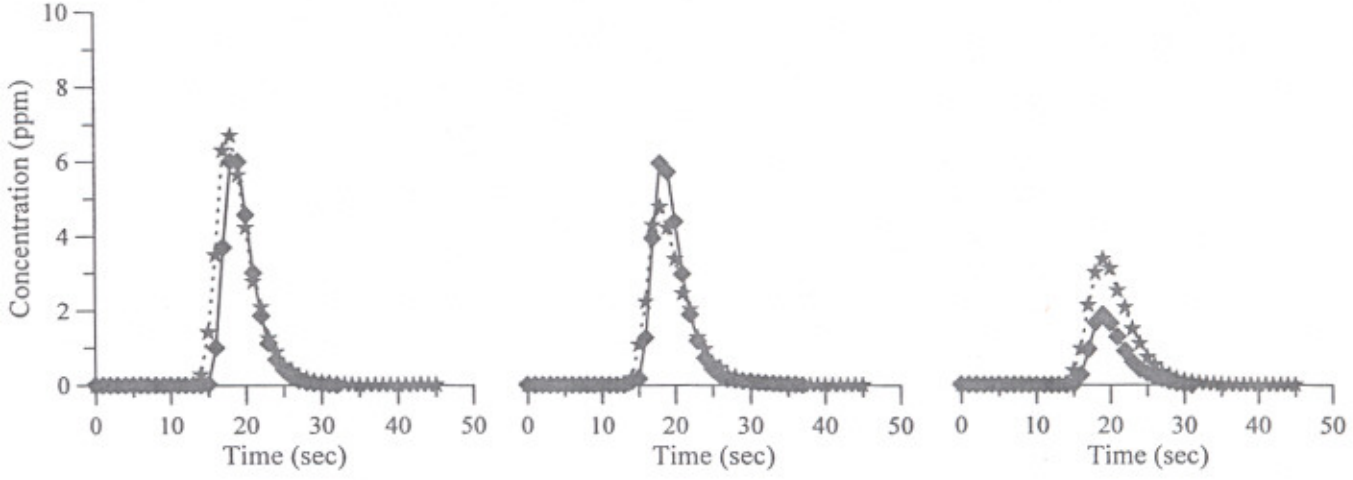

(d) x = 6 m

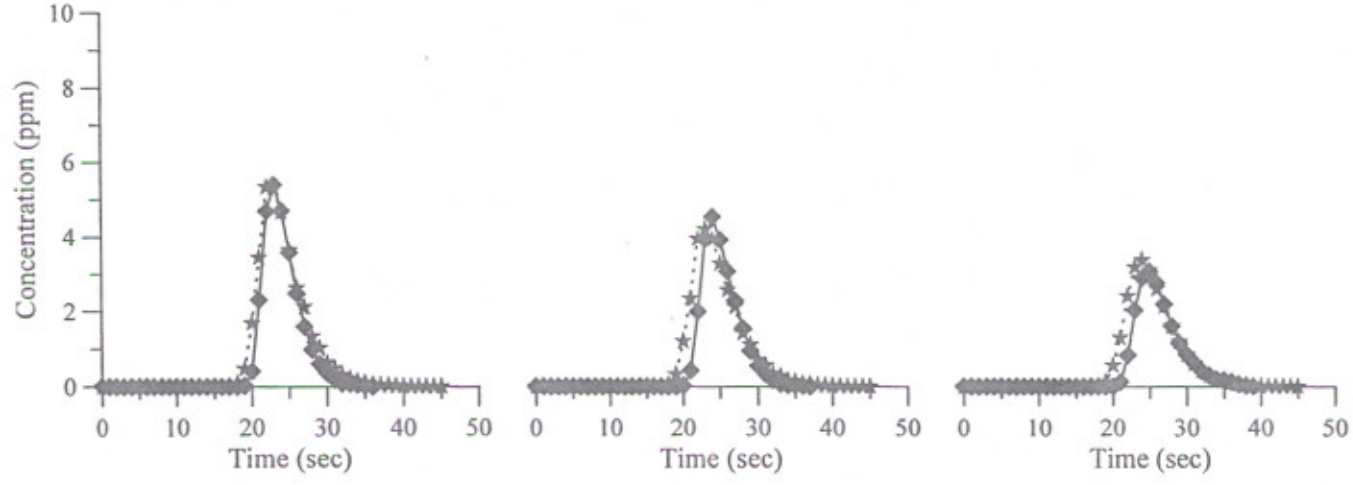

(e) x = 8 m

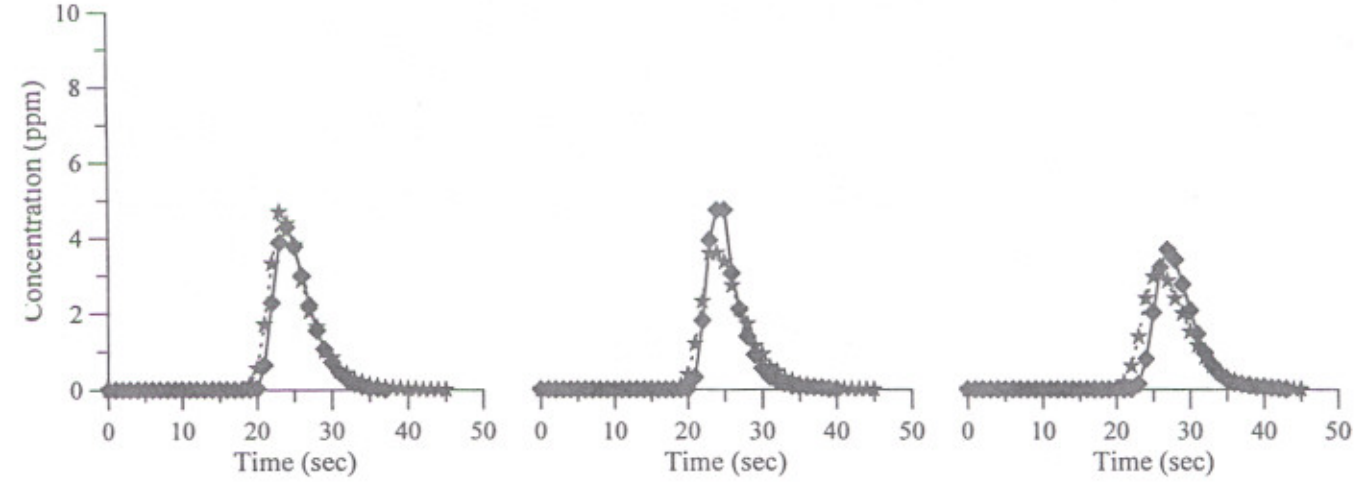

(f) x = 9 m

Fig. 5.13 Comparison between observed C-t curve and C-t curve computed using proposed numerical scheme with use of optimum value of E_x and vertical velocity distribution based value of E_y

channel characteristics which significantly influence the mixing coefficient E_x. It was found by Ahmad et al. (2004) that non-dimensional parameter $\frac{E_x}{qS_b}$ should be significantly affected by the variables $\frac{b}{d}$, $\frac{U}{U_*}$ and S_b. Based on the above study the following functional relationship is considered for determination of E_x for process of two-dimensional mixing in streams:

$$\frac{E_x}{qS_b} = \varphi\left(\frac{b}{d}, \frac{U}{U_*}, S_b\right) \tag{5.1}$$

Here φ represents the functional relationship and q is discharge per unit width. The variable qS_b has been included in the above relationship to account for the effect of unit stream power ($\tau_o U$) on the longitudinal mixing. Here τ_o is the average bed shear stress. Like wise, the parameters $\frac{b}{d}$, $\frac{U}{U_*}$ and S_b has been included to account for the effect of aspect ratio, velocity distribution and channel slope, respectively on E_x. Multiple regression analysis produced the following relationship for E_x.

$$\frac{E_x}{qS_b} = 43.54\left(\frac{b}{d}\right)^{2.51}\left(\frac{U}{U_*}\right)^{-2.39}(S_b)^{-1.01} \tag{5.2}$$

The multiple correlation coefficient for Eq. (5.2) is 0.802. Equation (5.2) has been derived by using the data collected during the present experimental study. In order to check the accuracy, the values of E_x computed using Eq. (5.2) are compared with corresponding observed values as shown in Fig. 5.14. The values lie within an error band of 2 to 1/2 times the observed values.

In order to check what effect such errors in the values of E_x as well as E_y would have on the C-t curves computed using these values of E_x and E_y, a sensitivity analysis of E_x and E_y values is carried out as discussed in the next section.

5.6 SENSITIVITY ANALYSIS FOR MIXING COEFFICIENTS

For the sensitivity analysis, two sets of data viz. 2CDCW6 and 4CDCW1 are used. The input C-t curves are shown in Fig. 5.15. Using the proposed numerical scheme, the C-t curves are predicted at the various downstream sections using the derived optimum value of E_x and E_y derived using measured velocity distribution in vertical direction and C-t curves of Fig. 5.15 being used as inputs at three elevations along the vertical, *i.e.*, y/d = 0, 0.5 and 1.0. The C-t curves are also recomputed using the present numerical scheme with altered values of E_x. For this, the values of E_x are altered by multiplying factors of 0.01, 0.1, 0.2, 0.5, 1.5 and 2. For

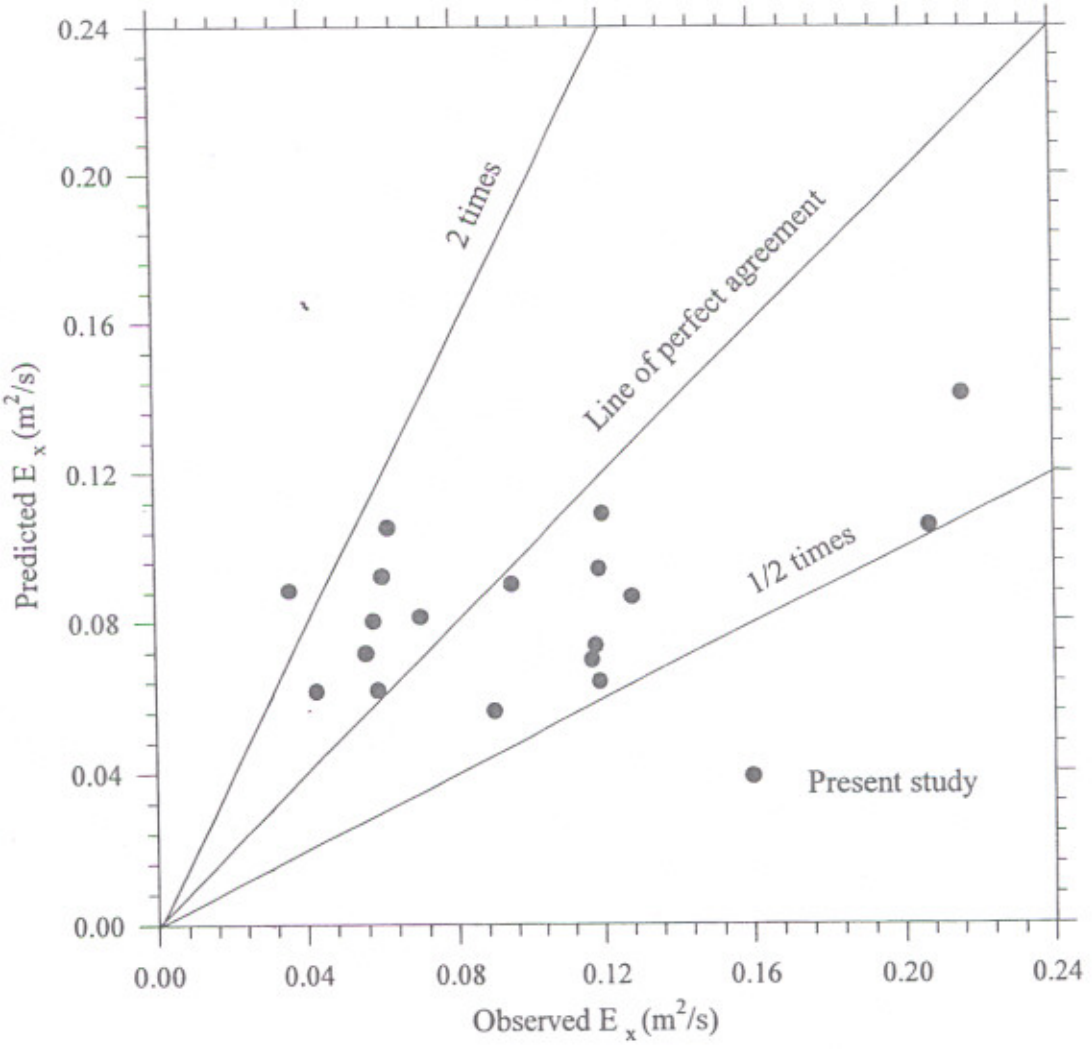

Fig.5.14 Verification of Eq. (5.2)

comparison, the ERR values (See; Eq. 3.32) are computed with the C-t curves computed with optimum E_x value taken as the reference, at various downstream stations. The accuracy of computations is then defined as (100-ERR). The values of the accuracy so computed are plotted against the corresponding $\frac{E_{x\ altered}}{E_{x\ optimum}}$ values and shown as illustration for the two sets in Fig. 5.16. A close study of Fig. 5.16 reveals that accuracy for computation of C-t curves reduces to about 60%, which is not considered to be significant when the value of E_x is altered with a multiplying factor from 0.2 to 2. However, the computed C-t curves are much less accurate while E_x values are altered beyond these limits.

A similar analysis for E_y (Fig. 5.17) reveals that accuracy for the computation of C-t curve reduces to about 50 to 70%, when optimum value of E_y is altered by factors from 0.5 to 2. However, less accurate results are obtained while E_y values are altered beyond these limits.

Also presented in Figs. 5.18 and 5.19, the variation of the dimensionless peak concentration of the C-t curve at the water surface (y/d = 1.0) with distance, when E_x and E_y values are changed from 0.01 to 2. These figures reveal that the peak of C-t curve does not change very much when E_x and E_y values are altered by 0.5 to 2 times the optimum value.

Thus in the light of above analysis, it is concluded that likely error in computation of E_x by using Eq. (5.2) and E_y by using Eq. (2.42) would not result in appreciable errors in computation of the C-t curves.

5.7 EFFECT OF SEDIMENT ON MIXING PROCESS

To study the effect of suspended sediment on mixing, C-t curves were observed for clear water flow and for suspended sediment-laden flow under nearly identical flow conditions, using sands of average diameter 0.064 mm and 0.024 mm with sand concentration ranging from 104 ppm to 6178 ppm by weight. The cross-sectional velocity distributions in clear-water flow (CWF) and sediment-laden flow (SLF) were also observed.

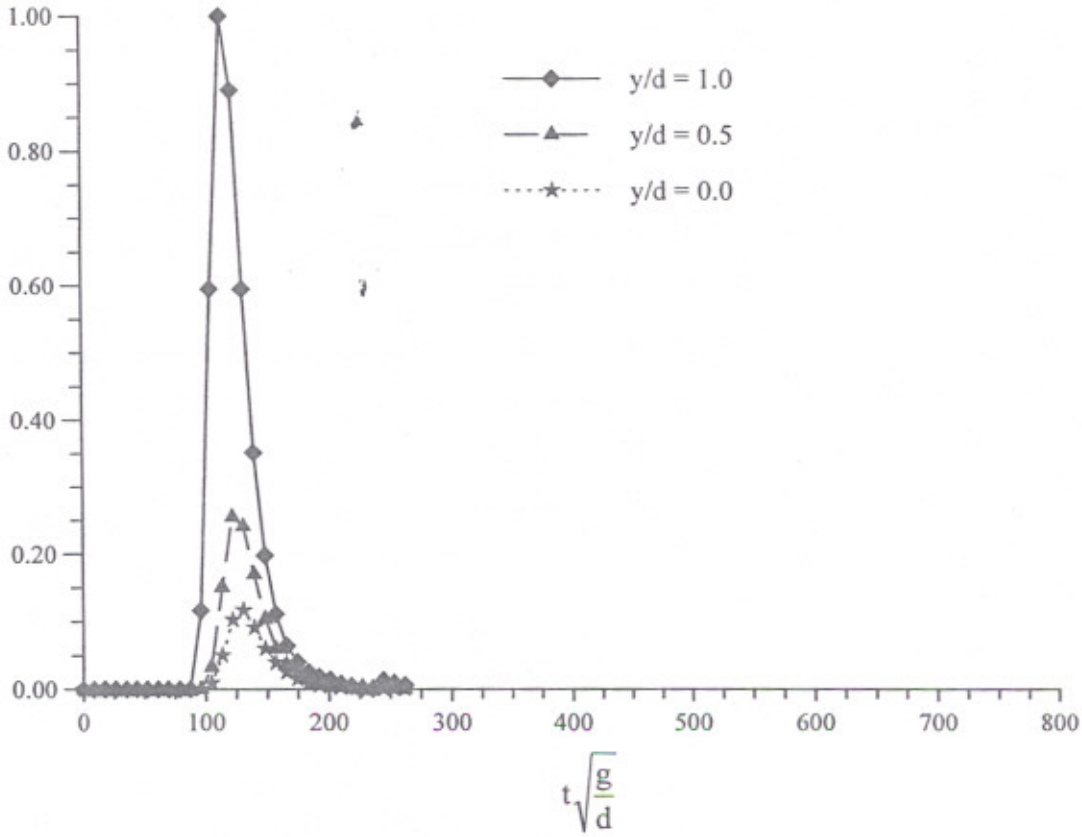

Fig.5.15 (a) Input C-t curves used in sensitivity analysis (Data set 4CDCW1)

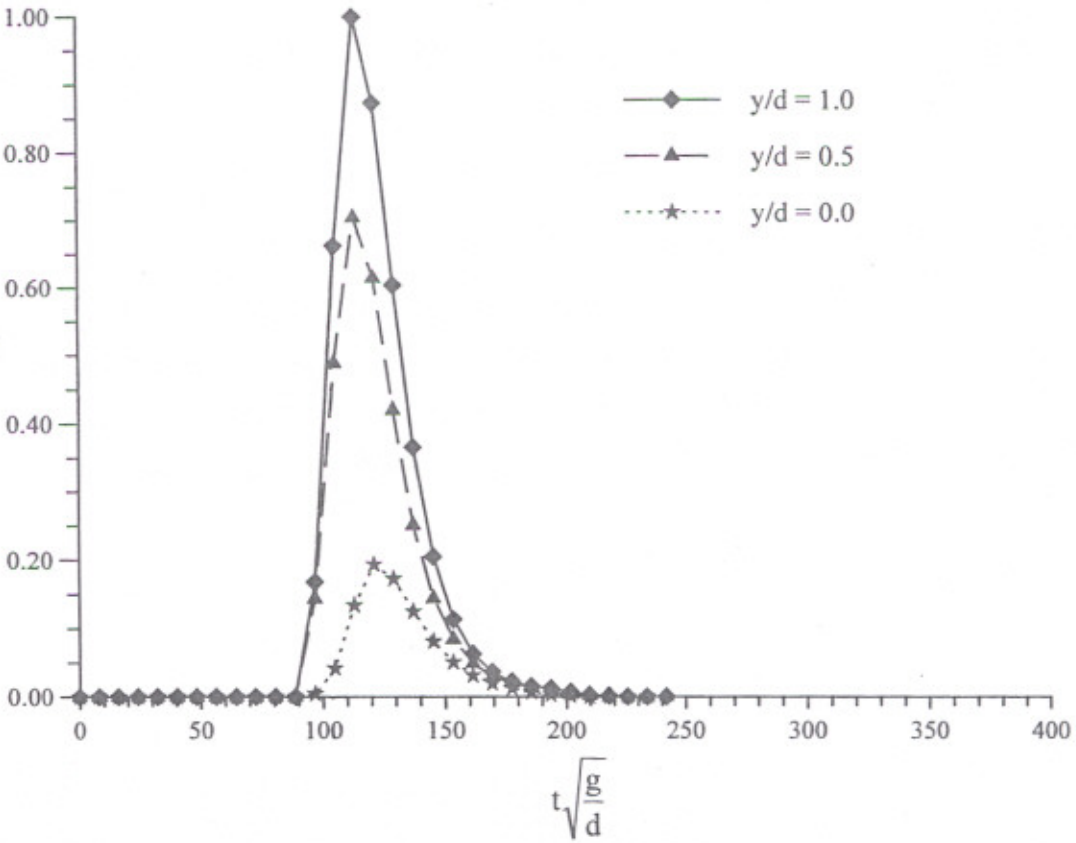

Fig.5.15 (b) Input C-t curves used in sensitivity analysis (Data set 2CDCW6)

The C-t curves observed for clear water flow and corresponding sediment-laden flows are superimposed on each other for studying the effect of sediment concentration on C-t curves, at different elevations along the depth and at various downstream locations. Such comparisons are shown for two sets of data in Figs. 5.20 and 5.21 as illustration. From these and many such other figures (not shown here), it is concluded that the presence of sediment within the range studied (suspended sediment concentration 104 ppm to 6178 ppm) does not have appreciable effect on mixing. These finding are in conformity with the findings of Singh et al. (1992) who has concluded that the presence of sediment with concentrations 90 ppm to 5000 ppm, has no effect on longitudinal dispersion. The measured vertical velocity distribution for the above two data sets for CWF and SLF are also superimposed and shown in Figs. 5.22 and 5.23. Within the range of sediment concentration studied in the present study, no appreciable changes in the velocity distribution for CWF and SLF are observed.

5.8 PROPOSED METHODOLOGY FOR PREDICTION OF TRACER CONCENTRATION IN STREAMS

For the computation of C-t curves, the stepwise procedure was described in Section 3.4. For this longitudinal mixing coefficient E_x is first estimated by using Eq. (5.2) and vertical mixing coefficient E_y is estimated by using Eq. (2.42). Then the C-t curves at different elevations along the depth and distances in the downstream are computed using the proposed numerical scheme, the algorithm of which is described in Fig. 3.3.

The computed C-t curves were plotted along with the corresponding observed C-t curves for graphical comparison using all the data for clear-water and sediment-laden flows. In Figs. 5.24 to Figs. 5.25, such a comparison is illustrated for some of the data sets. As revealed by these and many other such figures (not shown here), the prediction of C-t curves is satisfactorily (See; Figs. 5.24 and 5.25.

However the comparison between a few of the predicted C-t curves and the corresponding observed ones is poor as can be seen in Figs 5.24 and 5.25. This difference is attributed mainly to the measurement of errors particularly in the zone of two-dimensional mixing.

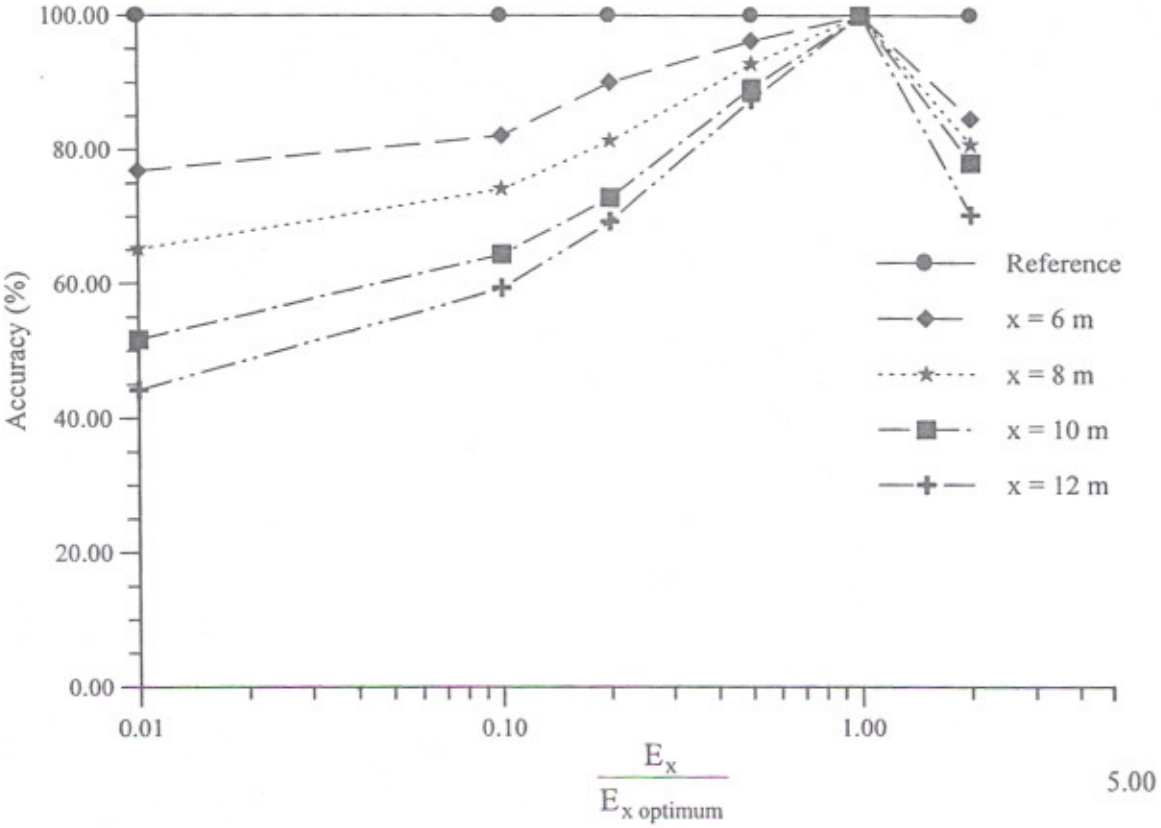

Fig.5.16 (a) Effect of variation of E_x on accuracy of predicted C-t curves (Data set 4CDCW1)

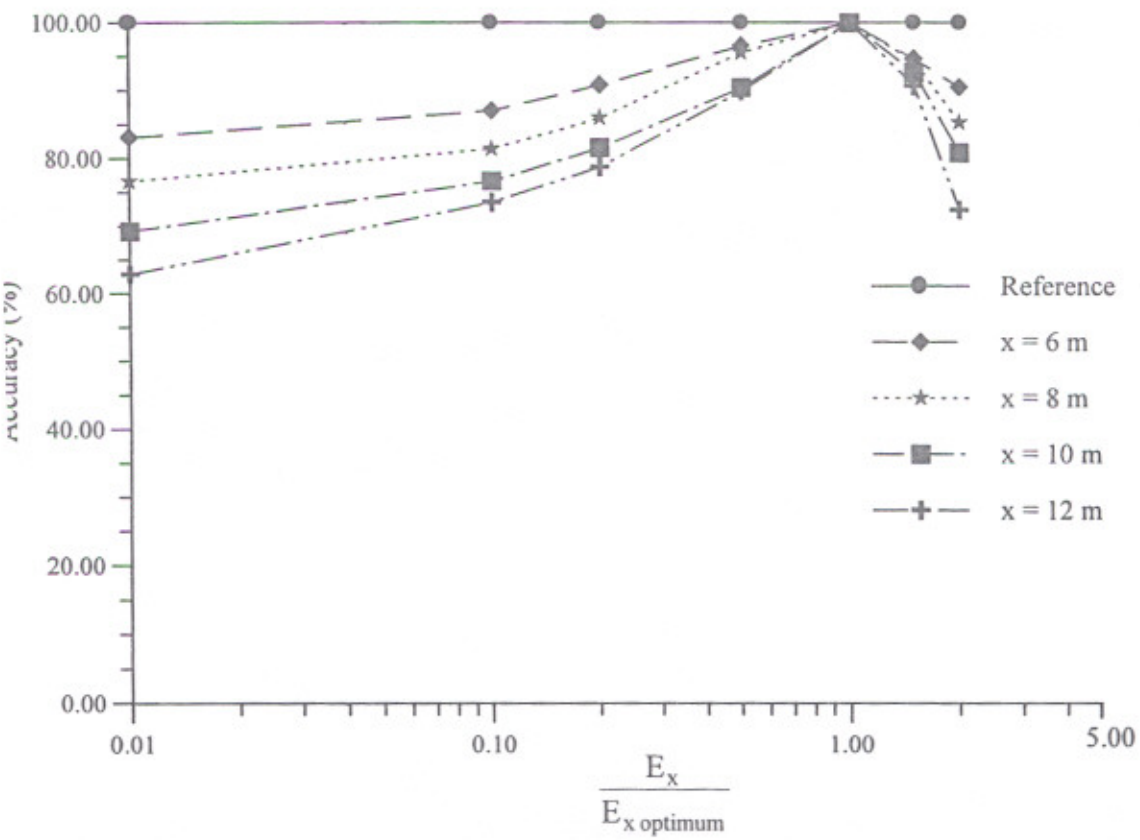

Fig.5.16 (b) Effect of variation of E_x on accuracy of predicted C-t curves (Data set 2CDCW6)

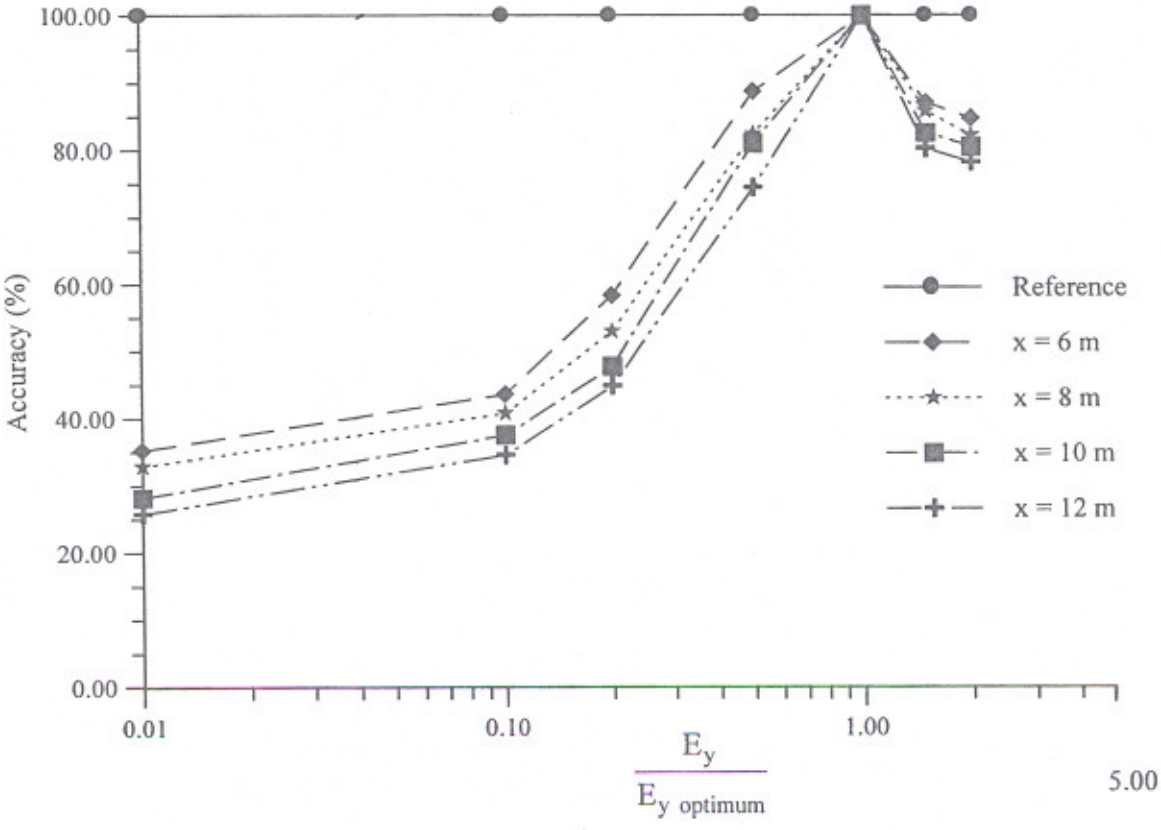

Fig.5.17(a) Effect of Variation of E_y on accuracy of predicted C-t curves (Data set 4CDCW1)

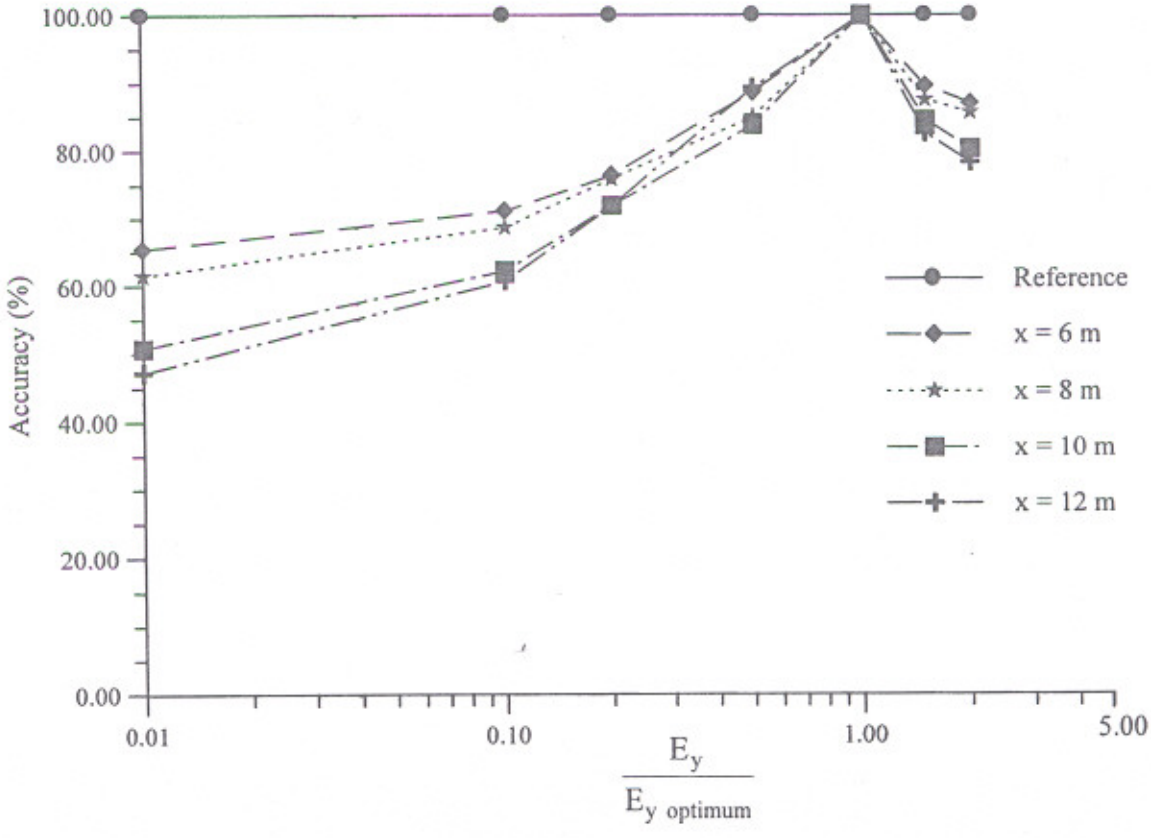

Fig. 5.17(b) Effect of variation of E_y on accuracy of predicted C-t curves (Data set 2CDCW6)

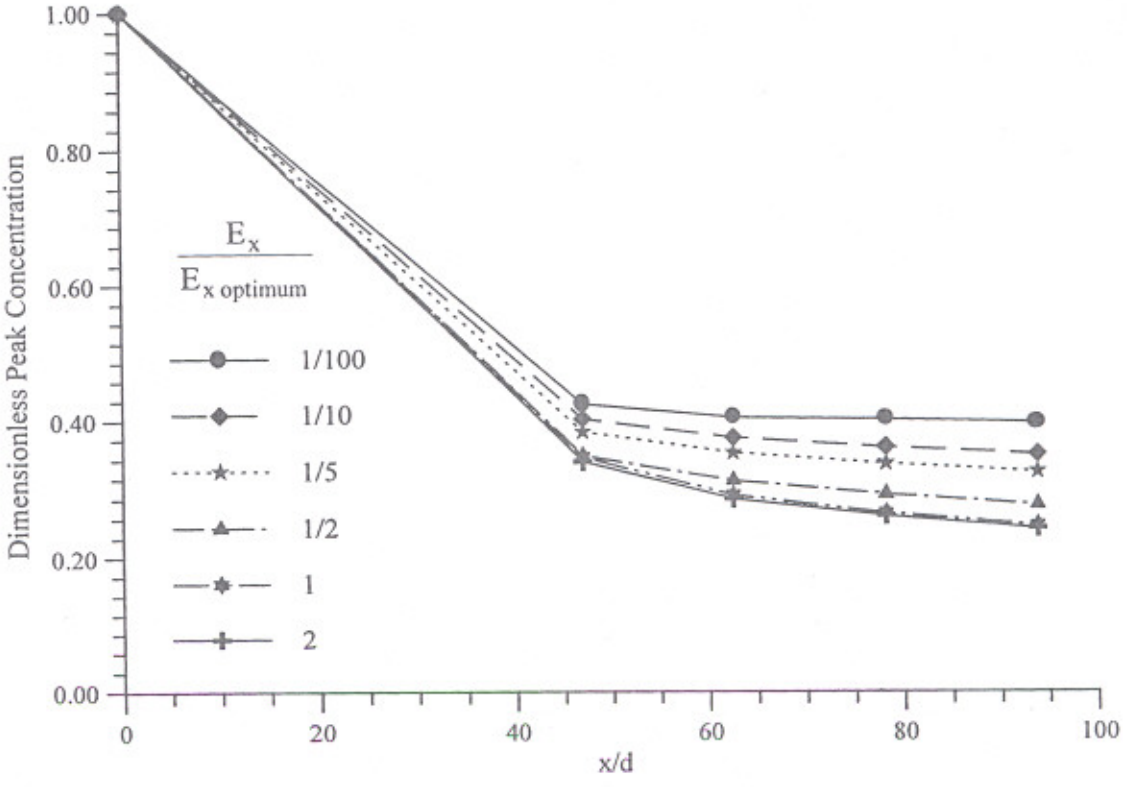

Fig. 5.18 (a) Effect of variation of E_x on accuracy of peak concentration at the water surface (y/d = 1.0) with distance (Data set 4CDCW1)

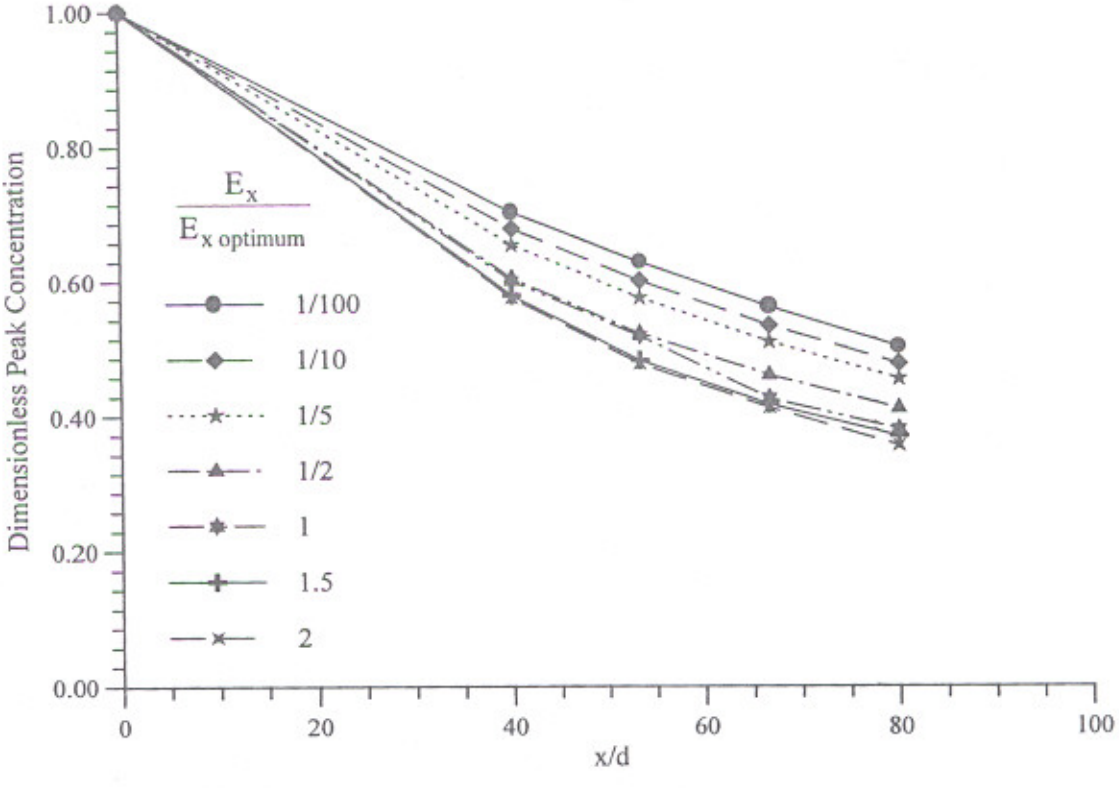

Fig. 5.18 (b) Effect of variation of E_x on accuracy of peak concentration at the water surface (y/d = 1.0) with distance (Data set 2CDCW6)

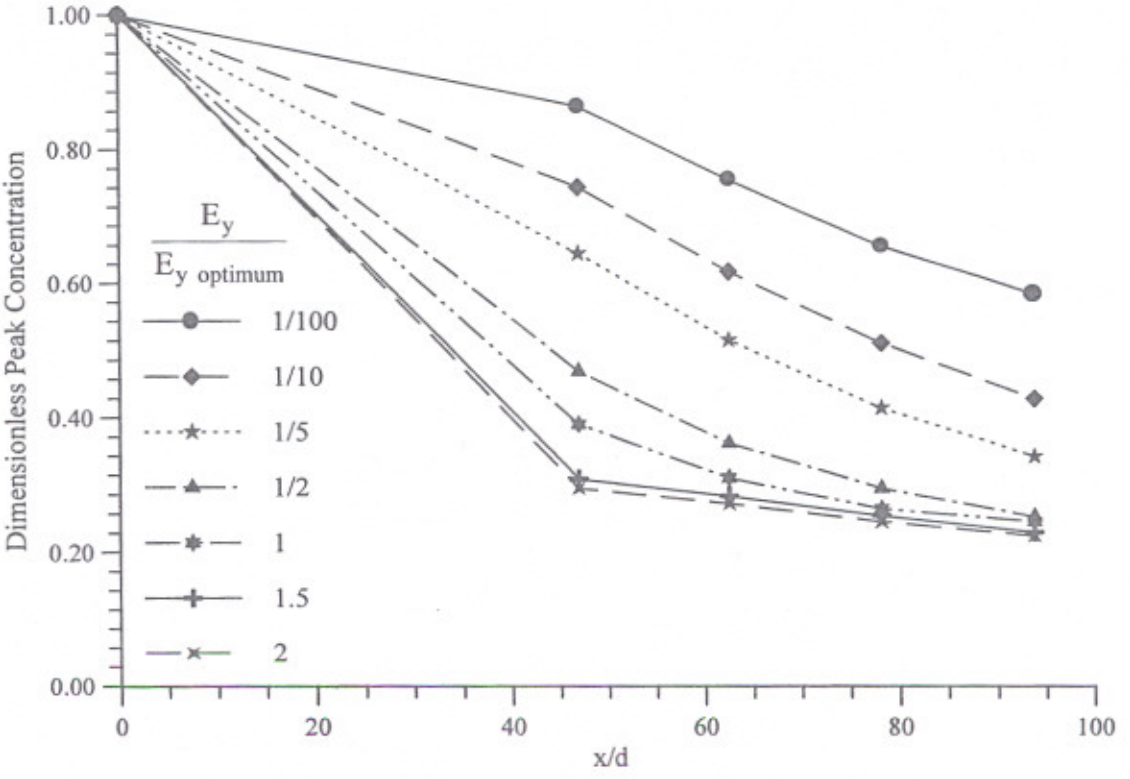

Fig.5.19 (a) Effect of variation of E_y on accuracy of peak concentration near the water surface(y/d = 1.0) with distance (Data set 4CDCW1)

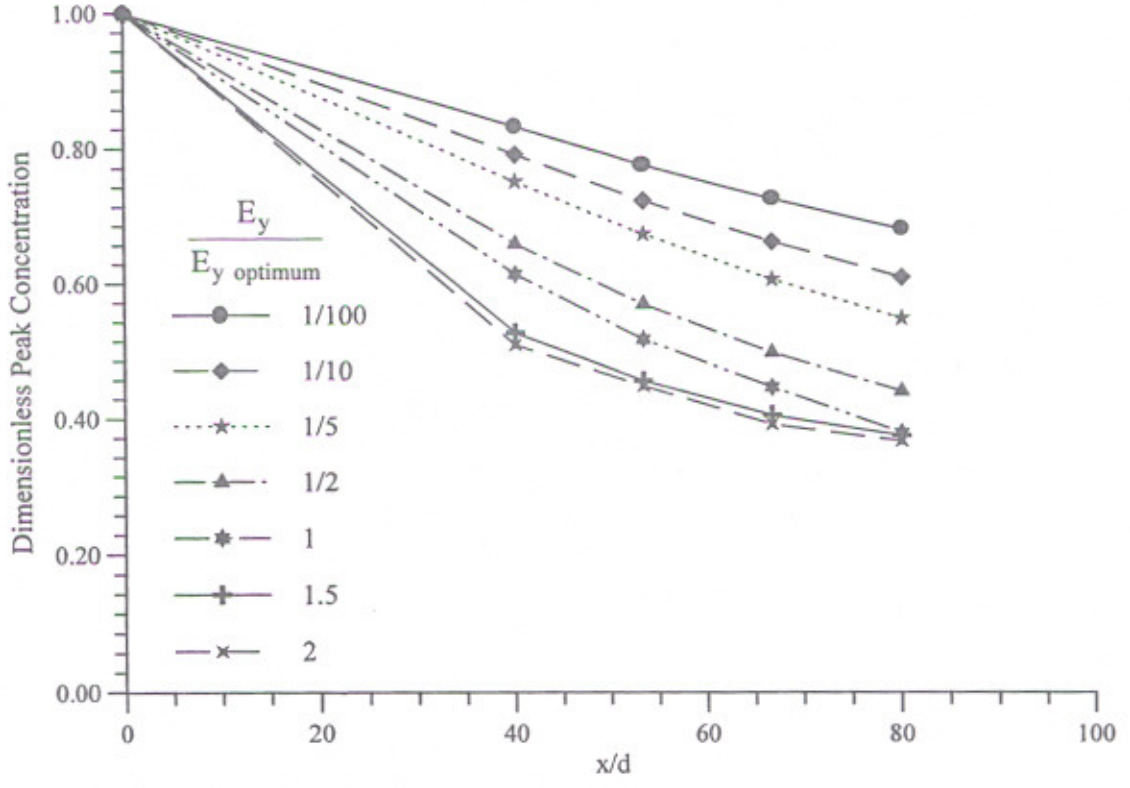

Fig.5.19 (b) Effect of variation of E_y on accuracy of peak concentration near the water surface (y/d = 1.0) with distance (Data set 2CDCW6)

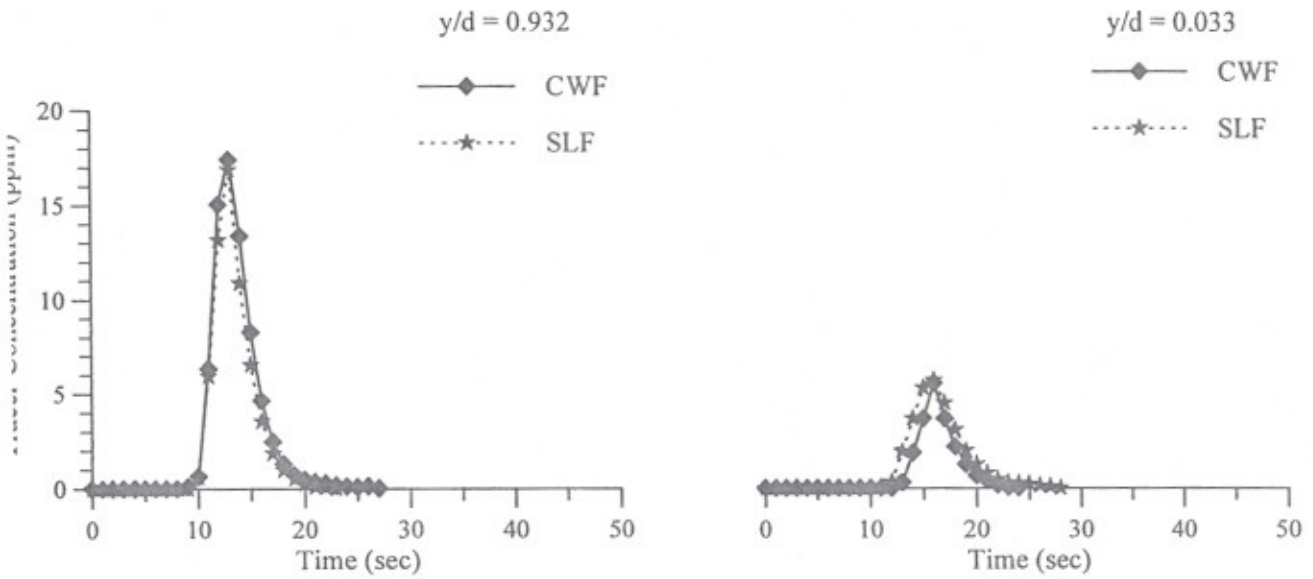

(a) x = 4 m

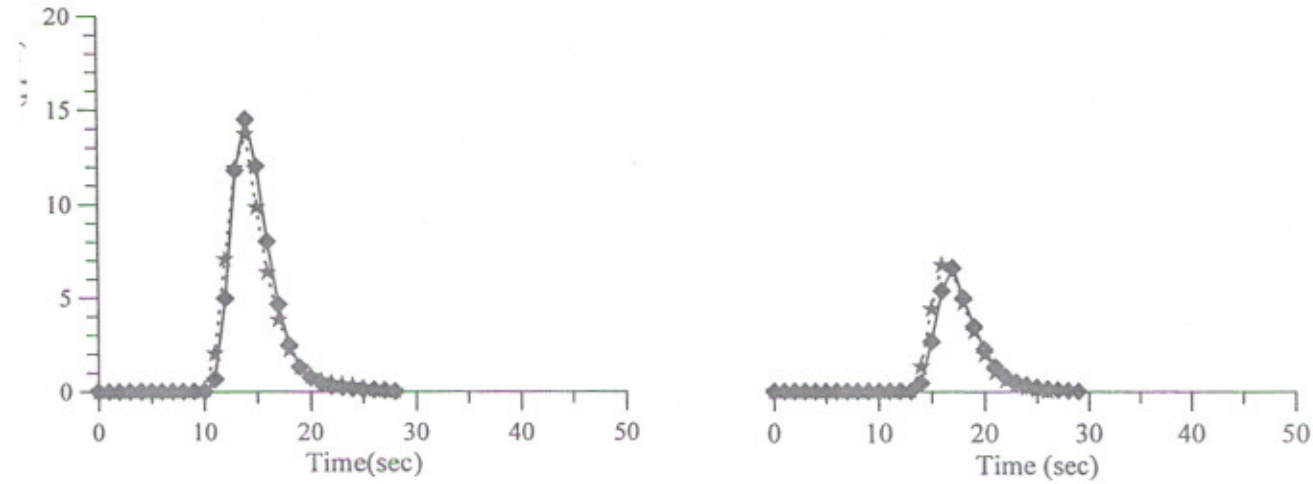

(b) x = 5 m

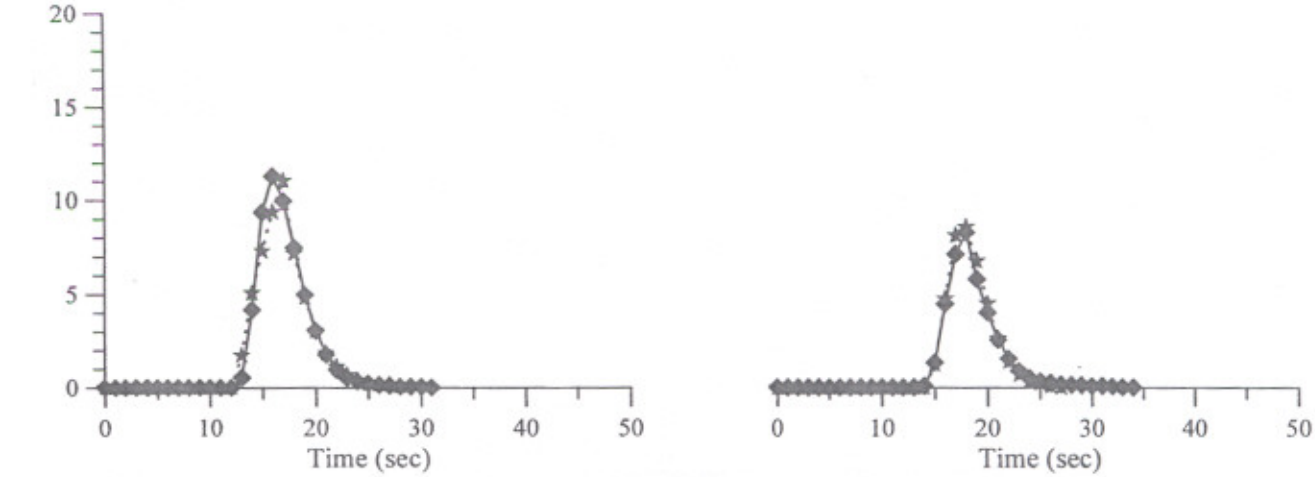

(c) x = 6 m

Continued....

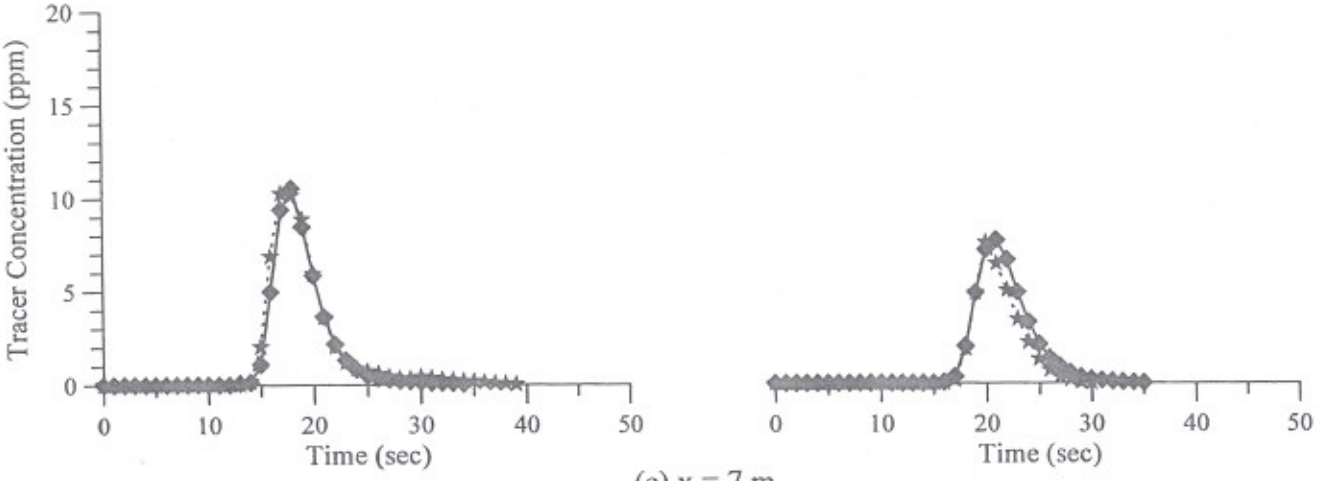

(e) x = 7 m

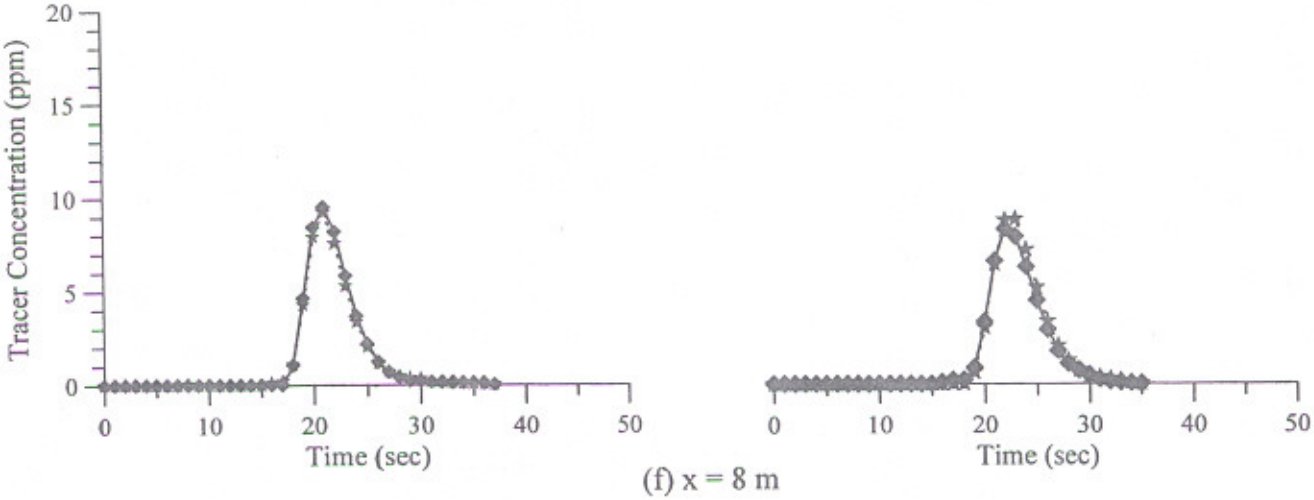

(f) x = 8 m

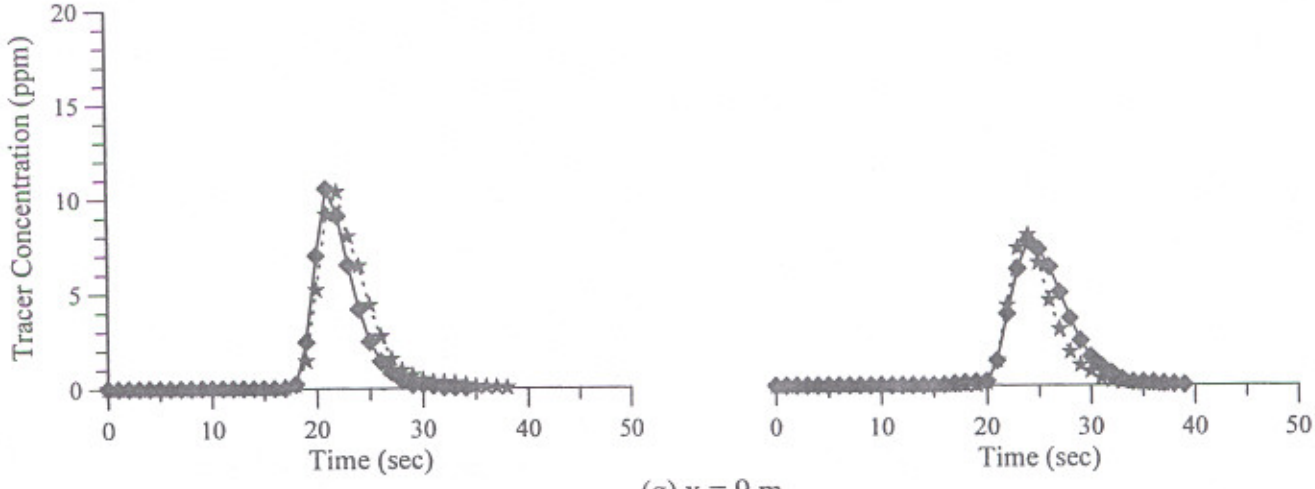

(g) x = 9 m

Fig. 5.20 Observed C-t curves for clear-water flow (CWF) and sediment-laden flow (SLF) (Data sets 3CDCW2 & 3CDSL24-Sediment concentration 993 ppm by weight)

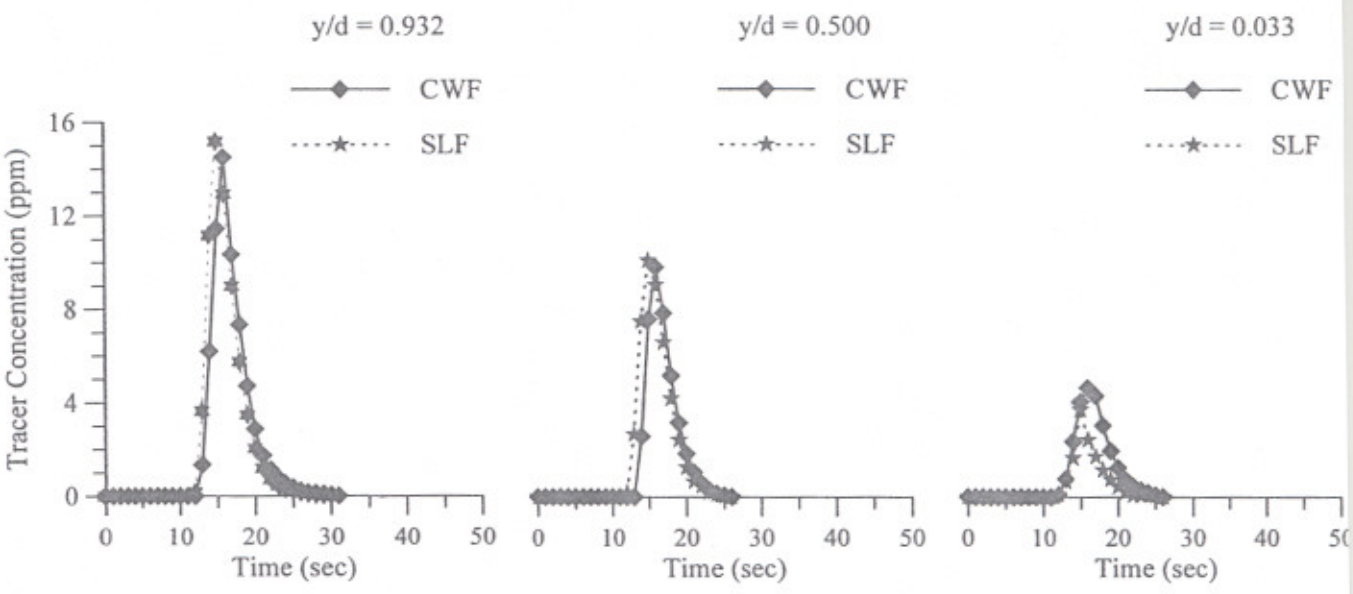

(a) x = 4 m

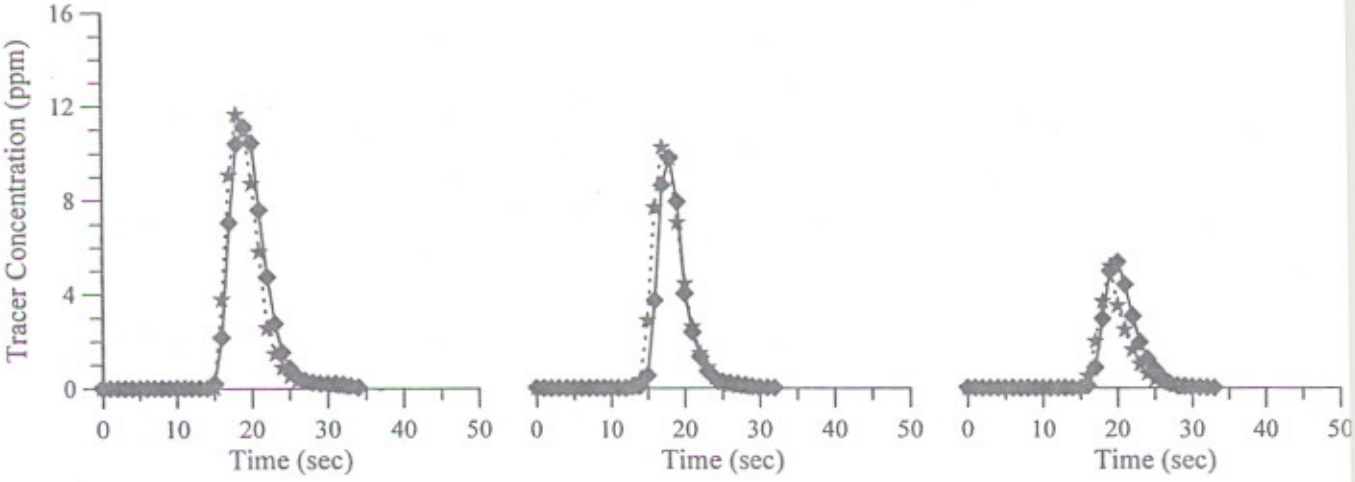

(b) x = 5 m

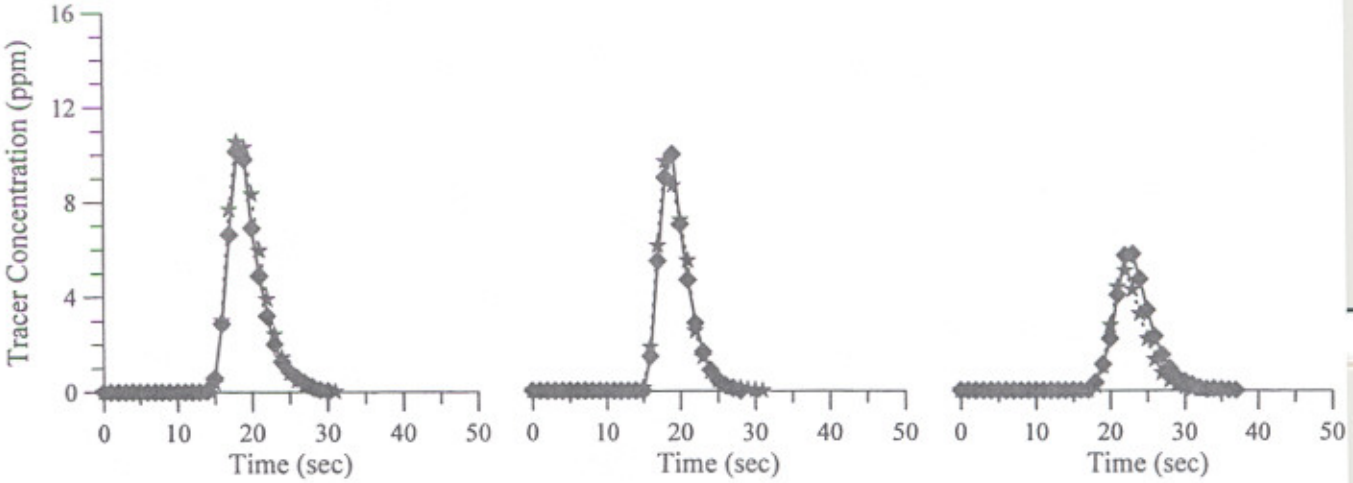

(c) x = 6 m

Continued....

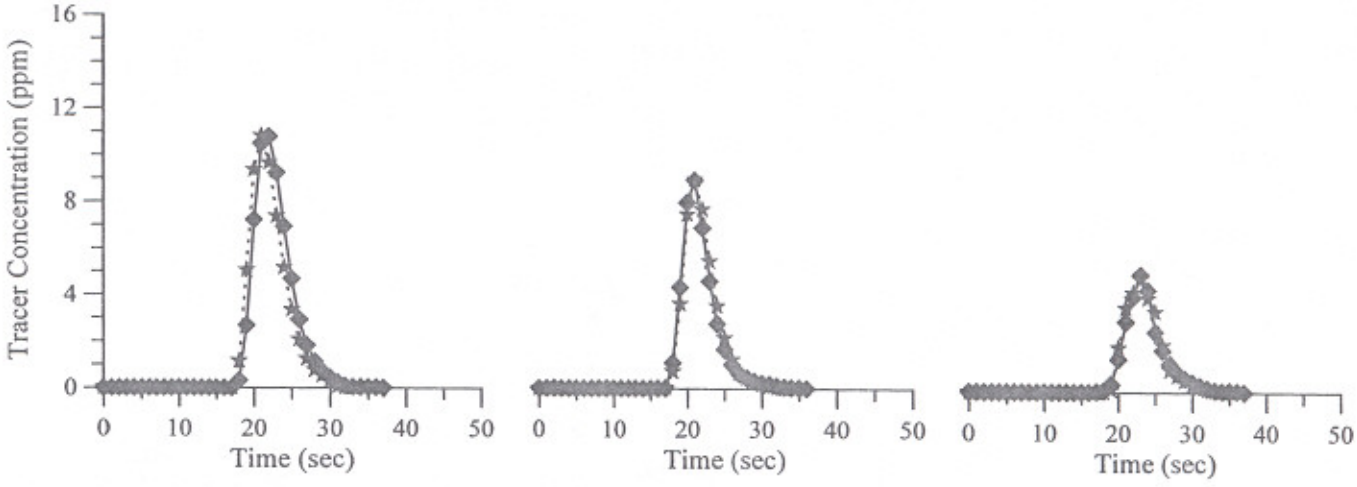

(d) x = 7 m

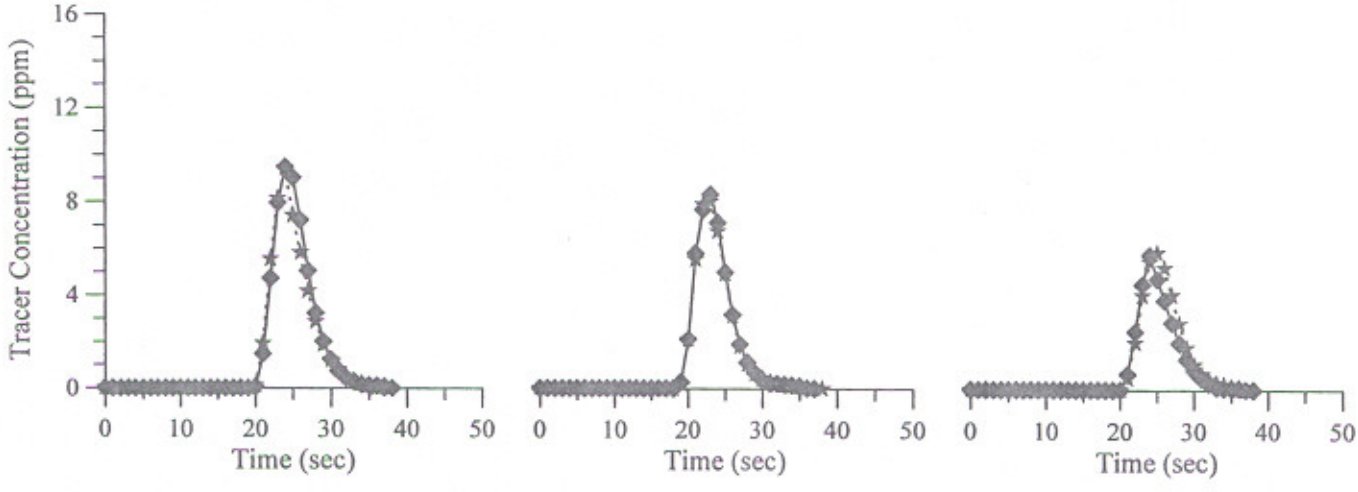

(e) x = 8 m

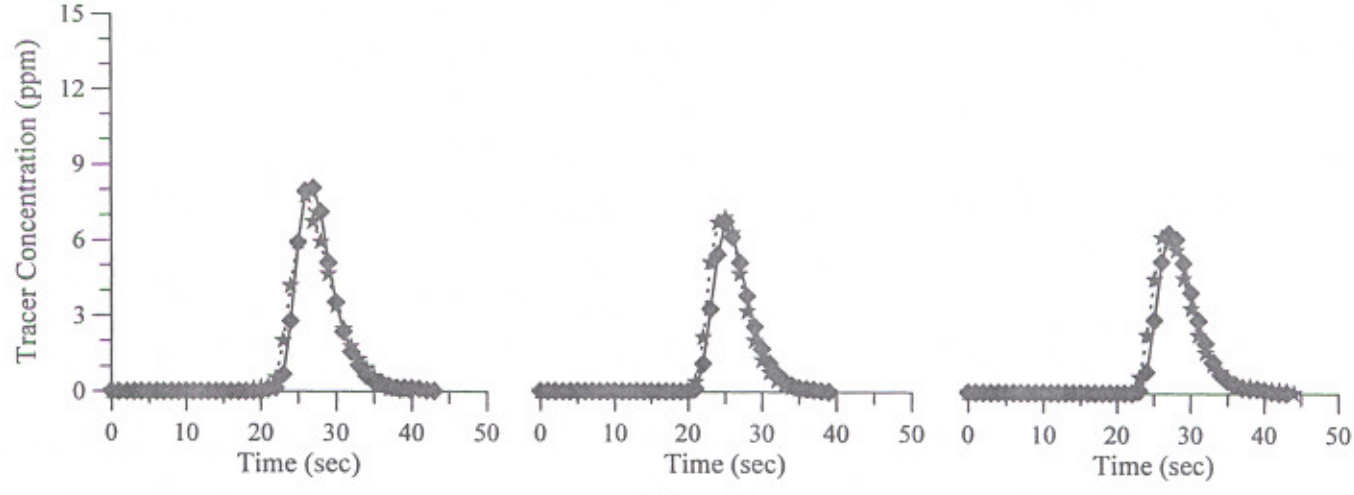

(f) x = 9 m

Fig. 5.21 Observed C-t curves for clear-water flow (CWF) and sediment-laden flow (SLF) (Data sets 4CDCW2 & 4CDSL2 - Sediment concentration 3802 ppm by weight)

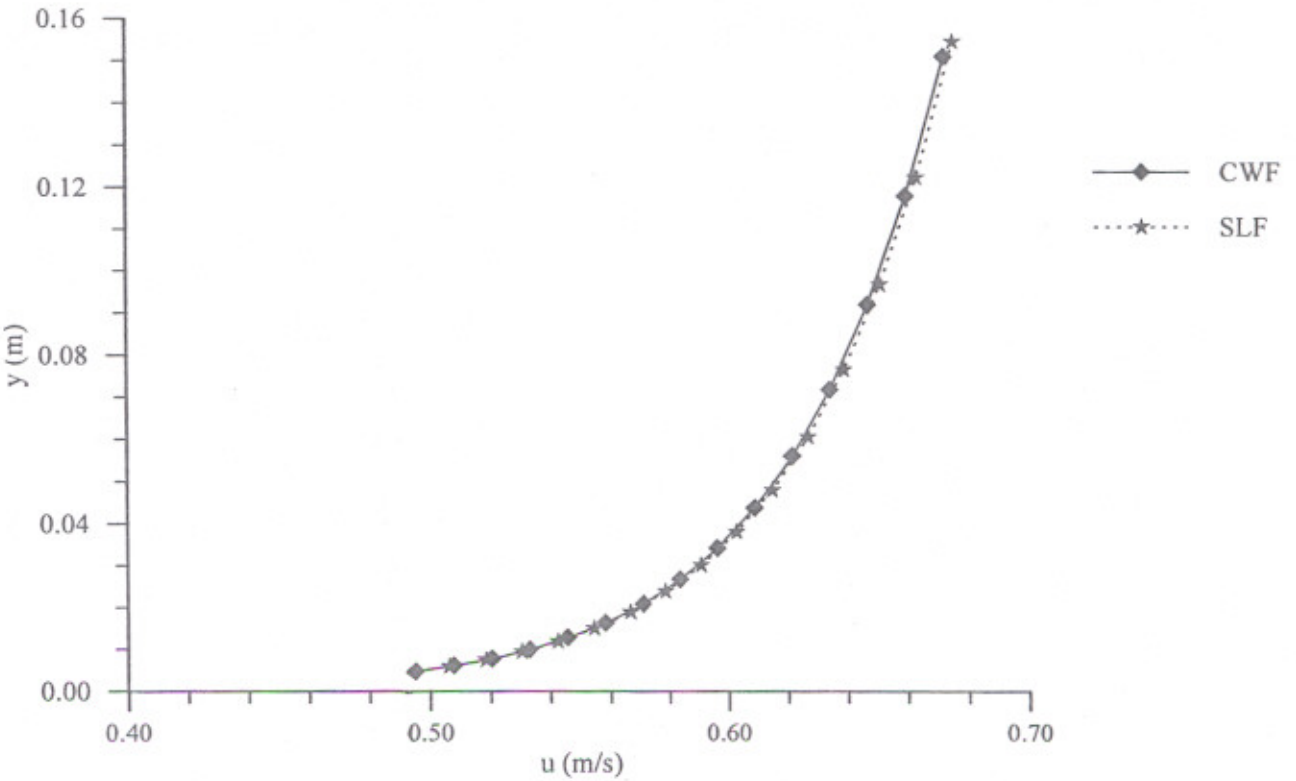

Fig. 5.22 Velocity distribution along a vertical in CWF and SLF (Data sets 3CDCW2 & 3CDSL24)

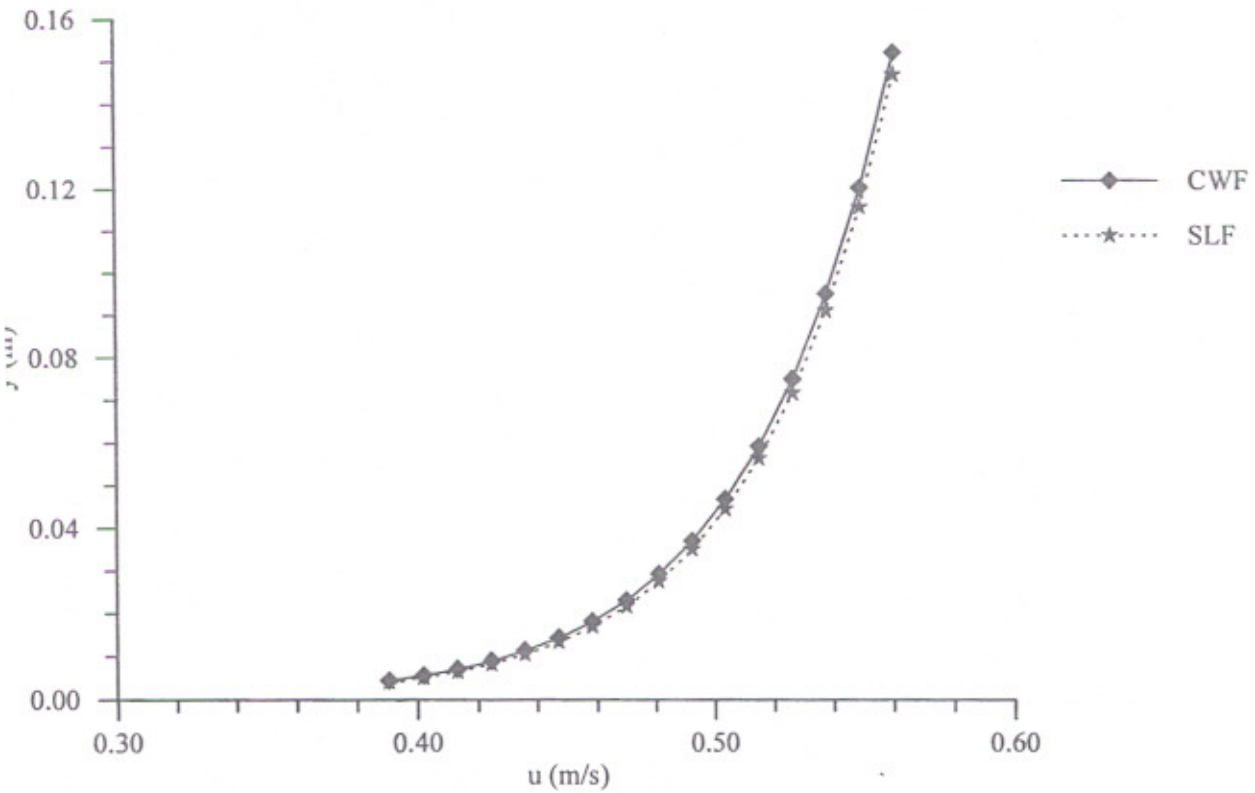

Fig.5.23 Velocity distribution along a vertical in CWF and SLF (Data sets 4CDCW2 & 4CDSL21)

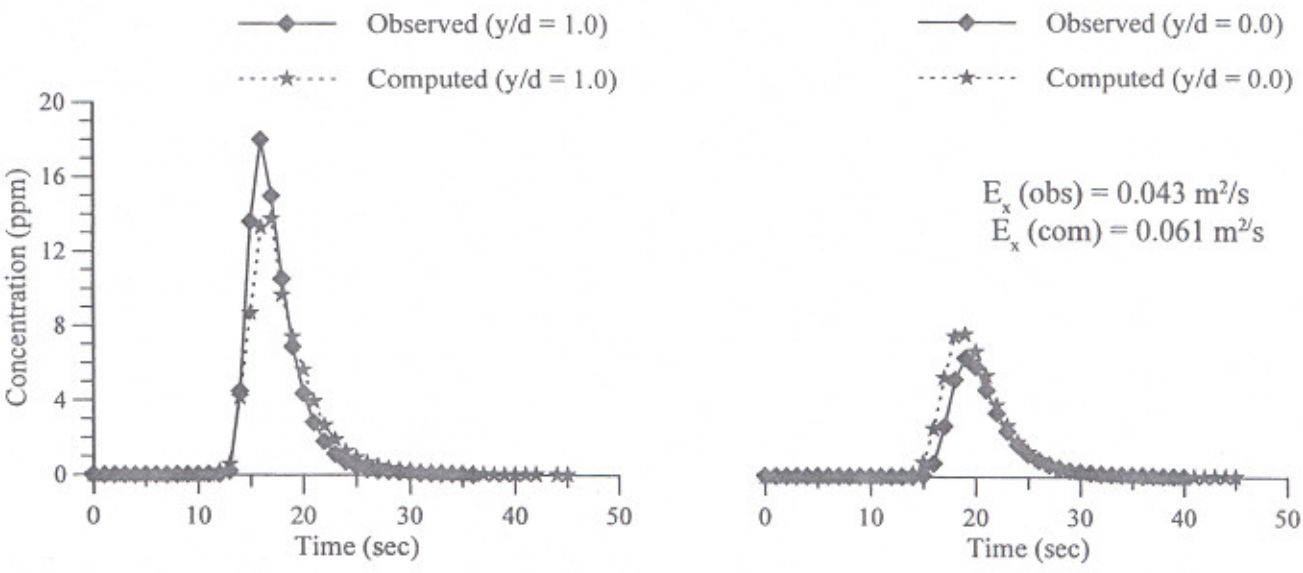

(a) x = 4 m

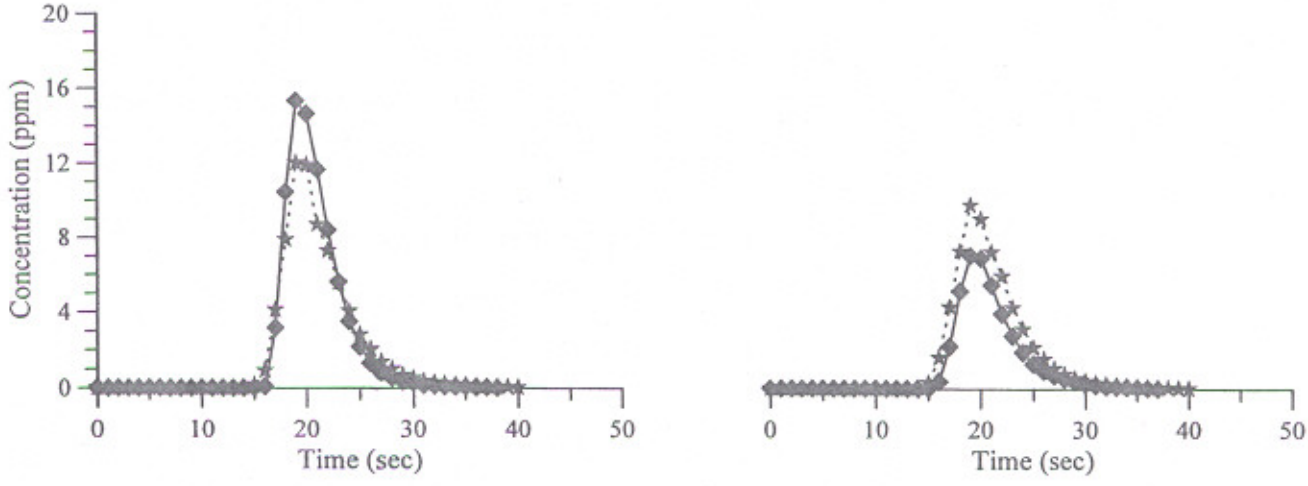

(b) x = 5 m

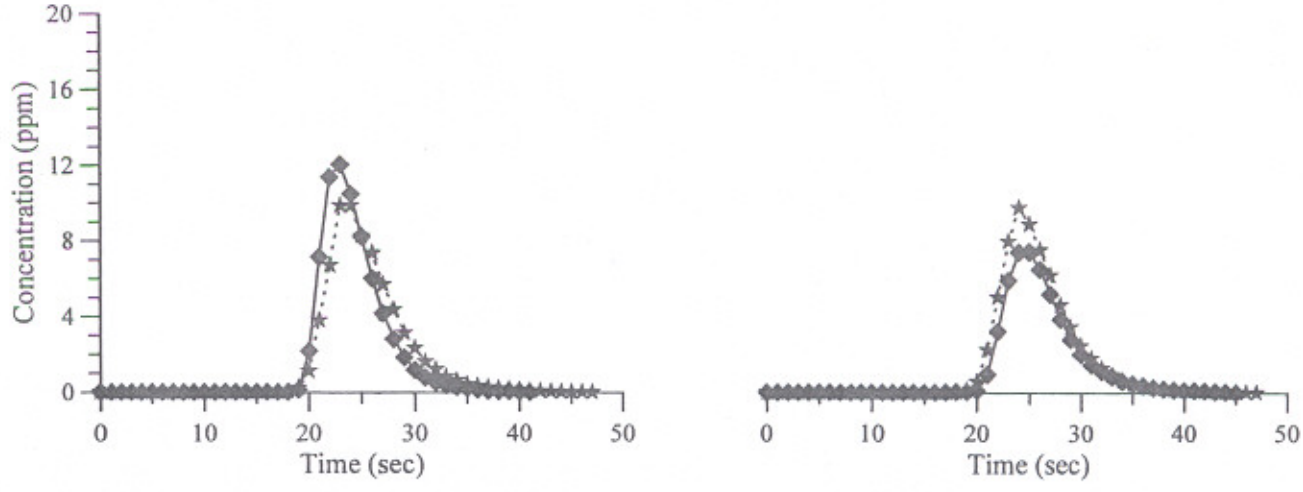

(c) x = 6 m

Continued....

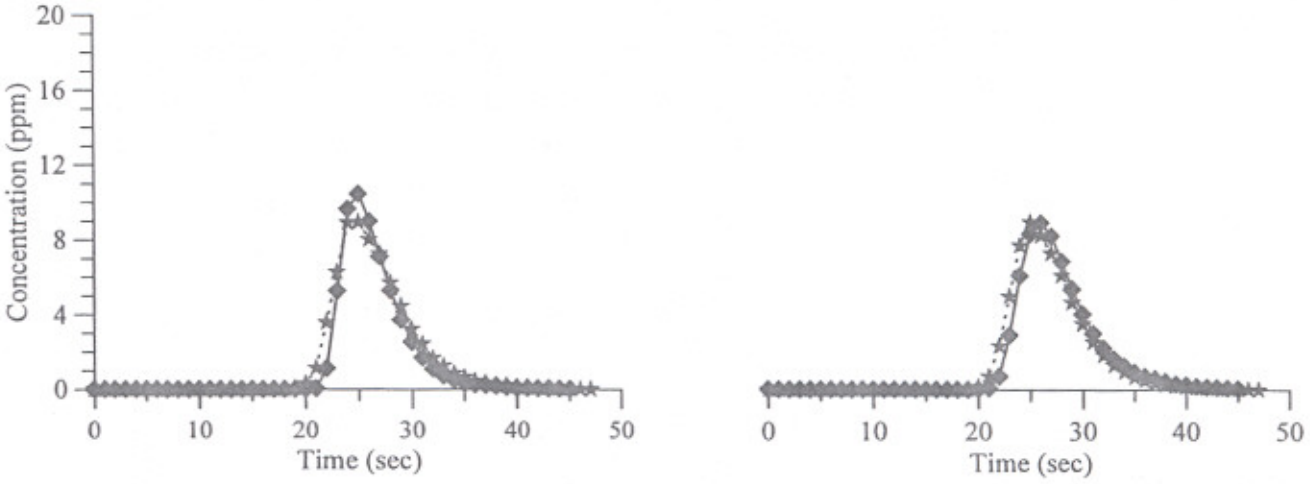

(d) x = 7 m

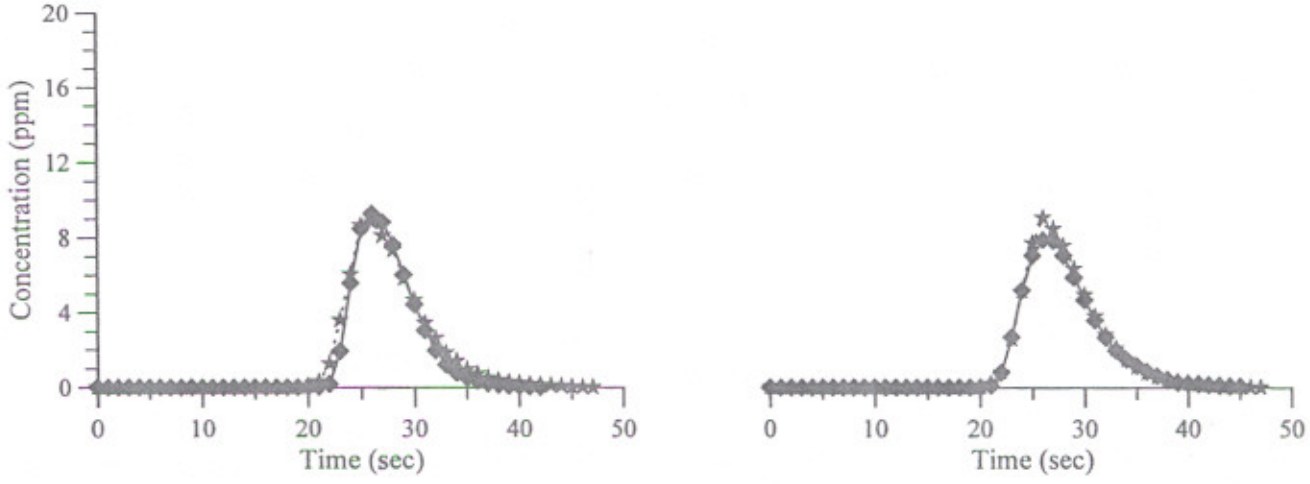

(e) x = 8 m

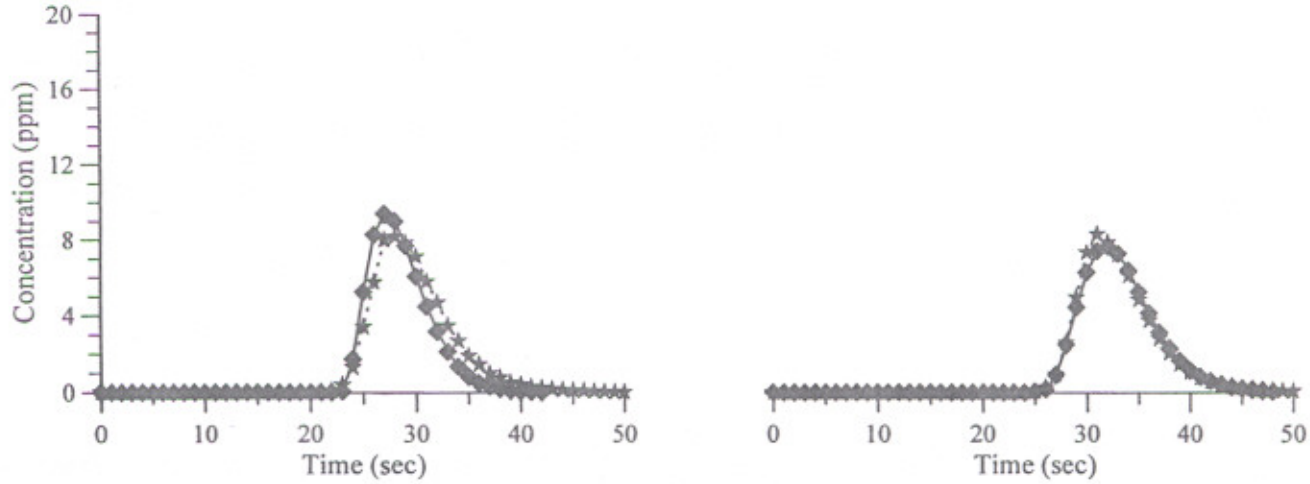

(f) x = 9 m

Fig. 5.24 Observed and computed C-t curves (Data set 1CDCW6)

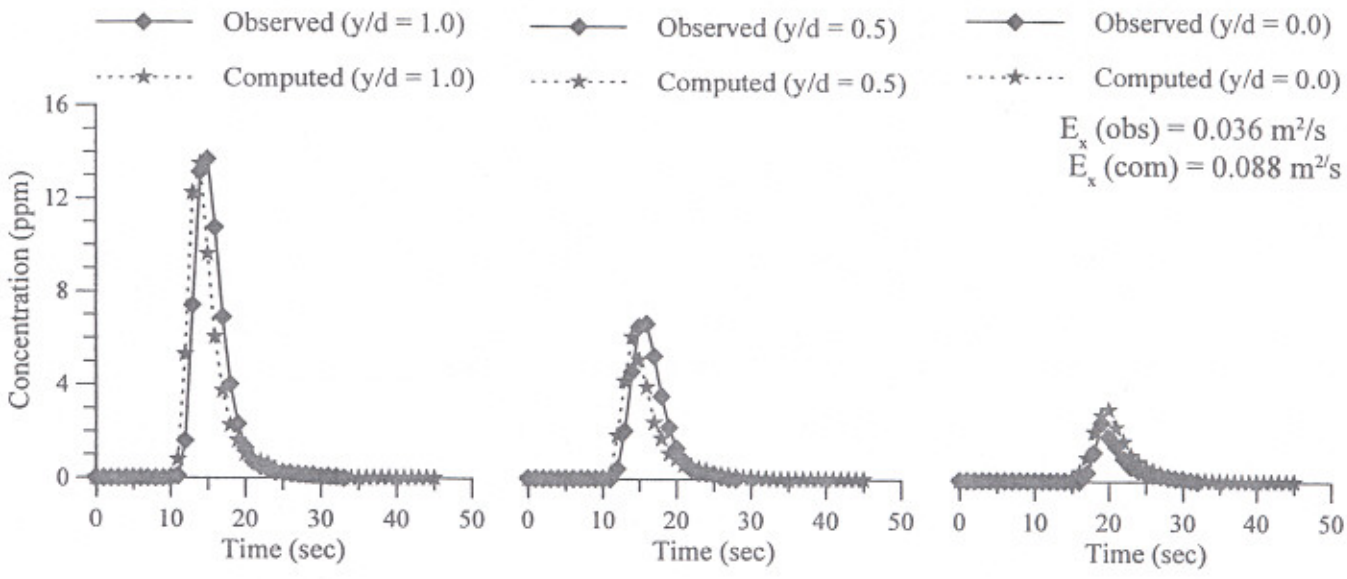

(a) x = 4 m

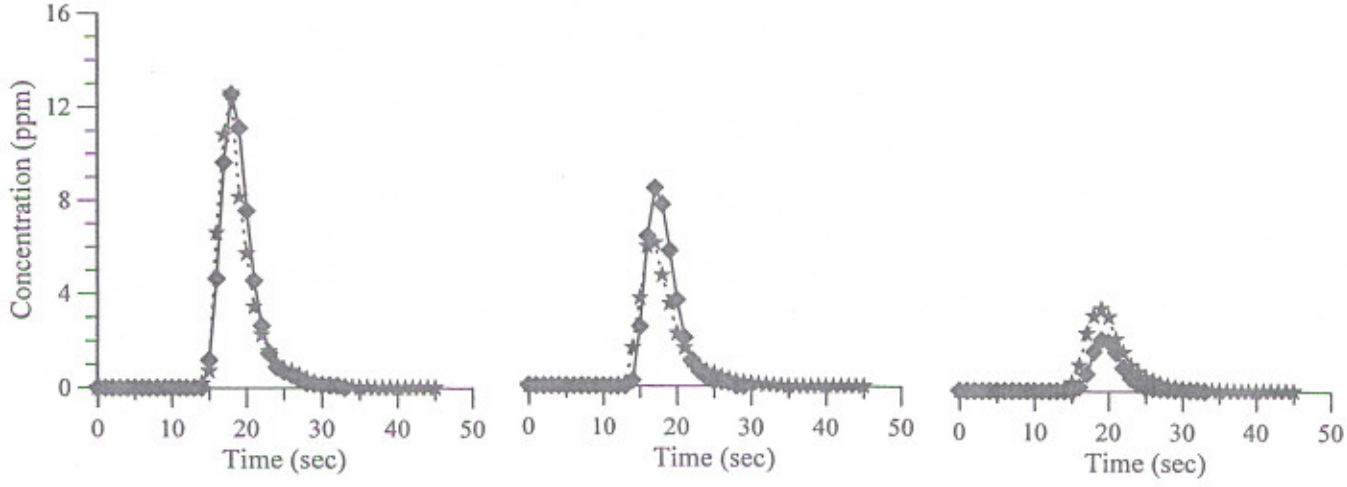

(b) x = 5 m

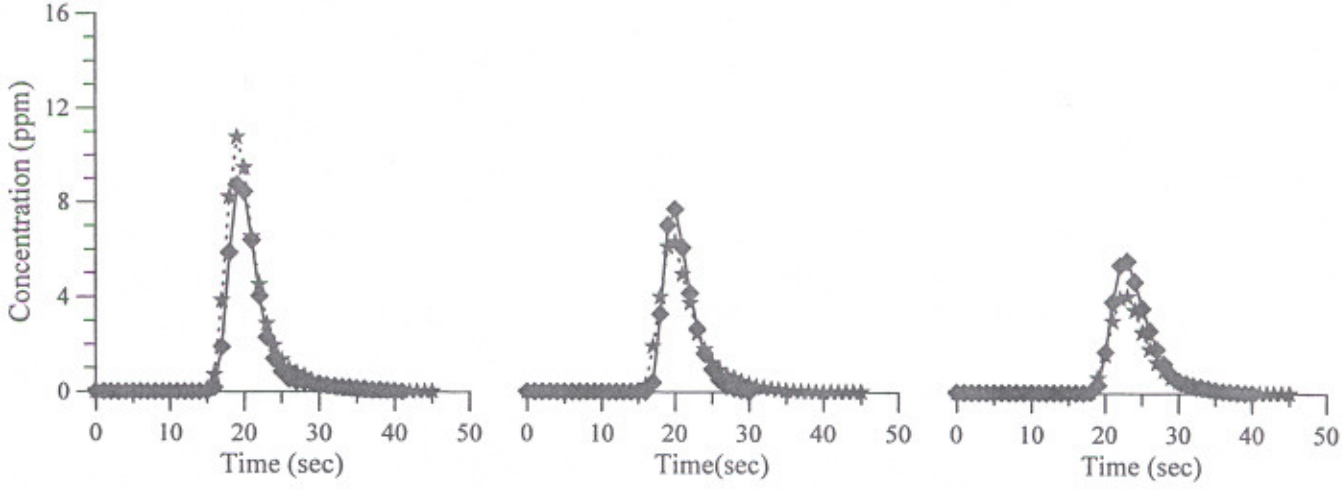

(c) x = 6 m

Continued....

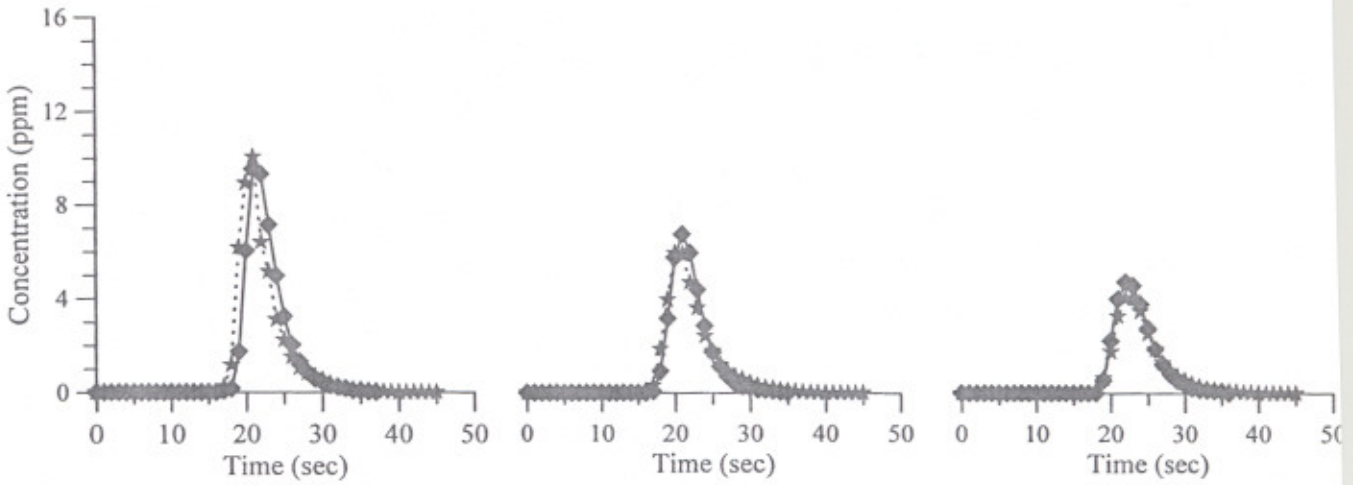

(d) x = 7 m

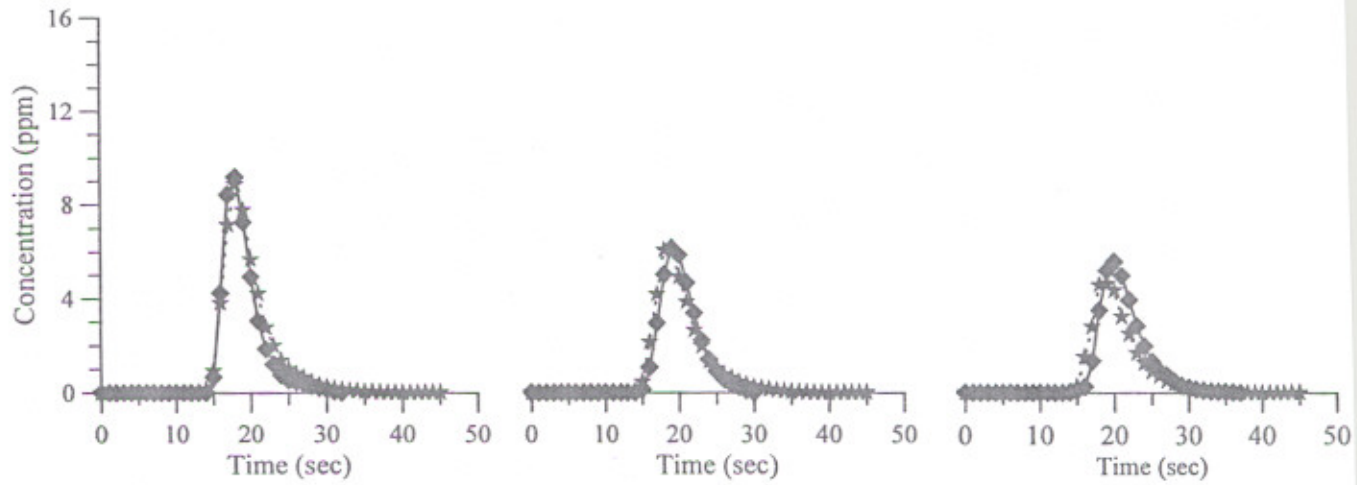

(e) x = 8 m

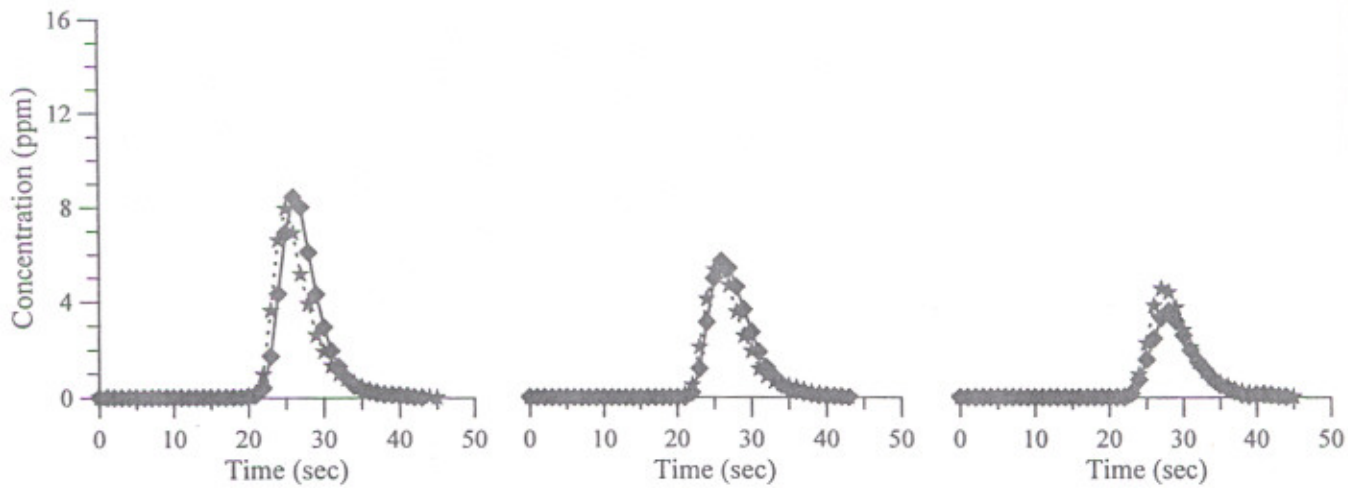

(f) x = 9 m

Fig. 5.25 Observed and computed C-t curves (Data set 4CDCW4)

5.9 CONCLUDING REMARKS

Analysis regarding the mixing characteristics in open channels due to slug transverse line injection of a conservative pollutant has been presented mainly by using the experimental data obtained in the present study. A new numerical scheme for the solution of Eq. (2.36) for two-dimensional mixing of pollutants resulting due to transverse line slug source has been proposed. The proof of the concepts tests for the proposed numerical scheme have been made by comparing its results with Fischer (1968) one-dimensional analytical model and analytical solution by Yotsukura and Cobb (1972) for continuous injection of transverse line source. The proposed numerical scheme has been extended for determination of the longitudinal mixing coefficient of the process of two-dimensional mixing. A predictor has been proposed for E_x for the mixing of the pollutant. A sensitivity analysis has been made to check the sensitivity of E_x and E_y on the prediction of C-t curves. It has been found that when the value of E_x and E_y is altered by a factor of 0.5 to 2, there is not a significant change in the predicted C-t curves at the downstream stations. The effect of suspended sediment on mixing has also been studied. It has been observed that the presence of sediment in suspension does not affect the mixing process significantly within the range of experimental data used in the present study.

6

CONCLUSIONS

The present study was carried out to evolve a mathematical model for the numerical solution of the two-dimensional mixing equation for the prediction of pollutants concentration in streams due to transverse line slug (source). The other aim of the study was to investigate the effect of suspended sediment load on the mixing process. Experiments were conducted both for clear-water and sediment-laden flows, to measure tracer concentration versus time profiles at the downstream stations at different elevations along the flow depth resulting due to horizontal line slug injection of tracer on the water surface at the upstream most section of the flume.

From the proposed numerical model for two-dimensional mixing and the analysis of the experimental data collected in the present investigation and available data from the literature, the following conclusions have been drawn.

1. A new numerical scheme based on the Split operator approach has been proposed for the solution of two-dimensional mixing equation, *i.e.*, Eq. (2.36) resulting due to transverse line slug source. The proposed model predicts concentration of pollutants downstream of the injection site both in near-field (*i.e.*, in longitudinal and vertical directions) and far-field (*i.e.*, in longitudinal direction). The validation tests for the proposed scheme have been made by comparing its results with Fischer (1968) one-dimensional analytical model and analytical solution for continuous injection of transverse line source.

   Exact solution of advection component of the mixing process has been obtained by developing a variable spatial grid corresponding to the velocity of flow at surface for computational nodes at y/d = 1.0, so that, the roots of the trajectory of the concentration at y/d = 1.0 falls at those computational nodes where the

concentration is known. For the computational nodes with y/d < 1.0, velocity of flow is smaller than the velocity at y/d = 1.0 due to velocity defect along the vertical. Therefore, the roots of the trajectory of the concentration for y/d < 1.0 do not fall at the computational nodes. Cubic spline interpolation scheme of Schohl and Holly (1991) has been used to interpolate the concentration at the roots of the trajectory by using the concentration at the neighborhood computational nodes. For simulation of diffusion process, alternate-direction implicit method (ADIM) suggested by Smith (1978) has been used. This is two-step approach method which is stable and convergent. The mass of the pollutant is fully conserved by the proposed numerical model.

2. The proposed numerical model can be used for the prediction of pollutant concentration immediately downstream of injection site of transverse line steady or unsteady source as well as for the far downstream region. Thus it applies to the initial mixing region as well as to the far-field. The model thus has a definite advantage over the traditional one-dimensional advection-diffusion models which are valid only in the far-field.

3. A two-dimensional grid search method has been employed to determine the optimum values of longitudinal mixing coefficient E_x and vertical mixing coefficient E_y, such that best matching is obtained between the observed and computed C-t curves at all the downstream stations. Initial estimate for E_x was made by using Fischer et al. (1979) triple integration of transverse profile of observed longitudinal velocity and initial estimate of E_y was obtained by using Eq. (2.45).

4. The existing predictor for vertical mixing coefficient E_y has been checked by using the data collected during present experimental study and data available from literature. It is found that E_y value predicted by Eq. (2.45) lie within a range of 2 to 1/2 times the observed values of E_y. The measured vertical velocity distribution at mid-width of the channel is also used to estimate the value of E_y, by using Eq.

(2.42). Thus computed values of E_y also lie within the range of 2 to 1/2 times the observed values of E_y but have better agreement with observed E_y. Therefore, values of E_y are computed using the observed velocity distribution and the optimum values of E_x were re-determined.

5. The proposed scheme has been extended by incorporating in it one-dimensional grid search method for determination of optimum E_x, by using E_y computed from velocity distribution and observations of C-t profiles. One-dimensional grid search method is based on the bisection procedure and can be used to find the optimum value of E_x, which is such that it produces maximum agreement between the observed and computed C-t curves at the all the downstream stations. Using observed pollutant concentration profiles at the upstream station as input, C-t curves at the downstream stations and at different elevations along the vertical were predicted by the proposed numerical scheme by first using a trial value of E_x. Thus computed C-t curves are compared with the corresponding observed C-t curves and the weighted error at each station is calculated by using Eq. (3.32). Average error, ERR was then calculated next by taking arithmetic mean of all the weighted errors. E_x corresponding to the minimum value of ERR is considered to be the optimum one.

6. A relationship viz. Eq. (5.2) has been proposed for prediction of longitudinal mixing coefficient E_x, by employing the channel and flow characteristics. Comparison was made between the values predicted from the proposed equation with the observed optimum E_x values. The predicted values are found to lie within 2 to 1/2 times the observed values.

7. A sensitivity analysis has also been carried out to check the sensitivity of E_x and E_y on the prediction of C-t curves. It has been found that when the value of E_x is altered with a multiplying factor varying from 0.2 to 2 and E_y is changed by a factor ranging from 0.5 to 2, there is no significant change in the predicted C-t

curves at the downstream stations. However, the computed C-t curves are less accurate while E_x and E_y values are altered beyond these limits.

8. The effect of suspended sediment on mixing has been studied by superimposing the observed C-t curves, for clear-water flows (CWF) and for sediment-laden flows (SLF). It has been observed that the presence of sediment does not affect the mixing process within the range of experimental data used in the present study. These finding are in conformity with the findings of Singh et al. (1992) who has concluded that the presence of sediment with concentrations 90 ppm to 5000 ppm, has no effect on longitudinal dispersion. No remarkable difference in vertical velocity distributions of clear-water and sediment-laden flows was found at the mid-width of the channel, within the range of the sediment concentration taken in the present study.

REFERENCES

1. Abbot, M. B. (1980), 'Computational Hydraulics', Volume 1, Pitman Advance Publishing Program, London.
2. Ahmad, Z. (1997), 'Longitudinal Dispersion of Conservative Pollutants in Open Channels', Ph.D. Thesis, Thapar Institute of Engineering & Technology (Deemed University), Patiala, India.
3. Ahmad, Z. and Kothyari, U. C. (2001), 'Time-Line Cubic Spline Interpolation Scheme for Solution of Advection Equation', Journal of Computers and Fluids, Elsevier, 30, pp. 737 – 752.
4. Ahmad, Z., Kothyari, U. C. and Ranga Raju, K. G. (1999a), 'Finite Difference Scheme for Longitudinal Dispersion', Journal of Hydraulic Research, International Association of Hydraulic Research, 37(3), pp. 389-406.
5. Ahmad, Z., Kothyari, U. C. and Ranga Raju, K. G. (1999b), 'Longitudinal Dispersion in Open Channels', Journal of Hydraulic Engineering, Indian Society for Hydraulics, 5(2), pp. 1-21.
6. Ahmad, Z., Kothyari, U. C. and Ranga Raju, K. G. (2004), 'Longitudinal Dispersion in Sediment-Laden Open Channels Flows', International Journal of Sediment Research, 19(1), pp. 1-14.
7. Alavian, V. (1986), 'Dispersion Tensor in Rotating Flows', Journal of Hydraulics Division, American Society of Civil Engineers, 112(8), pp. 771-777.
8. Arora, A. K. (1983), 'Velocity Distribution and Sediment Transport in Rigid-Bed Open Channels', Ph. D. thesis, University of Roorkee, Roorkee, India.
9. Asai, K., Fujisaki, K. and Awaya, Y. (1991), 'Effect of Aspect Ratio on Longitudinal Dispersion Coefficient, in Environmental Hydraulics', Edited by Lee and Cheung, Volume 2, Balkema, Rotterdam, Netherlands, pp. 493-498.

10. Bansal, M. K. (1971), 'Dispersion in Natural Streams', Journal of Hydraulics Division, American Society of Civil Engineers, 97(11), pp. 1867-1888.
11. Barnett, A. G. (1983), 'Exact and Approximate Solutions of the Advection-Diffusion Equation', XXth International Association of Hydraulic Research Congress, Moscow, Hydro. Tech. Inst., Moscow, 3, pp. 180-190.
12. Beltaos, S. (1975), 'Evaluation of Transverse Mixing Coefficients From Slug Tests', Journal of Hydraulic Research, International Association of Hydraulic Research, 4, pp. 351-360.
13. Beltaos, S. (1980), 'Transverse Mixing Tests in Natural Streams', Journal of Hydraulics Division, American Society of Civil Engineers, 106(10), pp. 1607-1625.
14. Bowden, K. F. (1983), 'Physical Oceanography of Coastal Waters', Ellis Horwood, Chichester.
15. Boxall, J. B. and Guymer, I. (2003a), 'Analysis and Prediction of Transverse Mixing Coefficients in Natural Channels', Journal of Hydraulic Engineering, American Society of Civil Engineers, 129(2), pp. 129-139.
16. Boxall, J. B. and Guymer, I. (2003b), 'Analysis and Prediction of Transverse Mixing Coefficients in Natural Channels', XXXth International Association of Hydraulic Research Congress, Greece, pp. 309-315.
17. Clearly and Adrain (1973), 'New Analytical Solutions for Dye Diffusion Equations', Journal of Environmental Engineering, American Society of Civil Engineers, 99(EE3), pp. 213-227.
18. Conte, S. D. and deBoor, C. (1980), 'Elementary Numerical Analysis: An algorithmic approach', Third Edition, McGraw-Hill, New York.
19. Cunge, J. A., Holly Jr., F. M. and Verwey, A. (1980), 'Practical Aspects of Computational River Hydraulics', Pitman Publishing Limited, London.
20. Deng, Z. Q., Singh, V. P. and Bengstsson, L. (2001), 'Longitudinal Dispersion Coefficient in Straight Rivers', Journal of Hydraulic Engineering, American Society of Civil Engineers, 127(11), pp. 919-927.
21. Deng, Z. Q., Singh, V. P. and Bengstsson, L. (2002), 'Longitudinal Dispersion Coefficient in Single-Channel Streams', Journal of Hydraulic Engineering, American Society of Civil Engineers, 128(10), pp. 901-916.

22. Egan, B. and Mahoney, J. R. (1972), 'Numerical Modeling of Advection and Diffusion of Urban Area Source Pollutants', Journal of Applied Meteorology, American Meteorological Society, 11(2), pp. 312-321.
23. Einstein, H. A. (1942), 'Formulas for the Transportation of Bed Load', Transactions of American Society of Civil Engineers, 107, pp. 561-597.
24. Einstein, H. A. and Chien, N. (1955), 'Effects of Heavy Sediment Concentration near the Bed on the Velocity and Sediment Distribution', Report No.8, U.S. Army Corps of Engineers, Missouri River Division, University of California, Berkeley, California.
25. Elder, J. W. (1959), 'The Dispersion of Marked Fluid Particles in Turbulent Shear Flow', Journal of Fluid Mechanics, Cambridge University Press, 5(4), pp. 544-560.
26. El-Hadi, N., Harrington, A., Hill, I., Lau, Y. L. and Krishnappan, B. G. (1984), 'River Mixing-A State of the Art Report', Canadian Journal of Civil Engineering, 11, pp. 585-609.
27. Fischer, H. B. (1967), 'The Mechanics of Dispersion in Natural Streams', Journal of Hydraulics Division, American Society of Civil Engineers, 93(6), pp. 187-216.
28. Fischer, H. B. (1968a), 'Methods for Predicting Dispersion Coefficients in Natural Streams with Application to Lower Reaches of the Green and Duwamist Rivers, Washington', Geological Survey Professional Paper, 582- A.
29. Fischer, H. B. (1968b), 'Dispersion Predictions in Natural Streams' Journal of Sanitary Engineering Division, American Society of Civil Engineers, 94, pp. 927-944.
30. Fischer, H. B. (1969), 'The Effects of Bends on Dispersion in Streams', Water Resources Research, American Geophysics Union, 5, pp. 496-506.
31. Fischer, H. B., List, E. J., Koh, R. C. Y., Imberger, J. and Brooks, N. H. (1979), 'Mixing in Inland and Coastal Waters', Academic Press, New York.
32. French, R. H. (1979), 'Transfer Coefficients in Stratified Channel Flow', Journal of Hydraulics Division, American Society of Civil Engineers, 105(9), pp. 1087-1101.
33. French, R. H. (1986), 'Open Channel Hydraulics', McGraw Hill, New York, USA.
34. Garde, R.J. and Ranga Raju, K.G. (2000), 'Mechanics of Sediment Transportation and Alluvial Stream Problems,' Wiley Eastern Limited,
35. Graf, W. H. and Altinkar, M. S. (1998), 'Fluvial Hydraulics: Flow and Transport Processes in Channels of Simple Geometry', John Wiley and Sons Limited, Chichester, England.

36. Guan, Y., Altinakar, M. S. and Krishnappan, B. G. (2002), 'Two-Dimensional Simulation of Advection-Dispersion in Open Channel flows' Proceedings of Fifth International Conference on Hydroinformatics, Cardiff, UK, pp. 226-231.
37. Henderson, F. M. (1967), 'Open Channel Flow', McMillan, New York.
38. Holley, E. R. (1969), 'Unified View of Diffusion and Dispersion', Journal of Hydraulics Division, American Society of Civil Engineers, 95(2), pp. 621-631.
39. Holley, E. R., Siemons, J. and Abraham, G. (1972), 'Some Aspects of Analyzing Transverse Dispersion in Rivers', Journal of Hydraulic Research, International Association of Hydraulic Research, 10(1), pp. 27-57.
40. Holly, F. M. and Preissmann (1977), 'Accurate Calculation of Transport in Two Dimensions', Journal of Hydraulics Division, American Society of Civil Engineers, 103(11), pp. 1259-1277.
41. Jain, M. K. (1991), 'Numerical Solution of Differential Equations', Wiley Eastern Limited, New Delhi.
42. James, Jr., R. W. and Helinsky, B. M. (1984), 'Time of Travel and Dispersion in the Jones Falls', Baltimore, Maryland, U.S. Geological Survey Water Resources Investigations, Rep. No. 84-4203.
43. Jaque, D. T. and Ball, J. E. (1994), 'Numerical Simulation of Advection-Diffusion Mass Transport', Journal of Hydroscience and Hydraulic Engineering, Japan Society of Civil Engineers, 11(2), pp. 49-56.
44. Jobson, H. E. and Sayre, W. W. (1970a), 'Predicting Concentration Profiles in Open Channels', Journal of Hydraulics Division, American Society of Civil Engineers, 96(10), pp. 1983-1996.
45. Jobson, H. E. and Sayre, W. W. (1970b), 'Vertical Transfer in Open Channel Flow', Journal of Hydraulics Division, American Society of Civil Engineers, 96 (3), pp. 703-724.
46. Jobson, H. E. (1997), 'Predicting Travel Time and Dispersion in Rivers and Streams', Journal of Hydraulic Engineering, American Society of Civil Engineers, 123(11), pp. 971-978.
47. Kilpatrick, F. A., Sayre, W. W. and Richardson, E. V. (1967), 'Discussion on Flow Measurements with Fluorescent Tracers by Replogle, J.A., Myers, L.E. and Brust, K.J.', Journal of Hydraulics Division, American Society of Civil Engineers, 93(4), pp. 298-308.

48. Komatsu, T., Holly, F. M. Jr., Nakashiki N. and Ohgushi K. (1985), 'Numerical Calculation of Pollutant Transport in One and Two Dimensions', Journal of Hydroscience and Hydraulic Engineering, 3(2), pp. 15-30.
49. Komatsu, T., Ohgushi, K., Asai K. and Holly, F. M. Jr. (1989), 'Accurate Numerical Simulation of Scalar Advective Transport', Journal of Hydroscience and Hydraulic Engineering, Japan Society of Civil Engineers, 7(1), pp. 63-73.
50. Komatsu, T., Ohgushi, K. and ASAI K. (1992), 'Development of Refined Numerical Scheme for Advective Transport in Diffusion Simulation', Journal of Hydraulic Division, American Society of Civil Engineers, 456 (21), pp. 37-46.
51. Komatsu, T., Ohgushi, K., ASAI K. and Holly, F. M. JR. (1997), 'Refined Numerical Scheme for Advective Transport in Diffusion Simulation', Journal of Hydraulic Engineering, American Society of Civil Engineers 123(1), pp. 41-50.
52. Lau, Y. L. (1983), 'Suspended Sediment Effect on Flow Residence', Journal of Hydraulics Division, American Society of Civil Engineers, 109(5), pp. 757-763.
53. Lau, Y. L. and Krishnappan, B.G. (1981), 'Modeling Transverse Mixing in Natural Streams', Journal of Hydraulics Division, American Society of Civil Engineers, 107(2), pp. 209-226.
54. Lau, Y. L. and Krishnappan, G. (1977), 'Transverse Dispersion in Rectangular Channels.' Journal of Hydraulics Division, American Society of Civil Engineers, 103(10), pp. 1173-1189.
55. Li, C. W. (1990), 'Advection Simulation by Minimax-Characteristics Method', Journal Hydraulic Engineering, American Society of Civil Engineers, 116(9), pp. 1138-44.
56. Li, C. W. and Yu, T. S. (1994), 'Conservative Characteristics-Based Schemes' Journal of Hydraulic Engineering, American Society of Civil Engineers, 120(9), pp. 1089-99.
57. Lipsett A. W. and Beltaos S. (1978), 'Tributary Mixing Characteristics Using Water Quality Parameters' Alberta Research Council, Report No. SWE-78/04.
58. Luk, G. K. Y., Lau, Y. L. and Watt, W. E. (1990), 'Two-Dimensional Mixing in Rivers with Unsteady Pollutant Source', Journal of Environmental Engineering, American Society of Civil Engineers, 116(1), pp.125-143.

59. Lung, W. S. and O'Connor, D. J. (1984), 'Two-Dimensional Mass Transport in Estuaries', Journal Hydraulic Engineering, American Society of Civil Engineers, 110(10), pp. 1340-1357.

60. McNulty, A. J (1983), 'Dispersion of a Continuous Pollutant Source in Open Channel Flow ', Ph.D. Thesis, University of Canterbury, Christchurch.

61. McNulty, A. J. and Wood, I. R. (1984), 'A New Approach to Predicting the Dispersion of a Continuous Pollutant Source' Journal of Hydraulic Research, International Association of Hydraulic Research, 22(1), pp. 23-34.

62. Morton, K. W. (1981), 'Finite Element Method for Non-Self-Adjoint Problems' Numerical Analysis Report 3/81, Department of Mathematics, University of Reading, Reading, England.

63. Nassiri, M. and Babarutsi, S. (1997), 'Computation of Dye Concentration in Shallow Recirculating Flow', Journal Hydraulic Engineering, American Society of Civil Engineers, 123(9), pp. 793-805.

64. Nokes, R. I., McNulty, A. J. and Wood, I. R. (1984), 'Turbulent Dispersion from a Steady Two-Dimensional Horizontal Source', Journal of Fluid Mechanics, Cambridge University Press, 149, pp. 147-159.

65. Nokes, R. I. (1986), 'Problems in turbulent dispersion', Ph.D. Thesis, University of Canterbury, Christchurch.

66. Nokes, R. I. and Wood, I. R. (1988), 'Vertical and Lateral Turbulent Dispersion: Some Experimental Results', Journal of Fluid Mechanics, Cambridge University Press, 187, pp. 373-394.

67. Nokes, R. I. and Huges, G. O. (1994), 'Turbulent Mixing in Uniform Channels of Irregular Cross-Sections', Journal of Hydraulic Research, International Association of Hydraulic Research, 32(1), pp.67-86.

68. Officer, C. B. (1976), Physical Oceanography of Estuaries, Wiley, London.

69. Patel, P. L. (1995), 'Initiation of Motion and Bed Load Transport of Non-Uniform Sediments', Ph. D. thesis, University of Roorkee, Roorkee, India.

70. Peaceman, D. W. and Rachford, H. H. (1955), 'The Numerical Solution of Parabolic and Elliptic Differential Equations', Journal of Society for Industrial and Applied Mathematics, 3, pp. 28-41.

71. Pepper, D. W. and Baker, A. J. (1980), 'A High Order Accurate Numerical Algorithm For 3D Transport Prediction', Journal of Computers and Fluids, Elsevier, 8(4), pp. 371-390.
72. Prakash, A. (1977), 'Convective Dispersion in Perennial Streams', Journal of Environmental Engineering Division, American Society of Civil Engineers, 103(EE2), pp. 321-340.
73. Ranga Raju, K. G. (1993), 'Flow Through Open Channel', Tata McGraw-Hill Publishing Company Limited, New Delhi.
74. Rutherford, J. C. (1994), 'River Mixing', John Wiley and Sons, New York.
75. Samaga, B. R., Ranga Raju, K. G. and Garde, R. J. (1986), 'Velocity Distribution in Alluvial Channel Flow', Journal of Hydraulic Research, International Association of Hydraulic Research, 24(4), pp. 297-308.
76. Sastry, S. S. (1995), 'Introductory Methods of Numerical Analysis', Second Edition, Prentice-Hall of India Private Limited, New Delhi.
77. Schiller, E. J. and Sayre, W. W. (1975), 'Vertical Temperature Profiles in Open Channel Flow', Journal of Hydraulics Division, American Society of Civil Engineers, 101(6), pp. 749-761.
78. Schohl, G. A. and Holly, Jr. F. M. (1991), 'Cubic-Spline Interpolation in Lagrangian Advection Computation', Journal of Hydraulic Engineering, American Society of Civil Engineers, 117(2), pp. 248-253.
79. Seo, W. and Cheon, T. S. (1998), 'Predicting Longitudinal Dispersion Coefficient in Natural Streams' Journal of Hydraulic Engineering, American Society of Civil Engineers, 124(1), pp. 25-32.
80. Seo, I. W. and Baek, K. O. (2004), 'Estimation of Longitudinal Dispersion Coefficient Using the Velocity Profile in Natural Streams' Journal of Hydraulic Engineering, American Society of Civil Engineers, 130(3), pp. 227-236.
81. Singh, U. P. (1987), 'Dispersion of Conservative Pollutants', Ph. D. thesis, University of Roorkee, Roorkee, India.
82. Singh, U. P., Garde, R. J. and Ranga Raju, K. G. (1992), 'Longitudinal Dispersion in Open-Channel Flow', International Journal of Sediment Research, International Research and Training Centre on Erosion and Sedimentation, China, 7(2), pp. 65-83.

83. Smith, G. D. (1978), 'Numerical Solution of Partial Differential Equations: Finite Difference Methods', Oxford University Press, Oxford.

84. Stefanovic, D. L. and Stefan, H. (2001), 'Accurate Two-Dimensional Solution of Advection-Diffusive-Reactive Transport' Journal of Hydraulic Engineering, American Society of Civil Engineers, 127(91) pp. 728-737.

85. Stone, H.L. and Brian, P. L. T. (1963), 'Numerical Solution of Convective Transport Problems', Journal of American Institute of Chemical Engineers, 9(5), pp. 681-688.

86. Tai, D. Y. and Rathbun, R. E. (1988), 'Photolysts of Rhodamine-WT dye', Chemosphere, Elsevier, 17(3), pp. 559-573.

87. Taylor, G. I. (1921), 'Diffusion by Continuous Movement', Proceedings of the London Mathematical Society', Series A, pp. 196-211.

88. Taylor, G. I. (1953), 'Dispersion of Soluble Matter in Solvent Flowing Slowly Through a Tube', Proceedings of the Royal Society London, A-219, pp. 186-203.

89. Taylor, G. I. (1954), 'The Dispersion of Matter in Turbulent Flow Through a Pipe', Proceedings of the Royal Society London, A-223, pp. 446-468.

90. Tsai, T. L., Yang, J. C and Hunag, L. H (2002), 'Hybrid Finite-Difference Scheme for Solving the Dispersion Equation', Journal of Hydraulic Engineering, American Society of Civil Engineers, 128(1) pp. 78-86.

91. Turner Designs (1993), 'User's Manual', Model 10-AU-005 Field Fluorometer, Turner Designs 845, W. Maude Avenue, Sunnyvale, USA.

92. Umeyama, M. and Gerristen, F. (1992). 'Velocity Distribution in Uniform Sediment Laden Flow', Journal of Hydraulic Engineering, American Society of Civil Engineers, 118(2), pp. 229-244.

93. Webel, G. and Schatzmann, M. (1984), 'Transverse Mixing in Open Channel Flow' Journal of Hydraulic Engineering, American Society of Civil Engineers, 110, pp. 423-435.

94. Wu, J. and Tsanis, I. K. (1994), 'Pollutant Transport and Residence Time in a Distorted Scale Model and a Numerical Model', Journal of Hydraulic Research, International Association of Hydraulic Research, 32(4), pp. 583-598.

95. Yang, J. C. and Hsu, E. L. (1990), 'Time-line Interpolation for Solution of the Dispersion Equation', Journal of Hydraulic Research, International Association of Hydraulic Research, 28(4), pp. 503-520.

96. Yotsukura, N. and Cobb, E. D. (1972), 'Transverse Diffusion of Solutes in Natural Streams', U.S. Geological Survey, Professional Paper 582-C.

97. Yotsukura, N. and Sayre, W. W. (1976), 'Transverse Mixing in Natural Channels' Water Resources Research', American Geophysics Union, 12 (4), pp. 695-704.

98. Young, P. C. and Wallis, S. G. (1993), 'Solute Transport and Dispersion in Channels', Channel Network Hydrology, Edited by K. Beven and M. J. Kirby, John Wiley & Sons Limited, London, U.K.

99. Zoppou, C. and Knight, J. H. (1997), 'Analytical Solutions for Advection and Advection-Diffusion Equations with Spatially Variable Coefficients', Journal of Hydraulic Engineering, American Society of Civil Engineers, 123(2), pp. 144-148.

100. Zoppou, C. and Knight, J. H. (1999), 'Analytical Solutions of a Spatially Variable Coefficient Advection-Diffusion Equation in Up to Three Dimensions', Journal of Applied Mathematical Modelling, Elesvier, 23, pp. 667-685.

APPENDIX-I

Notations used to report data of the present study are depicted in the following C-t curve

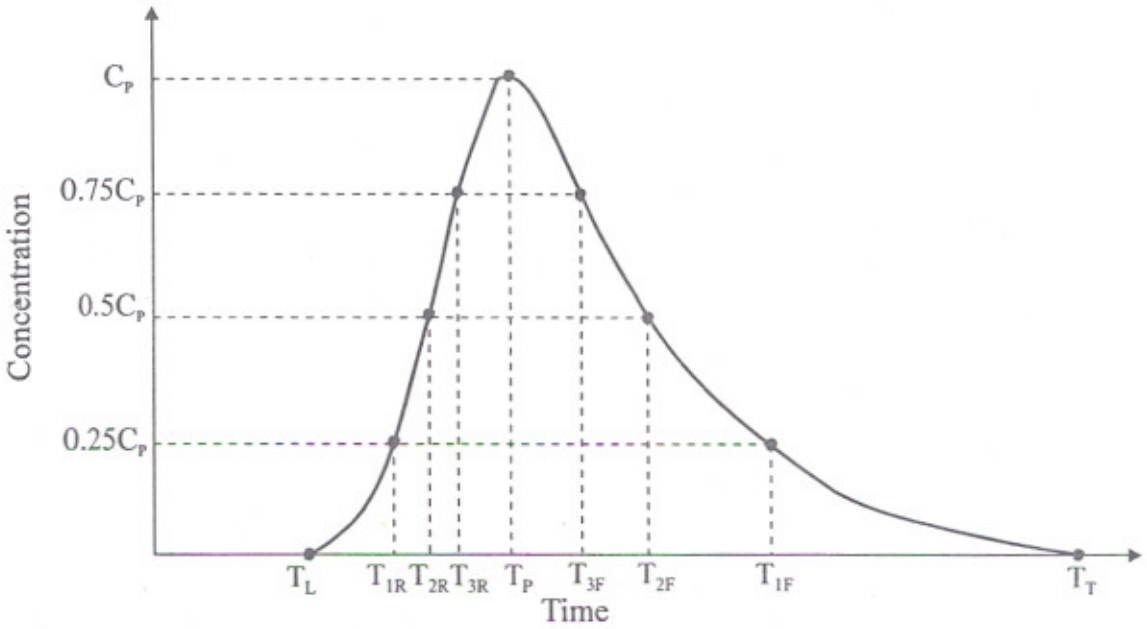

Fig. A-I Definition sketch of a C-t curve

C_p = Peak concentration

T_L = Elapsed time to the arrival of the leading edge of the tracer cloud

T_{1R} = Elapsed time to the arrival of the 25% of peak concentration of the tracer cloud on the rising limb

T_{2R} = Elapsed time to the arrival of the 50% of peak concentration of the tracer cloud on the rising limb

T_{3R} = Elapsed time to the arrival of the 75% of peak concentration of the tracer cloud on the rising limb

T_P = Elapsed time to the arrival of the peak concentration of the tracer cloud

T_{3F} = Elapsed time to the arrival of the 75% of peak concentration of the tracer cloud on the falling limb

T_{2F} = Elapsed time to the arrival of the 50% of peak concentration of the tracer cloud on the falling limb

T_{1F} = Elapsed time to the arrival of the 25% of peak concentration of the tracer cloud on the falling limb

T_T = Elapsed time to the arrival of the trailing edge of the tracer cloud

y = Vertical distance from the bed of the channel

d = Depth of flow

x = Longitudinal distance from the injection site

y/d = Dimensionless vertical location of concentration profile

Continued ....

TRAVEL TIME AND TWO-DIMENSIONAL MIXING DATA COLLECTED IN THE PRESENT STUDY

Data Set	x (m)	(y/d)	Cp (ppm)	T_L (s)	T_{1R} (s)	T_{2R} (s)	T_{3R} (s)	T_P (s)	T_{3F} (s)	T_{2F} (s)	T_{1F} (s)	T_T (s)
1CDCW1 (d = 0.123 m)	1 m	0.041	0.00	0.00	0.00	0.00	0.00	0.00	0.00	0.00	0.00	0.00
		0.500	0.27	10.00	10.17	10.59	11.04	12.00	12.84	16.61	14.54	16.00
		0.918	37.65	9.00	9.79	10.38	10.87	12.00	13.24	14.36	15.99	28.00
	2 m	0.041	2.55	13.00	13.85	14.44	14.96	16.00	17.45	18.67	21.59	32.00
		0.500	5.65	10.00	11.80	12.38	12.86	14.00	15.22	16.25	17.77	27.00
		0.918	34.06	11.00	12.09	12.60	13.18	14.00	15.53	16.71	18.44	37.00
	3 m	0.041	1.35	15.00	15.59	16.21	16.69	18.00	18.94	19.93	21.55	27.00
		0.500	7.22	13.00	15.20	15.73	16.33	17.00	18.50	19.54	21.21	33.00
		0.918	27.89	14.00	14.91	15.46	15.96	17.00	18.29	19.33	20.85	36.00
	4 m	0.041	2.53	17.00	18.24	18.95	19.63	21.00	22.87	24.34	26.51	38.00
		0.500	10.16	15.00	17.19	17.79	18.42	20.00	21.14	22.21	23.79	33.00
		0.918	14.05	17.00	17.57	18.32	18.94	20.00	22.15	23.53	25.57	37.00
	5 m	0.041	5.27	21.00	22.40	23.08	23.54	24.00	27.15	29.02	31.29	41.00
		0.500	10.31	18.00	19.41	20.05	20.63	22.00	23.62	24.98	26.85	40.00
		0.918	17.59	17.00	18.46	19.16	19.74	21.00	22.90	24.34	26.18	41.00
	6 m	0.041	3.99	21.00	23.06	23.78	25.41	26.00	29.40	31.16	33.16	45.00
		0.500	9.38	17.00	21.42	21.85	22.44	24.00	25.72	27.21	28.76	41.00
		0.918	14.90	20.00	19.66	20.36	20.95	22.00	24.39	26.03	28.36	38.00
	7 m	0.041	6.33	24.00	25.08	25.73	26.46	28.00	29.74	31.25	33.22	46.00
		0.500	10.38	17.00	20.30	20.98	21.61	23.00	24.68	26.26	29.35	40.00
		0.918	12.28	23.00	23.51	24.20	24.79	26.00	28.58	30.52	32.76	45.00
1CDCW2 (d = 0.155 m)	1 m	0.032	0.00	0.00	0.00	0.00	0.00	0.00	0.00	0.00	0.00	0.00
		0.500	7.22	10.00	11.27	11.79	12.37	13.00	14.55	15.66	17.35	28.00
		0.935	27.13	9.00	10.18	10.68	11.26	12.00	13.41	14.53	16.21	31.00
	2 m	0.032	0.22	14.00	15.70	16.44	17.08	18.00	19.42	20.33	21.50	26.00
		0.500	11.65	12.00	12.97	13.53	14.12	15.00	16.90	18.59	19.80	34.00
		0.935	22.39	13.00	13.67	14.30	14.82	16.00	17.44	18.62	20.28	36.00
	3 m	0.032	1.70	17.00	20.80	21.55	22.29	24.00	26.24	28.28	30.96	42.00
		0.500	8.94	16.00	16.57	17.26	17.83	19.00	20.85	22.06	23.78	40.00
		0.935	19.50	16.00	18.16	18.73	19.36	21.00	22.38	23.68	25.66	40.00
	4 m	0.032	1.80	22.00	23.42	24.30	25.15	27.00	29.35	31.18	33.48	44.00
		0.500	8.09	16.00	16.81	18.29	18.64	19.00	21.49	22.92	25.40	36.00
		0.935	18.37	16.00	16.98	17.44	17.89	19.00	21.72	22.80	25.24	39.00
	5 m	0.032	2.46	25.00	25.52	26.70	27.56	29.00	32.28	34.42	37.63	50.00
		0.500	6.28	18.00	19.43	20.09	20.62	23.00	24.31	25.71	27.76	41.00
		0.935	15.81	18.00	19.35	20.01	20.63	22.00	23.61	24.90	26.74	41.00
	6 m	0.032	2.68	27.00	29.98	30.96	32.00	34.00	37.52	40.05	43.69	59.00
		0.500	8.97	15.00	16.89	17.67	18.35	19.00	21.16	22.59	24.69	35.00
		0.935	9.70	20.00	20.59	21.30	21.90	23.00	25.33	26.80	28.77	39.00
	7 m	0.032	3.05	26.00	28.52	29.51	30.50	33.00	35.62	37.58	40.22	54.00
		0.500	7.96	23.00	25.43	26.12	26.72	28.00	29.95	31.48	33.61	44.00
		0.935	8.97	24.00	25.12	25.83	26.60	28.00	30.34	31.76	33.64	44.00
	8 m	0.032	4.82	30.00	34.25	35.24	36.27	39.00	41.72	44.17	47.38	65.00
		0.500	6.94	27.00	27.75	29.73	30.93	31.00	34.26	36.20	38.12	53.00
		0.935	7.55	22.00	27.19	27.91	28.66	30.00	32.78	34.57	36.83	54.00
	9 m	0.032	4.34	33.00	32.95	36.96	38.02	40.00	43.66	45.68	48.75	66.00
		0.500	7.32	26.00	30.70	31.39	31.97	33.00	37.46	37.46	39.73	53.00
		0.935	6.89	29.00	30.56	31.17	31.88	34.00	38.42	38.42	40.72	51.00
1CDCW3 (d = 0.1785)	1 m	0.028	0.00	0.00	0.00	0.00	0.00	0.00	0.00	0.00	0.00	0.00
		0.500	1.75	11.00	10.31	10.63	10.94	12.00	13.26	14.27	15.91	23.00
		0.944	22.15	8.00	9.89	10.67	11.36	12.00	13.95	16.00	17.71	32.00
	2 m	0.028	0.16	14.00	13.80	14.33	14.78	16.00	17.50	18.40	19.25	21.00
		0.500	8.91	11.00	12.28	12.82	13.40	14.00	15.97	17.06	18.71	30.00
		0.944	18.35	10.00	12.39	14.06	14.53	15.00	15.65	16.66	18.47	32.00
	3 m	0.028	0.30	16.00	16.27	16.85	17.55	19.00	21.42	23.00	24.75	29.00
		0.500	6.34	12.00	13.73	14.36	14.89	16.00	17.44	18.54	19.98	30.00
		0.944	15.37	13.00	13.85	14.45	14.97	16.00	17.53	18.61	20.12	35.00

Contiuned...

Data Set	x (m)	(y/d)	Cp (ppm)	T_L (s)	T_{1R} (s)	T_{2R} (s)	T_{3R} (s)	T_P (s)	T_{3F} (s)	T_{2F} (s)	T_{1F} (s)	T_T (s)
	4 m	0.028	0.48	18.00	19.00	19.80	20.64	22.00	23.90	25.14	28.00	33.00
		0.500	6.75	14.00	16.16	16.73	17.35	19.00	20.17	21.29	22.85	33.00
		0.944	15.60	16.00	16.87	17.45	17.97	19.00	20.54	21.64	23.15	32.00
	5 m	0.028	1.01	22.00	22.14	22.80	23.55	25.00	27.68	29.25	31.31	42.00
		0.500	7.31	18.00	19.25	19.81	20.40	21.00	23.18	24.35	25.97	41.00
		0.944	9.50	19.00	19.40	20.30	21.11	22.00	22.82	24.53	26.51	40.00
	6 m	0.028	1.76	22.00	23.00	23.71	24.50	26.00	28.13	30.05	32.36	40.00
		0.500	6.94	20.00	20.50	22.00	22.56	23.00	24.40	25.59	27.18	37.00
		0.944	10.41	19.00	21.04	21.44	21.84	23.00	24.30	25.41	26.93	36.00
	7 m	0.028	2.49	25.00	26.62	27.49	28.39	30.00	32.82	34.39	36.62	45.00
		0.500	6.27	22.00	22.51	23.16	23.72	25.00	26.57	27.82	29.65	42.00
		0.944	7.80	22.00	23.65	24.42	25.12	27.00	28.63	29.80	31.44	44.00
	8 m	0.028	2.14	28.00	28.92	29.72	30.58	32.00	34.82	36.55	38.92	50.00
		0.500	7.73	22.00	23.37	24.00	24.58	26.00	27.32	28.56	30.31	38.00
		0.944	6.52	22.00	24.21	24.55	24.90	26.00	28.64	29.98	31.92	41.00
	9 m	0.028	2.96	28.00	29.19	30.16	31.18	33.00	36.30	38.08	40.40	54.00
		0.500	5.15	25.00	24.86	25.48	26.08	27.00	29.27	30.79	32.87	42.00
		0.944	5.45	25.00	25.67	26.59	27.49	29.00	30.39	31.38	32.90	45.00
1CDCW4 (d = 0.0895 m)	1 m	0.056	0.00	0.00	0.00	0.00	0.00	0.00	0.00	0.00	0.00	0.00
		0.500	7.38	8.00	9.19	9.68	10.26	11.00	12.34	13.34	14.78	29.00
		0.882	49.20	7.00	8.20	8.69	9.27	10.00	11.20	12.08	13.45	27.00
	2 m	0.056	1.90	11.00	11.57	12.18	12.66	14.00	15.05	16.09	17.79	26.00
		0.500	11.66	9.00	10.05	10.51	10.98	12.00	12.97	13.83	15.12	28.00
		0.882	45.43	10.00	10.26	10.76	11.34	12.00	13.29	14.16	15.46	26.00
	3 m	0.056	4.75	13.00	13.70	14.32	14.83	16.00	17.32	18.46	20.14	30.00
		0.500	17.10	11.00	12.09	12.55	13.03	14.00	15.02	15.93	17.44	30.00
		0.882	25.70	12.00	12.31	12.86	13.43	14.00	15.70	16.69	18.13	32.00
	4 m	0.056	8.28	16.00	16.34	16.96	17.58	19.00	20.48	21.61	23.10	33.00
		0.500	15.38	15.00	15.41	16.02	16.57	18.00	19.16	20.21	21.73	35.00
		0.882	15.12	13.00	14.35	14.94	15.52	17.00	18.18	19.16	20.53	32.00
	5 m	0.056	11.25	17.00	17.66	18.31	18.84	20.00	21.60	22.83	24.59	37.00
		0.500	13.74	14.00	16.64	17.27	17.78	19.00	20.25	21.33	22.83	33.00
		0.882	17.73	15.00	16.10	16.63	17.24	18.00	19.88	20.93	22.40	33.00
	6 m	0.056	8.20	18.00	19.47	20.19	20.80	22.00	23.81	25.08	26.83	37.00
		0.500	13.51	16.00	17.99	18.54	19.14	20.00	21.72	22.84	24.46	38.00
		0.882	15.65	17.00	18.04	18.56	19.12	20.00	21.52	22.66	24.23	36.00
	7 m	0.056	11.29	21.00	22.05	22.66	23.35	25.00	26.69	28.10	30.05	44.00
		0.500	15.21	19.00	20.38	21.03	21.63	23.00	24.52	25.77	27.45	39.00
		0.882	13.37	19.00	19.60	20.34	20.97	22.00	23.98	25.04	26.61	36.00
	8 m	0.056	12.56	23.00	24.19	24.91	25.64	27.00	28.95	30.36	32.29	44.00
		0.500	12.71	19.00	22.28	22.96	23.63	25.00	26.98	28.45	30.35	46.00
		0.882	13.43	18.00	22.32	23.05	23.52	24.00	27.04	27.72	30.04	42.00
1CDCW5 (d = 0.1645 m)	1 m	0.030	0.00	0.00	0.00	0.00	0.00	0.00	0.00	0.00	0.00	0.00
		0.500	3.69	11.00	11.60	12.22	12.73	14.00	15.26	16.45	18.10	26.00
		0.940	36.65	10.00	10.52	11.15	11.68	13.00	14.33	15.57	17.33	33.00
	2 m	0.030	0.29	14.00	14.02	14.58	15.19	16.00	17.71	20.17	22.44	26.00
		0.500	6.85	12.00	11.79	12.49	13.33	15.00	16.44	17.86	19.80	28.00
		0.940	26.83	11.00	12.08	12.60	13.18	14.00	15.49	16.53	18.02	32.00
	3 m	0.030	2.43	15.00	16.18	16.76	17.38	19.00	20.24	21.59	23.66	35.00
		0.500	7.22	14.00	15.59	16.27	16.85	18.00	19.92	21.45	23.51	32.00
		0.940	18.19	14.00	14.34	14.94	15.51	17.00	18.11	19.14	20.63	33.00
	4 m	0.030	2.57	18.00	17.84	18.60	19.35	21.00	22.67	24.37	26.85	38.00
		0.500	7.48	17.00	17.21	17.85	18.53	20.00	21.45	22.72	24.57	36.00
		0.940	12.27	16.00	16.52	17.26	17.88	19.00	21.26	22.65	24.60	35.00
	5 m	0.030	3.44	20.00	20.22	20.90	21.58	23.00	24.85	26.67	28.76	40.00
		0.500	7.60	19.00	19.23	19.92	20.65	22.00	23.97	25.17	26.84	38.00
		0.940	10.62	19.00	18.59	19.65	20.40	21.00	22.61	23.83	25.70	37.00
	6 m	0.030	4.00	22.00	22.09	23.02	23.96	26.00	28.31	30.06	32.55	44.00
		0.500	8.19	21.00	22.37	23.08	23.73	25.00	27.29	28.71	30.69	39.00
		0.940	10.29	20.00	20.07	20.83	21.74	24.00	26.05	27.55	29.55	42.00

Contiuned....

Data Set	x (m)	(y/d)	Cp (ppm)	T_L (s)	T_{1R} (s)	T_{2R} (s)	T_{3R} (s)	T_P (s)	T_{3F} (s)	T_{2F} (s)	T_{1F} (s)	T_T (s)
	7 m	0.030	3.86	23.00	23.78	24.64	25.52	27.00	30.01	31.86	34.23	45.00
		0.500	8.34	23.00	23.64	24.33	24.90	26.00	27.82	29.07	30.92	45.00
		0.940	9.70	21.00	22.62	23.37	23.99	25.00	26.87	28.07	29.86	45.00
	8 m	0.030	4.34	24.00	23.86	24.82	25.79	28.00	30.42	32.41	35.19	48.00
		0.500	8.51	24.00	24.02	24.78	25.83	27.00	28.40	29.15	31.21	45.00
		0.940	9.06	22.00	22.67	23.53	24.40	26.00	28.35	29.86	31.93	44.00
	9 m	0.030	4.53	26.00	26.58	27.58	28.58	31.00	33.57	35.54	38.59	52.00
		0.500	8.55	25.00	27.00	27.61	28.33	30.00	31.31	32.60	34.44	46.00
		0.940	8.14	24.00	25.95	26.55	27.20	29.00	30.49	31.74	33.56	48.00
	10 m	0.030	4.66	27.00	27.72	28.90	30.78	32.00	33.19	36.20	39.31	54.00
		0.500	8.58	26.00	29.16	30.02	30.72	32.00	33.60	35.49	38.13	53.00
		0.94	7.64	25.00	27.60	28.71	29.58	31.00	32.91	34.62	37.04	54.00
1CDCW6 (d = 0.1005 m)	1 m	0.050	0.69	11.00	11.15	11.64	12.22	13.00	14.49	15.65	17.69	25.00
		0.900	34.77	9.00	9.66	10.21	10.60	11.00	12.31	13.12	14.52	32.00
	2 m	0.050	5.57	12.00	13.35	13.97	14.53	16.00	17.06	18.20	20.12	34.00
		0.900	25.83	10.00	10.94	11.72	12.39	13.00	14.23	14.84	16.68	35.00
	3 m	0.050	3.84	13.00	14.02	14.54	15.10	16.00	17.51	18.57	20.18	33.00
		0.900	14.17	13.00	13.29	13.83	14.41	15.00	16.97	17.91	19.37	38.00
	4 m	0.050	7.17	15.00	16.45	17.20	17.83	19.00	20.89	22.23	24.22	40.00
		0.900	20.21	13.00	14.00	14.50	14.99	16.00	17.33	18.41	19.94	36.00
	5 m	0.050	6.25	19.00	19.76	20.45	21.07	22.00	24.12	25.35	27.25	40.00
		0.900	13.61	16.00	17.09	17.62	18.22	19.00	21.05	22.26	23.84	38.00
	6 m	0.050	8.48	20.00	20.41	21.23	21.93	23.00	25.25	26.50	28.41	43.00
		0.900	14.03	17.00	18.29	18.92	19.56	21.00	22.40	23.59	25.32	44.00
	7 m	0.050	7.57	21.00	21.40	22.18	22.87	25.00	26.72	28.16	30.30	45.00
		0.900	12.26	19.00	20.17	20.78	21.45	23.00	24.64	25.99	27.84	41.00
	8 m	0.050	8.73	24.00	25.69	26.49	27.27	29.00	31.11	32.69	34.97	50.00
		0.900	10.23	22.00	22.36	22.99	23.59	25.00	26.61	28.04	29.93	46.00
	9 m	0.050	7.55	26.00	27.64	28.51	29.39	31.00	33.97	35.66	37.97	51.00
		0.900	8.88	23.00	23.11	23.74	24.48	26.00	28.42	29.86	31.66	42.00
	10 m	0.050	7.17	28.00	29.65	30.69	31.71	34.00	36.56	38.28	40.56	52.00
		0.900	8.78	26.00	26.18	26.85	27.60	29.00	31.39	32.86	34.77	44.00
1CDCW7 (d = 0.103 m)	1 m	0.048	3.87	11.00	11.43	12.02	12.53	14.00	15.09	16.27	17.98	30.00
		0.903	27.31	9.00	10.15	10.66	11.25	12.00	13.46	14.52	16.09	30.00
	2 m	0.048	2.91	13.00	13.71	14.34	14.85	16.00	17.43	18.65	20.53	28.00
		0.903	19.60	11.00	11.31	11.86	12.43	13.00	14.96	16.00	17.58	29.00
	3 m	0.048	5.55	15.00	15.75	16.42	16.98	18.00	20.06	21.49	23.66	40.00
		0.903	16.13	13.00	13.39	14.07	14.73	16.00	17.86	18.96	20.56	32.00
	4 m	0.048	5.82	18.00	19.21	19.95	20.66	22.00	23.78	25.11	27.27	38.00
		0.903	16.99	15.00	16.25	16.87	17.51	19.00	20.28	21.42	23.03	36.00
	5 m	0.048	7.92	20.00	21.29	22.05	22.75	24.00	26.17	27.65	29.90	45.00
		0.903	10.58	17.00	17.77	18.41	18.95	20.00	21.87	23.10	24.81	39.00
	6 m	0.048	5.71	23.00	23.54	24.34	25.08	27.00	28.88	30.56	32.92	48.00
		0.903	12.21	20.00	20.52	21.19	21.75	23.00	24.45	25.65	27.32	40.00
	7 m	0.048	7.27	25.00	26.19	27.01	27.76	29.00	31.39	32.91	35.34	52.00
		0.903	10.76	21.00	22.09	22.69	23.36	25.00	26.32	27.46	29.11	40.00
	8 m	0.048	6.25	27.00	28.25	29.09	29.91	32.00	34.51	36.32	38.85	53.00
		0.903	8.45	24.00	24.64	25.32	25.90	27.00	29.52	31.02	33.03	46.00
	9 m	0.048	6.49	28.00	28.76	29.61	30.46	32.00	34.31	35.95	38.44	55.00
		0.903	6.65	29.00	29.58	30.41	31.23	33.00	35.74	37.62	40.13	52.00
2CDCW1 (d = 0.124 m)	1 m	0.040	0.00	0.00	0.00	0.00	0.00	0.00	0.00	0.00	0.00	0.00
		0.500	5.91	14.00	14.07	14.44	14.80	16.00	17.75	18.63	20.28	34.00
		0.920	25.65	9.00	9.86	10.70	11.39	12.00	13.14	14.08	15.56	30.00
	2 m	0.040	0.85	15.00	14.79	15.43	15.99	17.00	19.14	20.63	22.97	34.00
		0.500	9.46	12.00	12.57	13.22	13.76	15.00	16.40	17.62	19.33	32.00
		0.920	14.25	11.00	11.63	12.26	12.76	14.00	15.16	16.22	17.78	32.00
	3 m	0.040	4.67	15.00	15.28	15.91	16.54	18.00	19.49	20.84	22.81	32.00
		0.500	8.71	13.00	14.05	14.58	15.17	16.00	17.69	18.80	20.41	29.00
		0.920	12.83	14.00	14.37	15.01	15.58	17.00	18.12	19.17	20.71	39.00
	4 m	0.040	2.67	18.00	18.35	19.04	19.70	21.00	22.89	24.34	26.39	35.00

Continued....

Data Set	x (m)	(y/d)	Cp (ppm)	T_L (s)	T_{1R} (s)	T_{2R} (s)	T_{3R} (s)	T_P (s)	T_{3F} (s)	T_{2F} (s)	T_{1F} (s)	T_T (s)
		0.500	7.94	16.00	16.93	17.52	18.13	19.00	20.91	22.10	23.88	34.00
		0.920	12.15	16.00	16.22	16.80	17.42	19.00	20.21	21.32	22.82	34.00
	5 m	0.040	3.36	19.00	19.66	20.40	21.02	22.00	24.40	25.87	28.13	42.00
		0.500	6.30	20.00	20.78	21.60	22.40	24.00	25.61	26.96	29.07	41.00
		0.920	8.31	17.00	17.61	18.31	18.89	20.00	22.03	23.32	25.02	36.00
	6 m	0.040	4.77	24.00	24.14	24.96	25.79	28.00	30.14	31.85	34.57	49.00
		0.500	6.62	21.00	21.30	22.00	22.69	24.00	26.56	28.21	30.34	42.00
		0.920	9.06	19.00	19.91	20.56	21.22	23.00	24.49	25.44	26.61	46.00
	7 m	0.040	3.91	24.00	25.32	26.19	26.93	29.00	30.71	32.24	34.57	49.00
		0.500	5.57	22.00	22.79	23.55	24.30	26.00	27.67	29.12	31.25	44.00
		0.920	7.45	21.00	21.24	21.84	22.50	24.00	25.72	27.06	28.86	42.00
	8 m	0.040	4.58	23.00	23.12	23.96	24.82	27.00	29.07	30.69	32.81	42.00
		0.500	6.39	23.00	25.17	26.00	26.82	29.00	30.83	32.29	34.28	44.00
		0.920	7.96	22.00	23.19	23.82	24.51	26.00	27.93	29.18	30.03	39.00
	9 m	0.040	4.85	27.00	28.23	29.14	29.99	32.00	34.50	36.14	38.24	48.00
		0.500	6.76	25.00	25.91	26.54	27.18	29.00	30.58	31.99	33.82	42.00
		0.920	6.47	24.00	25.20	25.93	26.69	28.00	30.57	32.27	34.31	44.00
	10 m	0.040	4.25	31.00	31.81	32.73	33.64	36.00	38.50	40.32	42.87	55.00
		0.500	4.53	28.00	28.61	29.63	30.77	34.00	36.69	38.55	41.22	55.00
		0.920	4.98	28.00	28.05	28.83	29.74	32.00	34.81	36.53	38.35	43.00
2CDCW2 (d = 0.134 m)	1 m	0.037	0.00	0.00	0.00	0.00	0.00	0.00	0.00	0.00	0.00	0.00
		0.500	3.24	8.00	8.17	8.67	9.26	10.00	11.27	12.14	13.40	21.00
		0.925	20.01	7.00	8.28	9.03	9.51	10.00	11.01	12.25	13.85	27.00
	2 m	0.037	0.39	12.00	12.45	13.09	13.66	15.00	16.42	17.64	19.56	26.00
		0.500	4.84	11.00	11.18	11.68	12.26	13.00	14.38	15.40	16.88	27.00
		0.925	12.18	10.00	10.52	11.14	11.64	13.00	13.95	14.86	16.16	26.00
	3 m	0.037	2.28	13.00	13.49	14.10	14.56	16.00	16.90	17.93	19.50	31.00
		0.500	6.78	12.00	13.07	13.58	14.16	15.00	16.47	17.53	18.97	32.00
		0.925	8.91	12.00	12.25	12.78	13.37	14.00	15.53	16.46	17.70	33.00
	4 m	0.037	2.09	15.00	16.06	16.61	17.23	18.00	19.98	21.20	22.84	32.00
		0.500	5.74	13.00	13.71	14.34	14.87	16.00	17.31	18.27	19.55	29.00
		0.925	9.99	13.00	13.57	14.20	14.70	16.00	17.04	17.94	19.25	31.00
	5 m	0.037	2.65	18.00	18.27	18.93	19.59	21.00	22.50	23.72	25.34	31.00
		0.500	6.41	16.00	16.16	16.69	17.29	18.00	19.78	20.82	22.22	36.00
		0.925	9.70	14.00	14.34	14.88	15.44	16.00	17.63	18.52	19.70	31.00
	6 m	0.037	2.63	19.00	20.13	20.76	21.46	23.00	24.59	25.89	27.90	37.00
		0.500	5.94	18.00	18.22	18.85	19.53	21.00	22.41	23.51	24.92	36.00
		0.925	7.79	17.00	17.50	18.16	18.71	20.00	21.33	22.43	23.90	36.00
	7 m	0.037	3.05	21.00	21.36	22.07	22.73	24.00	26.09	27.39	29.10	40.00
		0.500	6.02	20.00	20.10	20.40	20.70	21.00	22.71	23.73	25.15	38.00
		0.925	6.54	18.00	18.67	19.33	19.88	21.00	22.83	24.00	25.63	40.00
	8 m	0.037	4.29	22.00	23.45	24.27	25.00	27.00	28.63	29.51	30.69	45.00
		0.500	5.27	21.00	21.50	22.23	22.85	24.00	25.83	27.02	28.65	40.00
		0.925	5.40	21.00	21.82	22.48	23.11	25.00	26.54	27.72	29.17	39.00
	9 m	0.037	3.86	25.00	25.89	26.71	27.54	29.00	31.18	32.70	34.65	46.00
		0.500	5.34	22.00	23.04	23.62	24.27	26.00	27.36	28.52	30.17	44.00
		0.925	5.50	23.00	23.40	24.14	24.82	26.00	28.13	29.37	30.95	41.00
	10 m	0.037	3.45	28.00	28.36	29.20	29.95	31.00	33.47	35.03	37.13	48.00
		0.500	4.57	25.00	25.87	26.51	27.13	29.00	30.47	31.77	33.46	41.00
		0.925	4.79	25.00	26.03	26.68	27.44	29.00	31.01	32.44	34.22	46.00
2CDCW3 (d = 0.145 m)	1 m	0.034	0.00	0.00	0.00	0.00	0.00	0.00	0.00	0.00	0.00	0.00
		0.500	4.74	8.00	8.50	9.12	9.63	11.00	12.02	12.98	14.46	23.00
		0.931	18.42	8.00	8.90	10.09	10.54	11.00	11.68	12.63	14.34	27.00
	2 m	0.034	0.24	11.00	11.38	12.11	12.78	14.00	16.50	17.50	19.00	22.00
		0.500	6.46	10.00	10.82	11.39	11.88	13.00	14.15	15.08	16.45	28.00
		0.931	13.66	8.00	9.19	9.56	9.92	11.00	11.64	12.82	14.20	25.00
	3 m	0.034	1.88	14.00	14.59	15.21	15.72	17.00	18.26	19.43	21.06	32.00
		0.500	5.14	11.00	12.31	12.87	13.44	14.00	15.88	16.46	17.00	28.00
		0.931	11.01	12.00	12.49	13.11	13.61	15.00	15.96	16.86	18.10	29.00
	4 m	0.034	2.04	15.00	16.19	16.76	17.36	18.00	19.85	20.88	22.48	33.00

Continued....

Data Set	x (m)	(y/d)	Cp (ppm)	T_L (s)	T_{1R} (s)	T_{2R} (s)	T_{3R} (s)	T_P (s)	T_{3F} (s)	T_{2F} (s)	T_{1F} (s)	T_T (s)
		0.500	7.90	14.00	14.37	14.93	15.47	16.00	17.91	18.86	20.20	28.00
		0.931	8.57	13.00	14.06	14.59	15.18	16.00	17.65	18.65	19.97	30.00
	5 m	0.034	2.15	18.00	18.36	19.04	19.67	21.00	22.47	23.70	25.51	37.00
		0.500	6.44	15.00	16.02	16.52	17.04	18.00	19.34	20.34	21.71	33.00
		0.931	4.69	15.00	15.64	16.27	16.78	18.00	19.16	20.14	21.55	34.00
	6 m	0.034	1.76	20.00	20.30	20.98	21.64	23.00	24.66	25.91	27.76	35.00
		0.500	5.57	17.00	18.08	18.64	19.26	20.00	21.95	23.00	24.56	39.00
		0.931	5.64	18.00	18.19	18.74	19.35	20.00	22.04	23.00	24.47	34.00
	7 m	0.034	1.90	21.00	21.24	21.97	22.49	23.00	24.88	26.16	27.98	38.00
		0.500	5.25	19.00	19.88	20.51	21.12	22.00	23.78	24.81	26.23	37.00
		0.931	5.22	19.00	19.42	20.17	20.81	22.00	23.71	24.84	26.27	40.00
	8 m	0.034	2.58	24.00	24.91	25.58	26.31	28.00	29.80	31.16	33.34	42.00
		0.500	3.80	21.00	21.45	22.14	22.72	24.00	25.61	27.02	28.69	37.00
		0.931	4.53	21.00	21.50	22.16	22.73	24.00	25.58	26.80	28.39	37.00
	9 m	0.034	3.24	25.00	26.10	26.85	27.62	29.00	31.02	32.37	34.13	45.00
		0.500	4.18	23.00	23.58	24.26	24.82	26.00	27.70	28.71	30.43	42.00
		0.931	3.79	23.00	23.26	23.92	24.59	26.00	27.72	29.11	30.98	39.00
	10 m	0.034	1.73	27.00	27.64	28.51	29.38	31.00	34.01	35.48	37.51	47.00
		0.500	3.02	25.00	25.35	26.06	26.75	28.00	30.56	31.98	33.70	40.00
		0.931	3.51	24.00	24.07	24.62	25.24	26.00	28.42	29.73	31.65	46.00
2CDCW4 (d = 0.164 m)	1 m	0.030	0.00	0.00	0.00	0.00	0.00	0.00	0.00	0.00	0.00	0.00
		0.500	4.00	8.00	9.21	9.76	10.36	11.00	12.98	13.94	15.29	24.00
		0.940	12.11	8.00	9.12	9.94	10.48	11.00	11.72	12.61	13.91	26.00
	2 m	0.030	1.48	11.00	12.01	12.55	13.14	14.00	15.71	16.90	18.71	26.00
		0.500	5.55	10.00	10.81	11.42	11.95	13.00	14.30	15.27	16.61	28.00
		0.940	8.73	9.00	10.20	10.76	11.36	12.00	12.70	13.55	14.80	25.00
	3 m	0.030	1.35	14.00	14.60	15.36	15.99	17.00	19.11	20.46	22.33	31.00
		0.500	3.81	11.00	12.55	13.36	14.01	15.00	16.40	17.32	18.62	27.00
		0.940	6.87	12.00	13.48	14.29	14.92	16.00	17.49	18.54	19.93	33.00
	4 m	0.030	0.73	15.00	15.27	15.72	16.34	18.00	19.63	21.04	22.84	31.00
		0.500	4.92	12.00	13.14	13.74	14.36	16.00	16.98	17.91	19.21	28.00
		0.940	9.12	13.00	13.55	14.35	15.09	16.00	17.12	18.08	19.38	33.00
	5 m	0.030	1.35	16.00	18.04	18.44	18.84	20.00	21.06	22.27	23.86	31.00
		0.500	4.51	15.00	16.02	16.55	17.14	18.00	19.72	20.79	22.22	35.00
		0.940	5.73	15.00	16.11	16.67	17.29	18.00	20.09	21.10	22.48	33.00
	6 m	0.030	1.88	19.00	20.03	20.74	21.50	23.00	24.62	25.92	27.80	38.00
		0.500	3.85	17.00	17.42	18.16	18.77	20.00	21.48	22.60	24.14	32.00
		0.940	5.20	17.00	17.58	18.33	18.94	20.00	21.82	22.98	24.55	37.00
	7 m	0.030	2.66	21.00	21.53	22.32	22.99	25.00	26.77	28.23	30.20	39.00
		0.500	3.57	19.00	19.42	20.14	20.76	22.00	23.50	24.57	25.96	35.00
		0.940	3.65	18.00	18.36	19.08	19.75	21.00	23.58	24.92	26.55	37.00
	8 m	0.030	1.93	23.00	24.10	24.91	25.71	27.00	29.24	30.59	32.51	43.00
		0.500	3.37	22.00	22.74	23.45	24.10	26.00	27.44	28.72	30.44	41.00
		0.940	3.49	22.00	22.20	22.84	24.51	26.00	27.40	28.56	30.17	42.00
	9 m	0.030	2.00	25.00	27.44	28.34	29.12	31.00	32.67	34.31	36.56	48.00
		0.500	3.45	24.00	25.05	25.64	26.31	28.00	29.55	30.75	32.28	40.00
		0.940	3.26	24.00	24.30	25.06	25.82	27.00	29.01	30.38	31.97	40.00
	10 m	0.030	2.06	27.00	28.18	29.05	29.92	31.00	33.98	34.94	37.46	47.00
		0.500	2.98	26.00	26.90	27.61	28.34	30.00	31.62	32.98	34.84	43.00
		0.940	3.13	24.00	24.53	25.40	26.19	28.00	30.15	31.76	33.78	44.00
2CDCW5 (d = 0.196 m)	1 m	0.025	0.00	0.00	0.00	0.00	0.00	0.00	0.00	0.00	0.00	0.00
		0.500	1.18	10.00	9.95	10.45	10.93	12.00	13.15	14.13	15.53	22.00
		0.950	10.89	8.00	9.00	10.20	10.60	11.00	11.73	12.92	14.38	26.00
	2 m	0.025	0.00	0.00	0.00	0.00	0.00	0.00	0.00	0.00	0.00	0.00
		0.500	1.08	8.00	9.00	9.50	10.00	11.00	12.29	13.32	14.80	20.00
		0.950	6.25	10.00	11.15	11.71	12.33	13.00	14.96	15.91	17.29	29.00
	3 m	0.025	0.39	13.00	13.61	14.32	14.90	16.00	17.59	18.81	20.45	24.00
		0.500	3.21	14.00	13.82	14.40	14.92	16.00	17.24	18.21	19.58	28.00
		0.950	6.00	13.00	13.75	14.43	15.03	16.00	17.61	18.62	20.00	36.00
	4 m	0.025	0.16	17.00	17.17	17.83	18.60	20.00	21.00	22.60	23.67	26.00

Continued....

Data Set	x (m)	(y/d)	Cp (ppm)	T_L (s)	T_{1R} (s)	T_{2R} (s)	T_{3R} (s)	T_P (s)	T_{3F} (s)	T_{2F} (s)	T_{1F} (s)	T_T (s)
		0.500	2.41	15.00	15.08	15.65	16.27	17.00	18.66	19.59	20.89	28.00
		0.950	5.08	15.00	15.39	16.15	16.78	18.00	19.49	20.61	22.06	33.00
	5 m	0.025	0.38	18.00	18.50	19.27	19.90	21.00	22.94	24.17	25.90	29.00
		0.500	2.34	17.00	17.21	17.89	18.63	20.00	21.78	22.85	24.34	36.00
		0.950	3.90	16.00	16.97	17.65	18.43	20.00	22.28	23.58	25.21	37.00
	6 m	0.025	0.87	19.00	20.02	20.70	21.44	23.00	24.65	25.86	27.71	35.00
		0.500	1.78	18.00	18.18	18.89	19.57	21.00	22.27	23.39	24.94	34.00
		0.950	3.15	18.00	18.57	19.32	19.95	21.00	22.98	24.15	25.80	41.00
	7 m	0.025	1.59	22.00	22.40	22.86	23.52	25.00	26.70	28.10	29.91	40.00
		0.500	1.99	20.00	20.78	22.07	23.03	25.00	27.07	28.37	30.06	41.00
		0.950	2.72	20.00	20.53	21.25	21.87	23.00	24.95	26.15	27.79	40.00
	8 m	0.025	1.14	23.00	23.24	24.03	24.80	27.00	28.63	29.91	31.68	37.00
		0.500	2.17	22.00	23.11	23.89	24.68	26.00	28.20	29.42	31.20	44.00
		0.950	3.42	21.00	22.16	23.01	23.83	26.00	27.80	29.12	30.89	42.00
	9 m	0.025	1.55	26.00	26.99	28.04	29.08	31.00	33.54	34.88	36.60	47.00
		0.500	1.23	24.00	25.15	26.15	27.21	32.00	34.78	36.28	38.03	48.00
		0.950	2.28	24.00	24.90	26.06	27.20	29.00	32.09	33.64	35.37	48.00
2CDCW6 (d = 0.150 m)	1 m	0.033	4.17	13.00	14.07	14.60	15.19	16.00	17.57	18.63	20.09	27.00
		0.500	15.23	12.00	12.10	12.61	13.18	14.00	15.44	16.40	17.70	27.00
		0.934	21.62	12.00	12.17	12.67	13.26	14.00	15.46	16.43	17.72	28.00
	2 m	0.033	6.28	14.00	13.74	14.95	15.87	17.00	17.96	19.38	20.88	29.00
		0.500	13.42	13.00	13.05	13.58	14.16	15.00	16.69	17.74	19.18	29.00
		0.934	19.78	13.00	13.08	13.60	14.19	15.00	16.41	17.43	18.74	29.00
	3 m	0.033	6.90	14.00	14.82	15.50	16.17	18.00	19.38	20.57	22.22	31.00
		0.500	12.43	14.00	14.08	14.75	15.38	16.00	17.93	18.97	20.61	31.00
		0.934	18.04	13.00	14.05	14.55	15.08	16.00	17.39	18.49	19.86	30.00
	4 m	0.033	8.20	15.00	15.65	16.44	17.30	19.00	20.14	21.59	23.31	33.00
		0.500	12.10	14.00	14.97	15.75	16.41	17.00	19.16	20.21	21.90	32.00
		0.934	16.13	13.00	14.90	15.47	16.00	17.00	18.46	19.61	21.04	31.00
	5 m	0.033	8.33	15.00	16.58	17.38	17.98	20.00	21.58	22.86	24.65	35.00
		0.500	11.26	15.00	15.98	16.76	17.41	18.00	20.39	21.64	23.38	34.00
		0.934	14.91	14.00	15.84	16.44	16.96	18.00	19.52	20.76	22.39	34.00
	6 m	0.033	8.66	17.00	17.55	18.39	19.20	21.00	22.64	24.00	25.87	37.00
		0.500	10.34	15.00	16.98	17.70	18.37	19.00	21.68	23.06	24.87	36.00
		0.934	13.34	15.00	16.70	17.36	17.91	19.00	20.71	22.01	23.79	35.00
	7 m	0.033	8.55	17.00	18.53	19.39	20.10	22.00	23.91	25.33	27.22	38.00
		0.500	9.82	17.00	17.97	18.72	19.40	21.00	22.92	24.37	26.26	37.00
		0.934	12.40	17.00	17.66	18.34	18.89	20.00	21.93	23.25	25.16	36.00
	8 m	0.033	8.63	18.00	19.53	20.41	21.29	23.00	25.06	26.52	28.50	40.00
		0.500	9.38	18.00	18.99	19.71	20.42	22.00	24.18	25.66	27.64	39.00
		0.934	11.17	17.00	18.57	19.26	19.85	21.00	23.20	24.61	26.59	38.00
	9 m	0.033	8.35	19.00	20.53	21.43	22.23	24.00	26.30	27.83	29.86	41.00
		0.500	9.06	18.00	19.98	20.75	21.48	23.00	25.42	26.92	28.94	41.00
		0.934	10.46	18.00	19.53	20.26	20.86	22.00	24.45	25.91	27.91	40.00
2CDSL11 (d = 0.124 m)	1 m	0.040	0.00	0.00	0.00	0.00	0.00	0.00	0.00	0.00	0.00	0.00
		0.920	9.97	6.00	8.56	9.20	9.79	11.00	11.97	12.97	14.42	27.00
	2 m	0.040	1.71	12.00	13.19	13.74	14.34	15.00	17.02	18.37	20.35	29.00
		0.920	8.02	10.00	10.15	10.58	11.05	12.00	12.73	13.62	14.95	28.00
	3 m	0.040	0.56	15.00	16.04	16.63	17.28	19.00	20.33	21.67	24.33	32.00
		0.920	7.47	13.00	13.23	13.77	14.37	15.00	16.68	17.65	18.96	32.00
	4 m	0.040	1.02	18.00	18.45	19.26	19.99	22.00	24.03	25.56	27.45	35.00
		0.920	4.89	14.00	14.73	15.37	15.90	17.00	18.60	19.70	21.19	33.00
	5 m	0.040	2.29	20.00	20.35	21.11	21.80	23.00	25.48	26.99	29.04	38.00
		0.920	5.44	15.00	15.64	16.31	16.86	18.00	18.83	19.89	21.44	35.00
	6 m	0.040	1.59	22.00	22.35	22.78	23.39	25.00	26.71	28.20	30.33	39.00
		0.920	4.12	18.00	18.35	19.01	19.63	21.00	22.77	24.01	25.68	39.00
	7 m	0.040	2.48	23.00	23.68	24.45	25.17	27.00	28.70	30.14	32.10	43.00
		0.920	3.35	20.00	20.52	21.22	21.84	23.00	25.70	27.13	28.98	38.00
	8 m	0.040	2.37	25.00	25.65	26.51	27.37	29.00	31.57	33.34	35.69	46.00
		0.920	2.79	18.00	19.06	19.75	20.55	22.00	24.35	25.70	27.53	39.00

Continued...

Data Set	x (m)	(y/d)	Cp (ppm)	T_L (s)	T_{1R} (s)	T_{2R} (s)	T_{3R} (s)	T_P (s)	T_{3F} (s)	T_{2F} (s)	T_{1F} (s)	T_T (s)
	9 m	0.040	2.44	28.00	28.62	29.45	30.25	32.00	34.31	35.87	38.16	49.00
		0.920	2.48	25.00	25.14	25.78	26.52	28.00	30.94	32.76	34.96	47.00
	9.9 m	0.040	2.11	29.00	30.03	30.85	31.76	34.00	36.34	38.10	40.46	55.00
		0.920	2.58	25.00	24.93	25.59	26.34	28.00	30.84	32.55	34.54	45.00
2CDSL21 (d = 0.134 m)	1 m	0.037	0.00	0.00	0.00	0.00	0.00	0.00	0.00	0.00	0.00	0.00
		0.500	2.28	8.00	8.38	8.94	9.47	10.00	11.85	12.77	14.04	23.00
		0.925	13.50	7.00	8.51	9.20	9.60	10.00	10.60	11.36	12.66	25.00
	2 m	0.037	0.09	11.00	11.06	11.63	12.25	13.00	14.31	14.87	15.88	18.00
		0.500	2.37	9.00	9.63	10.25	10.75	12.00	12.93	13.83	15.22	24.00
		0.925	9.80	9.00	9.27	9.56	9.86	11.00	12.00	12.89	14.15	24.00
	3 m	0.037	1.17	13.00	13.73	14.38	14.92	16.00	17.59	18.77	20.52	26.00
		0.500	3.00	12.00	11.76	12.35	12.86	14.00	15.22	16.15	17.44	27.00
		0.925	6.19	11.00	11.32	11.77	12.34	13.00	14.36	14.93	16.14	28.00
	4 m	0.037	1.31	15.00	15.68	16.35	16.90	18.00	19.56	20.82	22.48	30.00
		0.925	3.77	13.00	13.32	13.69	14.16	15.00	16.48	17.49	18.55	29.00
	5 m	0.037	1.80	16.00	17.05	17.67	18.35	20.00	21.38	22.62	24.41	34.00
		0.925	3.20	16.00	16.30	17.02	17.66	19.00	20.63	21.86	23.47	35.00
	6 m	0.037	2.25	19.00	19.43	20.11	20.56	21.00	23.66	24.99	26.91	38.00
		0.925	4.04	17.00	17.12	17.77	18.59	21.00	21.75	22.76	24.25	36.00
	7 m	0.037	2.21	20.00	21.35	22.11	22.80	24.00	26.20	27.58	29.56	37.00
		0.925	4.06	18.00	18.91	19.62	20.36	22.00	23.54	24.71	26.23	35.00
	8 m	0.037	1.99	24.00	25.38	26.22	26.91	28.00	30.65	32.08	34.02	43.00
		0.925	2.68	21.00	23.06	23.66	24.34	26.00	28.00	29.60	31.69	41.00
	9 m	0.037	2.21	28.00	28.25	29.13	29.98	32.00	34.34	35.82	37.86	48.00
		0.925	2.59	25.00	25.35	26.24	27.16	29.00	31.45	33.01	35.01	46.00
3CDCW1 (d = 0.115 m)	1 m	0.043	0.00	0.00	0.00	0.00	0.00	0.00	0.00	0.00	0.00	0.00
		0.913	6.41	7.00	7.89	8.41	8.86	10.00	10.95	11.85	13.14	23.00
	2 m	0.043	0.20	11.00	11.00	11.50	12.00	13.00	14.20	15.33	17.00	22.00
		0.913	5.23	9.00	9.37	9.94	10.47	11.00	12.69	13.56	14.75	25.00
	3 m	0.043	0.50	10.00	10.62	11.24	11.74	13.00	14.04	14.93	16.25	21.00
		0.913	5.05	10.00	10.78	11.35	11.82	13.00	13.98	14.88	16.16	25.00
	4 m	0.043	0.64	14.00	15.14	15.71	16.33	17.00	19.00	20.09	21.86	28.000
		0.913	3.88	12.00	12.97	13.47	13.96	15.00	16.16	17.04	18.36	25.000
	5 m	0.043	1.65	16.00	17.33	18.08	18.54	19.00	20.95	22.08	23.69	30.00
		0.913	3.79	13.00	14.04	14.78	15.41	16.00	16.73	18.62	19.83	32.00
		0.913	2.08	15.00	15.61	16.29	16.86	18.00	19.40	20.41	21.81	30.00
	6 m	0.043	1.75	20.00	20.69	21.42	22.09	24.00	25.36	26.57	28.18	35.000
		0.913	1.99	19.00	19.79	20.43	20.98	22.00	23.83	25.02	26.73	33.000
	7 m	0.043	1.59	18.00	18.57	20.24	20.93	23.00	24.52	25.79	27.60	38.00
		0.500	1.89	18.00	18.39	18.83	19.48	21.00	22.54	23.73	25.29	33.00
		0.913	2.18	17.00	17.01	17.66	18.41	20.00	21.40	22.47	23.89	31.00
	8 m	0.043	1.53	23.00	23.29	24.07	24.80	26.00	28.62	29.98	31.76	38.00
		0.913	1.65	19.00	20.20	20.86	21.58	23.00	25.97	27.94	28.95	37.00
3CDSL11 (d = 0.115 m)	1 m	0.043	0.00	0.00	0.00	0.00	0.00	0.00	0.00	0.00	0.00	0.00
		0.913	10.38	6.00	7.30	7.90	8.45	9.00	9.83	10.55	11.57	21.00
	2 m	0.043	0.09	12.00	11.56	12.10	12.55	13.00	15.13	16.17	16.92	18.00
		0.913	7.14	9.00	9.91	10.42	10.88	12.00	12.92	13.77	14.95	27.00
	3 m	0.043	0.56	13.00	12.33	12.92	13.46	14.00	16.00	17.09	18.50	25.00
		0.913	5.61	12.00	13.12	13.61	14.17	15.00	16.20	17.11	18.50	28.00
	4 m	0.043	1.26	14.00	14.36	15.02	15.60	17.00	18.25	19.38	20.97	29.00
		0.913	2.85	12.00	12.55	13.18	13.69	15.00	16.04	16.97	18.38	26.00
	5 m	0.043	1.67	15.00	15.31	15.88	16.46	18.00	19.06	20.05	21.84	32.00
		0.913	2.76	14.00	14.19	14.73	15.34	16.00	17.68	18.63	19.90	28.00
	6 m	0.043	1.70	18.00	18.22	18.81	19.46	21.00	22.47	23.75	25.58	34.00
		0.913	2.65	17.00	17.30	17.91	18.52	20.00	21.28	22.45	24.16	34.00
	7 m	0.043	2.50	19.00	19.62	20.30	20.87	22.00	23.70	24.94	26.67	35.00
		0.500	2.58	17.00	18.07	18.63	19.26	20.00	22.18	23.35	24.93	33.00
		0.913	2.38	18.00	18.39	19.05	19.64	21.00	22.42	23.60	25.18	35.00
	8 m	0.043	1.56	20.00	21.46	22.24	22.90	24.00	26.12	27.31	29.00	37.00
		0.500	2.32	19.00	19.12	19.66	20.33	22.00	23.25	24.27	25.70	36.00

Continued...

Data Set	x (m)	(y/d)	Cp (ppm)	T_L (s)	T_{1R} (s)	T_{2R} (s)	T_{3R} (s)	T_P (s)	T_{3F} (s)	T_{2F} (s)	T_{1F} (s)	T_T (s)
3CDSL12		0.913	2.31	19.00	19.06	19.61	20.23	21.00	23.16	24.27	25.45	35.00
(d = 0.115 m)	1 m	0.043	0.00	0.00	0.00	0.00	0.00	0.00	0.00	0.00	0.00	0.00
		0.913	8.59	10.00	10.68	11.32	11.85	13.00	13.58	14.20	14.92	29.00
	2 m	0.043	0.44	11.00	11.32	11.89	12.45	13.00	14.64	15.55	17.00	22.00
		0.913	5.37	8.00	9.02	9.52	10.05	11.00	12.34	13.27	14.47	25.00
	3 m	0.043	1.57	11.00	11.44	12.09	12.64	14.00	15.18	16.17	17.64	26.00
		0.913	4.57	10.00	10.24	10.79	11.38	12.00	13.84	14.79	16.06	26.00
	4 m	0.043	1.26	13.00	13.23	13.84	14.49	16.00	17.20	18.20	19.72	28.00
		0.913	4.08	11.00	11.52	12.21	12.79	14.00	15.50	16.52	17.82	25.00
	5 m	0.043	1.82	14.00	14.58	15.26	15.83	17.00	18.50	19.60	21.03	30.00
		0.913	3.03	14.00	14.24	14.96	15.72	17.00	18.76	19.83	21.20	29.00
	6 m	0.043	1.73	16.00	16.49	17.20	17.82	19.00	21.03	22.24	23.86	33.00
		0.913	2.29	15.00	15.00	15.59	16.28	18.00	20.37	21.56	23.03	31.00
	7 m	0.043	2.19	19.00	19.68	20.38	20.97	22.00	23.99	25.19	26.83	36.00
		0.500	2.64	18.00	18.81	19.47	20.07	21.00	22.91	24.09	25.74	38.00
		0.913	2.63	18.00	18.36	19.09	19.76	21.00	22.71	23.84	25.30	31.00
	8 m	0.043	1.97	20.00	20.55	21.28	21.91	23.00	25.30	26.53	28.09	37.00
		0.913	2.25	17.00	17.42	18.17	18.81	20.00	22.23	23.58	25.35	34.00
3CDSL13	1 m	0.043	0.00	0.00	0.00	0.00	0.00	0.00	0.00	0.00	0.00	0.00
(d = 0.115 m)		0.913	8.73	7.00	7.74	8.25	8.63	9.00	10.11	10.98	11.71	22.00
	2 m	0.043	0.28	11.00	11.31	11.85	12.42	13.00	14.71	15.71	17.33	20.00
		0.913	3.33	9.00	9.33	9.88	10.50	12.00	12.93	13.83	15.10	23.00
	3 m	0.043	0.61	11.00	11.16	11.72	12.34	13.00	14.87	15.90	17.47	22.00
		0.913	3.74	10.00	10.70	11.33	11.85	13.00	14.35	15.35	16.66	24.00
	4 m	0.043	1.27	12.00	12.63	13.30	13.85	15.00	16.28	17.25	18.77	25.00
		0.913	3.10	12.00	12.51	13.19	13.75	15.00	16.16	17.03	18.35	26.00
	5 m	0.043	1.06	15.00	15.52	16.26	16.87	18.00	19.80	20.96	22.65	28.00
		0.913	2.64	13.00	13.82	14.41	14.93	16.00	17.52	18.72	20.23	28.00
	6 m	0.043	1.51	18.00	18.20	18.88	19.61	21.00	22.99	24.29	25.96	32.00
		0.913	2.18	15.00	15.73	16.40	16.96	18.00	20.01	21.17	22.74	31.00
	7 m	0.043	2.21	18.00	18.84	19.62	20.42	22.00	23.71	24.94	26.63	35.00
		0.500	2.36	17.00	16.80	17.42	17.98	19.00	20.74	21.87	23.44	32.00
		0.913	2.51	15.00	15.47	16.15	16.71	18.00	19.42	20.54	21.89	28.00
	8 m	0.043	1.97	20.00	20.91	21.65	22.43	24.00	26.17	27.59	29.62	36.00
		0.500	2.07	18.00	18.53	19.24	19.84	21.00	21.96	23.12	24.59	33.00
		0.913	2.10	19.00	19.15	19.76	20.45	22.00	23.67	24.98	26.70	35.00
3CDSL14	1 m	0.043	0.00	0.00	0.00	0.00	0.00	0.00	0.00	0.00	0.00	0.00
(d = 0.115 m)		0.913	8.67	7.00	7.37	7.92	8.46	9.00	9.74	10.36	10.90	19.00
	2 m	0.043	0.57	9.00	9.24	9.79	10.38	11.00	12.51	13.37	14.53	17.00
		0.913	3.45	9.00	9.99	10.51	11.05	12.00	13.37	14.29	15.58	24.00
	3 m	0.043	1.51	11.00	11.87	12.47	13.03	14.00	15.74	16.77	18.28	26.00
		0.913	3.36	10.00	10.79	11.40	11.91	13.00	14.24	15.14	16.46	25.00
	4 m	0.043	1.57	12.00	12.78	13.40	13.94	15.00	16.69	17.72	19.18	27.00
		0.913	2.67	12.00	12.50	13.20	13.80	15.00	16.41	17.38	18.65	25.00
	5 m	0.043	1.55	14.00	14.74	15.39	15.93	17.00	18.67	19.83	21.25	27.00
		0.913	2.19	13.00	13.18	13.73	14.34	15.00	16.78	17.70	18.91	26.00
	6 m	0.043	1.48	16.00	16.62	17.32	17.92	19.00	21.00	22.00	23.45	29.00
		0.913	2.34	12.00	12.53	13.21	13.78	15.00	16.59	17.70	19.02	27.00
	7 m	0.043	1.53	19.00	19.51	20.27	20.94	23.00	24.51	25.67	27.34	34.00
		0.500	1.91	18.00	18.48	19.17	19.78	21.00	22.84	24.01	25.55	35.00
		0.913	1.85	18.00	18.32	18.99	19.64	21.00	22.54	23.72	25.39	32.00
	8 m	0.043	1.60	20.00	21.49	22.30	23.00	25.00	26.47	27.71	29.35	37.00
		0.500	2.07	19.00	20.04	20.80	21.61	23.00	25.04	26.19	27.66	34.00
		0.913	1.90	16.00	16.33	17.04	17.72	19.00	20.98	22.24	23.72	31.00
	9 m	0.043	1.48	21.00	20.79	21.43	22.03	23.00	25.35	26.63	28.43	34.00
		0.913	1.85	20.00	20.31	21.02	21.78	24.00	26.09	27.37	28.82	36.00
3CDSL15	1 m	0.043	0.00	0.00	0.00	0.00	0.00	0.00	0.00	0.00	0.00	0.00
(d = 0.115)		0.913	9.16	7.00	7.68	8.22	8.61	9.00	9.62	10.36	11.53	24.00
	2 m	0.043	0.28	11.00	11.00	11.54	12.12	13.00	14.38	15.40	17.33	22.00
		0.913	4.03	9.00	10.44	11.04	11.54	13.00	13.95	14.95	16.48	27.00

Continued....

Data Set	x (m)	(y/d)	Cp (ppm)	T_L (s)	T_{1R} (s)	T_{2R} (s)	T_{3R} (s)	T_P (s)	T_{3F} (s)	T_{2F} (s)	T_{1F} (s)	T_T (s)
	3 m	0.043	0.46	11.00	11.63	12.27	12.80	14.00	15.35	16.38	19.13	24.00
		0.913	4.92	10.00	10.36	10.92	11.46	12.00	13.71	14.60	16.37	25.00
	4 m	0.043	0.86	12.00	13.01	13.61	14.26	15.00	16.93	17.95	19.41	27.00
		0.913	3.40	11.00	12.30	12.87	13.43	14.00	15.83	16.71	17.90	27.00
	5 m	0.043	1.07	15.00	15.51	16.21	16.81	18.00	19.68	20.85	22.52	27.00
		0.913	2.72	13.00	13.83	14.48	15.08	16.00	17.54	18.46	19.68	29.00
	6 m	0.043	1.28	16.00	17.15	17.83	18.55	20.00	21.26	22.24	23.56	30.00
		0.913	2.41	15.00	15.50	16.17	16.71	18.00	19.17	20.20	21.71	30.00
	7 m	0.043	1.43	18.00	18.62	19.34	19.95	21.00	23.16	24.40	26.10	31.00
		0.913	2.32	16.00	16.84	17.49	18.09	19.00	21.02	22.11	23.63	34.00
	8 m	0.043	1.28	17.00	20.85	22.29	22.74	24.00	26.04	27.22	28.93	37.00
		0.500	1.91	16.00	17.36	17.99	18.60	20.00	22.11	22.63	23.49	29.00
		0.913	2.13	17.00	17.40	18.08	18.68	21.00	21.51	22.05	23.28	32.00
	9 m	0.043	1.36	20.00	21.06	21.77	22.52	24.00	25.53	26.71	28.13	34.00
		0.913	1.98	18.00	18.70	19.25	19.63	20.00	20.92	22.03	23.52	28.00
3CDSL16 (d = 0.115 m)	1 m	0.04	0.00	0.00	0.00	0.00	0.00	0.00	0.00	0.00	0.00	0.00
		0.91	7.74	7.00	7.36	7.91	8.45	9.00	9.69	10.56	11.83	22
	2 m	0.043	0.14	10.00	10.17	11.20	11.90	13.00	14.50	15.67	17.75	20.00
		0.913	6.61	8.00	9.23	9.75	10.34	11.00	11.61	12.36	13.60	22.00
	3 m	0.043	0.66	12.00	11.79	12.37	12.89	14.00	15.50	16.64	18.10	26.00
		0.913	4.13	11.00	11.74	12.35	12.85	14.00	15.19	16.12	17.44	25.00
	4 m	0.043	1.05	13.00	14.49	15.24	15.85	17.00	18.51	19.59	21.07	27.00
		0.913	3.28	12.00	12.76	13.37	13.89	15.00	16.36	17.32	18.61	27.00
	5 m	0.043	1.65	14.00	15.15	15.70	16.31	17.00	18.86	19.85	21.25	31.00
		0.913	2.91	12.00	12.38	13.00	13.55	15.00	16.09	17.08	18.43	25.00
	6 m	0.043	2.52	16.00	17.26	17.95	18.62	20.00	21.56	22.72	24.31	33.00
		0.913	2.27	13.00	15.14	15.70	16.32	17.00	19.18	20.24	21.64	27.00
	7 m	0.043	1.39	19.00	20.04	20.73	21.51	23.00	25.11	26.38	28.04	36.00
		0.913	1.69	18.00	18.36	19.10	19.79	21.00	23.39	24.63	26.12	32.00
	8 m	0.043	1.37	21.00	21.68	22.48	23.25	25.00	26.68	27.94	29.72	38.00
		0.913	1.51	19.00	18.74	19.37	19.94	21.00	23.20	24.38	26.09	33.00
	9 m	0.043	1.14	21.00	21.19	21.97	22.74	24.00	26.51	27.94	29.82	36.00
		0.913	1.14	20.00	20.36	21.06	21.73	23.00	24.98	26.22	27.90	36.00
3CDSL17 (d = 0.115 m)	1 m	0.043	0.00	0.00	0.00	0.00	0.00	0.00	0.00	0.00	0.00	0.00
		0.913	10.15	7.00	8.23	8.77	9.37	10.00	10.65	11.42	12.55	24.00
	2 m	0.043	0.92	11.00	11.30	11.92	12.47	13.00	14.68	15.71	17.18	23.00
		0.913	7.04	9.00	9.70	10.51	11.26	12.00	13.02	13.89	15.07	25.00
	3 m	0.043	1.43	12.00	12.51	13.19	13.73	15.00	16.24	17.29	18.76	26.00
		0.913	6.36	11.00	11.19	11.72	12.32	13.00	14.60	15.52	16.75	24.00
	4 m	0.043	1.53	12.00	12.17	12.73	13.35	15.00	16.18	17.18	18.61	25.00
		0.913	5.32	11.00	11.80	12.41	12.94	14.00	15.39	16.33	17.59	29.00
	5 m	0.043	1.32	14.00	14.70	15.37	15.92	17.00	18.66	19.82	21.47	29.00
		0.913	3.79	12.00	12.31	12.93	13.50	15.00	15.98	16.89	18.15	29.00
	6 m	0.043	2.09	15.00	16.35	17.03	17.64	19.00	20.34	21.48	22.99	33.00
		0.913	3.28	16.00	16.69	17.43	18.11	20.00	21.12	22.12	23.50	33.00
	7 m	0.043	1.93	19.00	19.08	19.73	20.44	22.00	23.49	24.65	26.26	34.00
		0.500	3.30	17.00	17.88	18.58	19.33	21.00	22.40	23.51	24.95	31.00
		0.913	3.20	17.00	17.34	17.99	18.63	20.00	21.74	22.97	24.52	33.00
	8 m	0.043	2.27	21.00	21.48	22.26	22.93	24.00	26.30	27.52	29.31	39.00
		0.913	3.05	18.00	20.05	20.84	21.68	23.00	25.11	26.26	27.74	41.00
	9 m	0.043	2.03	23.00	23.45	24.39	25.27	27.00	28.74	30.02	31.73	37.00
		0.913	2.77	20.00	20.34	21.07	21.77	23.00	25.50	26.72	28.27	35.00
3CDSL19 (d = 0.115 m)	1 m	0.043	0.17	10.00	11.21	11.92	12.47	13.00	13.61	14.75	16.38	18.00
		0.913	47.77	7.00	7.75	8.27	8.64	9.00	9.54	10.25	11.71	26.00
	2 m	0.043	1.89	11.00	11.78	12.41	12.93	14.00	15.52	16.72	18.60	25.00
		0.913	38.49	9.00	9.54	10.13	10.56	11.00	11.84	12.72	13.92	25.00
	3 m	0.043	2.45	13.00	12.89	13.47	14.03	15.00	16.69	17.82	19.53	28.00
		0.913	26.42	10.00	11.30	11.88	13.19	14.00	14.92	15.80	16.98	29.00
	4 m	0.043	6.09	15.00	15.69	16.42	17.06	18.00	20.06	21.17	22.79	33.00
		0.913	15.04	13.00	13.82	14.44	14.99	16.00	17.56	18.51	19.75	28.00

Continued....

Data Set	x (m)	(y/d)	Cp (ppm)	T_L (s)	T_{1R} (s)	T_{2R} (s)	T_{3R} (s)	T_P (s)	T_{3F} (s)	T_{2F} (s)	T_{1F} (s)	T_T (s)
	5 m	0.043	4.40	14.00	14.44	15.14	15.73	17.00	18.39	19.59	21.38	33.00
		0.913	15.19	11.00	11.96	12.51	13.06	14.00	15.60	16.63	18.00	27.00
	6 m	0.043	11.20	17.00	17.81	18.45	19.01	20.00	21.72	22.81	24.35	34.00
		0.913	16.62	15.00	15.98	16.52	17.10	18.00	19.72	20.77	22.13	31.00
	7 m	0.043	12.18	19.00	19.56	20.31	20.94	22.00	24.20	25.34	26.85	37.00
		0.913	13.00	16.00	16.70	17.37	17.93	19.00	21.12	22.31	23.81	32.00
	8 m	0.043	9.22	20.00	20.84	21.58	22.35	24.00	25.81	27.06	28.66	39.00
		0.913	11.27	18.00	18.53	19.27	19.90	21.00	23.12	24.24	25.67	36.00
	9 m	0.043	9.85	21.00	22.61	23.36	24.00	26.00	27.58	28.92	30.84	39.00
		0.913	10.28	19.00	19.62	20.32	20.90	22.00	24.20	25.49	27.04	36.00
3CDSL110 (d = 0.115 m)	1 m	0.043	0.00	0.00	0.00	0.00	0.00	0.00	0.00	0.00	0.00	0.00
		0.913	32.82	7.00	7.33	7.85	8.42	9.00	10.38	11.19	12.30	28.00
	2 m	0.043	1.88	10.00	10.59	11.18	11.70	13.00	14.08	14.96	16.36	21.00
		0.913	25.39	8.00	8.70	9.23	9.62	10.00	12.54	13.25	14.32	25.00
	3 m	0.043	8.67	12.00	12.16	12.70	13.31	14.00	15.74	17.43	18.09	30.00
		0.913	21.91	9.00	11.16	11.69	12.29	13.00	14.47	15.38	16.60	27.00
	4 m	0.043	7.76	14.00	14.79	15.41	15.94	17.00	18.40	19.49	20.97	30.00
		0.913	20.36	12.00	12.46	13.08	13.59	15.00	15.88	16.74	17.88	25.00
	5 m	0.043	9.90	16.00	16.37	17.08	17.71	19.00	20.59	21.75	23.43	33.00
		0.913	18.17	13.00	13.56	14.18	14.68	16.00	16.98	17.85	19.00	26.00
	6 m	0.043	9.21	16.00	16.39	17.10	17.72	19.00	20.46	21.55	22.98	30.00
		0.913	13.03	14.00	15.04	15.56	16.14	17.00	18.63	19.60	20.84	28.00
	7 m	0.043	9.69	17.00	18.15	18.75	19.41	21.00	22.20	23.25	24.70	33.00
		0.913	12.40	16.00	17.23	17.82	18.45	20.00	21.15	22.17	23.56	34.00
	8 m	0.043	9.63	20.00	21.11	21.84	22.61	24.00	26.14	27.46	29.07	37.00
		0.913	10.94	17.00	18.39	19.10	19.75	21.00	23.25	24.52	27.11	38.00
	9 m	0.043	9.74	21.00	22.31	23.09	23.80	25.00	27.21	28.48	30.07	38.00
		0.913	9.12	19.00	19.73	20.48	21.25	23.00	25.37	26.71	28.37	34.00
3CDSL111 (d = 0.115 m)	1 m	0.043	0.00	0.00	0.00	0.00	0.00	0.00	0.00	0.00	0.00	0.00
		0.913	37.72	7.00	7.47	8.25	8.63	9.00	10.02	10.79	11.87	24.00
	2 m	0.043	1.24	10.00	10.22	10.78	11.38	12.00	13.53	14.41	15.63	21.00
		0.913	24.72	9.00	9.93	10.48	11.00	12.00	13.19	13.97	15.06	26.00
	3 m	0.043	4.76	11.00	11.48	12.11	12.63	14.00	15.02	15.90	17.14	24.00
		0.913	20.11	8.00	8.42	9.02	9.52	11.00	11.73	12.51	13.57	25.00
	4 m	0.043	4.75	13.00	13.98	14.54	15.15	16.00	17.77	18.84	20.31	27.00
		0.913	13.22	11.00	11.52	12.13	12.63	14.00	14.85	15.68	16.80	26.00
	5 m	0.043	8.46	16.00	16.20	16.80	18.40	19.00	20.22	21.26	22.74	29.00
		0.913	15.97	14.00	13.57	14.13	14.62	16.00	16.91	17.78	18.95	30.00
	6 m	0.043	8.21	16.00	16.86	17.49	19.08	20.00	21.11	22.15	23.63	34.00
		0.913	10.57	14.00	15.23	15.78	16.38	18.00	19.23	20.33	21.75	33.00
	7 m	0.043	8.97	18.00	18.94	19.69	20.47	22.00	23.64	24.85	26.33	36.00
		0.913	10.11	16.00	16.78	17.44	18.00	19.00	21.13	22.17	23.60	33.00
	8 m	0.043	7.76	20.00	20.54	21.33	22.01	24.00	25.49	26.77	28.40	38.00
		0.500	9.08	18.00	19.06	19.68	20.38	22.00	23.39	24.48	25.84	34.00
		0.913	10.44	17.00	17.04	17.71	18.49	20.00	21.91	22.98	24.39	36.00
	9 m	0.043	6.91	21.00	22.29	23.10	23.82	25.00	27.20	28.44	30.02	36.00
		0.913	8.98	20.00	20.80	21.43	21.98	23.00	24.93	26.22	27.87	38.00
3CDSL112 (d = 0.115 m)	1 m	0.043	0.00	0.00	0.00	0.00	0.00	0.00	0.00	0.00	0.00	0.00
		0.913	35.88	6.00	7.26	8.01	8.51	9.00	11.90	10.44	9.66	23.00
	2 m	0.043	0.46	10.00	10.06	10.50	10.94	12.00	13.13	14.07	14.83	17.00
		0.913	29.69	8.00	8.28	8.81	9.39	10.00	10.58	11.26	12.44	28.00
	3 m	0.043	0.65	12.00	12.22	12.78	13.37	14.00	15.96	16.97	19.25	23.00
		0.913	21.83	9.00	9.99	10.49	10.98	12.00	13.13	13.95	15.08	25.00
	4 m	0.043	4.14	14.00	14.31	14.89	15.49	17.00	18.09	19.06	20.42	27.00
		0.913	15.39	12.00	12.87	13.46	13.99	15.00	16.46	17.42	18.66	25.00
	5 m	0.043	5.99	15.00	15.89	16.50	17.09	18.00	19.64	20.71	22.16	29.00
		0.913	13.39	14.00	14.16	14.70	15.31	16.00	17.73	18.66	19.86	30.00
	6 m	0.043	8.25	16.00	16.31	16.95	17.58	19.00	20.38	21.52	23.00	32.00
		0.913	13.09	15.00	16.12	16.69	17.32	19.00	20.17	21.16	22.52	29.00
	7 m	0.043	8.42	17.00	17.28	17.97	18.64	20.00	21.56	22.69	24.12	31.00

Continued....

Data Set	x (m)	(y/d)	Cp (ppm)	T_L (s)	T_{1R} (s)	T_{2R} (s)	T_{3R} (s)	T_P (s)	T_{3F} (s)	T_{2F} (s)	T_{1F} (s)	T_T (s)
		0.913	10.83	17.00	17.55	18.23	18.81	20.00	21.89	23.01	24.47	33.00
	8 m	0.043	6.78	21.00	21.50	22.28	22.95	24.00	26.24	27.35	28.85	35.00
		0.913	9.95	18.00	18.55	19.30	19.94	22.00	23.37	24.44	25.75	42.00
	9 m	0.043	7.76	22.00	22.71	23.47	24.19	26.00	27.50	28.77	30.54	40.00
		0.913	9.41	21.00	21.22	21.85	22.53	24.00	25.83	27.26	29.02	40.00
3CDCW2 (d = 0.15 m)	1 m	0.033	0.00	0.00	0.00	0.00	0.00	0.00	0.00	0.00	0.00	0.00
		0.933	35.35	7.00	8.01	8.34	8.67	9.00	9.61	10.33	11.48	25.00
	2 m	0.033	0.35	10.00	10.55	11.09	11.64	13.00	14.11	15.83	17.13	18.00
		0.933	25.48	8.00	8.64	10.04	10.52	11.00	11.85	12.70	13.87	25.00
	3 m	0.033	2.80	12.00	12.49	13.12	13.64	15.00	16.00	16.91	18.46	29.00
		0.933	21.11	10.00	11.15	11.65	12.23	13.00	14.21	14.99	16.12	27.00
	4 m	0.033	3.41	13.00	13.44	14.05	14.60	16.00	17.22	18.23	19.46	24.00
		0.933	15.19	11.00	11.66	12.28	12.77	14.00	15.06	15.91	17.12	29.00
	5 m	0.033	5.68	15.00	15.49	16.14	16.70	18.00	19.28	20.34	21.77	30.00
		0.933	13.67	12.00	12.69	13.33	13.87	15.00	16.29	17.23	18.46	29.00
	6 m	0.033	7.79	16.00	16.15	16.74	17.37	19.00	20.19	21.25	22.72	35.00
		0.933	12.07	14.00	14.63	15.29	15.83	17.00	18.60	19.73	21.18	32.00
	7 m	0.033	8.21	18.00	18.97	19.65	20.40	22.00	23.50	24.64	26.21	36.00
		0.933	11.08	15.00	16.39	17.04	17.63	19.00	20.27	21.31	22.70	35.00
	8 m	0.033	8.41	19.00	19.50	20.25	20.89	22.00	24.03	25.19	26.71	35.00
		0.933	9.63	18.00	18.37	19.03	19.66	21.00	22.45	23.50	24.86	37.00
	9 m	0.033	6.21	20.00	22.21	22.94	23.70	25.00	27.61	28.93	30.63	40.00
		0.933	9.05	19.00	20.04	20.62	21.26	22.00	23.46	24.53	25.89	35.00
3CDSL21 (d = 0.15 m)	1 m	0.033	0.00	0.00	0.00	0.00	0.00	0.00	0.00	0.00	0.00	0.00
		0.933	31.98	7.00	7.32	7.85	8.42	9.00	10.38	11.18	12.35	21.00
	2 m	0.033	2.86	10.00	10.45	11.04	11.55	13.00	13.98	14.92	16.33	22.00
		0.933	19.45	9.00	9.10	9.59	10.13	11.00	12.11	12.86	13.90	19.00
	3 m	0.033	4.03	13.00	13.70	14.36	14.91	16.00	17.63	18.79	20.42	27.00
		0.933	14.06	10.00	10.16	10.67	11.25	12.00	13.32	14.17	15.32	27.00
	4 m	0.033	3.35	13.00	13.61	14.32	14.90	16.00	17.58	18.59	19.87	31.00
		0.933	13.41	11.00	12.02	12.54	13.10	14.00	15.40	16.27	17.41	33.00
3CDSL22 (d = 0.15 m)	1 m	0.033	0.00	0.00	0.00	0.00	0.00	0.00	0.00	0.00	0.00	0.00
		0.933	29.82	7.00	7.56	8.15	8.57	9.00	9.76	10.57	11.70	26.00
	2 m	0.033	0.48	10.00	11.27	11.82	12.40	13.00	14.33	14.78	16.38	19.00
		0.933	24.61	8.00	8.38	8.96	9.48	10.00	10.72	11.52	12.64	28.00
	3 m	0.033	1.68	11.00	11.46	12.14	12.73	14.00	15.46	16.44	17.59	25.00
		0.933	15.67	10.00	10.38	10.94	11.47	12.00	13.62	14.47	15.64	30.00
	4 m	0.033	4.87	13.00	13.30	13.93	14.54	16.00	17.24	18.30	19.73	29.00
		0.933	14.78	11.00	11.39	11.96	12.48	13.00	14.72	15.57	16.73	30.00
	5 m	0.033	4.37	14.00	14.57	15.23	15.78	17.00	18.30	19.23	20.56	31.00
		0.500	10.50	13.00	13.52	14.16	14.69	16.00	17.15	18.11	19.45	30.00
		0.933	12.32	12.00	13.20	13.77	14.37	15.00	16.88	17.78	18.98	27.00
	6 m	0.033	5.05	17.00	17.20	17.76	18.36	19.00	21.04	22.07	23.52	32.00
		0.500	8.49	14.00	15.13	15.68	17.29	18.00	18.95	19.87	21.12	29.00
		0.933	11.22	16.00	16.76	17.36	17.87	19.00	20.40	21.37	22.66	33.00
	7 m	0.033	8.49	19.00	19.48	20.15	20.76	22.00	23.50	24.54	25.89	33.00
		0.500	8.57	17.00	17.63	18.31	18.87	20.00	21.48	22.56	23.97	36.00
		0.933	11.51	17.00	17.18	17.74	18.34	19.00	20.98	21.92	23.24	34.00
	8 m	0.033	6.25	20.00	21.01	21.73	22.53	24.00	25.79	27.00	28.72	41.00
		0.500	9.74	19.00	19.56	20.25	20.82	22.00	23.52	24.63	26.05	43.00
		0.933	9.58	18.00	18.47	19.14	19.72	21.00	22.37	23.40	24.73	37.00
3CDSL23 (d = 0.15 m)	1 m	0.033	0.00	0.00	0.00	0.00	0.00	0.00	0.00	0.00	0.00	0.00
		0.933	30.00	7.00	7.41	7.97	8.49	9.00	9.64	10.39	11.52	22.00
	2 m	0.033	0.96	9.00	9.58	10.39	10.98	12.00	13.18	13.88	15.00	24.00
		0.933	28.24	9.00	9.19	9.70	10.29	11.00	11.52	12.09	13.26	26.00
	3 m	0.033	1.44	10.00	10.49	10.97	11.67	13.00	13.92	14.79	16.00	21.00
		0.933	20.75	11.00	11.18	11.97	12.49	13.00	13.47	13.94	15.36	30.00
	4 m	0.033	1.82	14.00	14.27	14.77	15.35	16.00	17.68	18.86	20.73	27.00
		0.933	15.10	11.00	11.42	12.00	12.50	13.00	14.67	15.49	16.62	33.00

Continued....

Data Set	x (m)	(y/d)	Cp (ppm)	T_L (s)	T_{1R} (s)	T_{2R} (s)	T_{3R} (s)	T_P (s)	T_{3F} (s)	T_{2F} (s)	T_{1F} (s)	T_T (s)
	5 m	0.033	5.35	15.00	15.62	16.38	17.02	18.00	20.19	21.10	22.44	35.00
		0.933	10.87	13.00	14.00	14.52	15.07	16.00	17.39	18.31	19.56	32.00
	6 m	0.033	5.31	17.00	17.85	18.46	19.00	20.00	21.64	22.71	24.23	33.00
		0.933	10.68	15.00	15.80	16.44	16.99	18.00	19.90	20.93	22.30	31.00
	7 m	0.033	5.88	18.00	18.73	19.55	20.28	21.00	22.38	23.66	25.54	34.00
		0.933	8.77	16.00	16.73	17.39	17.94	19.00	20.72	21.74	23.07	37.00
	8 m	0.033	5.26	20.00	21.68	22.40	22.99	24.00	26.20	27.42	29.26	39.00
		0.933	9.12	18.00	18.80	19.48	20.11	21.00	23.01	24.02	25.49	39.00
3CDSL24 (d = 0.15 m)	1 m	0.033	0.00	0.00	0.00	0.00	0.00	0.00	0.00	0.00	0.00	0.00
		0.933	35.97	7.00	7.40	7.94	8.47	9.00	9.35	9.70	10.29	22.00
	2 m	0.033	0.43	11.00	10.54	11.12	11.94	13.00	13.63	14.75	19.04	21.00
		0.933	25.93	8.00	8.80	10.02	10.51	11.00	11.64	12.42	13.78	25.00
	3 m	0.033	3.26	11.00	11.05	11.56	12.12	13.00	14.53	15.51	16.82	25.00
		0.933	15.86	10.00	10.40	11.01	11.54	13.00	13.90	14.78	15.98	29.00
	4 m	0.033	5.84	13.00	14.80	15.46	16.07	17.00	18.80	19.92	21.52	30.00
		0.933	13.35	12.00	12.57	13.19	13.69	15.00	15.99	16.83	17.96	25.00
	5 m	0.033	6.00	15.00	15.12	15.67	16.28	17.00	18.80	19.88	21.27	27.00
		0.933	11.39	14.00	14.23	14.86	15.51	17.00	18.09	19.00	20.39	31.00
	6 m	0.033	6.59	17.00	17.26	17.87	18.50	20.00	21.15	22.11	23.38	29.00
		0.500	8.23	16.00	16.48	17.16	17.74	19.00	20.45	21.53	22.99	33.00
		0.933	8.34	15.00	14.79	15.61	17.07	18.00	19.13	20.22	21.72	30.00
	7 m	0.033	5.55	18.00	18.91	19.51	20.10	21.00	22.96	24.04	25.55	31.00
		0.500	8.72	17.00	17.63	18.29	18.84	20.00	21.44	22.48	23.87	32.00
		0.933	9.50	16.00	17.17	17.76	18.39	20.00	21.10	22.10	23.46	41.00
	8 m	0.033	7.73	20.00	20.67	21.42	22.09	24.00	25.27	26.40	27.86	36.00
		0.933	7.84	18.00	19.37	20.06	20.68	22.00	23.36	24.41	25.82	38.00
	9 m	0.033	6.67	21.00	21.23	21.91	22.57	24.00	25.26	26.34	27.80	37.00
		0.933	8.75	20.00	20.31	21.00	21.65	23.00	24.14	25.61	27.10	39.00
3CDSL25 (d = 0.15 m)	1 m	0.033	0.00	0.00	0.00	0.00	0.00	0.00	0.00	0.00	0.00	0.00
		0.933	30.71	7.00	7.12	7.59	8.13	9.00	9.46	9.91	10.97	22.00
	2 m	0.033	1.24	17.00	10.24	10.76	11.35	12.00	13.49	14.57	16.07	19.00
		0.933	23.10	9.00	9.33	9.72	10.22	11.00	11.78	13.29	14.44	25.00
	3 m	0.033	2.52	12.00	11.66	12.27	12.81	14.00	15.27	16.14	17.45	21.00
		0.933	18.29	10.00	10.53	11.24	12.14	13.00	14.40	15.05	16.09	29.00
	4 m	0.033	4.86	13.00	13.84	14.45	14.99	16.00	17.44	18.46	19.92	28.00
		0.933	15.75	11.00	11.79	12.39	12.91	14.00	15.16	15.98	17.11	29.00
	5 m	0.033	5.16	15.00	15.27	15.97	16.84	18.00	18.72	19.77	21.18	29.00
		0.500	8.84	13.00	13.51	14.14	14.66	16.00	16.94	17.78	18.93	26.00
		0.933	14.17	13.00	13.02	13.52	14.02	15.00	16.23	17.09	18.28	30.00
	6 m	0.033	6.33	16.00	16.46	17.16	17.76	19.00	20.46	21.59	22.94	32.00
		0.500	10.55	15.00	16.00	16.50	16.99	18.00	19.21	20.07	21.24	27.00
		0.933	12.19	14.00	14.55	15.23	15.80	17.00	18.32	19.16	20.63	32.00
	7 m	0.033	4.61	18.00	18.28	18.89	19.53	21.00	22.30	23.34	24.79	31.00
		0.500	8.87	16.00	16.46	17.12	17.68	19.00	20.25	21.53	22.76	31.00
		0.933	10.72	16.00	16.50	17.18	17.75	19.00	20.40	21.44	22.78	37.00
	8 m	0.033	4.56	19.00	19.58	20.31	20.93	22.00	24.29	25.35	26.62	38.00
		0.500	8.97	18.00	18.63	19.31	19.87	21.00	22.58	23.66	25.04	35.00
		0.933	9.07	17.00	17.68	18.33	18.87	20.00	21.96	22.66	23.76	36.00
	9 m	0.033	4.91	22.00	22.51	23.35	24.11	26.00	27.55	28.80	30.59	37.00
		0.933	9.05	19.00	19.85	20.48	21.07	22.00	24.17	25.32	26.91	40.00
3CDSL26 (d = 0.15 m)	1 m	0.033	0.00	0.00	0.00	0.00	0.00	0.00	0.00	0.00	0.00	0.00
		0.933	30.14	7.00	7.18	7.45	7.73	8.00	8.98	9.73	11.30	23.00
	2 m	0.033	1.71	10.00	10.22	10.67	12.21	13.00	13.72	14.52	15.57	18.00
		0.933	19.76	10.00	10.41	11.08	12.27	13.00	13.51	14.18	16.08	30.00
	3 m	0.033	1.35	13.00	13.06	13.60	14.20	15.00	16.61	17.54	18.87	21.00
		0.933	18.12	10.00	10.37	10.96	11.75	13.00	13.78	14.61	15.73	29.00
	4 m	0.033	4.54	13.00	13.12	13.71	14.36	16.00	17.14	18.10	19.64	27.00
		0.933	15.15	12.00	12.63	13.27	13.78	15.00	15.99	16.80	17.93	26.00
	5 m	0.033	5.04	15.00	16.04	16.61	17.24	18.00	20.18	21.22	22.67	36.00
		0.500	8.86	14.00	14.52	15.17	15.69	17.00	18.01	18.89	20.12	28.00

Continued....

Data Set	x (m)	(y/d)	Cp (ppm)	T_L (s)	T_{1R} (s)	T_{2R} (s)	T_{3R} (s)	T_P (s)	T_{3F} (s)	T_{2F} (s)	T_{1F} (s)	T_T (s)
		0.933	16.20	14.00	14.67	15.32	15.85	17.00	18.16	18.98	20.11	31.00
	6 m	0.033	5.84	18.00	19.03	19.65	20.33	22.00	23.25	24.31	25.85	34.00
		0.500	9.48	15.00	15.35	15.98	16.56	18.00	19.09	19.99	21.25	30.00
		0.933	10.07	15.00	15.79	16.41	16.94	18.00	19.29	20.23	21.50	29.00
	7 m	0.033	5.05	18.00	18.85	19.54	20.22	22.00	23.26	24.38	25.82	31.00
		0.500	8.57	17.00	17.54	18.18	18.71	20.00	21.13	22.02	23.33	32.00
		0.933	9.63	17.00	17.71	18.73	19.43	20.00	21.62	22.56	23.82	35.00
	8 m	0.033	5.81	21.00	21.36	22.16	22.85	24.00	26.02	27.10	28.57	37.00
		0.500	7.71	19.00	19.35	20.02	20.64	22.00	22.68	23.59	24.98	33.00
		0.933	9.24	18.00	18.91	19.50	20.08	21.00	22.68	23.69	24.93	38.00
	9 m	0.033	5.54	22.00	22.27	23.00	23.74	25.00	27.16	28.33	30.11	36.00
		0.933	7.49	20.00	20.62	21.27	21.82	23.00	24.56	25.74	27.40	37.00
4CDCW1	1 m	0.040	0.00	0.00	0.00	0.00	0.00	0.00	0.00	0.00	0.00	0.00
(d = 0.128 m)		0.922	51.25	6.00	7.00	7.47	7.94	9.00	9.94	10.75	11.86	26.00
	2 m	0.040	0.27	11.00	10.84	11.37	11.82	13.00	14.25	17.50	19.63	23.00
		0.500	13.61	10.00	10.13	10.64	11.22	12.00	13.39	14.36	15.67	26.00
		0.922	29.22	9.00	9.49	10.12	10.64	12.00	12.94	13.81	14.99	29.00
	3 m	0.040	3.76	12.00	12.50	13.16	13.72	15.00	16.12	17.07	18.69	28.00
		0.500	8.23	12.00	12.26	12.81	13.39	14.00	15.69	16.64	17.92	29.00
		0.922	32.32	11.00	11.28	11.80	12.38	13.00	14.47	15.39	16.66	27.00
	4 m	0.040	4.00	14.00	14.07	14.60	15.19	16.00	17.57	18.63	20.08	26.00
		0.500	14.60	13.00	13.10	13.61	14.18	15.00	16.44	17.40	18.70	28.00
		0.922	20.72	13.00	13.17	13.67	14.26	15.00	16.46	17.44	18.72	32.00
	5 m	0.040	7.21	15.00	16.52	17.21	17.77	19.00	20.41	21.53	23.17	33.00
		0.500	14.86	14.00	14.52	15.15	15.68	17.00	18.10	19.03	20.41	31.00
		0.922	16.77	14.00	14.02	14.53	15.08	16.00	17.53	18.59	20.01	36.00
	6 m	0.040	8.17	16.00	16.55	17.26	17.85	19.00	20.68	21.89	23.61	36.00
		0.500	12.97	16.00	16.39	17.06	17.63	19.00	20.08	21.04	23.41	29.00
		0.922	14.26	15.00	15.31	15.87	16.43	17.00	18.98	19.99	21.49	38.00
	7 m	0.040	9.12	19.00	19.22	19.75	20.80	23.00	24.30	25.48	26.99	38.00
		0.500	10.98	17.00	17.47	18.16	18.76	20.00	20.74	21.74	23.15	34.00
		0.922	10.27	18.00	17.80	19.11	19.56	20.00	22.46	23.45	24.91	38.00
	8 m	0.040	8.39	21.00	21.98	22.69	23.48	25.00	26.91	28.18	29.90	42.00
		0.500	11.93	19.00	19.50	20.20	20.79	22.00	23.62	24.75	26.25	40.00
		0.922	12.12	19.00	20.15	20.78	21.48	23.00	24.60	25.80	27.31	35.00
	9 m	0.040	9.38	23.00	23.58	24.37	25.05	27.00	28.40	29.60	31.26	43.00
		0.500	9.85	21.00	21.77	22.49	23.18	25.00	26.48	27.66	29.25	43.00
		0.922	10.94	22.00	22.99	23.58	24.23	26.00	27.42	28.55	30.10	43.00
4CDSL11	1 m	0.040	0.00	0.00	0.00	0.00	0.00	0.00	0.00	0.00	0.00	0.00
(d = 0.128 m)		0.922	26.17	8.00	8.28	8.80	9.38	10.00	11.39	12.23	13.44	28.00
	2 m	0.040	0.21	10.00	10.03	10.69	11.34	12.00	13.81	17.37	19.75	23.00
		0.500	6.49	9.00	9.23	9.80	10.39	11.00	12.60	13.52	14.83	27.00
		0.922	16.86	9.00	9.20	9.69	10.27	11.00	12.16	12.96	14.10	33.00
	3 m	0.040	2.38	12.00	12.23	12.78	13.37	14.00	16.07	17.02	18.30	28.00
		0.500	6.17	11.00	11.45	12.04	12.54	14.00	14.83	15.72	16.95	29.00
		0.922	9.58	10.00	10.51	11.17	11.72	13.00	14.09	14.99	16.47	28.00
	4 m	0.040	2.38	13.00	13.70	14.34	14.88	16.00	17.45	18.48	19.82	26.00
		0.500	9.72	13.00	13.35	13.95	14.50	16.00	16.94	17.88	19.21	25.00
		0.922	9.32	12.00	12.98	13.46	13.94	15.00	16.08	16.99	18.47	29.00
	5 m	0.040	3.24	16.00	16.94	17.57	18.22	20.00	21.20	22.24	23.61	30.00
		0.500	7.02	13.00	13.51	14.20	14.81	16.00	17.90	19.06	19.93	28.00
		0.922	8.78	15.00	16.13	16.62	17.19	18.00	18.98	19.96	21.38	28.00
	6 m	0.040	5.21	17.00	18.17	18.86	19.56	21.00	22.49	23.70	25.33	34.00
		0.500	6.99	16.00	16.49	17.19	17.80	19.00	20.95	23.08	23.93	33.00
		0.922	9.01	14.00	14.83	15.42	15.93	17.00	18.56	19.66	22.01	30.00
	7 m	0.040	6.49	19.00	19.55	21.11	22.31	23.00	24.52	25.61	27.36	40.00
		0.500	8.98	17.00	18.22	18.77	19.37	20.00	21.97	23.05	24.64	35.00
		0.922	7.45	17.00	17.32	17.98	18.49	19.00	20.58	21.32	21.94	38.00
	8 m	0.040	4.61	21.00	22.07	22.83	23.62	25.00	26.91	28.15	29.90	40.00
		0.500	7.48	20.00	20.66	21.38	21.98	23.00	25.00	26.10	27.74	36.00

Continued....

Data Set	x (m)	(y/d)	Cp (ppm)	T_L (s)	T_{1R} (s)	T_{2R} (s)	T_{3R} (s)	T_P (s)	T_{3F} (s)	T_{2F} (s)	T_{1F} (s)	T_T (s)
		0.922	8.07	19.00	19.69	20.52	21.37	23.00	25.02	26.23	27.79	38.00
	9 m	0.040	5.06	22.00	22.66	23.41	24.08	27.00	28.32	28.98	31.55	45.00
		0.500	5.81	21.00	21.61	22.26	22.76	24.00	24.93	25.93	27.46	38.00
		0.922	7.47	21.00	21.38	22.11	22.78	24.00	26.12	27.26	28.97	44.00
4CDSL12	1 m	0.040	0.00	0.00	0.00	0.00	0.00	0.00	0.00	0.00	0.00	0.00
(d = 0.128 m)		0.922	6.20	7.00	22.06	22.53	22.99	24.00	26.30	27.36	28.94	33.00
	2 m	0.040	2.57	9.00	10.95	11.48	11.97	13.00	14.18	15.17	16.99	25.00
		0.922	16.20	9.00	9.73	10.24	10.62	11.00	12.02	13.28	14.80	30.00
	3 m	0.040	1.64	12.00	12.26	12.83	13.41	14.00	15.70	16.67	18.00	22.00
		0.922	13.05	11.00	11.93	12.44	12.92	14.00	15.09	16.04	17.62	36.00
	4 m	0.040	3.09	14.00	14.27	14.80	15.39	16.00	17.72	18.73	20.33	26.00
		0.922	11.65	12.00	12.77	13.38	13.88	15.00	16.36	17.49	19.20	32.00
	5 m	0.040	5.17	16.00	17.87	18.45	18.97	20.00	21.48	22.66	24.36	31.00
		0.922	9.48	13.00	14.47	15.13	15.65	17.00	18.07	19.11	20.83	36.00
	6 m	0.040	4.17	18.00	19.20	19.90	20.60	22.00	23.62	24.86	26.63	34.00
		0.922	7.29	17.00	17.25	17.80	18.59	20.00	21.06	22.02	23.45	33.00
	7 m	0.040	4.54	21.00	21.14	21.70	22.32	24.00	25.24	26.39	28.07	35.00
		0.922	9.25	18.00	18.30	19.01	19.68	21.00	22.85	23.93	25.38	39.00
	8 m	0.040	3.54	22.00	22.01	22.60	23.26	25.00	26.49	27.76	29.85	42.00
		0.922	6.85	20.00	20.17	20.78	21.47	23.00	25.48	27.09	28.77	47.00
	9 m	0.040	5.77	23.00	22.65	23.35	23.94	25.00	27.03	28.23	29.98	37.00
		0.922	7.93	21.00	21.37	22.08	22.71	24.00	25.46	26.60	28.05	37.00
4CDCW2	1 m	0.034	0.00	0.00	0.00	0.00	0.00	0.00	0.00	0.00	0.00	0.00
(d = 0.147 m)		0.932	36.36	8.00	8.47	9.08	9.58	11.00	11.88	12.76	13.96	28.00
	2 m	0.034	1.97	13.00	13.69	14.30	14.81	16.00	17.39	18.42	19.76	26.00
		0.500	12.98	10.00	10.13	10.64	11.23	12.00	13.63	14.64	15.95	29.00
		0.932	16.65	9.00	10.24	10.80	11.39	12.00	13.78	14.72	16.04	27.00
	3 m	0.034	3.56	11.00	11.22	11.82	12.41	13.00	15.06	16.18	17.55	26.00
		0.500	13.31	11.00	11.19	11.70	12.30	13.00	14.42	15.34	16.70	23.00
		0.932	15.50	12.00	11.67	12.43	13.37	15.00	16.81	17.74	19.07	30.00
	4 m	0.034	5.39	14.00	14.28	15.04	15.74	17.00	18.54	19.58	21.08	27.00
		0.500	10.91	15.00	13.95	14.46	14.95	16.00	17.18	18.13	19.54	26.00
		0.932	13.87	15.00	14.37	15.01	15.61	17.00	18.32	19.41	20.86	32.00
	5 m	0.034	5.77	16.00	17.23	17.88	18.53	20.00	21.28	22.33	23.84	33.00
		0.500	10.60	15.00	15.61	16.24	16.74	18.00	19.15	19.77	20.95	32.00
		0.932	12.65	15.00	15.72	16.30	16.77	19.00	20.14	21.04	22.38	34.00
	6 m	0.034	5.83	18.00	18.40	20.10	20.74	22.00	23.57	24.75	26.46	37.00
		0.500	9.50	17.00	17.26	17.88	18.58	20.00	20.84	21.86	23.29	29.00
		0.932	11.15	16.00	16.52	17.30	18.06	19.00	19.78	21.00	22.68	31.00
	7 m	0.034	6.00	20.00	20.52	21.41	22.93	24.00	24.52	25.15	27.02	38.00
		0.500	9.35	18.00	18.36	19.04	19.65	21.00	22.08	23.07	24.48	36.00
		0.932	11.32	18.00	19.01	19.60	20.27	22.00	23.49	24.68	26.20	37.00
	8 m	0.034	6.41	22.00	22.43	23.20	23.91	25.00	26.46	27.98	29.78	39.00
		0.500	9.23	20.00	20.99	21.56	22.23	24.00	25.41	26.46	27.85	38.00
		0.932	10.50	21.00	21.28	22.00	22.74	24.00	26.05	27.17	28.69	38.00
	9 m	0.034	7.64	23.00	24.37	25.13	25.81	27.00	29.33	30.72	32.50	43.00
		0.500	7.70	21.00	22.23	22.97	23.71	25.00	27.23	28.47	30.13	39.00
		0.932	9.60	21.00	21.54	22.26	22.87	24.00	25.98	27.24	28.86	40.00
4CDSL21	1 m	0.034	0.00	0.00	0.00	0.00	0.00	0.00	0.00	0.00	0.00	0.00
(d = 0.147 m)		0.932	28.12	8.00	8.23	8.87	9.44	10.00	10.73	12.13	13.37	26.00
	2 m	0.034	0.09	6.00	6.21	6.58	6.96	12.00	14.05	14.50	14.95	18.00
		0.500	6.51	9.00	10.23	10.77	11.37	12.00	13.59	14.54	15.81	27.00
		0.932	22.24	8.00	8.90	9.55	10.22	11.00	11.47	11.94	13.50	28.00
	3 m	0.034	0.57	12.00	13.09	13.63	14.25	15.00	17.36	18.21	20.55	24.00
		0.500	9.04	11.00	12.11	12.61	13.18	14.00	15.34	16.25	17.51	25.00
		0.932	14.37	11.00	11.89	12.47	13.00	14.00	15.37	16.29	17.57	30.00
	4 m	0.034	2.24	14.00	14.72	16.25	16.62	17.00	18.42	19.51	21.08	28.00
		0.500	7.96	13.00	12.94	13.49	14.03	15.00	16.59	17.64	18.94	26.00
		0.932	11.93	12.00	13.02	13.52	14.05	15.00	16.39	17.43	18.86	29.00
	5 m	0.034	2.98	16.00	16.37	17.07	17.68	19.00	20.36	21.44	22.94	29.00

Continued....

Data Set	x (m)	(y/d)	Cp (ppm)	T_L (s)	T_{1R} (s)	T_{2R} (s)	T_{3R} (s)	T_P (s)	T_{3F} (s)	T_{2F} (s)	T_{1F} (s)	T_T (s)
		0.500	7.70	14.00	14.93	15.52	16.12	17.00	18.64	19.64	20.94	29.00
		0.932	9.12	14.00	15.42	15.84	16.64	18.00	18.90	20.39	21.08	33.00
	6 m	0.034	3.56	18.00	19.12	19.81	20.53	22.00	23.64	24.78	26.17	34.00
		0.500	6.83	15.00	16.11	16.65	17.26	18.00	19.81	21.47	22.19	31.00
		0.932	7.85	15.00	16.86	17.49	18.08	19.00	21.18	22.33	23.85	32.00
	7 m	0.034	3.52	19.00	19.31	19.67	21.06	22.00	24.28	25.24	25.95	35.00
		0.500	6.42	18.00	18.52	19.22	19.80	21.00	22.43	23.50	24.93	33.00
		0.932	7.76	18.00	18.40	19.08	19.71	21.00	22.68	23.89	25.50	33.00
	8 m	0.034	4.53	22.00	22.64	23.46	24.25	26.00	27.70	28.90	30.44	38.00
		0.500	6.18	19.00	19.96	20.56	21.21	23.00	24.40	25.50	26.84	38.00
		0.932	6.48	20.00	21.06	21.63	22.30	24.00	25.68	26.98	28.74	36.00
	9 m	0.034	5.19	23.00	23.54	24.33	25.02	26.00	29.00	30.29	32.16	44.00
		0.500	6.10	21.00	21.38	22.01	22.57	25.00	26.08	27.20	28.74	39.00
		0.932	6.20	21.00	22.06	22.53	22.99	24.00	26.30	27.36	28.94	43.00
4CDCW3 (d = 0.162 m)	1 m	0.031	0.00	0.00	0.00	0.00	0.00	0.00	0.00	0.00	0.00	0.00
		0.938	30.73	8.00	8.65	9.24	9.72	11.00	11.95	12.90	14.31	26.00
	2 m	0.031	0.13	12.00	12.04	12.58	13.19	14.00	15.05	15.70	16.44	18.00
		0.500	12.85	9.00	9.41	9.97	10.48	11.00	12.53	13.40	14.65	22.00
		0.938	18.22	8.00	8.49	9.12	9.63	11.00	11.98	12.85	14.02	25.00
	3 m	0.031	2.14	12.00	12.17	12.70	13.31	14.00	15.57	16.58	17.96	25.00
		0.500	11.07	11.00	11.96	12.45	12.93	14.00	15.04	15.91	17.18	25.00
		0.938	10.65	10.00	10.56	11.20	11.94	14.00	15.26	16.25	16.84	28.00
	4 m	0.031	5.45	13.00	14.12	14.65	15.26	16.00	18.01	19.08	20.55	29.00
		0.500	10.40	13.00	14.28	14.61	14.94	16.00	17.15	18.08	19.41	25.00
		0.938	15.40	12.00	12.57	13.23	13.76	15.00	16.30	17.29	18.59	31.00
	5 m	0.031	3.94	15.00	15.67	16.37	16.96	18.00	19.86	20.90	22.44	34.00
		0.500	10.88	16.00	15.41	15.83	16.38	17.00	18.95	19.87	21.15	30.00
		0.938	13.66	14.00	14.24	14.80	15.41	17.00	18.08	18.98	20.23	30.00
	6 m	0.031	6.78	17.00	18.05	18.71	19.45	21.00	22.89	24.32	25.31	36.00
		0.500	8.62	16.00	16.25	16.77	17.36	18.00	20.03	21.02	22.39	29.00
		0.938	13.47	15.00	16.13	16.66	17.26	18.00	19.54	20.52	21.82	37.00
	7 m	0.031	6.46	19.00	20.01	20.67	21.40	23.00	24.50	25.77	27.51	37.00
		0.500	7.60	18.00	18.86	19.49	20.09	21.00	23.24	24.56	26.21	34.00
		0.938	7.68	17.00	18.42	18.86	19.42	21.00	22.06	23.01	24.42	37.00
	8 m	0.031	7.15	21.00	21.66	22.50	23.25	24.00	25.49	26.79	28.46	39.00
		0.500	7.29	20.00	20.49	21.17	21.83	24.00	24.92	25.92	27.33	34.00
		0.938	10.67	19.00	19.78	20.39	20.93	22.00	23.68	24.77	26.09	38.00
	9 m	0.031	6.02	23.00	24.00	24.64	25.37	27.00	28.88	30.37	32.11	41.00
		0.500	10.07	23.00	23.21	23.76	24.36	25.00	26.93	27.92	29.36	41.00
		0.938	7.50	21.00	21.31	22.06	22.82	25.00	26.75	28.02	29.68	39.00
4CDSL31 (d = 0.162)	1 m	0.031	0.00	0.00	0.00	0.00	0.00	0.00	0.00	0.00	0.00	0.00
		0.938	29.44	8.00	9.33	10.12	10.56	11.00	11.59	12.53	14.47	30.00
	2 m	0.031	0.17	13.00	13.03	13.56	14.15	15.00	19.38	20.07	20.68	22.00
		0.500	7.19	10.00	9.83	10.56	11.27	12.00	12.89	13.75	14.92	22.00
		0.938	22.89	10.00	10.33	11.18	11.59	12.00	12.78	14.06	15.29	24.00
	3 m	0.031	0.60	13.00	13.15	13.73	14.38	16.00	17.17	18.00	19.20	22.00
		0.500	9.21	11.00	11.17	11.66	12.25	13.00	13.79	14.66	16.54	25.00
		0.938	18.83	11.00	11.69	12.31	12.81	14.00	14.52	15.10	16.34	33.00
	4 m	0.031	2.64	14.00	14.72	15.37	15.91	17.00	18.47	19.49	21.32	31.00
		0.500	10.81	13.00	14.05	14.56	15.11	16.00	17.32	18.24	19.53	28.00
		0.938	10.94	12.00	13.15	13.70	14.31	15.00	16.89	17.91	19.35	33.00
	5 m	0.031	3.58	16.00	16.76	17.45	18.65	21.00	21.57	23.06	23.85	32.00
		0.500	8.19	15.00	15.84	16.44	16.97	18.00	19.55	20.57	21.84	33.00
		0.938	9.70	15.00	15.52	16.26	16.88	18.00	19.57	20.58	21.82	31.00
	6 m	0.031	4.64	18.00	18.59	19.31	19.90	21.00	22.66	23.80	25.39	35.00
		0.500	7.97	17.00	17.29	17.96	18.62	20.00	21.48	22.54	23.88	34.00
		0.938	8.38	16.00	17.20	17.73	18.33	19.00	20.96	22.14	23.76	33.00
	7 m	0.031	3.62	20.00	20.94	21.68	22.45	24.00	25.61	26.83	28.34	37.00
		0.500	6.58	19.00	19.80	20.47	21.10	22.00	24.12	25.23	26.69	37.00
		0.938	7.78	19.00	19.85	20.67	21.53	23.00	24.80	25.96	27.55	34.00

Continued....

Data Set	x (m)	(y/d)	Cp (ppm)	T_L (s)	T_{1R} (s)	T_{2R} (s)	T_{3R} (s)	T_P (s)	T_{3F} (s)	T_{2F} (s)	T_{1F} (s)	T_T (s)
	8 m	0.031	3.31	22.00	22.86	23.58	24.31	26.00	27.79	29.10	30.98	37.00
		0.500	7.45	20.00	21.10	21.64	22.25	23.00	24.96	26.06	27.61	38.00
		0.938	6.74	20.00	20.70	21.32	21.89	23.00	25.08	26.31	28.01	37.00
	9 m	0.031	3.45	21.00	27.74	28.55	29.39	31.00	33.30	34.58	36.74	45.00
		0.938	6.98	22.00	22.12	22.69	23.31	24.00	25.87	27.11	28.79	40.00
4CDSL32 (d = 0.162 m)	1 m	0.031	0.00	0.00	0.00	0.00	0.00	0.00	0.00	0.00	0.00	0.00
		0.500	2.11	7.00	8.90	9.47	9.99	11.00	32.23	33.12	34.37	18.00
		0.938	27.83	8.00	8.20	8.69	9.27	10.00	10.51	11.02	12.14	21.00
	2 m	0.031	0.10	7.00	4.50	5.00	5.83	13.00	16.12	16.75	17.37	19.00
		0.500	4.26	10.00	8.31	9.05	9.81	12.00	13.70	14.98	16.71	22.00
		0.938	20.58	9.00	9.97	10.33	10.66	11.00	11.54	12.23	13.87	28.00
	3 m	0.031	1.12	12.00	13.30	13.81	14.39	15.00	16.67	17.86	19.33	24.00
		0.500	4.55	11.00	6.10	6.75	7.52	9.00	11.56	13.11	15.01	24.00
		0.938	9.89	11.00	11.18	11.74	12.35	13.00	14.96	15.82	16.96	26.00
	4 m	0.031	1.23	13.00	14.48	15.17	15.78	17.00	17.99	19.02	20.52	26.00
		0.500	5.68	12.00	14.35	15.09	15.76	17.00	19.06	20.29	22.10	29.00
		0.938	9.34	12.00	12.79	13.41	13.96	15.00	16.54	17.48	18.73	30.00
	5 m	0.031	2.29	16.00	16.70	17.34	17.92	19.00	20.82	21.82	23.25	29.00
		0.500	5.88	15.00	15.26	15.90	16.56	18.00	19.48	20.66	22.14	30.00
		0.938	8.03	14.00	14.13	15.34	15.98	17.00	18.28	18.87	20.05	30.00
	6 m	0.031	2.62	19.00	18.81	19.47	20.11	22.00	23.48	24.70	26.82	33.00
		0.500	6.00	18.00	19.14	19.65	20.24	21.00	22.30	23.12	24.29	33.00
		0.938	7.66	16.00	15.52	16.31	16.97	19.00	20.58	21.76	23.30	31.00
	7 m	0.031	2.90	21.00	21.19	22.04	22.52	23.00	23.68	24.89	26.50	34.00
		0.500	6.37	19.00	19.80	20.37	20.86	22.00	23.16	24.10	25.50	36.00
		0.938	7.10	18.00	18.35	19.12	19.83	21.00	23.30	24.58	25.86	37.00
	8 m	0.031	3.23	22.00	22.83	23.78	24.43	25.00	25.65	26.82	28.42	34.00
		0.500	6.84	21.00	21.26	21.83	22.43	24.00	25.01	25.91	27.21	37.00
		0.938	6.28	20.00	21.02	21.69	22.35	23.00	24.85	25.89	27.35	39.00
	9 m	0.031	3.85	23.00	23.39	24.21	24.98	27.00	28.88	30.27	31.99	41.00
		0.500	6.91	22.00	22.61	23.26	23.79	25.00	26.24	27.26	28.72	41.00
		0.938	6.24	20.00	20.91	21.53	22.19	24.00	26.60	27.86	29.59	36.00
4CDCW4 (d = 0.184 m)	1 m	0.027	0.00	0.00	0.00	0.00	0.00	0.00	0.00	0.00	0.00	0.00
		0.500	1.75	8.00	8.51	9.04	9.55	11.00	11.95	12.74	13.81	18.00
		0.946	30.18	7.00	8.24	9.00	9.50	10.00	10.63	11.88	13.10	27.00
	2 m	0.027	2.31	12.00	12.20	12.67	13.24	14.00	15.31	16.34	18.30	24.00
		0.500	5.46	9.00	9.96	10.52	11.11	12.00	13.45	14.42	15.86	31.00
		0.946	18.31	9.00	9.89	10.42	10.89	12.00	12.94	13.78	14.97	29.00
	3 m	0.027	1.41	14.00	14.30	14.91	15.51	17.00	18.37	19.65	21.42	31.00
		0.500	11.47	12.00	12.47	13.07	13.58	15.00	15.90	16.81	18.09	25.00
		0.946	14.09	11.00	11.43	11.98	12.49	13.00	14.65	15.52	16.76	30.00
	4 m	0.027	2.00	16.00	17.71	18.30	18.80	20.00	21.40	22.40	24.00	32.00
		0.500	6.96	13.00	13.38	14.11	14.77	16.00	17.47	18.49	19.90	29.00
		0.946	13.46	12.00	13.32	13.90	14.50	16.00	17.13	18.01	19.34	34.00
	5 m	0.027	1.83	16.00	16.68	17.39	17.97	19.00	20.99	21.86	23.01	33.00
		0.500	7.05	14.00	14.82	15.44	15.99	17.00	18.71	19.73	20.97	29.00
		0.946	10.50	15.00	15.57	16.33	16.95	18.00	19.48	20.42	21.73	33.00
	6 m	0.027	6.02	18.00	19.77	20.51	21.22	23.00	24.46	25.83	27.74	40.00
		0.500	8.30	17.00	17.53	18.15	18.67	20.00	21.15	22.20	23.69	30.00
		0.946	9.41	16.00	17.08	17.63	18.24	19.00	20.91	21.86	23.12	41.00
	7 m	0.027	4.41	20.00	20.38	21.08	21.74	23.00	25.25	26.45	28.10	37.00
		0.500	6.30	19.00	19.35	20.08	20.73	22.00	23.57	24.66	26.08	36.00
		0.946	8.87	18.00	19.15	19.70	20.32	21.00	23.01	24.13	25.71	37.00
	8 m	0.027	5.25	21.00	24.03	24.68	25.41	27.00	28.76	30.04	31.86	44.00
		0.500	5.82	21.00	22.26	23.07	23.81	25.00	27.03	28.24	29.80	36.00
		0.946	8.69	19.00	19.46	20.08	20.63	22.00	23.16	24.17	25.61	36.00
	9 m	0.027	4.06	24.00	24.73	25.84	26.85	28.00	30.23	31.70	34.04	46.00
		0.500	6.30	22.00	22.65	23.39	24.03	26.00	27.83	29.33	31.15	43.00
		0.946	9.81	21.00	22.75	23.54	24.39	26.00	27.20	28.40	30.15	42.00

continued....

Data Set	x (m)	(y/d)	Cp (ppm)	T_L (s)	T_{1R} (s)	T_{2R} (s)	T_{3R} (s)	T_P (s)	T_{3F} (s)	T_{2F} (s)	T_{1F} (s)	T_T (s)
4CDSL41	1 m	0.027	0.00	0.00	0.00	0.00	0.00	0.00	0.00	0.00	0.00	0.00
(d = 0.184 m)		0.500	1.22	8.00	8.35	8.81	9.36	10.00	11.15	11.86	12.74	16.00
		0.946	27.02	6.00	7.95	9.13	9.57	10.00	10.46	10.93	12.76	29.00
	2 m	0.027	0.00	0.00	0.00	0.00	0.00	0.00	0.00	0.00	0.00	32.00
		0.500	8.32	9.00	9.33	9.87	10.43	11.00	11.68	12.50	13.71	23.00
		0.946	17.19	7.00	9.29	9.90	10.45	11.00	11.56	12.47	13.95	26.00
	3 m	0.027	0.53	12.00	13.37	14.10	14.63	16.00	16.95	18.64	20.75	25.00
		0.500	6.08	11.00	11.30	11.82	12.39	13.00	14.57	15.51	16.79	24.00
		0.946	15.82	11.00	12.17	12.71	13.31	14.00	14.66	15.48	16.70	29.00
	4 m	0.027	1.01	12.00	14.84	15.61	16.35	18.00	19.20	20.02	20.99	24.00
		0.500	5.35	13.00	13.48	14.15	14.71	16.00	17.23	18.22	19.62	26.00
		0.946	9.48	14.00	14.45	15.08	15.64	17.00	18.17	19.11	20.54	35.00
	5 m	0.027	0.89	15.00	17.06	17.70	18.35	19.00	21.27	22.96	24.06	30.00
		0.500	6.17	14.00	14.98	15.59	16.24	17.00	18.83	19.78	21.14	31.00
		0.946	8.72	14.00	14.29	14.93	15.55	17.00	18.17	19.11	20.42	34.00
	6 m	0.027	1.80	17.00	18.78	19.45	20.02	21.00	23.07	24.18	25.52	34.00
		0.500	4.66	16.00	17.26	17.81	18.40	19.00	21.43	22.55	24.17	36.00
		0.946	7.62	16.00	17.19	17.89	18.59	20.00	21.37	22.36	23.69	32.00
	7 m	0.027	2.01	18.00	20.19	20.92	21.62	23.00	24.54	25.76	27.62	36.00
		0.500	3.85	17.00	19.17	19.71	20.33	22.00	23.37	24.39	25.82	33.00
		0.946	5.64	16.00	19.11	19.53	19.94	21.00	23.00	24.19	25.75	37.00
	8 m	0.027	2.44	22.00	23.00	23.70	24.55	26.00	28.17	29.42	31.12	38.00
		0.500	5.40	18.00	20.17	20.78	21.43	23.00	24.20	25.24	26.68	35.00
		0.946	5.35	18.00	20.39	21.36	22.22	24.00	25.00	26.16	27.75	42.00
	9 m	0.027	2.68	23.00	24.23	25.17	26.00	28.00	30.13	31.67	33.88	42.00
		0.500	3.82	22.00	22.51	23.23	23.85	25.00	27.33	28.58	30.23	38.00
		0.946	4.62	21.00	24.80	25.64	26.52	28.00	30.66	32.00	34.13	41.00
4CDSL42	1 m	0.027	0.00	0.00	0.00	0.00	0.00	0.00	0.00	0.00	0.00	0.00
(d = 0.184 m)		0.946	14.86	7.00	7.85	8.40	8.88	10.00	10.93	11.75	12.89	22.00
	2 m	0.027	0.55	9.00	9.75	10.50	11.14	12.00	13.52	14.94	16.52	19.00
		0.500	3.53	9.00	9.41	9.97	10.49	11.00	12.66	13.48	14.60	20.00
		0.946	11.80	8.00	9.27	9.84	10.42	11.00	11.76	12.67	13.79	30.00
	3 m	0.027	0.98	12.00	12.12	12.93	13.68	15.00	16.30	17.82	21.38	26.00
		0.500	5.24	11.00	11.82	12.41	12.93	14.00	15.17	15.99	17.22	24.00
		0.946	8.33	11.00	11.51	12.18	12.76	14.00	15.21	16.09	17.38	24.00
	4 m	0.027	2.11	15.00	15.28	15.59	15.89	17.00	18.33	19.25	20.64	26.00
		0.500	4.76	12.00	12.45	13.11	13.70	15.00	16.03	16.86	18.05	26.00
		0.946	8.50	11.00	12.34	12.94	13.50	15.00	15.90	16.79	18.05	28.00
	5 m	0.027	1.68	16.00	16.28	17.10	17.80	20.00	21.22	21.95	23.12	30.00
		0.500	4.46	13.00	14.89	15.43	15.92	17.00	18.10	19.05	20.52	29.00
		0.946	6.27	12.00	14.33	14.94	15.53	17.00	18.08	18.97	20.17	26.00
	6 m	0.027	1.31	18.00	18.53	19.23	19.87	21.00	22.66	23.80	25.73	32.00
		0.500	4.69	17.00	17.08	17.38	17.69	18.00	19.99	20.98	22.47	30.00
		0.946	4.77	17.00	17.30	17.89	18.53	20.00	21.30	22.39	23.84	31.00
	7 m	0.027	2.07	20.00	20.93	21.58	22.26	24.00	25.30	26.47	28.33	36.00
		0.500	4.33	19.00	18.48	19.14	19.73	21.00	22.40	23.44	24.91	28.00
		0.946	4.52	19.00	19.36	19.71	20.27	22.00	22.98	24.78	26.57	35.00
	8 m	0.027	2.59	21.00	22.79	24.04	24.52	25.00	25.64	27.27	29.97	35.00
		0.500	5.08	20.00	19.72	20.41	20.98	22.00	23.60	24.69	26.24	32.00
		0.946	5.46	20.00	20.27	21.09	22.02	23.00	23.97	25.64	27.86	41.00
	9 m	0.027	1.92	23.00	23.27	23.92	24.60	26.00	28.56	29.89	31.68	41.00
		0.500	4.06	22.00	21.30	21.94	22.56	24.00	25.46	26.78	28.66	39.00
		0.946	4.58	21.00	20.77	21.48	22.14	24.00	25.74	27.09	28.70	38.00
4CDCW5	1 m	0.045	0.00	0.00	0.00	0.00	0.00	0.00	0.00	0.00	0.00	0.00
(d = 0.109 m)		0.908	41.93	8.00	8.63	9.18	9.59	10.00	10.51	11.05	13.19	25.00
	2 m	0.045	3.58	9.00	9.14	9.62	10.18	11.00	12.20	13.06	14.25	20.00
		0.908	27.24	8.00	8.38	9.07	9.54	10.00	10.98	12.35	13.51	27.00
	3 m	0.045	8.97	11.00	11.15	11.65	12.23	13.00	14.26	15.15	16.48	28.00
		0.908	19.24	10.00	10.82	12.03	12.51	13.00	13.81	15.01	15.89	26.00
	4 m	0.045	8.80	12.00	12.92	13.47	13.97	15.00	16.34	17.32	18.63	24.00

Continued....

Data Set	x (m)	(y/d)	Cp (ppm)	T_L (s)	T_{1R} (s)	T_{2R} (s)	T_{3R} (s)	T_P (s)	T_{3F} (s)	T_{2F} (s)	T_{1F} (s)	T_T (s)
		0.908	17.91	11.00	11.75	12.36	12.87	14.00	15.16	16.00	17.19	29.00
	5 m	0.045	10.66	14.00	15.35	15.93	16.47	17.00	18.80	19.90	21.58	29.00
		0.908	14.89	12.00	12.89	13.44	13.94	15.00	16.23	17.16	18.46	32.00
	6 m	0.045	10.54	15.00	15.91	16.49	17.05	18.00	19.79	20.85	22.30	32.00
		0.908	13.93	13.00	14.45	15.11	15.67	17.00	18.19	19.14	20.41	28.00
	7 m	0.045	10.71	17.00	18.05	18.61	19.24	20.00	22.17	23.25	24.76	36.00
		0.908	13.42	15.00	16.90	17.47	17.99	19.00	20.39	21.36	22.68	35.00
	8 m	0.045	10.68	18.00	20.27	20.93	21.59	23.00	24.39	25.50	26.98	40.00
		0.908	10.55	17.00	17.80	18.46	19.06	20.00	22.00	22.97	24.31	33.00
	9 m	0.045	11.13	20.00	20.64	21.37	21.98	23.00	24.79	25.84	27.29	37.00
		0.908	11.29	19.00	19.95	20.53	21.14	22.00	23.92	24.92	26.33	38.00
4CDSL51 (d = 0.109 m)	1 m	0.045	0.12	5.00	5.50	6.25	7.00	8.00	9.00	9.60	10.50	12.00
		0.908	32.22	8.00	8.47	9.19	9.59	10.00	10.51	11.03	12.27	22.00
	2 m	0.045	0.20	11.00	11.15	11.54	11.92	13.00	14.25	14.87	15.67	17.00
		0.908	22.69	8.00	8.08	8.54	9.01	10.00	10.57	11.47	12.85	22.00
	3 m	0.045	0.93	12.00	12.22	12.77	13.37	14.00	16.01	16.81	17.81	22.00
		0.908	14.13	10.00	10.36	10.93	11.47	12.00	13.81	14.66	15.78	23.00
	4 m	0.045	6.19	12.00	13.49	14.14	14.67	16.00	17.17	18.12	19.45	28.00
		0.908	13.48	11.00	12.42	13.02	13.54	15.00	15.90	16.77	17.94	29.00
	5 m	0.045	4.44	14.00	14.76	15.39	15.92	17.00	18.53	19.56	20.89	27.00
		0.908	13.01	13.00	13.45	14.05	14.55	16.00	16.88	17.76	18.92	27.00
	6 m	0.045	5.35	16.00	18.04	18.61	19.25	20.00	22.17	23.26	24.92	33.00
		0.908	9.37	15.00	15.56	16.25	16.82	18.00	19.45	20.48	21.81	32.00
	7 m	0.045	5.84	19.00	20.17	20.84	21.56	23.00	24.62	25.89	27.62	37.00
		0.908	9.33	16.00	16.99	17.53	18.11	19.00	20.55	21.55	22.86	31.00
	8 m	0.045	6.71	21.00	22.83	23.55	24.29	26.00	27.84	29.19	31.04	40.00
		0.908	8.87	18.00	18.39	18.99	19.54	21.00	22.07	23.00	24.30	31.00
	9 m	0.045	6.32	22.00	23.16	23.93	24.70	26.00	28.44	29.76	31.56	41.00
		0.908	8.12	21.00	22.16	22.73	23.36	25.00	26.26	27.34	28.74	37.00
4CDSL52 (d = 0.109 m)	1 m	0.045	0.38	10.00	9.56	10.10	10.55	11.00	12.25	12.78	13.46	15.00
		0.908	22.66	7.00	8.02	8.34	8.67	9.00	9.75	11.16	12.26	21.00
	2 m	0.045	0.31	11.00	10.86	11.41	11.89	13.00	13.97	14.68	16.21	18.00
		0.908	20.65	8.00	9.32	9.85	10.42	11.00	11.62	12.73	14.44	26.00
	3 m	0.045	1.86	12.00	12.22	12.80	13.40	14.00	16.01	16.98	18.39	25.00
		0.908	16.09	10.00	10.80	11.36	11.84	13.00	14.04	14.90	16.06	28.00
	4 m	0.045	1.70	14.00	14.33	14.88	15.46	17.00	18.07	18.96	20.34	28.00
		0.908	11.34	11.00	12.13	12.66	13.25	14.00	15.55	16.50	17.74	26.00
	5 m	0.045	3.34	15.00	15.13	15.66	16.27	17.00	18.70	19.74	20.98	27.00
		0.908	10.75	13.00	13.40	13.99	14.53	16.00	17.02	17.93	19.19	26.00
	6 m	0.045	5.03	17.00	17.66	18.33	18.89	20.00	21.62	22.73	24.31	36.00
		0.908	8.96	16.00	16.36	16.99	17.50	18.00	19.51	20.51	22.43	27.00
	7 m	0.045	5.43	18.00	18.59	19.31	19.92	21.00	22.98	24.08	25.61	33.00
		0.908	8.95	17.00	16.88	17.46	17.98	19.00	20.51	21.55	22.92	30.00
	8 m	0.045	5.72	20.00	20.58	21.31	21.91	23.00	24.87	26.09	27.88	36.00
		0.908	8.66	18.00	18.36	19.00	19.59	21.00	22.27	23.37	24.82	38.00
	9 m	0.045	6.32	21.00	21.56	22.33	22.98	24.00	26.27	27.43	28.88	35.00
		0.908	7.72	19.00	19.27	19.90	20.49	22.00	23.11	24.25	25.75	36.00

MIXING COEFFICIENTS AND HYDRAULIC PARAMETERS

Data Set	d (m)	Q (m^3/s)	b (m)	A (m^2)	P (m)	U (m/s)	R_h (m)	S_b	U_* (m/s)	C_s (ppm)	d_{50} (mm)	E_y (m^2/s)	OE_x (m^2/s)	$(U_x)_1$ (m/s)	$(U_x)_2$ (m/s)	$(U_x)_3$ (m/s)
1CDCW1	0.123	0.0195	0.39	0.048	0.636	0.407	0.092	0.0009174	0.029	-	-	0.000492	0.056	0.378	0.446	0.455
1CDCW2	0.155	0.0224	0.39	0.060	0.700	0.370	0.121	0.0009174	0.033	-	-	0.000552	0.060	0.327	0.375	0.386
1CDCW3	0.1785	0.0305	0.39	0.070	0.747	0.438	0.128	0.0009174	0.034	-	-	0.000793	0.09	0.414	0.465	0.468
1CDCW4	0.0895	0.0158	0.39	0.035	0.569	0.454	0.063	0.0009174	0.024	-	-	0.000275	0.117	0.400	0.479	0.488
1CDCW5	0.1645	0.0259	0.39	0.064	0.719	0.404	0.123	0.0009174	0.033	-	-	0.000653	0.119	0.378	0.437	0.448
1CDCW6	0.1005	0.0184	0.39	0.039	0.591	0.470	0.069	0.0009174	0.025	-	-	0.000229	0.043	0.413	0.496	0.506
1CDCW7	0.103	0.0198	0.39	0.040	0.596	0.492	0.068	0.0009174	0.025	-	-	0.000456	0.107	0.364	0.420	0.428
2CDCW1	0.124	0.0210	0.39	0.048	0.638	0.434	0.095	0.0011765	0.033	-	-	0.000278	0.062	0.362	0.440	0.459
2CDCW2	0.134	0.0263	0.39	0.052	0.658	0.504	0.095	0.0011765	0.033	-	-	0.000398	0.118	0.442	0.516	0.527
2CDCW3	0.145	0.0276	0.39	0.057	0.680	0.487	0.105	0.0011765	0.034	-	-	0.000304	0.070	0.397	0.478	0.500
2CDCW4	0.164	0.0318	0.39	0.064	0.718	0.498	0.117	0.0011765	0.037	-	-	0.000526	0.058	0.405	0.486	0.503
2CDCW5	0.196	0.0394	0.39	0.076	0.782	0.515	0.137	0.0011765	0.040	-	-	0.000417	0.059	0.475	0.530	0.536
2CDCW6	0.15	0.0282	0.39	0.0585	0.69	0.482	0.109	0.0011765	0.035	-	-	0.00035	0.026	0.380	0.470	0.550
2CDSL11	0.124	0.0210	0.39	0.048	0.638	0.434	0.095	0.0011765	0.033	104	0.064	0.000244	0.071	0.431	0.494	0.500
2CDSL21	0.134	0.0263	0.39	0.052	0.658	0.504	0.095	0.0011765	0.033	300	0.064	0.000296	0.071	0.442	0.516	0.527
3CDCW1	0.115	0.0263	0.39	0.045	0.620	0.587	0.087	0.0020408	0.042	-	-	0.000659	0.216	0.495	0.590	0.602
3CDCW2	0.15	0.0341	0.39	0.059	0.690	0.583	0.114	0.0020408	0.048	-	-	0.00069	0.12	0.551	0.632	0.627
3CDSL11	0.115	0.0263	0.39	0.045	0.620	0.587	0.087	0.0020408	0.042	192	0.064	0.000588	0.179	0.502	0.581	0.592
3CDSL12	0.115	0.0263	0.39	0.045	0.620	0.587	0.087	0.0020408	0.042	391	0.064	0.000683	0.069	0.483	0.570	0.562
3CDSL13	0.115	0.0263	0.39	0.045	0.620	0.587	0.087	0.0020408	0.042	681	0.064	0.000407	0.06	0.450	0.560	0.592
3CDSL14	0.115	0.0263	0.39	0.045	0.620	0.587	0.087	0.0020408	0.042	1118	0.064	0.000352	0.046	0.469	0.562	0.572
3CDSL15	0.115	0.0263	0.39	0.045	0.620	0.587	0.087	0.0020408	0.042	654	0.064	0.000457	0.008	0.484	0.563	0.565

$(U_x)_1$ = Width – averaged velocity up to bottom $1/3^{rd}$ depth of flow
$(U_x)_2$ = Width – averaged velocity up to middle $1/3^{rd}$ depth of flow
$(U_x)_3$ = Width – averaged velocity up to top $1/3^{rd}$ depth of flow

Continued....

Data Set	d (m)	Q (m^3/s)	b (m)	A (m^2)	P (m)	U (m/s)	R_b (m)	S_b	U_* (m/s)	C_s (ppm)	d_{50} (mm)	E_y (m^2/s)	OE_x (m^2/s)	$(U_x)_1$ (m/s)	$(U_x)_2$ (m/s)	$(U_x)_3$ (m/s)
3CDSL16	0.115	0.0263	0.39	0.045	0.620	0.587	0.087	0.00204	0.042	758	0.024	0.000631	0.111	0.453	0.541	0.551
3CDSL17	0.115	0.0263	0.39	0.045	0.620	0.587	0.087	0.00204	0.042	1513	0.024	0.000387	0.359	0.505	0.580	0.584
3VDSL18	0.115	0.0263	0.39	0.045	0.620	0.587	0.087	0.00204	0.042	915.2	0.024	0.0004	-	0.486	0.571	0.581
3CDSL19	0.115	0.0263	0.39	0.045	0.620	0.587	0.087	0.00204	0.042	1035	0.024	0.000588	0.18	0.498	0.575	0.580
3CDSL110	0.115	0.0263	0.39	0.045	0.620	0.587	0.087	0.00204	0.042	2060	0.024	0.00056	0.057	0.495	0.574	0.583
3CDSL111	0.115	0.0263	0.39	0.045	0.620	0.587	0.087	0.00204	0.042	3765	0.024	0.000355	0.239	0.483	0.562	0.561
3CDSL112	0.115	0.0263	0.39	0.045	0.620	0.587	0.087	0.00204	0.042	3285	0.024	0.000508	0.124	0.499	0.582	0.581
3CDSL22	0.15	0.0341	0.39	0.059	0.690	0.583	0.114	0.00204	0.048	2510	0.024	0.000968	0.05	0.541	0.628	0.618
3CDSL23	0.15	0.0341	0.39	0.059	0.690	0.583	0.114	0.00204	0.048	3075	0.024	0.000484	0.191	0.531	0.624	0.629
3CDSL24	0.15	0.0341	0.39	0.059	0.690	0.583	0.114	0.00204	0.048	993	0.024	0.000601	0.03	0.550	0.627	0.628
3CDSL25	0.15	0.0341	0.39	0.059	0.690	0.583	0.114	0.00204	0.048	1787	0.024	0.000715	0.034	0.550	0.627	0.627
3CDSL26	0.15	0.0341	0.39	0.059	0.690	0.583	0.114	0.00204	0.048	2395	0.024	0.000673	0.063	0.553	0.644	0.629
4CDCW1	0.128	0.0258	0.39	0.050	0.646	0.517	0.096	0.00147	0.037	-	-	0.000498	0.132	0.479	0.563	0.577
4CDCW2	0.147	0.0290	0.39	0.057	0.684	0.506	0.111	0.00147	0.040	-	-	0.001464	0.207	0.437	0.510	0.512
4CDCW3	0.162	0.0318	0.39	0.063	0.714	0.503	0.123	0.00147	0.042	-	-	0.000739	0.119	0.461	0.522	0.526
4CDCW4	0.184	0.0367	0.39	0.072	0.758	0.512	0.138	0.00147	0.045	-	-	0.000426	0.036	0.467	0.532	0.542
4CDCW5	0.109	0.0235	0.39	0.043	0.608	0.554	0.078	0.00147	0.034	-	-	0.000207	0.028	0.548	0.630	0.620
4CDSL11	0.128	0.0258	0.39	0.050	0.646	0.517	0.096	0.00147	0.037	3787	0.024	0.000596	0.08	0.448	0.518	0.528
4CDSL12	0.128	0.0258	0.39	0.050	0.646	0.517	0.096	0.00147	0.037	3882	0.024	0.000427	0.036	0.440	0.519	0.519
4CDSL21	0.147	0.0290	0.39	0.057	0.684	0.506	0.111	0.00147	0.040	3802	0.024	0.001097	0.226	0.442	0.515	0.516
4CDSL31	0.162	0.0318	0.39	0.063	0.714	0.503	0.123	0.00147	0.042	2458	0.024	0.000825	0.13	0.468	0.547	0.548
4CDSL32	0.162	0.0318	0.39	0.063	0.714	0.503	0.123	0.00147	0.042	3308	0.024	0.000958	0.177	0.445	0.517	0.520
4CDSL41	0.184	0.0367	0.39	0.072	0.758	0.512	0.138	0.00147	0.045	3067	0.024	0.001335	0.118	0.482	0.546	0.547
4CDSL42	0.184	0.0367	0.39	0.072	0.758	0.512	0.138	0.00147	0.045	4610	0.024	0.001755	0.281	0.461	0.539	0.543
4CDSL51	0.109	0.0235	0.39	0.043	0.608	0.554	0.078	0.00147	0.034	4460	0.024	0.000369	0.056	0.487	0.573	0.585
4CDSL52	0.109	0.0235	0.39	0.043	0.608	0.554	0.078	0.00147	0.034	6178	0.024	0.000287	0.03	0.502	0.592	0.608